

ABSTRACT

Title of Dissertation / Thesis: EMPLOYING A REMOTE CONFORMATIONAL BIAS, INHIBITION OF GAMMA-BUTYROLACTONE FORMATION, AND A SODIUM TEMPLATE TO ENHANCE MACROCYCLIZATION IN CARBENE ADDITION REACTIONS

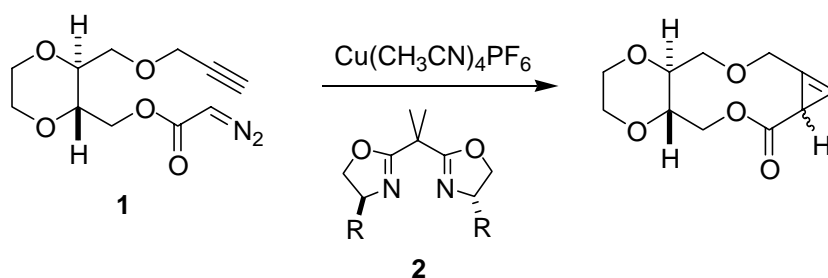
Thomas M. Weathers, Jr., Doctor of Philosophy, 2005

Dissertation / Thesis Directed By: Professor Michael P. Doyle, Department of Chemistry and Biochemistry

Ring closure via dirhodium(II) catalyzed diazo decomposition of diazoacetates is an efficient method of asymmetric macrocycle formation, affording up to 28-membered rings without the high dilution requirement of many other macrocyclization methods. To overcome reaction pathways that compete with macrocyclization, such as γ -butyrolactone formation via C-H insertion, and to enhance control of the stereocenters formed in carbene addition reactions, remote conformational bias of a diazoacetate, inhibition of γ -butyrolactone formation, and template directed macrocycle formation, were each independently investigated.

The influence of a remote conformational bias in a diazoacetate on diastereoselectivity in carbene addition reactions was evaluated using diazoacetates prepared from threitol 2,3-diprotected as a 1,4-dioxane (**1**) or a 1,3-dioxolane. Diazo decomposition of **A** with chiral dirhodium(II) and copper(I) catalysts afforded

diastereoisomer ratios as high as 99:1 and match/mismatch interactions between substrate and catalyst, while diazo decomposition of 1,3-dioxolane derived diazoacetates afforded no greater than 90:10 diastereoselectivity, and no match/mismatch relationship was found when using dirhodium(II) carboxamidate catalysts, though one is believed to exist when using a chiral copper(I)/**2**. Results indicate that the influence of a remote conformational bias on diastereoselectivity is the dihedral angle from the template.



In a separate study, effective inhibition of competitive γ -butyrolactone formation was accomplished by using a 1,2-benzenedimethanol linker, allowing the formation of up to 28-membered macrocycles via carbene addition to an allyl ether C=C bond with good yields. Catalysts such as $\text{Rh}_2(\text{MEOX})_4$ and $\text{Rh}_2(\text{DOSP})_4$, which have been ineffective in macrocycle formation, can catalyze diazo decomposition of these diazoacetates to afford macrocycles in greater than 50% yield. The elimination of γ -butyrolactone formation allows a greater number of dirhodium(II) catalysts to be used for macrocycle formation.

The influence of a sodium ion from NaBPh_4 and of copper(I) as a template on diazo decomposition reaction selectivity was evaluated using substrates that link a diazoacetate to an allyl ether through penta(ethylene glycol). Sodium ion inhibits

oxonium ylide formation and modifies diastereoselectivity in copper(I) catalyzed reactions to afford cyclopropanes in a ratio of 80:20 (*Z:E*) versus a 57:43 ratio without the template.

EMPLOYING A REMOTE CONFORMATIONAL BIAS, INHIBITION OF
GAMMA-BUTYROLACTONE FORMATION, AND A SODIUM TEMPLATE TO
ENHANCE MACROCYCLIZATION IN CARBENE ADDITION REACTIONS

By

Thomas M. Weathers, Jr.

Dissertation submitted to the Faculty of the Graduate School of the
University of Maryland, College Park, in partial fulfillment
of the requirements for the degree of
Doctor of Philosophy in the
subject of Chemistry
2005

Advisory Committee:
Professor Michael P. Doyle, Chair
Professor Philip DeShong
Professor Steven Rokita
Assoc. Professor Lyle Isaacs
Assoc. Professor Peter Kofinas

© Copyright by
Thomas M. Weathers, Jr.
2005

Dedication

To my grandma Roberta, whom I will always love,
and to my parents, who have supported me in everything with unfailing love.

Acknowledgements

As I reach the conclusion of this adventure known as graduate school, I have paused several times to reflect back to the people and events that have transpired during this seven year journey. The people that have inspired and encouraged me are many, and I cannot fully state the emotions that I have for these special individuals with a few simple words. Until the time that I find a way to express all that I feel please accept this substitute.

I will forever owe a debt of gratitude to my family (parents, sibling, cousins, aunts, uncles, grandparents, and even my great-grandmother Lee Otha) who have supported and encouraged me innumerable times. It is your love and support that started me on this journey.

I would be remiss if I did not recognize the people from two great research labs that I have had the pleasure of working in. I have learned a great deal in science and in life from Son, Mike and Abhi during my time in the Gervay-Hague lab, and I respect and appreciate all your contributions. With the changes that life brings I was warmly welcomed and accepted into the Doyle lab where I have formed friendships that I never expected. The challenges and changes I have been through with John, Marcela, Christine, Art, Darren, Penglin, Jason, Al, JP, Kousik, and Ray have brought me friendships that I take with me. I thank each of you for your support and honesty during our academic pursuits, and for your friendship that went beyond the lab walls. To the undergraduate students Hans and Sid who endeavored to work with me, I

appreciate all your work and your contribution to the lab. I have also enjoyed your company and your delightful zest for life.

As with anything in life, there are people that I have met along the way that have been my support in times of need, my escape in times of desperation, and my friends through it all. I thank God for my friends Joe and Erin; you have given of yourselves in your time and your concern for your beleaguered friend. My friend Jeremy has been the answer to prayer. With your boyish charm and carefree attitude you gave me an escape from the pressures of school that I continue to enjoy. To the Guerra family as a whole, and especially to Beth, I thank you for your unceasing support and friendship; there were times that it was the difference for me. To all my friends at church in Tucson and Flagstaff, I thank you for the kindness and support you showed me of your own free will and without thought of anything in return.

During the trials and triumphs of graduate school I have found many friends that I hold common ground with. To rob kevwitch, Taya (Peterson) Kevwitch, Chris Mullen, Chris Orrendorf, Eric Ross, Gemma D'Ambrusso, Brian Rolan, Hugh Selby, Mike Palian, Jason Cox, Jason Imbriglio, Emily Weinert, and Jim Watson, thanks for all the fun times and for the competitive spirit that you provided.

Finally, I would like to thank Prof. Mike Doyle for all his support. You have pushed, prodded, and coaxed me through a great deal of learning. For your mentorship and support and your relentless pursuit of perfection I thank you.

Table of Contents

Dedication	ii
Acknowledgements	iii
Table of Contents	v
List of Tables	vii
List of Figures	viii
List of Schemes	ix
List of Abbreviations	xi
Chapter 1: Introduction	1
1.1 Background	2
1.2 Methods for Ring Closure	5
1.2.1 Lactonization	8
1.2.2 Carbon-Carbon Bond Formation	9
1.2.3 Heteroatom Alkylation	11
1.2.4 Ring Closing Metathesis	12
1.2.5 Metal Carbene Insertion and Addition	13
1.3 Catalysts for Diazo Decomposition	16
1.4 Macrocyclization from Metal Carbene Addition Reactions	19
1.4.1 Functional Groups and Selectivity in Carbene Addition Macrocyclization	20
1.4.3 Competitive Reactions in Macrocyclization	27
1.4.4 Formation of Rings Larger Than 10-Membered	31
1.4.5 Insertion Reactions to Form Macrocycles	41
1.4.6 Summary	42
Chapter 2	44
2.1 Introduction	44
2.2 Semi-Empirical Prediction of Double Diastereoselectivity	46
2.3 Application of Dirhodium(II) Carboxamidates to Match/Mismatch Reactions	49
2.4 Formation of Ten-membered Rings by Carbene Addition Reactions	52
2.4.1 Intramolecular Cyclopropanation of Olefins	53
2.4.2 Intramolecular Cyclopropanation in Macrocycles	54
2.5 Linking a Diazoacetate to the Functional Group with a Chiral Tether	55
2.6 Conformationally Biased Diazoacetate Substrates	57
2.6.1 Synthesis Conformationally Biased Diazoacetates	58
2.6.2 Cyclopropane Diastereoselectivity with Chiral Di-acetal Substrates	59
2.6.3 Cyclopropene Diastereoselectivity with Chiral Di-acetal Substrates	70
2.6.4 Modification of the Conformational Bias	75
2.6.5 Cyclopropane Diastereoselectivity with Chiral Dioxolane Substrates	76
2.6.6 Cyclopropene Diastereoselectivity with Chiral Dioxolane Substrates	82
2.7 Discussion and Conclusions	86
2.8 Experimental Procedures	98
Chapter 3. Enhancing the Macrocyclization Reaction Pathway	127
3.1. Macrocyclization	127

3.1.1 The Dilution Principle.....	128
3.1.2 Carbene Addition Reactions in Macrocycle Formation.....	131
3.2 Macrocycle Ring Size Limits.....	135
3.2.1 Functional Group Variants.....	136
3.2.2 Linker Modification	137
3.3 Inhibition of γ -Lactone Formation.....	139
3.3.2 Diazoacetates where γ -C-H Insertion is Inhibited: Selectivity	142
3.4 Conclusions and Future Directions	155
3.5 Experimental Procedures	157
Chapter 4 – Templated Macrocycle Formation of Metal Carbenes.....	184
4.1 Introduction and Background	184
4.1.1 Templates for Macrocycle Formation.....	185
4.1.2 Substrate Modifications	187
4.1.3 Template Cyclization	188
4.1.2 Selectivity Between Oxonium Ylide and Carbene Addition Pathways...	192
4.2 Template Macrocyclic Cyclopropanation.....	195
4.2.1 Copper Templating Effects	196
4.2.2 Use of a Sodium Template.....	205
4.2.3 Product Complexes of Sodium	212
4.3 Conclusions and Future Work	215
4.4 Experimental Procedures	217
Chapter 5. Summary and Conclusions.....	219
Appendix A.....	221

List of Tables

Table 1.1 Product Selectivity from Diazo Decomposition of 51 ^a	23
Table 1.2 Selectivity in the Diazo Decomposition Reactions of 100 and 101	36
Table 1.3 Chemoselectivity and Regioselectivity of Diazo Decomposition of 102 ...	37
Table 1.4 Diastereoselectivity in Diazo Decomposition of 123	40
Table 2.1 Diastereoselectivity in Double Diastereoselective Aldol Reactions.....	48
Table 2.2 Enantiomeric Ratios for Diazo Decomposition of 27 at 40° C ^a	56
Table 2.3 Selectivity in Diazo Decomposition Reactions of 36 ^a	62
Table 2.4 Select Bond Angles and Bond Distances.....	64
Table 2.5 Product Selectivity in Diazo Decomposition of 42 ^a	67
Table 2.6 Reaction Selectivity in Diazo Decomposition of 48 ^a	72
Table 2.7 Selectivity in Diazo Decomposition of 49 with Select Catalysts	74
Table 2.8 Product Selectivity in Diazo Decomposition of 56 ^a	78
Table 2.9 Product Selectivity in Diazo Decomposition of 58 ^a	80
Table 2.10 Product Selectivity in Diazo Decomposition of 62	83
Table 2.11 Diazo Decomposition of 64	85
Table 2.12 Comparison of Diastereoselectivity Between Copper(I) and Rh ₂ (5 <i>R</i> - MEPY) ₄	89
Table 3.1 Effective Molarity of Lactonization of ω-Bromoalkanoate ions ^a	130
Table 3.2 Selectivity in the Diazo Decomposition of 30 ^a	138
Table 3.3 Diazo Decomposition ^a of 56 with Selected Dirhodium(II) Catalysts.....	144
Table 3.4 Diazo Decomposition ^a of 56 with Selected Copper(I) Catalysts.....	147
Table 3.5 Synthesis of Cyclopropanes with Varying Ring Size ^a	149
Table 3.6 Diazo Decomposition of Substrates with Selected Functional Groups ^a ...	152
Table 3.7 Yields of Reactions Catalyzed by Rh ₂ (pfb) ₄ versus Rh ₂ (OAc) ₄	155
Table 4.1 Ring Size Product Ratios for Copper(I) Diazo Decomposition ^a	198
Table 4.2 Catalyst Loading and Product Selectivity in Diazo Decomposition of 33b ^a	200
Table 4.3 Copper Decomposition with Various Functional Groups.....	203
Table 4.4 Chemical Shifts in the ¹ H NMR Spectra of 33b	208
Table 4.4 Selectivity in Diazo Decomposition of 30b with a Na Template	209
Table 4.5 IR Absorbances of 31a with and without a Na Template ^a	214

List of Figures

Figure 1.1 Select Ring Closure Methods in Macrocycle Formation	8
Figure 1.2 Grubbs Ruthenium Catalysts	13
Figure 1.3 Catalysts Used in Diazo Decomposition of 26	16
Figure 1.4 Structural Configurations of Dirhodium(II) Carboxamidates	17
Figure 1.5 Select Dirhodium(II) Carboxamidate Catalysts	18
Figure 1.6 1,2-Benzenedimethanol Linked Diazoacetate Substrates	21
Figure 1.7 Macrocyclization with Select Functional Groups	34
Figure 2.1 Chiral-Tethered Diazoacetates	55
Figure 2.2 Impact of a Conformational Bias	58
Figure 2.3 Chiral Catalysts and Ligands Used in Diazo Decomposition of Conformationally Biased Diazoacetates	60
Figure 2.4 ORTEP Diagram of 39a with Absolute Stereochemical Structure	64
Figure 2.5 Major Diastereoisomer Selectivity	69
Figure 2.6 Diazoacetate Structures	86
Figure 2.7 Rhodium-Carbene Intermediate	91
Figure 2.8 Copper Catalyzed Diastereoselectivity	92
Figure 3.1 Diazoacetates	137
Figure 3.2 Diazoacetate Precursors	141
Figure 3.2 Macrocycles formed from Catalytic Diazo Decomposition of 56	143
Figure 3.3 Additional Catalysts Used in the Decomposition of 56	153
Figure 3.4 Diazoacetates 56, 58, and 59	154
Figure 4.1 Template Derived Reaction Control	186
Figure 4.2 Cation Template Geometries	191
Figure 4.3 Diazoacetates with Ethylene Glycol Linkages to Functional Groups	192
Figure 4.4 Geometry of Copper Coordination	196
Figure 4.5 Diazoacetate Compounds for Macrocyclization	197
Figure 4.6 Diazoacetate Precursors With Various Functional Groups	201
Figure 4.7 ¹ H Spectra of 30b without NaBPh ₄	206
Figure 4.8 ¹ H Spectra of 30b with NaBPh ₄	207
Figure 4.8 Configuration of 30b with Sodium Template	211
Figure 4.9 ¹ H NMR Spectra of 31a with and without NaBPh ₄	213

List of Schemes

Scheme 1.1 Methods of Macrocycle Formation	2
Scheme 1.2 Reactions of Linear Precursors of Macrocycles.....	5
Scheme 1.3 Ring Enlargement by the Zip Reaction	6
Scheme 1.4 Bond Cleaving Ring Expansion ^a	7
Scheme 1.5 Lactonization Ring Closure by Ester Activation.....	9
Scheme 1.6 Macrocycle Formation from a Diels-Alder Reaction ^a	10
Scheme 1.7 O-H Insertion to Produce Macrocycles	13
Scheme 1.8 Synthesis of (±) – casbene	14
Scheme 1.9 Macrocycles from Dirhodium(II) Catalysts	15
Scheme 1.10 Chiral Ester Projection and Carbene Intermediate Conformations	19
Scheme 1.11 1,2-Benzenedimethanol Linked Cyclopropanation	22
Scheme 1.12 Olefin Substitution and Diazo Decomposition Products.....	23
Scheme 1.13 Asymmetric Cyclopropanation Using Various Catalysts.....	24
Scheme 1.14 Addition of a Carbene to 1,2-Benzenedimethanol	25
Scheme 1.15 Competitive and Conformational Investigations.....	26
Scheme 1.16 Diazo Decomposition Using 1,8-Naphthalenedimethanol as a Linker .	27
Scheme 1.17 Regioselectivity with a 1,2-Benzenedimethanol Linker	28
Scheme 1.18 Competitive Allylic Cyclopropanation versus Cyclopropanation	29
Scheme 1.19 Cyclopropanation versus Cyclopropanation in Macrocycle Formation	30
Scheme 1.20 Selective Cyclopropanation of Geraniol Diazoacetate.....	31
Scheme 1.21 Carboxamidate versus Carboxylate Catalysts	33
Scheme 1.22 Large Ring Cyclopropanation	34
Scheme 1.23 Diazo Decomposition of 100, and 101	36
Scheme 1.24 Diazo Decomposition of 102.....	37
Scheme 1.25 Ring formation with Alkane Linkers	38
Scheme 1.26 Carbene Dimerization Process	39
Scheme 1.27 Carbene Dimerization with Diazoketones.....	39
Scheme 1.28 Carbene Dimerization by Select Catalysts	40
Scheme 1.29 Synthesis of Patulolides A and B	41
Scheme 1.30 General O-H Insertion Reactions	41
Scheme 1.31 C-H Insertion for Macrocycle Formation.....	42
Scheme 2.1 Removal of Configurational Bias.....	46
Scheme 2.2 Double Diastereoselective Aldol.....	48
Scheme 2.3 Decomposition of Chiral Diazoacetate 16	50
Scheme 2.4 Match and Mismatch Decompositions of 18 with Rh ₂ (MEOX) ₄	51
Scheme 2.5. 1,2-Benzenedimethanol Linked Cyclopropanation.....	54
Scheme 2.6 Asymmetric Cyclopropanation Forming Ten-membered Rings.....	54
Scheme 2.7 Diazo Decomposition of 27.....	56
Scheme 2.8 Synthesis of a Conformationally Biased Diazoacetate	59
Scheme 2.9 Diazo Decomposition of 36.....	62
Scheme 2.10 Diazo Decomposition of 41.....	67
Scheme 2.11 Synthesis of 48	70
Scheme 2.12 Diazo Decomposition of 48.....	72
Scheme 2.13 Hydrogenation of 49a.....	73

Scheme 2.14 Diazo Decomposition of 49.....	74
Scheme 2.15 Dimethyldioxolane Formation	76
Scheme 2.16 Product Selectivity in Diazo Decomposition of 56	78
Scheme 2.17 Diazo Decomposition of 58.....	80
Scheme 2.18 Synthesis of 62	82
Scheme 2.19 Diazo decomposition of 62	83
Scheme 2.20 Diazo Decomposition of 64.....	85
Scheme 2.21 Influence of Dirhodium(II) Carboxamidate on Olefin Trajectory	88
Scheme 2.22 Chiral Influence of Copper(I)/3 Complex on Olefin Trajectory	89
Scheme 2.23 Stereochemistry by Conformation	96
Scheme 3.1 Ring Closing Metathesis in the Synthesis of Mygrastatin	131
Scheme 3.2 Intramolecular Reaction Pathways of Diazo Decomposition	133
Scheme 3.3 Carboxamidate versus Carboxylate Catalysts	134
Scheme 3.4. Large ring cyclopropanation	136
Scheme 3.5 Macrocyclization with Various Functional Groups	137
Scheme 3.6 Ring Formation with Alkane Linkers.....	138
Scheme 3.7 Synthesis of Diazo Precursors.....	140
Scheme 3.8 Synthesis of Macrocycle Precursors with Functional Group Diversity	142
Scheme 3.9 Hydride Abstraction in 1,2-Benzenedimethanol Diazoacetates.....	146
Scheme 3.10 Diazo Decomposition of Substrates with Variable Linker Lengths....	149
Scheme 3.11 Macrocyclization with Allyl, Methallyl, and Propargyl Functional Groups.....	151
Scheme 4.1 Erythromycin Lactonization with Configurational Constraints	187
Scheme 4.2 Effective Molarity of Ring Closure with Select Phenol Compounds ^a ..	188
Scheme 4.3 Formation of Benzo-18-crown-6 Templated by Potassium ^a	189
Scheme 4.4 Template Macrocyclization.....	190
Scheme 4.5 Decomposition of 20 Using Copper(I).....	193
Scheme 4.6 Intramolecular Addition Reactions to Furans	194
Scheme 4.7 Diazo Decomposition of 30b with a Na Template	209

List of Abbreviations

$\text{Rh}_2(5S\text{-MEPY})_4$	dirhodium(II) tetrakis[methyl 2-oxopyrrolidine-5(<i>S</i>)-carboxylate]
$\text{Rh}_2(4S\text{-MEOX})_4$	dirhodium(II) tetrakis[methyl 2-oxooxazolidin-4(<i>S</i>)-carboxylate]
$\text{Rh}_2(4S\text{-MEAZ})_4$	dirhodium(II) tetrakis[methyl 2-oxaazetidine-4(<i>S</i>)-carboxylate]
$\text{Rh}_2(4S\text{-MPPIM})_4$	dirhodium(II) tetrakis[methyl 1-(3-phenylpropanoyl)-2-oxoimidazolidin-4(<i>S</i>)-carboxylate]
$\text{Rh}_2(4S\text{-DOSP})_4$	dirhodium(II) tetrakis[<i>N</i> -(4-dodecylbenzene-sulfonyl)-proline]
$\text{Rh}_2(\text{cap})_4$	dirhodium(II) tetrakis(caprolactamate)
$\text{Rh}_2(\text{pfb})_4$	dirhodium(II) tetrakis(perfluorobutyrate)
$\text{Rh}_2(\text{oct})_4$	dirhodium(II) tetrakis(octanoate)
(<i>S,S</i>)- <i>t</i> Bu-BOX	2,2-bis[2-[4(<i>S</i>)- <i>tert</i> -butyl-1,3-oxazolinyl]]propane
DCM	dichloromethane
THF	tetrahydrofuran
HPLC	high performance liquid chromatography
GC	gas chromatography
ee	enantiomeric excess
d.r.	diastereomeric ratio

Chapter 1: Introduction

Despite their relative inaccessibility, macrocycles are common in chemistry and chemical biology.¹ Their structural diversity and the unique physical properties of these compounds makes them both challenging synthetic targets and important materials for commercial applications. Insight gained from employing macrocycles to their greatest possible advantage has expanded and advanced science in many areas including drug targets, host-guest chemistry, display technologies, catalysis, and molecular machines.² Many naturally occurring substrates contain large rings, and the unique configurational arrangement of these substrates provides important properties such as ion complexation and templating that contribute to their biological activity.³ As the complexity of macrocycles increases, the need increases for cyclization reactions that occur regioselectively, diastereoselectively, chemoselectively, and with tolerance of a broad range of functional groups.

Methods to form rings include cleavage of internal bonds, ring expansion, and end-to-end cyclization (Scheme 1.1). Of these methods, end-to-end cyclization is most preferred for large ring formation.⁴ Cyclization of linear substrates (**1**) is a synthetic challenge due to the internal entropy of the substrate making this an energetically

¹ Deitrich, B.; Viout, P.; Lehn, J.-M. Macrocyclic Chemistry, VCH Publishers: New York, 1993.

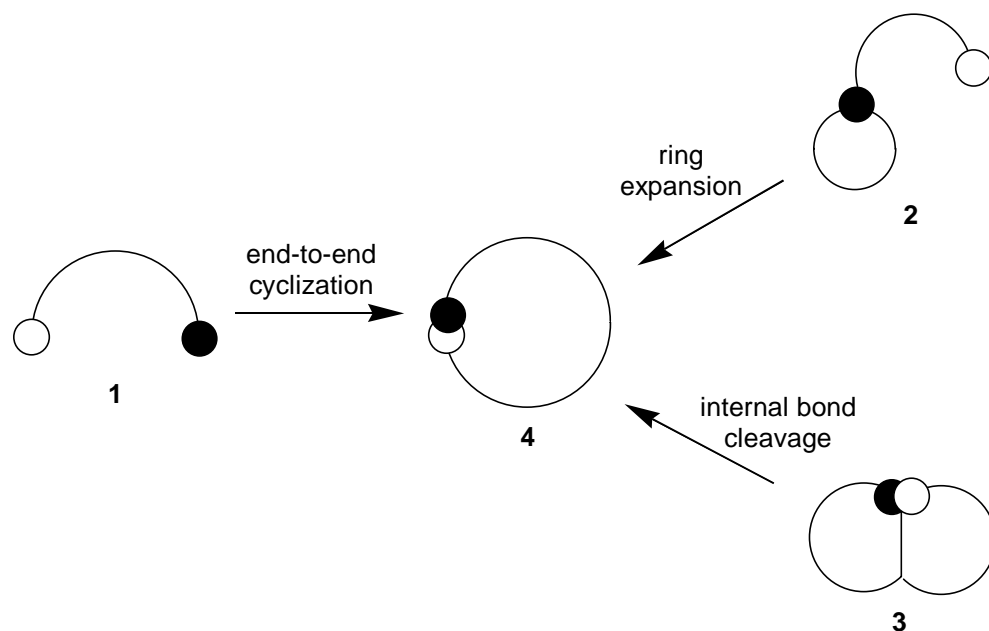
² For representative examples see: (a) Zhang, X.X.; Bradshaw, J.S.; Izatt, R.M. *Chem. Rev.* **1997**, *97*, 3313; (b) Gokel, G.W.; Leevy, W.M.; Weber, M.E. *Chem. Rev.* **2004**, *104*, 2723. (c) Schalley, C.A.; Beizai, K.; Vögtle, F. *Acc. Chem. Res.* **2001**, *34*, 465. (d) Meunie, B.; de Visser, S.P.; Shaik, S. *Chem. Rev.* **2004**, *104*, 3947. (e) Takahashi, K. *Chem. Rev.* **1998**, *98*, 2013; (f) Rychnovsky, S.D. *Chem. Rev.* **1995**, *95*, 2021; (g) Kovbasyuk, L.; Krämer, R. *Chem. Rev.* **2004**, *104*, 3161; (h) Balzani, V.; Credi, A.; Raymo, F.M.; Stoddart, J. F. *Angew. Chem. Int. Ed* **2000**, *39*, 3349.

³ Macrolides : Chemistry, Pharmacology, and Clinical Uses Bryskier, A.J. Ed.; Arnette Blackwell: Boston, 1993.

⁴ Roxborgh, C.J. *Tetrahedron* **1995**, *51*, 1995.

unfavorable process.⁵ Many approaches have been used to improve the current state-of-the-art for macrocycle synthesis.^{4,6} One approach to macrocycle formation is end-to-end cyclizations via carbon-carbon bond forming reactions. These reactions provide a means to asymmetric induction in the ring formation step that can potentially be used in any organic macrocycle.

Scheme 1.1 Methods of Macrocycle Formation



1.1 Background

Prelog and Brown first devised a classification system for molecular rings with separation between classes based on the heat of combustion per methylene group for saturated aliphatic rings.⁷ The four classes are: small rings ($n = 3$ and 4), possessing high ring strain energy, common rings ($n = 5, 6$ and 7) with heats of combustion

⁵ Ruzieka, L.; Brugger, W.; Pfeiffer, M.; Sehin, H.; Stoll, M. *Helv. Chem. Act.* **1926**, 9, 499.

⁶ Meng, Q.; Hesse, M. Ring Closure Methods in the Synthesis of Macrocyclic Natural Products. In *Topics in Current Chemistry: Macrocycles*, 161; Dewar, M.J.S., Dunitz, J.D., Hafner, K., Ito, S., Lehn, J.-M., Niedenzu, K.; Raymond, K.N.; Rees, C.W.; Vögtle, F. Springer-Verlag:Berlin, 1992.

⁷The classification was discussed in a personal communication between V. Prelog and H.C. Brown as cited in: Brown, H.C.; Fletcher, R.S.; Johannesen, R.B. *J. Am. Chem. Soc.* **73**, 212.

similar to those of acyclic aliphatic compounds, medium rings ($n = 8-12$), which also deviate from combustion values for linear aliphatic compounds, and large rings, or macrocycles ($n = 13$ and larger), which also have heats of combustion similar to acyclic aliphatic compounds.

Ring size is directly correlated to the rate of lactonization in small to medium ring lactones, but the rate of cyclization does not vary significantly in the formation of thirteen membered lactones or larger (Graph 1.1).⁸ Heteroatoms, atom hybridization, carbon substitution, solvent effects, and conformational control are known to enhance small and common ring cyclization reactions.^{1,9} However, these substrate modifications generally have little or no effect on macrocyclization rates or yields, and in some cases are deleterious to the reaction.¹⁰ The only substrate modification reported to enhance ring closure is addition of rigid groups to the acyclic precursor, lowering the number of degrees of freedom and the internal entropy of the substrate.¹¹

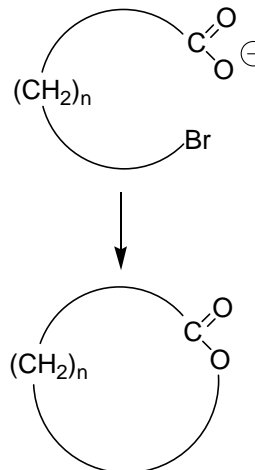
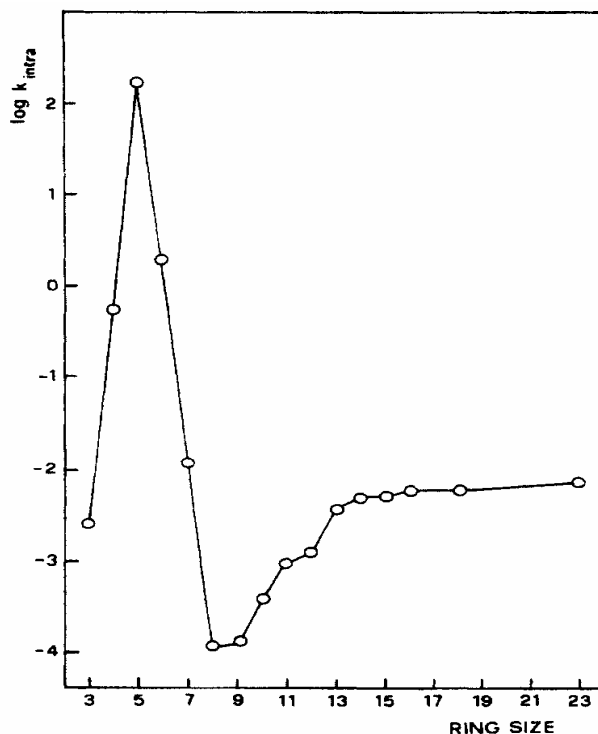
⁸ Illuminati, G.; Mandolini, L. *Acct. Chem. Res.* **1981**, *14*, 95.

⁹ Eliel, E.L. *Stereochemistry of Carbon Compounds* McGraw-Hill: New York, 1962, pp.188-201.

¹⁰ (a) Borgen, G.; Dale, J. *Acta Chem. Scand.* **1972**, *26*, 952; (b) Galli, C.; Giovannelli, G.; Illuminati, G.; Mandolini, L. *J. Org. Chem.* **1979**, *44*, 1258.

¹¹ a) Illuminati, G.; Mandolini, L.; Masci, B. *J. Am. Chem. Soc.* **1977**, *99*, 6308; b) Galli, C.; Illuminati, G.; Mandolini, L. *J. Am. Chem. Soc.* **1973**, *95*, 8374; c) Galli, C.; Mandolini, L. *Chem. Comm.* **1982**, 251; d) Ruzieka, L.; Stoll, M.; Sehin, H. *Helv. Chem. Act.* **1926**, *9*, 249.

Graph 1.1 Intramolecular Lactone Formation Rates by Ring Size^a



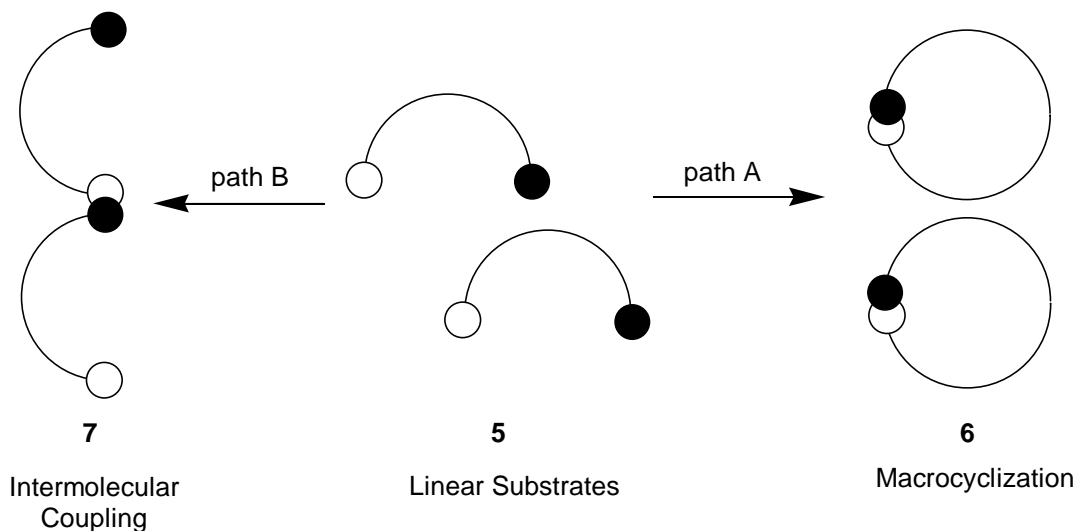
(a) taken from: Illuminati, G.; Mandolini, L. *Acc. Chem. Res.* **1981**, *14*, 95.

Large ring formation is inherently difficult due to the degrees of freedom in the substrate. Ring closure occurs by the coupling of two reactive termini within the same molecule (Scheme 1.2). A reactive terminus may react with any counterpart terminus in both intramolecular (path A) and intermolecular (path B) reactions. Intermolecular reactions form dimers (7), and can propagate to generate polymer chains instead of ring closure. To form macrocycles in reasonable yields, the rate of path A must be significantly higher than that of path B.¹² It is the rate difference between intramolecular cyclization and intermolecular dimer formation that helps

¹² Knops, P.; Sendhoff, N.; Mekelbirger, H.-B.; Vögtle, F. 'High Dilution Reactions- New Synthetic Applications' *Topics in Current Chemistry: Macrocycles* ed. Dewar, M.J.S.; Dunitz, J.D.; Hafner, K.; Ito, S.; Lehn, J.-M.; Niedenzu, K.; Raymond, K.N.; Rees, C.W.; Vögtle, F. Springer-Verlag:Berlin, 1992, pp.1-106.

define good macrocyclization reactions. If undesired, the intermolecular reaction rate is most commonly diminished by high dilution techniques, and this technique is discussed in section 3.1.1.

Scheme 1.2 Reactions of Linear Precursors of Macrocycles

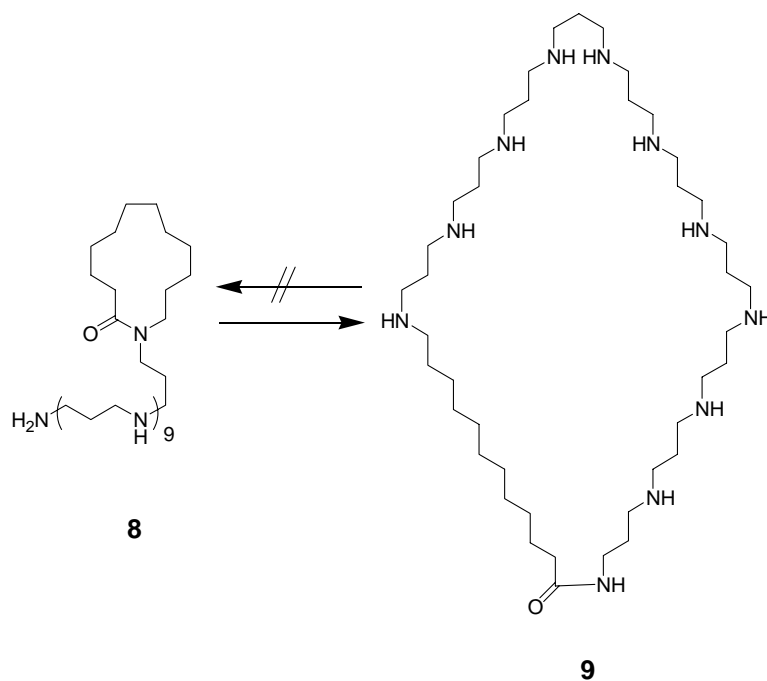


1.2 Methods for Ring Closure

Macrocycle formation can be accomplished in a variety of ways including ring enlargement by incorporating a side chain into an existing ring, ring expansion cleaving a bridgehead bond, and end-to-end cyclization of a linear substrate (Scheme 1.1). Ring enlargement by side chain incorporation has been utilized to create very large rings, and the “Zip reaction”, which is a trans-amidation process, is a method capable of creating rings of almost limitless size by side chain incorporation (Scheme 1.3).¹³

¹³ Kramer, U.; Guggisberg, A.; Hesse, M.; Schmid, H. *Angew. Chem., Int. Ed. Engl.* **1978**, *17*, 200.

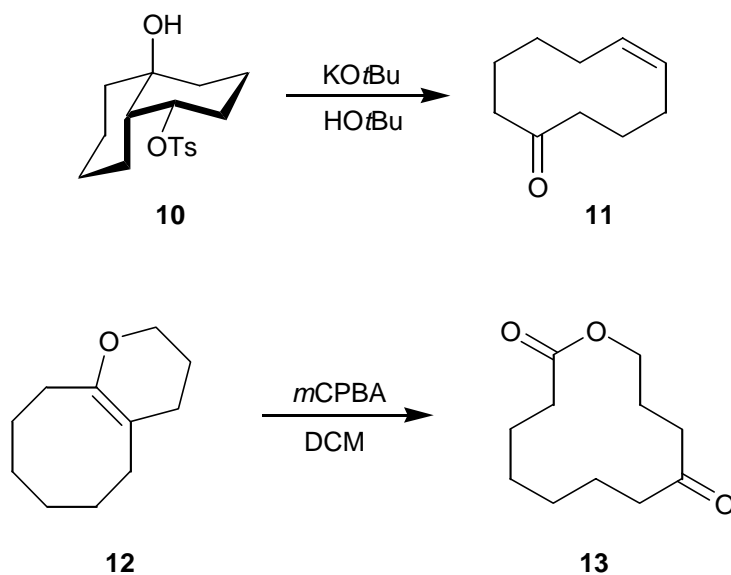
Scheme 1.3 Ring Enlargement by the Zip Reaction



Ring expansion by bond cleavage is also an elegant method for the synthesis of medium and large rings. By using a bicyclic material and destroying the bridgehead bond, rings may be rapidly expanded (Scheme 1.4).¹⁴

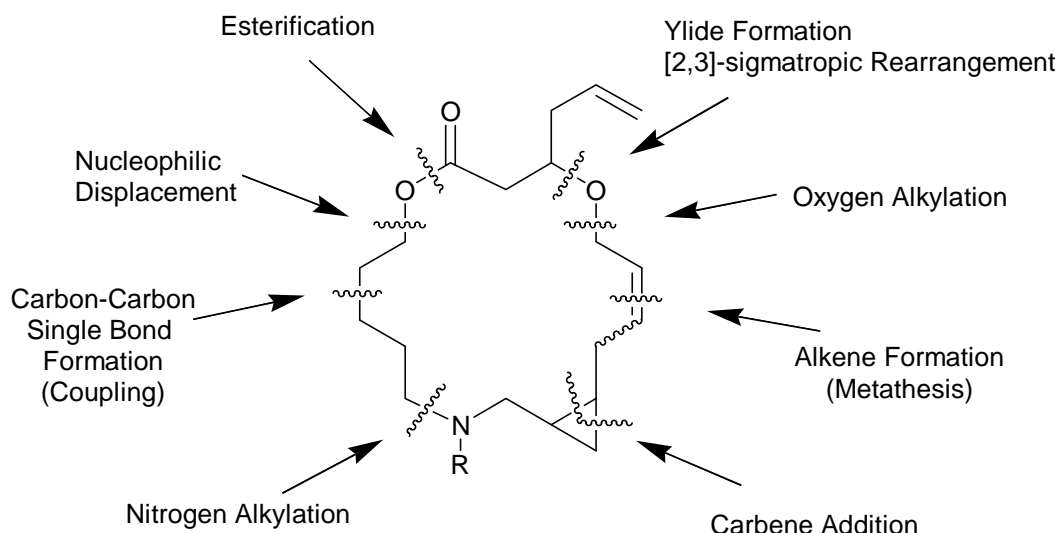
¹⁴ Hesse, M. Ring Enlargement in Organic Chemistry VCH: New York, 1991.

Scheme 1.4 Bond Cleaving Ring Expansion^a



End-to-end cyclization of a linear substrate is generally the most preferred method of macrocycle formation.⁴ Ring formation may be viewed in a retro-synthetic manner to select which bond in the ring is most amenable to ring formation (Figure 1.1). A variety of methods are available, including esterification, C-C bond formation, C=C bond formation, heteroatom alkylation, ylide formation, and carbene addition. In sections 1.2.1 through 1.2.4 we review the most common end-to-end cyclization methods used for macrocycle formation.

Figure 1.1 Select Ring Closure Methods in Macrocycle Formation



1.2.1 Lactonization

Activated esters and carboxylic acid derivatives with functional groups designed to promote internal esterification have proven successful in large ring lactone formation (macrolactonization). The method developed by Corey using a 2-pyridinthioester illustrates how a reagent may be used to activate a carboxylate for ester formation (Scheme 1.5).¹⁵ Many other examples of reagents used to activate carboxylic acids for lactonization are reported.¹⁶ The number of such reagents has continually increased with the drive to provide milder and more functional groups tolerant reaction conditions. Alcohol activating reagents for macrolactonization have also been reported.¹⁷ In general, however, these reactions are reported using high dilution

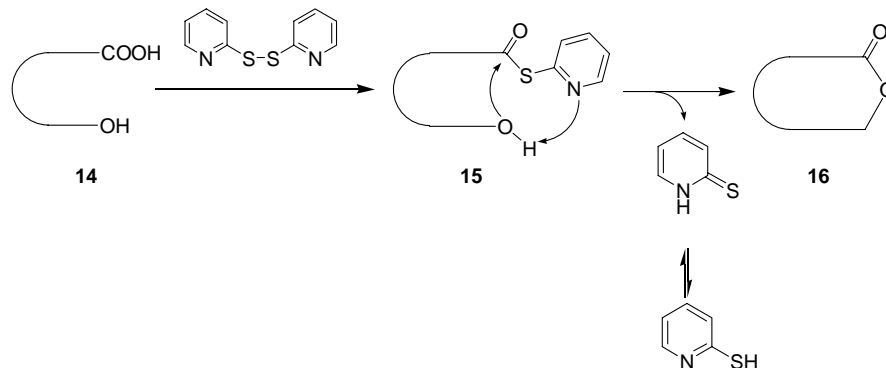
¹⁵ Corey, E.J.; Nicolaou, K.C. *J. Am. Chem. Soc.* **1974**, *96*, 5614.

¹⁶ For reviews of various activated esters see [4] and [5]; For current examples see: (a) Nicolaou, K.C.; Ninkovic, S.; Sarabia, F.; Vourloumis, D.; He, .Y.; Vallberg, H.; Finlay, M.R.V.; Yang, Z. *J. Am. Chem. Soc.* **1997**, *119*, 7974; (b) Dwoden, J.; Edwards, P.D.; Flack, S.S.; Kilburn, J.D. *Chem. Eur. J.* **1999**, *5*, 79; (c) Nicolaou, K.C.; Ritzén, A.; Namoto, K.; Buey, R.M.; Díaz, J.F.; Andreu, J.M.; Wartmann, M.; Altmann, K.-H.; O'Brate, A.; Giannakakou, G. *Tetrahedron* **2002**, *58*, 6413; (d) Nicolaou, K.C.; Zak, M.; Safina, B.S.; Lee, S.H.; Estrada, A.A. *Angew. Chem. Int. Ed.* **2004**, *43*, 5092.

¹⁷ For recent examples see: (a) Sasaki, T.; Inoue, M.; Hirama, M. *Tetrahedron Lett.* **2001**, *42*, 5299; (b) Moreau, X.; Campagne, J.-M. *J. Org. Chem.* **2003**, *68*, 5346.

reaction conditions with substrate concentrations of less than 0.01 millimolar (mM) to diminish intermolecular esterification reactions.

Scheme 1.5 Lactonization Ring Closure by Ester Activation



1.2.2 Carbon-Carbon Bond Formation

Carbon-carbon bond forming reactions, including nucleophilic addition to carbonyl containing compounds,¹⁸ alkylation of activated alkanes,¹⁹ radical cyclization,²⁰ and pericyclic reactions²¹ exemplify the diversity of reactions providing ring closure for macrocycle formation.

Nucleophilic addition to carbonyl carbon atoms is the most extensively used method of carbon-carbon bond forming macrocyclization.⁵ For example, aldol reactions, sulfone-carbonyl coupling, and addition of allylstannanes have all been used in

¹⁸ For examples see: (a) Takeda, K.; Yano, S. Yoshii, E. *Tetrahedron Lett.* **1988**, 29, 6951; (b) Danishefsky, S.J.; Mantlo, N.B.; Yamashita, D.S. *J. Am. Chem. Soc.* **1988**, 110, 6890.

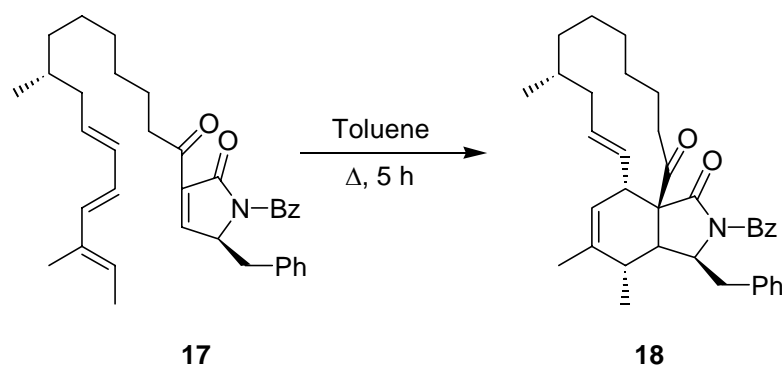
¹⁹ For examples see: (a) Takahashi, T.; Nagashima, T.; Tsuji, J. *Tetrahedron Lett.* **1981**, 22, 1359; (b) Marshall, J.A.; Cleary, D.G. *J. Org. Chem.* **1986**, 51, 858.

²⁰ For examples see: (a) Porter, N.A.; Chang, V.H-T. *J. Am. Chem. Soc.* **1987**, 109, 4976; (b) Cox, N.J.G.; Pattenden, G.; Mills, S.D. *Tetrahedron Lett.* **1989**, 30, 621; (c) Boger, D.L.; Mathvink, R.J. *J. Am. Chem. Soc.* **1990**, 112, 4008.

²¹ (a) Graetz, B.R.; Rychnovsky, S.D. *Org. Lett.* **2003**, 5, 3357; (b) McCauley, J.A.; Nagasawa, K.; Lander, P.A.; Mischke, S.G.; Semones, M.A.; Kishi, Y. *J. Am. Chem. Soc.* **1998**, 120, 7647; (c) Evans, D.A.; Ripin, D.H.B.; Halstead, D.P.; Campos, K.R. *J. Am. Chem. Soc.* **1999**, 121, 6816.

nucleophilic addition to an aldehyde.²² Alkylation is also possible, and has been demonstrated in the nucleophilic displacement of alkyl iodides.²³ Pericyclic reactions forming C-C bonds have also been utilized in the formation of macrocycles with examples using both a Diels-Alder reaction and [3+2] dipolar cycloaddition.²² In an example of an intramolecular pericyclic reaction that forms a macrocycle, the two components at opposite ends of an acyclic substrate come together to react and form both the macrocycle and the ring resulting from the pericyclic reaction simultaneously, as illustrated in Scheme 1.6.

Scheme 1.6 Macrocycle Formation from a Diels-Alder Reaction^a



Further development of ring closure methods with metal mediated C-C bond forming reactions includes McMurray coupling,²⁴ nickel mediated bis-halide coupling,²⁵ and metal initiated free-radical macrocyclization.²⁶ The use of palladium mediated

²² For recent examples see: (a) Yang, W.; Digits, C.A.; Hatada, M.; Narula, S.; Rozamus, L.W.; Huestis, C.M.; Wong, J.; Dalgarno, D.; Holt, D.A. *Org. Lett.* **1999**, *1*, 2003; (b) Zajac, M.A.; Vedejs, E. *Org. Lett.* **2004**, *6*, 237.

²³ (a) Belanger, G.; Deslongchamps, P. *J. Org. Chem.* **2000**, *65*, 7070; (b) Dineen, T.A.; Rousch, W.R. *Org. Lett.* **2004**, *6*, 2043; (c) Smith, A.B.; Adams, C.M.; Kozmin, S.A.; Paone, D.V. *J. Am. Chem. Soc.* **2001**, *123*, 5925.

²⁴ For a review see: McMurray, J.E. *Acc. Chem. Res.* **1983**, *16*, 405.

²⁵ For examples see: (a) Corey, E.J.; Hamanaka, E. *J. Am. Chem. Soc.* **1964**, *86*, 1641; (b) Dauben, W.G.; Beasley, G.H.; Broadhurst, M.D.; Muller, B.; Peppard, D.J.; Pesnelle, P.; Sutter, C. *J. Am. Chem. Soc.* **1974**, *96*, 4724.

²⁶ (a) Paterson, I.; Lombart, H.-G.; Allerton, C. *Org. Lett.* **1999**, *1*, 19; (b) Quéron, E.; Lett, R. *Tetrahedron Lett.* **2004**, *45*, 4539; (c) Boger, D.L.; Mathvink, R.J. *J. Am. Chem. Soc.* **1990**, *112*, 4008.

allylic alkylation to affect ring closure has also been reported by Trost and coworkers.²⁷ Each of these methods provides macrocycles with moderate to good yields. Many additional methods for C-C bond forming ring closure have also been reported, and have been reviewed.⁶

The most common method of macrocycle formation by C=C bond forming reactions is the Horner-Wadsworth-Emmons reaction, which has been employed in the synthesis of a number of macrocyclic natural products.²⁸ Both the Horner-Wadsworth-Emmons and Wittig reactions couple a carbonyl compound such as an aldehyde with a carbon nucleophile to form a carbon-carbon double bond. Metathesis is also a very important C=C bond forming reaction with significant contributions to effective macrocyclization, and will be discussed separately (section 1.2.4).

1.2.3 Heteroatom Alkylation

The electrophilic alkylation of oxygen and nitrogen is most prevalent in template cyclization and host-guest chemistry, where the counter-ion of the reacting nucleophile may also act as a template. The use of a template in these reactions accelerates the rate of reaction, allowing reactions to be performed with higher substrate concentrations.²⁹ Ether forming reactions including Williamson ether synthesis, and alcohol-dithioketal coupling that do not incorporate a template have

²⁷ Trost, B.M.; Ohmori, M.; Boyd, S.A.; Okawara, H.; Brickner, S.J. *J. Am. Chem. Soc.* **1989**, *111*, 8281.

²⁸ For recent examples see: (a) Märkl, G.; Amrhein, J.; Stoiber, T.; Stiebl, U.; Kreitmeier, P. *Tetrahedron* **2002**, *58*, 2551; (b) Zheng, G.; Shibata, M.; Dougherty, T.J.; Pandey, R.K. *J. Org. Chem.* **2000**, *65*, 543.

²⁹ For further discussion on this and pertinent references see section 3.1.1

also been used in macrocyclic ring closure.³⁰ Alkylation of a nitrogen atom has also been used as a method of ring closure in macrocycle formation. Palladium mediated allylic alkylation of a primary amine and alkylation of a sulfonamide nitrogen atom have been reported as reactions for macrocycle formation.³¹

1.2.4 Ring Closing Metathesis

Ruthenium based organometallic catalysts have pioneered the use of metathesis as a means of macrocyclization.³² Ring closing metathesis (RCM) catalyzed by metal carbene species has been utilized in the formation of many medium and large rings. Application of metathesis to macrocycle formation was first reported in 1980,³³ and continues to be a featured method of ring closure in total synthesis of natural products.³⁴ Of the many catalysts available, the Grubbs ruthenium catalysts are preferred because of their stability in air, and their activity in solvents having a wide spectrum of polarity, including acidic water³⁵ and hydrocarbons (Figure 1.2). The most significant drawback of using this method of macrocycle formation is that in many cases high dilution must be used to suppress intermolecular metathesis reactions.²⁹

³⁰ For examples see: (a) Marshall, J.A.; Jenson, T.M.; DeHoff, B.S. *J. Org. Chem.* **1986**, *51*, 4316; (b) Nicolaou, K.C.; Duggan, M.E.; Hwang, C.-K. *J. Am. Chem. Soc.* **1986**, *108*, 2468; (c) Reid, R.C.; Kelso, M.J.; Scanion, M.J.; Fairlie, D.P. *J. Am. Chem. Soc.* **2002**, *124*, 5673.

³¹ For examples see: (a) Goekjian, P.G.; Wu, G.-Z.; Chen, S.; Zhou, L.; Jirousek, M.R.; Gillig, J.R.; Balla, L.M.; Dixon, J.T. *J. Org. Chem.* **1999**, *64*, 4238; (b) Rodríguez, G.; Lutz, M.; Spek, A.L.; van Koten, G. *Chem. Eur. J.* **2002**, *8*, 46.

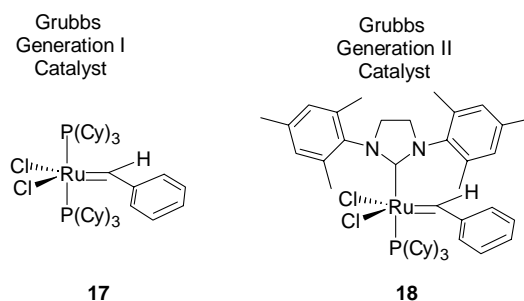
³² Trnka, T.M.; Grubbs, R.H. *Acc. Chem. Res.* **2001**, *34*, 18.

³³ Tsuji, J.; Hashiguchi, S. *Tetrahedron Lett.* **1980**, *21*, 2955.

³⁴ For recent examples see: (a) Gaul, C.; Njardarson, J.T.; Shan, D.; Wu, K.-D.; Tong, W.P.; Huang, X.-Y.; Moore, M.A.S.; Danishefsky, S.J. *J. Am. Chem. Soc.* **2004**, *126*, 11326; (b) Ojima, I.; Lin, S.; Inoue, T.; Miller, M.L.; Borella, C.P.; Geng, X.; Walsh, J.J. *J. Am. Chem. Soc.* **2000**, *122*, 5343.

³⁵ Mohr, B.; Lynn, D.M.; Grubbs, R.H. *J. Am. Chem. Soc.* **1998**, *120*, 1627.

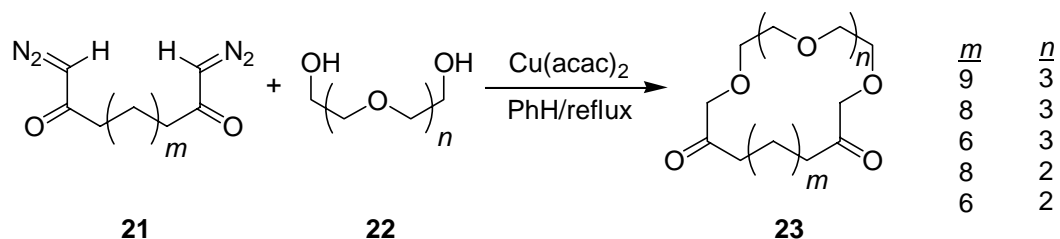
Figure 1.2 Grubbs Ruthenium Catalysts



1.2.5 Metal Carbene Insertion and Addition

Metal mediated carbene intermediates undergo chemical transformations beyond metathesis. In 1981, Kulkowit and McKervey demonstrated copper carbene intermediates derived from diazoketone **21** undergo O-H insertion to produce α -keto-ethers (Scheme 1.7) with an array of ring sizes.³⁶

Scheme 1.7 O-H Insertion to Produce Macrocycles



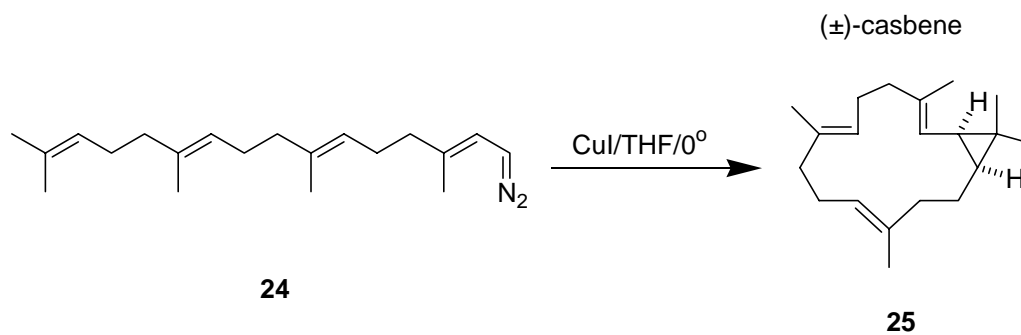
The earliest report of macrocycle formation via cyclopropanation was the synthesis of casbene by Takahashi and co-workers as reported in 1982.³⁷ The final step of the synthesis was the CuI catalyzed cyclopropanation of **24** to form (\pm)-casbene (**25**) in 14% overall yield from geranylgeraniol (Scheme 1.8). This initial report of macrocycle formation by a carbene addition reaction was not further pursued, and the

³⁶ Kulkowit, S.; McKervey, M.A. *J. Chem. Soc., Chem. Commun.* **1981**, 616.

³⁷ Toma, K.; Miyazaki, E.; Murae, T.; Takahashi, T. *Chem. Lett.* **1982**, 863.

application of carbene addition reactions to macrocycle formation lay dormant until the report by Doyle, Poulter, and co-workers of dirhodium(II) catalyzed formation of new macrocyclic compounds.

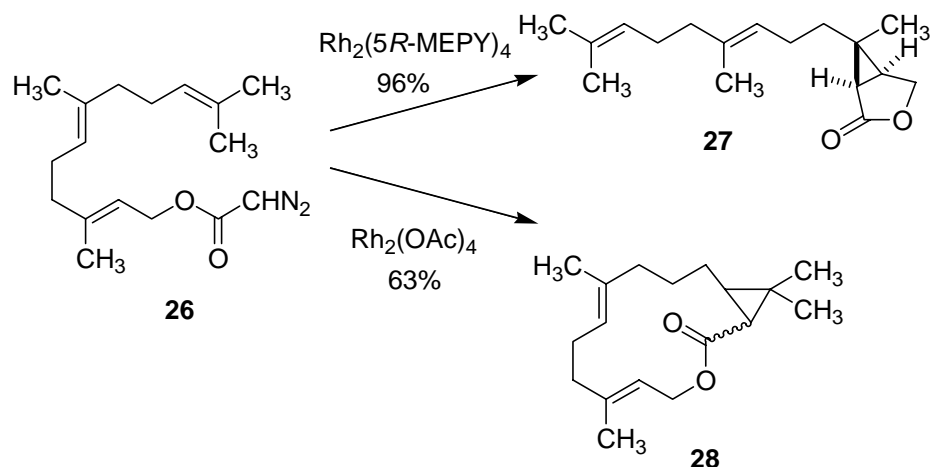
Scheme 1.8 Synthesis of (±) – casbene



A 1995 report by Doyle, Poulter, and co-workers showed decomposition of *trans*, *trans*-farnasyl diazoacetate **26** by $\text{Rh}_2(5R\text{-MEPY})_4$ produced γ -butyrolactone **27** exclusively in greater than 94% enantiomeric excess.³⁸ However, the use of dirhodium(II) tetraacetate catalyzed decomposition of diazoacetate **26** resulted in the formation of the thirteen membered ring **28** via allylic cyclopropanation with complete regioselectivity (Scheme 1.9). The unexpected regioselectivity seen for the dirhodium(II) tetraacetate catalyzed decomposition of **26** prompted further investigation of regioselectivity in the decomposition of diazoacetate compounds having multiple carbon-carbon double bonds.

³⁸ Doyle, M.P.; Protopopova, M.N.; Poulter, C.D.; Rogers, D.H. *J. Am. Chem. Soc.* **1995**, *117*, 7281.

Scheme 1.9 Macrocycles from Dirhodium(II) Catalysts

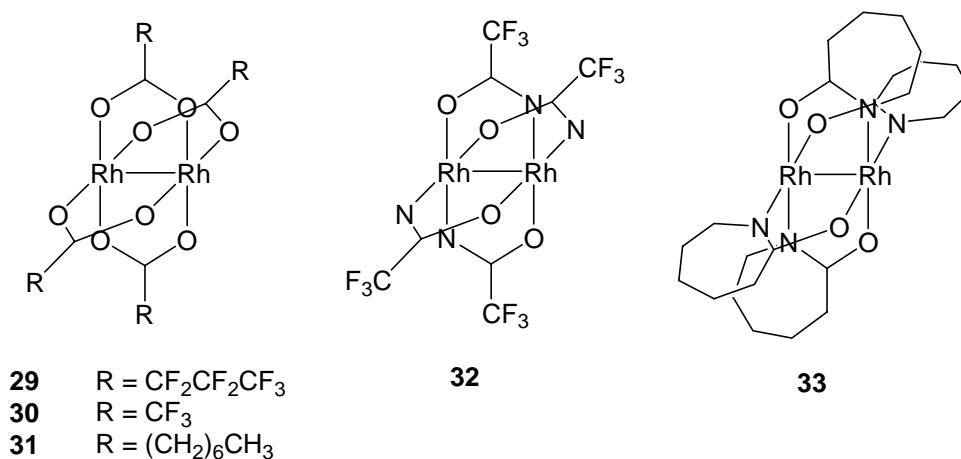


The influence of dirhodium(II) catalyst ligands on product distribution,³⁹ previously established to effectively control chemoselectivity, regioselectivity, and stereoselectivity in intermolecular cyclopropanation,⁴⁰ was applied to the selection of catalysts employed in the decomposition of **26**. Decomposition of diazoacetate **26** with dirhodium(II) perfluorobutyrate (**29**), dirhodium(II) trifluoroacetate (**30**), dirhodium(II) trifluoroacetamidate (**32**), and dirhodium(II) octanoate (**31**) (Figure 1.3), like dirhodium(II) tetraacetate, all produced **28** exclusively. Decomposition of **26** by dirhodium(II) caprolactamate (**33**) afforded **27** as the exclusive regioisomer.

³⁹ Padwa, A.; Austin, D.J. *Angew. Chem., Int. Ed. Engl.* **1994**, 33, 1797.

⁴⁰ Doyle, M.P.; Bagheri, V.; Wandless, T.J.; Harn, N.K.; Brinker, D.A.; Eagle, C.T.; Loh, K.-L. *J. Am. Chem. Soc.* **1990**, 112, 1906.

Figure 1.3 Catalysts Used in Diazo Decomposition of 26



1.3 Catalysts for Diazo Decomposition

The development of metal catalysts for diazo decomposition has evolved considerably since copper bronze and copper sulfate were first used with diazo compounds.⁴¹ The introduction of dirhodium(II) tetraacetate as a catalyst for diazo decomposition by Teyssie in 1973 was the first reported use of a dirhodium(II) species in catalytic diazo decomposition.⁴² Since the initial report by Teyssie, dirhodium(II) catalysts have been utilized in a wide variety of diazo decomposition reactions, and are considered to be effective and versatile catalysts for diazo decomposition.⁴³ Dirhodium(II) tetraacetate has D_{4h} symmetry and possesses a metal-metal single bond, one vacant coordination site per metal atom, and is readily prepared from rhodium(III) chloride and acetic acid.⁴⁴ Ligand exchange of the acetate with other carboxylic acids has produced dirhodium(II) species with unique

⁴¹ Doyle, M.P.; McKervey, M.A.; Ye, T. Modern Catalytic Methods for Organic Synthesis with Diazo Compounds: from Cyclopropanes to Ylides, Wiley-Interscience: New York, 1998.

⁴² Pauissenen, R.; Reimlinger, H.; Hayez, E.; Hubert, A.J.; Teyssie, P. *Tetrahedron Lett.* **1973**, 2233.

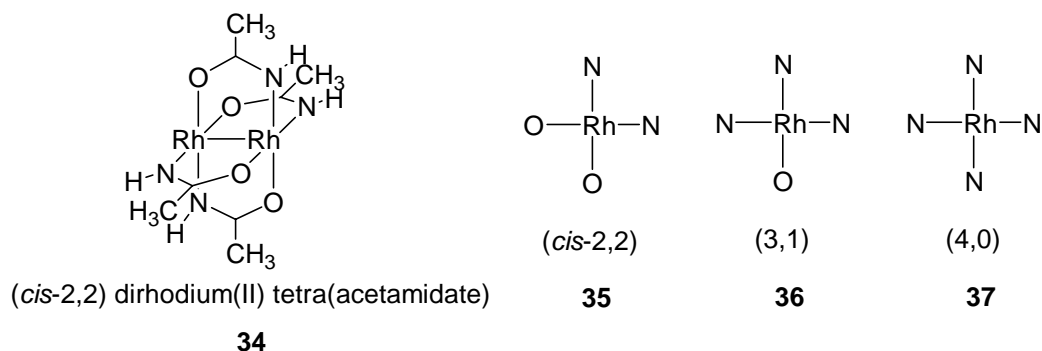
⁴³ (a) Davies, H.M.L. *Tetrahedron*, **1993**, 49, 5203; (b) Padwa, A.; Krumpe, K.E. *Tetrahedron*, **1992**, 48, 5385; (c) Mass, G. *Top. Curr. Chem.* **1987**, 137, 76; (d) Doyle, M.P. *Chem. Rev.* **1986**, 86, 919.

⁴⁴ Rempel, G.A.; Legzdins, P.; Smith, H.; Wilkinson, G. *Inorg. Syn.* **1972**, 13, 90.

physical structures and properties according to the characteristics of the ligands.⁴¹ Ligand substitution has also been achieved to produce dirhodium(II) phosphates, orthometallated phosphines, and carboxamides.⁴¹

The first preparation of a dirhodium(II) carboxamidate was dirhodium(II) acetamidate (**34**) reported by Bear, who, in cooperation with Bernal, described the structure of these compounds as having a (*cis*-2,2) geometry (**35**) with two nitrogens and two oxygens bound to each rhodium atom (Figure 1.4).⁴⁵ In addition to the (*cis*-2,2) geometry (**35**), the (3,1) structure (**36**) of dirhodium(II) *N*-phenylacetamide has been confirmed,⁴⁶ and more recently the (4,0) structure (**37**)⁴⁷ of a dirhodium(II) *N*-acylimidazolidin-2-one has also been reported.

Figure 1.4 Structural Configurations of Dirhodium(II) Carboxamides



The utility of dirhodium(II) carboxamides as catalysts for diazo decomposition was made possible by the development of a convenient procedure for their synthesis. Bear and coworkers previously described carboxamidate preparation in a melt at 140°C, but incomplete conversion to dirhodium(II) tetra(acetamidate) occurred, and

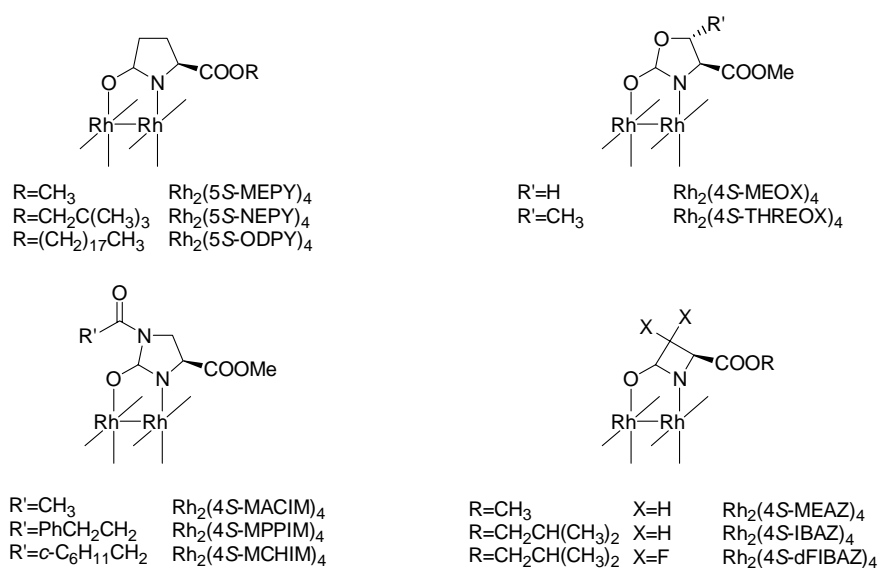
⁴⁵ Ahsan, M.Q.; Bernal, I.; Bear, J.L. *Inorg. Chem.* **1986**, 25, 260.

⁴⁶ Lifsey, R.S.; Lin, X.Q.; Chavan, M.Y.; Ahsan, M.Q.; Kadish, K.M.; Bear, J.L. *Inorg. Chem.* **1987**, 26, 830.

⁴⁷ Doyle, M.P.; Raab, C.E.; Roos, G.H.P.; Lynch, V.; Simonsen, S.H. *Inorg. Chim. Acta* **1997**, 266, 13.

isolation of the desired product was laborious.⁴⁵ However, ligand exchange on dirhodium(II) tetraacetate by a carboxamidate compound is accomplished in refluxing chlorobenzene with a Soxhlet extractor containing sodium carbonate to trap the displaced acetic acid, as described by Doyle.⁴⁰ Using this procedure, Doyle and coworkers have developed an extensive array of chiral carboxamidates for asymmetric catalysis, and a representative listing is found in Figure 1.5.⁴¹

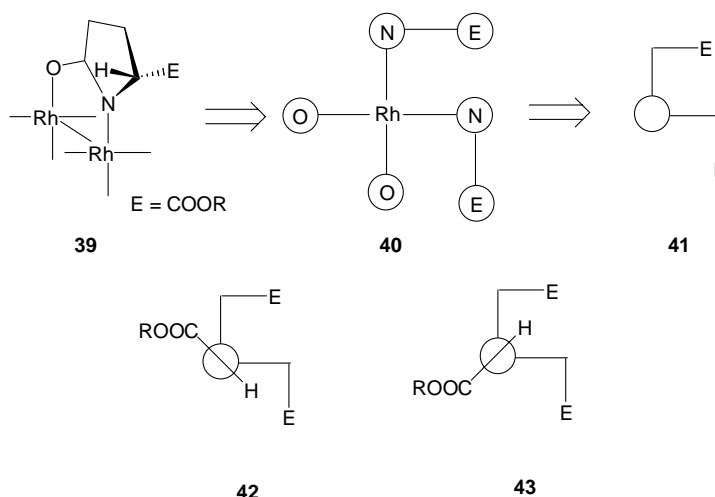
Figure 1.5 Select Dirhodium(II) Carboxamidate Catalysts



The chiral carboxamidate ligands that have been effectively employed in ligand exchange onto dirhodium(II) are enantiomerically pure α -substituted carboxamidates based on 2-oxapyrrolidine, 2-oxazolidinone, *N*-acylimidazolidin-2-one, and 2-azetidinone. The most effective dirhodium(II) carboxamidate catalysts for enantiocontrol are those with a chiral carboxylate ester at the α position of the carboxamidate, and for many of those listed in Figure 1.5 both enantiomers have been prepared. X-ray crystal structures of the bis-acetonitrile complex or the bis-benzonitrile complex of many of these dirhodium(II) carboxamidates have been

obtained and reveal that all of them possess the (*cis*-2,2) geometry.⁴⁸ The characteristic geometry of these structures is the projection of the chiral ester from the nearly perpendicular plane of the ligand (**39**), which is the source of the enantiocontrol that these catalysts exhibit (Scheme 1.10). From CACHE calculations⁴⁹ a carbene bound to rhodium has two minimum energy conformations (**42** and **43**), each restricting substrate approach to one side of the carbene center and controlling enantioselectivity.

Scheme 1.10 Chiral Ester Projection and Carbene Intermediate Conformations



1.4 Macrocycle Formation from Metal Carbene Addition Reactions

Reactions that cause ring closure with regioselectivity and enantiocontrol provide access to macrolactones (macrolides)⁵⁰ with substrate chirality. Addition reactions of metal carbene intermediates are known to proceed with chemoselectivity, regioselectivity, and enantioselectivity.⁴¹ The selectivity of metal carbene

⁴⁸ A list of dirhodium(II) carboxamidates with crystal structures and reference to the initial publication of them can be found in ref. 41.

⁴⁹ Doyle, M.P.; Winchester, W.R.; Hoorn, J.A.A.; Lynch, V.; Simonsen, S.H.; Ghosh, R. *J. Am. Chem. Soc.* **1993**, *115*, 9968.

⁵⁰ Woodward, R.B. *Angew. Chem.*, **1957**, *69*, 50.

intermediates in addition reactions has been applied to macrocycle formation, which has been shown to proceed with both regioselectivity and enantioselectivity.⁵¹

Macrocyclization is controlled by entropic factors, and attempts to direct reactions toward intramolecular ring closure over intermolecular oligomerization have led to the use of the “dilution principle”,⁵² requiring low substrate concentration and large amounts of solvent.⁵³ Chiral dirhodium(II) and copper(I) catalysts are known to promote enantioselective and diastereoselective intramolecular carbene addition reactions with a high degree of regioselectivity using slow addition techniques, avoiding high dilution of the substrate.⁵⁴ The contributions of dirhodium(II) catalysts to macrocycle formation including the limitations of the method and comparative studies using copper(I) catalysts are reviewed.⁵¹

1.4.1 Functional Groups and Selectivity in Carbene Addition Macrocyclization

In the discussion of macrocyclization from carbene addition reactions, it is important to consider the influence of the functional groups in the diazoacetate compounds on both chemoselectivity and regioselectivity. Studies to date have examined a variety of functional groups that undergo carbene addition including substituted olefins,^{54,55} alkynes,⁵⁶ arenes,⁵⁷ and furans.⁵⁸ In each of these studies copper(I) hexafluorophosphate, dirhodium(II) carboxylates, and dirhodium(II) carboxamides

⁵¹ For a review see : Doyle, M.P.; Hu, W. *Synlett* **2001**, 1364.

⁵² Ruggli, P. *Ann.* **1912**, 392, 92.

⁵³ For discussion on the dilution principle see section 3.1.1

⁵⁴ Doyle, M.P.; Hu, W.; Chapman, B.; Marnett, A.B.; Peterson, C.S.; Vitale, J.P.; Stanley, S.A. *J. Am. Chem. Soc.* **2000**, 122, 5718.

⁵⁵ Doyle, M.P.; Peterson, C.S.; Parker, D.L. *Angew. Chem. Int. Ed. Eng.* **1993**, 35, 1334.

⁵⁶ Doyle, M.P.; Ene, D.G.; Peterson, C.S.; Lynch, V. *Angew. Chem. Int. Ed.* **1996**, 38, 700.

⁵⁷ Doyle, M.P.; Protopopova, M.N.; Peterson, C.S.; Vitale, J.P. *J. Am. Chem. Soc.* **1996**, 118, 7865.

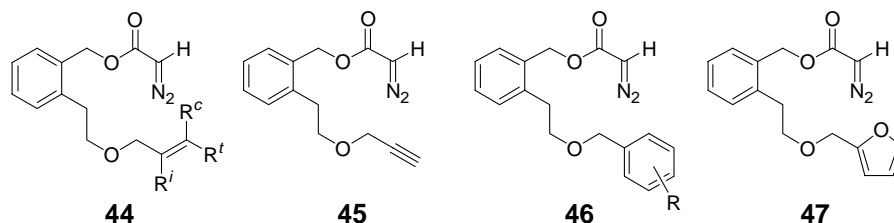
⁵⁸ Doyle, M.P.; Chapman, B.J.; Hu, W.; Peterson, C.S.; McKervey, M.A.; Garcia, C.F. *Org. Lett.* **1999**, 1, 1327.

have been used as catalysts to compare the reaction selectivity of different catalytic species.

1.4.1.1 Functional Groups Used in Macrocyclization

The use of asymmetric catalysts to cyclize prochiral substrates and create chiral macrocycles in carbene addition reactions provides a valuable method for the synthesis of new chiral materials. Studies that use olefins (**44**),^{54,55} alkynes (**45**),⁵⁶ arenes (**46**),⁵⁷ and furans (**47**)⁵⁸ as the reactive functional group linked through 1,2-benzenedimethanol to a diazoacetate have been reported (Figure 1.6). Diazo decomposition of these compounds has provided a great deal of information on the enantioselectivity, chemoselectivity, and regioselectivity of macrocycle forming carbene addition reactions.

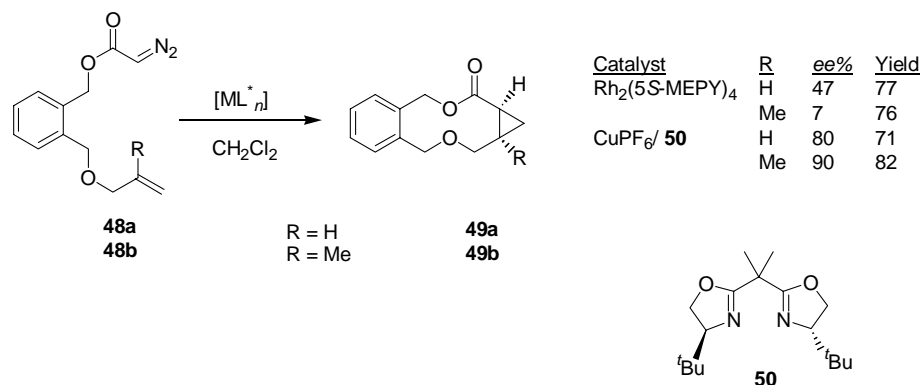
Figure 1.6 1,2-Benzenedimethanol Linked Diazoacetate Substrates



The first report of asymmetric macrocycle formation from carbene addition was the diazo decomposition of substrates **48a** and **48b**. Each substrate has a diazoacetate coupled through 1,2-benzenedimethanol to an allyl and methallyl functional group respectively (Scheme 1.11).⁵⁵ Diazo decomposition of **48a** and **48b** by Rh₂(5*S*-MEPY)₄ or the Cu(CH₃CN)₄PF₆/**50** complex results in formation of *cis* isomers **49a**

and **49b** respectively, which contrasts the intermolecular reactions of diazo esters, in which the predominate product is generally the *trans* diastereoisomers.⁵⁹

Scheme 1.11 1,2-Benzenedimethanol Linked Cyclopropanation



1.4.1.2 Effects of Olefin Substitution on Ring Formation

In a study examining the impact of olefin substitution on enantioselectivity, the allyl derivatives possessing *cis* (**52**), *trans* (**51**), and trisubstituted olefins (**53**) were decomposed with dirhodium(II) carboxamidate and copper(I) catalysts (Scheme 1.12).⁵⁴ Diazo decomposition by rhodium(II) carboxamidate catalysts resulted in cyclopropane products **56** and **57**, but formation of products from hydride abstraction⁶⁰ at the benzylic position was competitive, forming products **58** and **59** (Table 1.1). The formation of **58** and **59** was believed to occur as a result of the stereoelectronic factors involved in the cyclopropane forming process. It should be noted that in the diazo decomposition of both **48a** and **48b**, the Cu(CH₃CN)₄PF₆/**50** complex afforded the higher enantioselectivity.

⁵⁹ (a) Pfaltz, A. *Acc. Chem. Res.* **1993**, 26, 339; (b) Müller, P.; Baud, C.; Ene, D.; Motallebi, S.; Doyle, M.P.; Brandes, B.D.; Dyatkin, A.B.; See, M.M. *Helv. Chim. Acta* **1995**, 78, 459; (c) Nishiyama, H. Itoh, Y.; Sugawara, Y.; Matsumoto, Aoki, K.; Itoh, K. *Bull. Chem. Soc. Jpn.* **1995**, 68, 1247.

⁶⁰ Hydride abstraction from the benzylic position is a process known to occur with dirhodium carboxamidate catalysts and was first reported in : Doyle, M.P.; Dyatkin, A.B.; Autry, C.L.J. *J. Chem. Soc., Perkin Trans. 1* **1995**, 619.

Scheme 1.12 Olefin Substitution and Diazo Decomposition Products

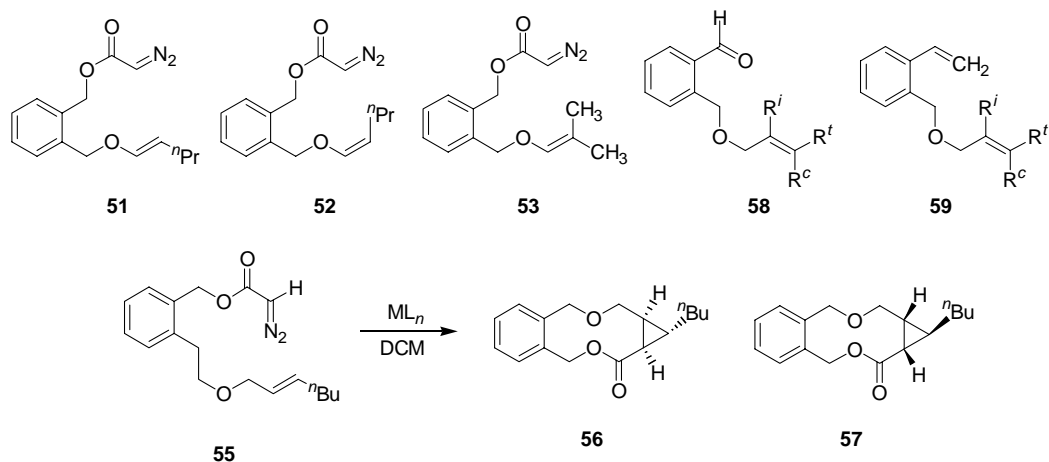
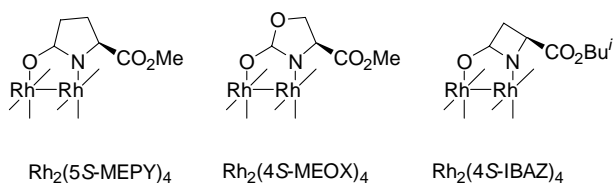


Table 1.1 Product Selectivity from Diazo Decomposition of 51

Catalyst	Isolated Yield(%) 56 + 57	Relative Yield(%) 56 + 57 (56:57)	Relative Yield(%) 58 + 59 (58:59)
Rh ₂ (5 <i>S</i> -MEPY) ₄	78	23 (>99:1)	77 (87:13)
Rh ₂ (4 <i>S</i> -MEOX) ₄	70	39 (94:6)	61 (70:30)
Rh ₂ (4 <i>S</i> -IBAZ) ₄	77	57 (>99:1)	43 (58:42)

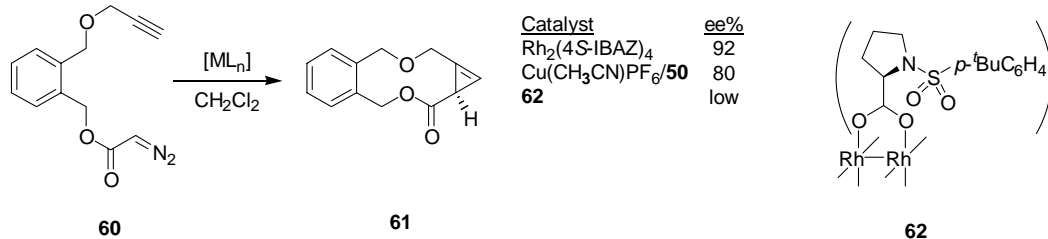


1.4.1.3 Intramolecular Cyclopropanation in Macrocycles

Asymmetric carbene addition to **43** with an alkyne functional group yields cyclopropene **44** in high enantiomeric excess (62 to 92%) and good yields (Scheme 1.13).⁵⁶ The chiral environment around the metal center yields much higher enantioselectivity in cyclopropanation than in the analogous cyclopropanation of **48a**. In the formation of **61**, Rh₂(4*S*-IBAZ)₄ is superior to all other catalysts. Product

yields using dirhodium(II) carboxamidates average 80%, making this a very effective method of enantioselective macrocycle formation.

Scheme 1.13 Asymmetric Cyclopropanation Using Various Catalysts

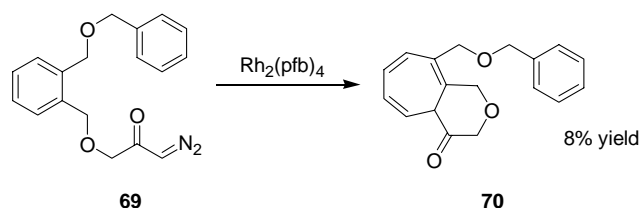


1.4.1.6 Conclusions on Carbene Addition to Select Functional Groups

The formation of ten membered rings from diazoacetates tethered through 1,2-benzenedimethanol to allyl, methallyl, and propargyl functional groups have shown the relative ability of dirhodium(II) carboxamidates, dirhodium(II) carboxylates, and copper(I) hexafluorophosphate to form macrocycles through carbene addition to π bonds. The 1,2-benzenedimethanol linker provides an important function in the diazo decomposition of diazoacetates **48a**, **48b**, and **60**, exhibiting very low susceptibility to carbene addition or aryl C-H insertion at the benzylic positions. The only reported case of carbene addition into the aryl ring of 1,2-benzenedimethanol is using the highly reactive $\text{Rh}_2(\text{pfb})_4$ catalyst in combination with diazo acetate **69** (Scheme 1.14).⁵⁷ Because of the very low susceptibility to carbene addition or aryl C-H insertion of 1,2-benzenedimethanol, substrates can be constructed using a linker (between the diazoacetate and the reactive functional group) that has low susceptibility to carbene addition, therefore favoring macrocycle formation. The only competitive reaction process reported to occur with diazoacetates of 1,2-

benzenedimethanol is that of hydride abstraction,⁵⁴ and is only observed in diazoacetates with 1,2-disubstituted or trisubstituted olefins.

Scheme 1.14 Addition of a Carbene to 1,2-Benzenedimethanol

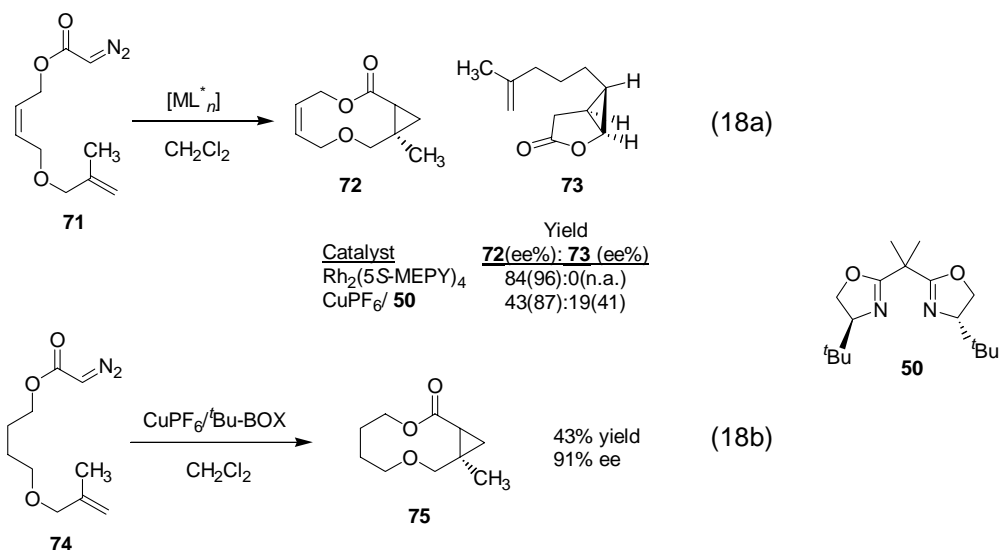


1.4.2.1 Conformation in Ring Formation

The linker 1,2-benzenedimethanol has an aryl ring between the diazoacetate and reacting functional group, limiting the number of conformations that the metal carbene intermediate may adopt for ring formation. In addition, the 1,2-benzenedimethanol linker has very low reactivity toward metal carbene intermediates compared to other functional groups. To ascertain if the aromatic linker promotes macrocyclization due to conformational restriction from the aryl group two additional diazoacetates were synthesized.⁵⁵ Compound **71** was synthesized using *Z*-2-butene-1,4-diol in place of 1,2-benzenedimethanol to investigate catalyst regioselectivity while retaining the geometry found with a 1,2-benzenedimethanol linker (Scheme 1.15). Diazo decomposition of **71** demonstrated dirhodium(II) carboxamidates prefer γ -lactone formation (**73**) and copper catalysts prefer macrocycle formation (**72**). The second diazoacetate synthesized to investigate the influence of substrate conformation on macrocycle formation possessed an aliphatic linker (**74**) in place of 1,2-benzenedimethanol (Scheme 1.18).^{40a} Removal of the conformational restrictions of the *cis*-olefin did not impact reaction selectivity, demonstrating that the fixed

conformation of **48**, **60**, or **71** is not an *a priori* requirement for the formation of macrocycles via cyclopropanation, and metal carbene intermediates selectively undergo addition to olefins.

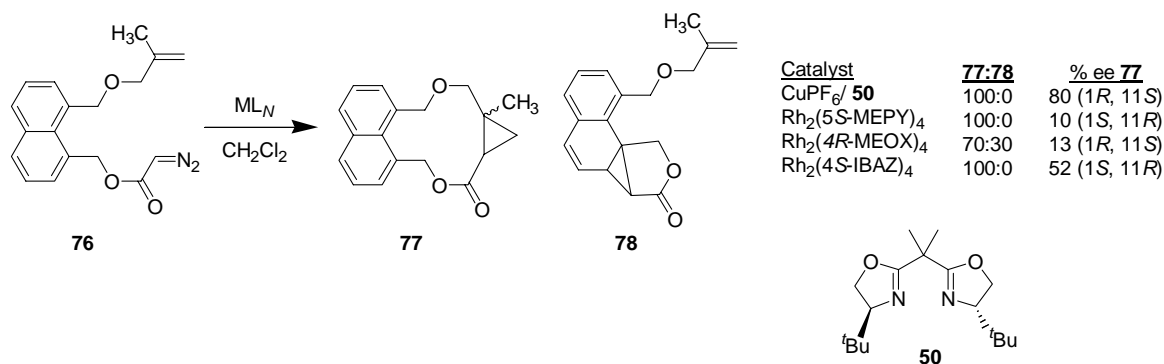
Scheme 1.15 Competitive and Conformational Investigations



1.4.2.2 Reaction Selectivity Using 1,8-Naphthalenedimethanol as a Linker

A second investigation of the impact of the 1,2-benzenedimethanol linker on selectivity considered the enantiocontrol of the reaction by modification of the linker to 1,8-naphthalenedimethanol, which retains the aromatic nature of the linker.⁵⁴ In contrast to studies using 1,2-benzenedimethanol, aromatic cycloaddition occurred in competition with cyclopropanation using $\text{Rh}_2(4R\text{-MEOX})_4$ (Scheme 1.16). Enantioselectivity seen in the decomposition of **76** did not vary significantly from that observed using the analogous substrate with the 1,2-benzenedimethanol linker (**48b**).

Scheme 1.16 Diazo Decomposition Using 1,8-Naphthalenedimethanol as a Linker

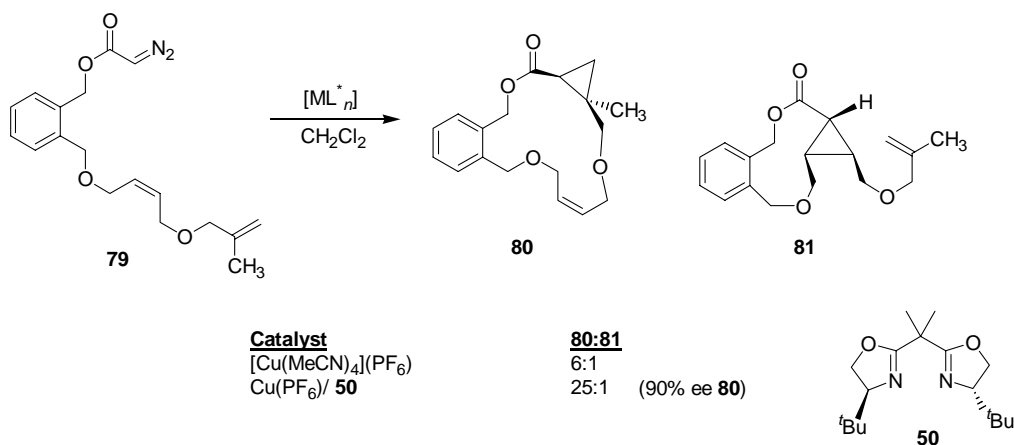


1.4.3 Competitive Reactions in Macrocycle Formation

Regioselectivity and chemoselectivity are important considerations in macrocycle formation. The ability of a metal mediated carbene reaction to differentiate between two reaction pathways such as two different olefins in the same compound (regioselectivity), or an olefin and an alkyne (chemoselectivity) allows substrates with multiple functional groups to be used in macrocycle formation from metal carbene intermediates.

Regioselectivity in macrocycle formation was investigated using diazoacetate **79**, which had two olefins, each removed from the diazoacetate by a different number of atoms (Scheme 1.17).⁵⁴ The enhanced regioselectivity seen by addition of bis-oxazoline ligand **50** demonstrates the contribution of ligands to copper catalysts in macrocycle formation.

Scheme 1.17 Regioselectivity with a 1,2-Benzenedimethanol Linker

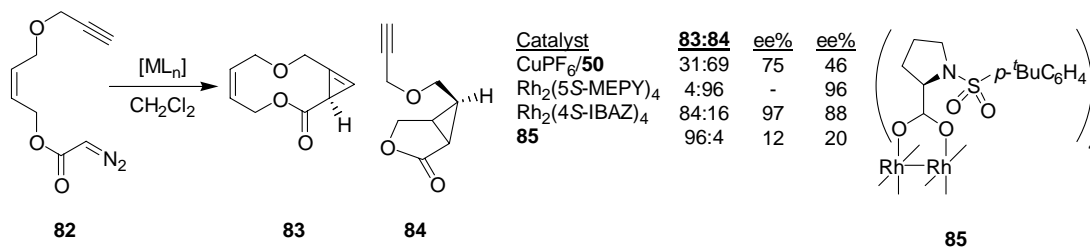


1.4.3.1 Competitive Cyclopropanation

To ascertain the differences in chemoselectivity towards alkenes and alkynes, substrate **82** was synthesized (Scheme 1.18).⁵⁶ Because studies prior to this had reported that dirhodium(II) carboxamidate catalyzed reactions yield allylic cyclopropanation in preference to addition to remote double bonds,⁶¹ while CuPF_6 /**50** favors addition to the terminal site (see Scheme 1.15), the same outcome was expected in diazo decomposition of **82**.⁵⁶ Whereas $\text{Rh}_2(5S\text{-MEPY})_4$ exhibited the chemoselectivity expected, almost complete reversal of regioselectivity was seen in the $\text{Rh}_2(4S\text{-IBAZ})_4$ catalyzed reaction and CuPF_6 /**50** prefers allylic cyclopropanation to terminal cyclopropanation.

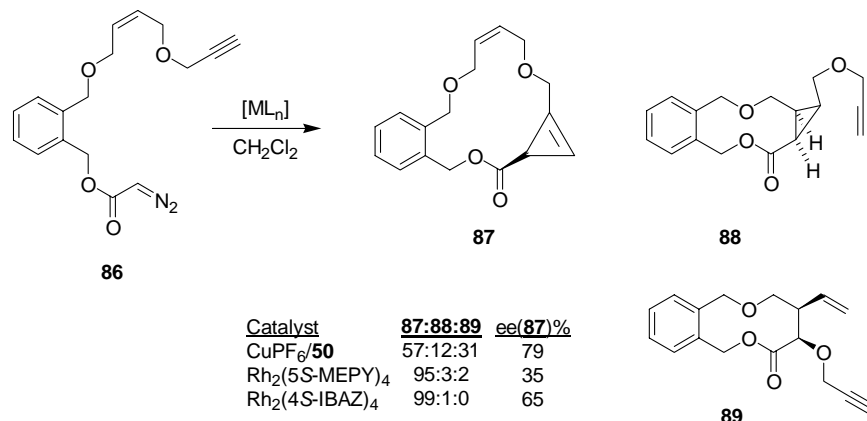
⁶¹ Doyle, M.P.; Austin, R.E.; Bailey, A.S.; Dwyer, M.P.; Dyatkin, A.B.; Kalinin, A.V.; Kwan, M.M.Y.; Liras, S.; Oalman, C.J.; Pieters, R.J.; Protopopova, M.N.; Raab, C.E.; Roos, G.H.P.; Zhou, Q.-L.; Martin, S.F. *J. Am. Chem. Soc.* **1995**, *117*, 5763.

Scheme 1.18 Competitive Allylic Cyclopropanation versus Cyclopropanation



A second competitive study using the 1,2-benzenedimethanol linker was also reported (Scheme 1.19).⁵⁶ In this case each dirhodium(II) carboxamidate exhibited exceptional chemoselectivity for cyclopropanation, and Rh₂(4*S*-IBAZ)₄ was clearly superior in selectivity for addition to the C≡C of those employed. The copper(I)/**50** catalyst demonstrates the lowest chemoselectivity, but the highest cyclopropanation enantioselectivity of all the catalysts used in this reaction. This reaction also illustrated that copper(I) catalysts can form oxonium ylides followed by [2,3]-sigmatropic rearrangement (**89**) to effectively produce macrocycles. The study showed conclusively that the terminal alkyne of **86** is the preferred site of carbene addition over the internal alkene regardless of the catalyst used.

Scheme 1.19 Cyclopropanation versus Cyclopropanation in Macrocyclic Formation

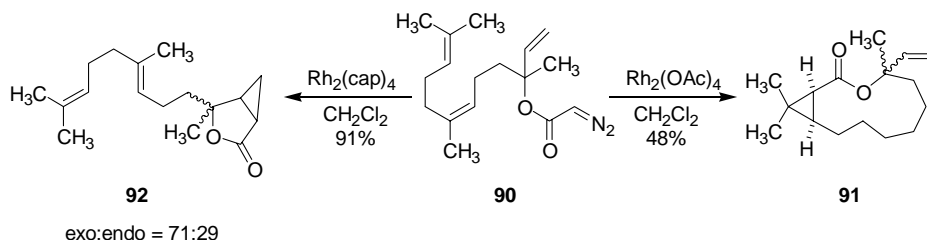


Competitive carbene addition was also carried out using **90**, which presents a terminal olefin and two tri-substituted olefins (Scheme 1.20).⁶² Regioselective cyclopropanation is observed and, as anticipated from previous results,³⁸ Rh₂(cap)₄ catalyzes the formation of allylic cyclopropanation product **92**, whereas dirhodium(II) tetraacetate produces macrolide **91** from carbene addition to the tri-substituted olefin further removed from the carbene center. Compound **91** is observed as the *cis* isomer exclusively, but diastereocontrol at the methyl/vinyl substituted carbon was random (50:50). Limited diastereocontrol was also achieved in the formation of **92**, which is consistent with prior studies.⁶³

⁶² Doyle, M.P.; Peterson, C.S.; Protopopova, M.N.; Marnett, A.B.; Parker, D.L., Jr.; Ene, D.G.; Lynch, V. *J. Am. Chem. Soc.* **1997**, *119*, 8826.

⁶³ Martin, S.F.; Spaller, M.R.; Liras, S.; Hartmann, B. *J. Am. Chem. Soc.* **1994**, *116*, 4493.

Scheme 1.20 Selective Cyclopropanation of Geraniol Diazoacetate



1.4.4 Formation of Rings Larger Than 10-Membered

Further development of macrocyclization through carbene addition reactions has focused on the formation of rings beyond 10 atoms. Reaction control changes as ring size grows larger, until the limit is reached at intermolecular reactions, which have no linker between the diazoacetate and the reacting functional group. Diazoacetates that can form rings larger than ten membered in size produce products that differ in enantioselectivities, regioselectivities, and chemoselectivities.⁶⁴ In addition, carbene addition to olefins more than ten atoms removed has been shown to form both *cis* and *trans* cyclopropanes.^{54,62}

1.4.4.1 Substrate Considerations

Macrocyclization resulting from carbene addition reactions is dependent on both the metal carbene intermediate and on the functional group undergoing carbene addition. The longer the linker between the metal carbene intermediate and the reacting functional group, the greater the number of degrees of freedom, and the lower the probability of the metal carbene intermediate meeting the reactive functional group to

⁶⁴ Doyle, M.P.; Hu, W. *J. Org. Chem.* **2000**, 65, 8839.

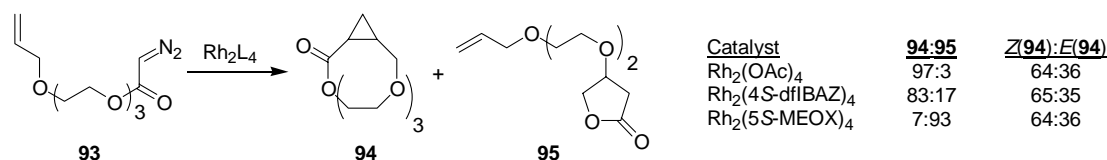
react. Competitive studies with select functional groups linked to 1,2-benzenedimethanol (see section 1.4.3) demonstrate that both steric and electronic factors contribute to reaction selectivity. As linkers become longer, reaction selectivity changes, due to the change in internal entropy. A series of reports using both ethylene glycol linkers and 1,2-benzenedimethanol linkers have described macrocycle formation using metal mediated carbene addition reactions with selected functional groups.^{54-56,65} The reports show that chemoselectivity can change drastically with the length of the linker used in these macrocyclization reactions.

Using ethylene glycol based linkers, Doyle and Hu demonstrated that dirhodium carboxamidates were less likely to undergo cyclopropanation with a remote olefin than dirhodium tetraacetate, and would undergo γ -butyrolactone formation in a competitive reaction pathway, as illustrated in Scheme 1.21.⁶⁴ In addition, the general structure of the carboxamidate ligand was also shown to be critical to the reaction selectivity. $\text{Rh}_2(4R\text{-dFIBAZ})_4$, having enhanced electron withdrawing capacity due to the fluorine substitution on the ligand, and an elongated rhodium-rhodium bond due to the azetidinone bite angle,⁶⁶ undergoes macrocyclic cyclopropanation much more readily than $\text{Rh}_2(4S\text{-MEOX})_4$ in the diazo decomposition of **93**. The dramatic effect ligands have on the chemoselectivity of metal carbene intermediates does not change the diastereoselectivity seen in **94**. Selectivity between *E* and *Z* isomers is nearly identical for all dirhodium(II) catalysts.

⁶⁵ Doyle, M.P.; Hu, W. *Tetrahedron Lett.* **2000**, *41*, 6265.

⁶⁶ (a) Doyle, M.P.; Hu, W.; Phillips, I.M.; Moody, C.J.; Pepper, A.G.; Slawin, A.M.Z. *Adv. Synth. Catal.* **2001**, *343*, 112; (b) Doyle, M.P.; Zhou, Q.-L.; Simonsen, S.H.; Lynch, V. *Synlett*, **1996**, 697.

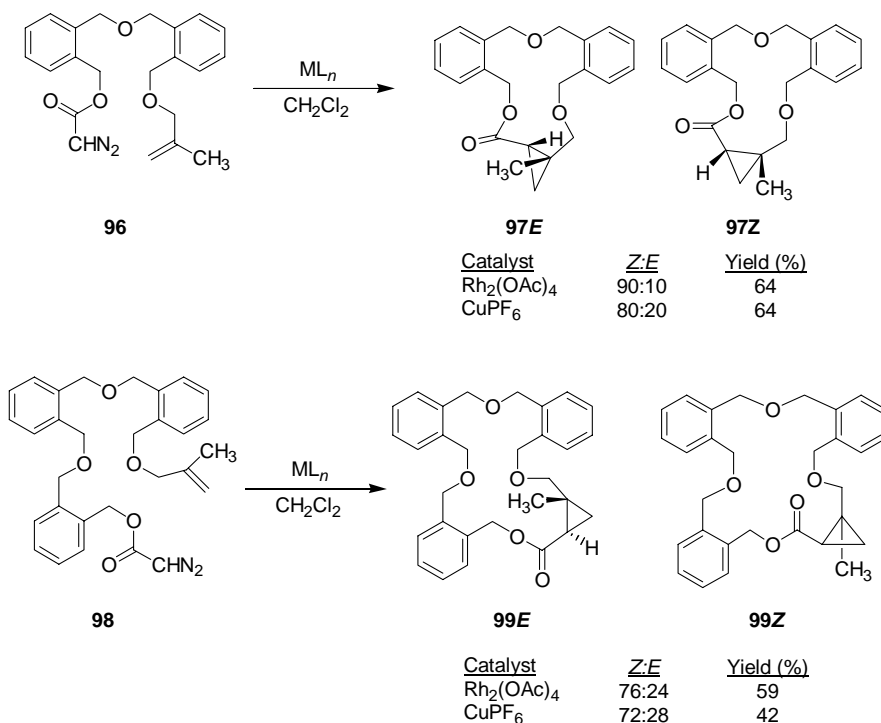
Scheme 1.21 Carboxamidate versus Carboxylate Catalysts



1.4.4.2 Macrocycle Ring Size Limits

Successful use of 1,2-benzenedimethanol as an unreactive linker in macrocycle formation prompted their incorporation into substrates that could form larger macrocycles (Scheme 1.22).⁵⁴⁻⁵⁷ Diazo decomposition to yield the largest ring structures formed via cyclopropanation reported to date was based on these substrates.⁵⁴ Only five possible intramolecular products can be formed from these substrates: cyclopropanation, aromatic addition, ylide formation and rearrangement, hydride abstraction, and benzylic C-H insertion. Of these five, only cyclopropanation is observed, demonstrating that diazo decomposition of these substrates is a highly chemoselective process due to the relative susceptibility of the various sites to carbene addition. Also of note, as ring size increases, *E* to *Z* ratios approach those consistent with intermolecular reactions, showing that cyclopropanation forming large rings begins to achieve the selectivities of the intermolecular reaction dictated by the olefin conformations that may approach the metal carbene intermediate to undergo carbene addition.

Scheme 1.22 Large Ring Cyclopropanation

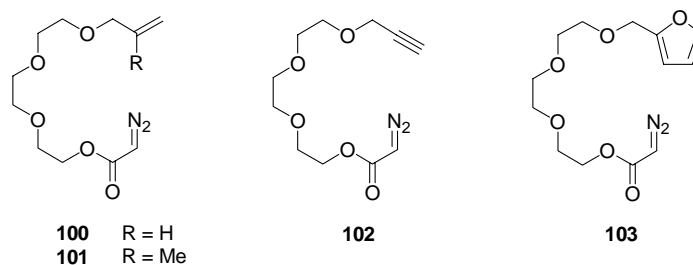


1.4.4.3 Functional Group Variants

Work has also been conducted using an allyl (**100**), methallyl (**101**), propargyl (**102**), or furfuryl group (**103**) linked by tri(ethylene glycol) to a diazoacetate (Figure 1.7).⁶⁵

The aim of this investigation was to evaluate the effect of select functional groups on the selectivity seen in diazo decomposition.

Figure 1.7 Macrocyclization with Select Functional Groups



1.4.4.4 Olefin Substitution

Diazo decomposition of **100** and **101** yielded three separate materials that could be identified; cyclopropanes (**104**, **105**), γ -butyrolactones (**106**, **107**), and 12-membered rings resulting from oxonium ylide formation followed by [2,3]-sigmatropic rearrangement (**108**, **109**) (Scheme 1.23).⁶⁵ Comparison of allyl versus methallyl shows that electron donation by alkyl substituents is more favorable for cyclopropanation in large rings (Table 1.2).⁶⁵ Chemoselectivity for cyclopropanation is diminished going from dirhodium(II) tetraacetate and copper(I) catalysts to dirhodium(II) carboxamidate catalysts. Reported *E* to *Z* ratios in diazo decomposition of **101** show a greater degree of selectivity than those reported for decomposition of **100**, though diastereoselectivity for both diazoacetates is virtually independent of the catalyst employed. It should also be noted that only with copper catalysts is oxonium ylide formation followed by [2,3]-sigmatropic rearrangement observed.

Scheme 1.23 Diazo Decomposition of **100**, and **101**

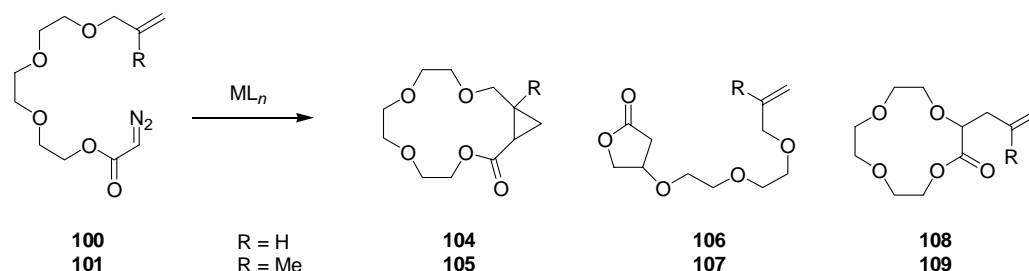


Table 1.2 Selectivity in the Diazo Decomposition Reactions of **100 and **101****

catalyst	104:106:108 ^b	105:107:109 ^b	104Z:E ^b	105Z:E ^b	104, %ee ^c		105, %ee ^c	
					Z	E	Z	E
Rh ₂ (OAc) ₄	97:3:0	100:0:0	64:36	87:13				
Cu(MeCN) ₄ PF ₆	86:0:14	94:0:6	56:44	91:9				
CuPF ₆ / 50	83:13:4	100:0:0	40:60	86:14	88	80	89	62
Rh ₂ (4 <i>S</i> -IBAZ) ₄	53:47:0	54:46:0	65:35	88:12	59	44	35	66
Rh ₂ (5 <i>S</i> -MEPY) ₄	13:87:0	28:72:0	63:37	88:12	49	44	55	7
Rh ₂ (4 <i>R</i> -MEOX) ₄	7:93:0	8:92:0	64:36	88:12	47	33	30	13

a) reproduced from : Doyle, M.P.; Hu, W. *Tetrahedron Lett.* **2000**, *41*, 6265.

b) Determined by GC on a SPB-5 column.

c) Determined by GC on a Chiraldex B-PH column.

1.4.4.5 Alkynes

Reaction selectivity in the diazo decomposition of propargyl-linked diazoacetate **102** is quite different from that seen in the decomposition of **100** and **101** (Table 1.3).⁶⁵

Copper(I) hexafluorophosphate catalyzed reactions show a pronounced affinity for oxonium ylide formation with a corresponding [2,3] sigmatropic rearrangement to produce the macrocycle **112** with an allene side chain, whereas CuPF₆/**50** preferred carbene addition to form **110**. This unprecedented high chemoselectivity for ylide formation with Cu(CH₃CN)₄PF₆/**50** was suggested to result from coordination of ether oxygens to the copper catalysts, directing the reaction pathway.⁶⁵ The dirhodium(II) carboxamidate catalyzed decomposition of **102** proceeded through

carbene addition with a higher degree of chemoselectivity than that reported in dirhodium(II) carboxamidate catalyzed reactions with **100** and **101** (Table 1.3).

Scheme 1.24 Diazo Decomposition of **102**

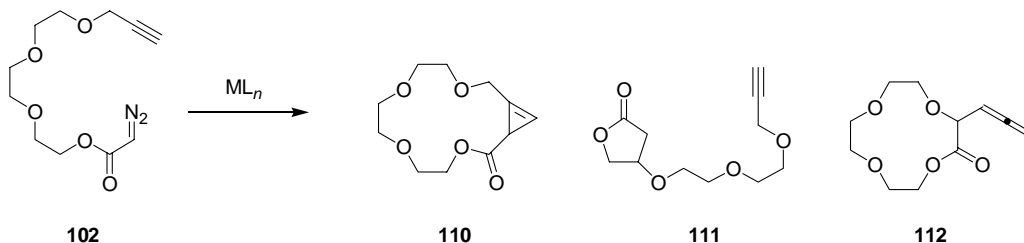
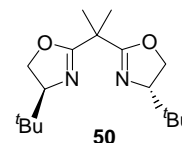


Table 1.3 Chemoselectivity and Regioselectivity of Diazo Decomposition of **102**

Catalyst	110-112 Yield, %	110:111:112 ^b	%ee, 110 ^c
Rh ₂ (OAc) ₄	62	96:4:0	
Cu(MeCN) ₄ PF ₆	61	25:0:75	
CuPF ₆ / 50	70	84:16:0	61
Rh ₂ (4 <i>S</i> -IBAZ) ₄	70	80:20:0	76
Rh ₂ (5 <i>S</i> -MEPY) ₄	82	60:40:0	72
Rh ₂ (4 <i>R</i> -MEOX) ₄	85	35:65:0	42



a) Reproduced from : Doyle, M.P.; Hu, W. *Tetrahedron Lett.* **2000**, *41*, 6265.

b) Determined by GC on a SPB-5 column.

c) Determined by GC on a Chiraldex B-PH column after catalytic hydrogenation over 10% Pd/C.

1.4.4.7 Summary of Functional Groups in Large Ring Carbene Addition

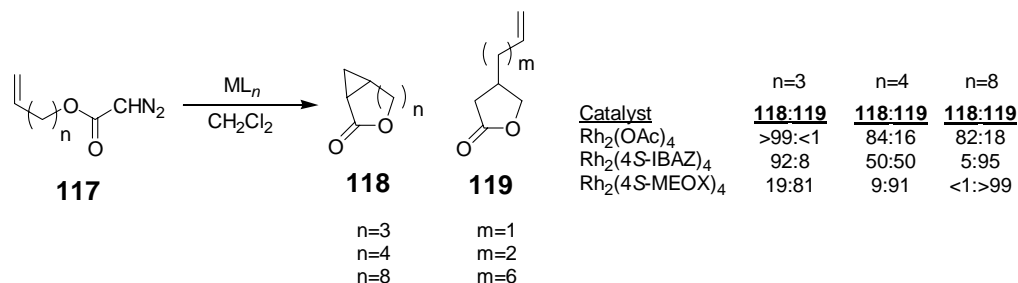
From the results of diazo decomposition of **100**, **101**, **102**, and **103** it was concluded that more reactive catalysts favor macrocycle formation over C-H insertion regardless of the functional group used. Order of preference of addition is determined to be: propargyl > furfuryl > methallyl > allyl.⁶⁵ The investigation showed that both catalyst and functional group influence the chemoselectivity seen in the addition of metal carbenes to form macrocycles. Reactions using copper(I) hexafluorophosphate in combination with polyether substrates exhibit unique chemo- and regioselectivity towards ylide formation with subsequent [2,3]-sigmatropic rearrangement not seen with dirhodium(II) catalysts. This unique behavior has yet to be intentionally utilized

in reaction control, and full understanding of the reason for the selectivity is not currently known.

1.4.4.8 Aliphatic Chains

Doyle and Phillips reported a series of intramolecular cyclopropanation reactions using aliphatic linkers between the olefin and diazoacetate (Scheme 1.25).⁶⁷ As the length of the aliphatic linker increases, γ -lactone formation from C-H insertion becomes a more predominant product. The diazo decomposition of the only substrate capable of forming a macrocycle ring yielded chemoselectivity comparable to that reported using ethylene glycol based linkers.⁶⁴

Scheme 1.25 Ring formation with Alkane Linkers



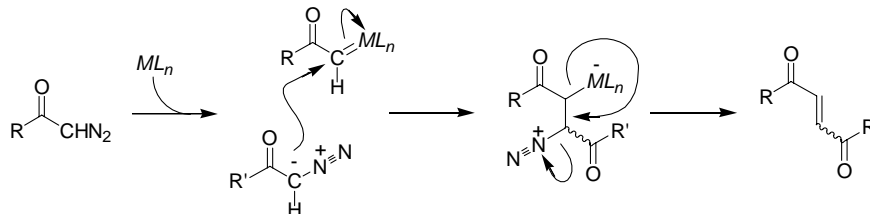
1.4.4.9 Carbene Dimerization

The so-called “carbene dimer” formation, constructing a carbon-carbon double bond from the condensation of two diazocarbonyl groups has also been used in macrocycle formation. The reaction requires that a metal carbene intermediate react with a second diazocarbonyl group to produce the final product (Scheme 1.26). Addition of the carbene leads to the formation of a metal diazoium intermediate, allowing the

⁶⁷ Doyle, M.P.; Phillips, I.M. *Tetrahedron Lett.* **2001**, 42, 3155.

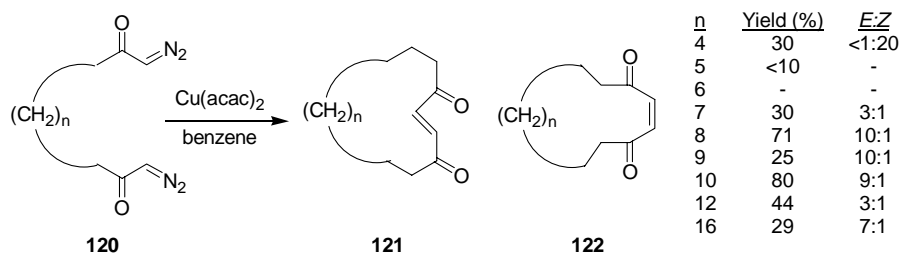
formation of both *E* and *Z* isomers. When both diazocarbonyl groups in the reaction are linked together, "carbene dimerization" results in macrocycle formation.

Scheme 1.26 Carbene Dimerization Process



Carbene dimerization was first utilized for macrocycle construction by Kulkowit and McKervey.⁶⁸ Using substrates having bis-diazo ketones, they reported forming up to twenty membered rings (Scheme 1.27). Substrates used in the study were decomposed using Cu(acac)₂ and, with the exception of eight membered ring formation, selectively formed the *E* isomer in a three to one ratio or higher.

Scheme 1.27 Carbene Dimerization with Diazoketones



Macrocycle formation by carbene dimerization was further advanced by Doyle, Wee, and co-workers in a similar investigation using diazoacetates connected by a hexa(ethylene glycol) linker (Scheme 1.28). The geometry of the resulting olefin was examined and copper catalysts preferentially formed the *E* isomer, whereas dirhodium(II) carboxamides predominately formed the *Z* isomer (Table 1.4).⁶⁹ It

⁶⁸ Kulkowit, S.; McKervey, M.A. *J. Chem. Soc., Chem. Commun.* **1983**, 1069.

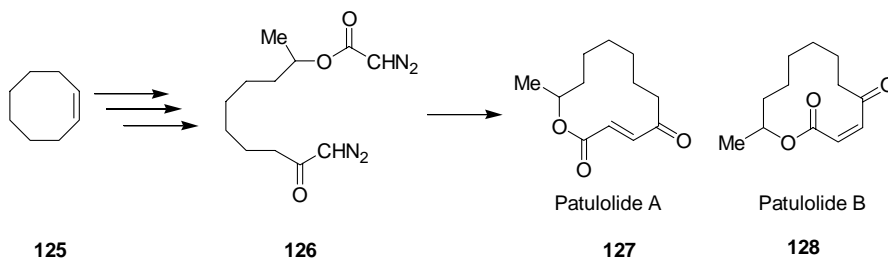
⁶⁹ Doyle, M.P.; Hu, W.; Phillips, I.M.; Wee, A.G.H. *Org. Lett.* **2000**, 2, 1777.

Scheme 1.28 Carbene Dimerization by Select Catalysts



Application of "carbene dimerization" to macrocycle formation was seen in the synthesis of patulolides A and B (Scheme 1.29).⁶⁹ This synthesis coupled the termini of **126** using a diazoacetate and a diazoketone to afford both *E* (**127**) and *Z* (**128**) isomers.

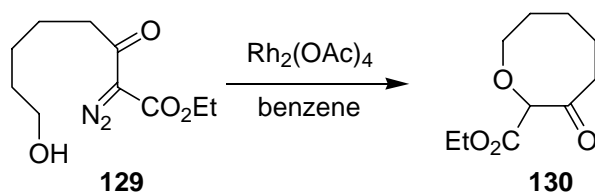
Scheme 1.29 Synthesis of Patulolides A and B



1.4.5 Insertion Reactions to Form Macrocycles

Carbene insertion reactions for macrocycle formation are not as prevalent in the literature as carbene addition reactions. After the initial report by Kulkowit and McKervey³⁰ using O-H insertion to form macrocycles, Moody and co-workers also reported a number of cyclizations using β -keto-diazoacetates to form eight membered rings as illustrated in Scheme 1.30.⁷⁰

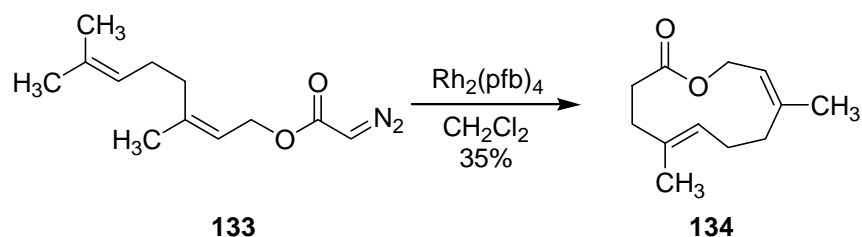
Scheme 1.30 General O-H Insertion Reactions



Macrocycle formation via C-H insertion has been reported in only one instance. Using dirhodium(II) perfluorobutyrate to decompose nerol diazoacetate insertion into a methyl C-H bond was the sole product isolated (Scheme 1.31).³⁸ In contrast, the *E*-isomer of this compound (geraniol diazoacetate) did not produce any intramolecular reaction products. This unique example has not been matched in any subsequent report.

⁷⁰ Helsin, J.C.; Moody, C.J. *J. Chem. Soc., Perkin Trans. 1* **1988**, 1417.

Scheme 1.31 C-H Insertion for Macrocycle Formation



1.4.6 Summary

The formation of macrocycles using metal carbene addition reactions has been investigated using a wide variety of substrates to produce macrocycles of ring size between 10 and 23 members with both dirhodium(II) and copper(I) catalysts. Carbene insertion reactions have also been reported to form macrocycles, as has ylide formation followed by [2,3]-sigmatropic rearrangement in copper catalyzed reactions. The studies demonstrate that the catalytic metal center and the ligands coordinated to it play a significant role in chemoselectivity, regioselectivity, and enantioselectivity of metal carbene macrocyclization reactions. Electronic contributions from ligands are the determining factor in relative reactivity of dirhodium(II) catalysts, with catalysts ligated by more electron deficient ligands generally forming macrocycles in better yields, but lower selectivity than those having less electron deficient ligands.

Limitations to this method of macrocycle formation appear to be few. Carbon-carbon bond formation by carbene addition can be achieved with chemoselectivity, regioselectivity, and enantioselectivity. Ylide formation followed by [2,3]-sigmatropic rearrangement is also seen in copper(I) hexafluorophosphate catalyzed diazo decompositions, but no investigations have focused on the enhancement of this reaction pathway in macrocyclization with metal carbene intermediates. The reaction

pathway that most impedes the formation of larger macrocycles is C-H insertion to form γ -lactones; and in the diazo decomposition of compounds containing 1,2-disubstituted and trisubstituted olefins, hydride abstraction may be a competitive reaction pathway. The asymmetric addition of carbenes to terminal olefins and alkynes leads to the formation of chiral macrocycles from chiral metal carbene intermediates, but dirhodium(II) carboxamidate catalysts, which are most suitable for asymmetric induction in carbene addition reactions, are the catalysts most severely limited by the competitive C-H insertion reaction pathway forming γ -butyrolactones. A second limitation of this method is the lack of information regarding the effects of stereocenters placed within the diazo precursors on reaction selectivity.

Chapter 2

2.1 Introduction

Developments in asymmetric catalysis have evolved rapidly in recent years.¹ Whereas an optically active compound can be formed through the reaction of an achiral substrate with a chiral catalyst in (*single*) asymmetric synthesis, the use of a chiral reactant in combination with a chiral catalyst has been described as *double* asymmetric synthesis.² The interaction between chiral reactants and chiral catalysts to create new stereocenters in processes including asymmetric hydrogenation and epoxidation has been an important facet of the rapid evolution of asymmetric catalysis.^{2,3} As a part of the development of double asymmetric synthesis, chiral dirhodium(II) carboxamidates have been used in combination with chiral diazoacetates, such as *cis*-(2-methyl)-1-cyclohexyl diazoacetate, to catalyze intramolecular carbon-hydrogen insertion reactions⁴ as well as carbene addition reactions⁵ such as the diazo decomposition of cyclohex-2-en-1-yl diazoacetate,^{5b} yielding products with a high degree of diastereoselectivity and regioselectivity.

Many types of reactions, including aldol,² Diels-Alder,⁶ and addition of allyl boronates to aldehydes,⁷ have been utilized in the examination of the influence of

¹ *Catalytic Asymmetric Synthesis*, 2nd Ed.; Ojima, Iwao editor; Wiley-VCH: New York, 2000.

² Masamune, S.; Choy, W.; Petersen, J.S.; Sita, L.R. *Angew. Chem. Int. Ed. Engl.* **1985**, *24*, 1.

³ Kolodiazhnyi, O.I. *Tetrahedron* **2003**, *59*, 5953

⁴ For examples see: (a) Doyle, M.P.; Dyatkin, A.B.; Autry, C. L. *J. Chem. Soc., Perkins Trans. 1* **1995**, 619; (b) Doyle, M.P.; Davies, S.B.; May, E.J. *J. Org. Chem.* **2001**, *66*, 8112; (c) Doyle, M.P.; Kalinin, A.V.; Ene, D.G. *J. Am. Chem. Soc.* **1996**, *118*, 8837.

⁵ (a) Martin, S.F.; Spaller, M.R.; Liras, S.; Hartmann, B. *J. Am. Chem. Soc.* **1994**, *116*, 4493; (b) Doyle, M.P.; Dyatkin, A.B.; Kalinin, A.V.; Ruppar, D.A.; Martin, S.F.; Spaller, M.R.; Liras, S. *J. Am. Chem. Soc.* **1995**, *117*, 11021.

⁶ Kim, P.; Nantz, M.H.; Kurth, M.J.; Olmstead, M.M. *Org. Lett.* **2000**, *2*, 1831.

stereocenters more than one atom removed from the reaction center (remote stereocenters)⁸ in double asymmetric synthesis. However, the influence of remote chiral stereocenters on the diastereoselectivity and chemoselectivity of intramolecular diazo decomposition reactions catalyzed by chiral dirhodium(II) carboxamidates is not known. Herein, we describe the synthesis and diazo decomposition of diazoacetates having a remote conformational bias to yield ten-membered lactones with apparent match/mismatch selectivity.

Doyle and co-workers have investigated the use of metal carbene intermediates to form macrocyclic lactones (macrolides)⁹ ranging in size from 10- to 23-membered.^{10,11} Asymmetric synthesis using chiral dirhodium(II) carboxamidates to catalyze intramolecular carbene addition reactions has made available an array of [8.1.0]-bicyclic compounds with non-racemic chiral ring fusion.¹² Many of the substrates use 1,2-benzenedimethanol or *cis*-2-butene-1,4-diol to link the diazoacetate to the reacting allyl or propargyl group.^{10,11} Whereas the 1,2-benzenedimethanol group linking the diazoacetate to the functional group (**1a**) has a constrained conformation, an analogous diazoacetate using butane-1,4-diol (**1b**), which removes

⁷ Roush, W.R.; Hoong, L.K.; Palmer, M.A.J.; Straub, J.A.; Palkowitz, A.D. *J. Org. Chem.* **1990**, *55*, 4117.

⁸ Still, W.C.; Darst, K.P. *J. Am. Chem. Soc.* **1980**, *102*, 7385.

⁹ The term "macrolide" was coined by R.B. Woodward in : Woodward, R.B. *Angew. Chem.*, **1957**, *69*, 50.

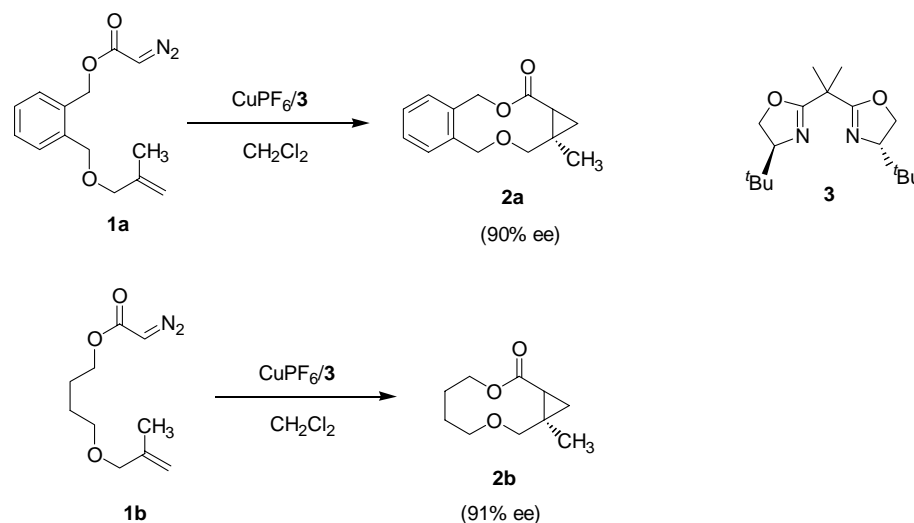
¹⁰ Doyle, M.P.; Protopopova, M.N.; Poulter, C.D.; Rogers, D.H. *J. Am. Chem. Soc.* **1995**, *117*, 7281-2.

¹¹ (a) Doyle, M.P.; Peterson, C.S.; Protopopova, M.N.; Marnett, A.B.; Parker, D.L. Jr.; Ene, D.G.; Lynch, V. *J. Am. Chem. Soc.* **1997**, *119*, 8826-37; (b) Doyle, M.P.; Chapman, B.J.; Hu, W.; Peterson, C.S.; McKerver, M.A.; Garcia, C.F. *Org. Lett.* **1999**, *1*, 1327; (c) Doyle, M.P.; Hu, W. *Synlett.* **2001**, *9*, 1364.

¹² (a) Doyle, M.P.; Peterson, C.S.; Parker, D.L. *Angew. Chem. Int. Ed. Eng.* **1996**, *35*, 1334; (b) Doyle, M.P.; Hu, W.; Chapman, B.; Marnett, A.B.; Peterson, C.S.; Vitale, J.P.; Stanley, S.A. *J. Am. Chem. Soc.* **2000**, *122*, 5718; (c) Doyle, M.P.; Ene, D.G.; Peterson, C.S.; Lynch, V. *Angew. Chem. Int. Ed.* **1999**, *38*, 700.

the conformational constraint imposed by 1,2-benzenedimethanol, has also been synthesized. Diazo decomposition of **1b** produced similar enantioselectivity to that for diazo decomposition of **1a**, demonstrating that the conformational bias from 1,2-benzenedimethanol is not the *a priori* cause for macrocycle formation (Scheme 2.1).^{10a} Though the tether does not influence macrocycle formation, the impact of the conformation of the tether in double asymmetric synthesis has not been explored. We have, therefore, investigated how the conformation imposed by the tether between the diazoacetate and the reacting functional group influences reaction selectivity when using chiral dirhodium(II) carboxamidates.

Scheme 2.1 Removal of Configurational Bias



2.2 Semi-Empirical Prediction of Double Diastereoselectivity

Processes involving two chiral reactants have been categorized by the terms “double asymmetric induction”¹³ and “double asymmetric synthesis.”² Because asymmetry

¹³ Horeau, A.; Kagan, H.B.; Vigneron, J.-P. *Bull. Soc. Chim. Fr.*, **1968**, 3795.

cannot really be qualified, the description “double stereodifferentiation”¹⁴ has also been applied in reactions incorporating racemic mixtures of substrates to avoid confusion.¹⁵ In reactions where two enantiomerically pure chiral reactants are coupled, when stereoselectivity is enhanced relative to a reference reaction in which only one of the reactants is chiral, the reactants are described as “matched.” Conversely, if the stereoselectivity relative to the reference reaction with one chiral reactant is diminished, the reactants are regarded as “mismatched”.¹⁶

Semi-empirical prediction of reaction diastereoselectivity between two chiral reactants has been described by Masamune and co-workers.² To illustrate how the prediction of diastereoselectivity is used, a double diastereoselective aldol reaction was described (Scheme 2.2).¹⁷ First, the use of chiral enolate **S-4** with an achiral aldehyde (reaction 1), and chiral aldehyde **9** with achiral enolate **5** (reaction 2), were examined. Chiral aldehyde **9** was then reacted with each enantiomer of chiral enolate **4** (reaction 3 and 4), and the diastereoselectivities of these reactions was compared against control reactions 1 and 2. The resulting diastereoselectivity from each of these reactions is listed in Table 2.1.

¹⁴ Izumi, Y.; Tai, A. *Stereodifferentiating Reactions*, Academic Press: New York, **1977**.

¹⁵ Heathcock, C.H.; White, C.T. *J. Am. Chem. Soc.* **1979**, *101*, 7076.

¹⁶ Eliel, E.L.; Wilen, S.H.; Mander, L.N. *Stereochemistry of Organic Compounds*, Wiley: New York, 1994; p. 969.

¹⁷ Results cited from : Masamune, S.; Ali, S.A.; Snitman, D.L.; Garvey, D.S. *Angew. Chem. Int. Ed. Engl.* **1980**, *19*, 557.

Scheme 2.2 Double Diastereoselective Aldol

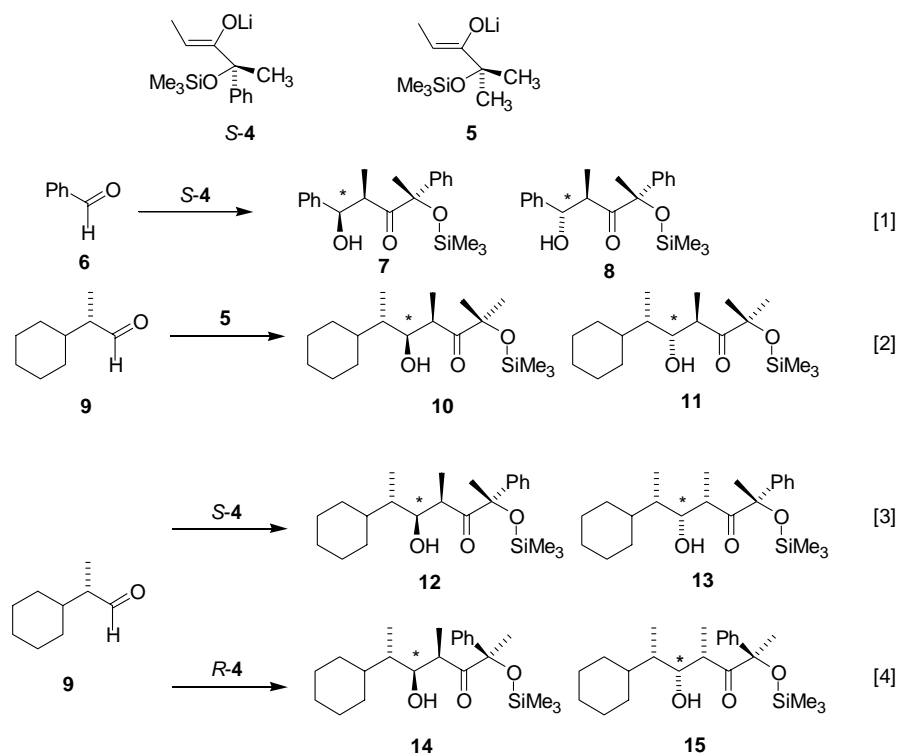


Table 2.1 Diastereoselectivity in Double Diastereoselective Aldol Reactions

Aldehyde	Enolate	Diastereoisomer Ratio	Theoretical
6	S-4	3.5 : 1	
9	5	2.7 : 1	
9	S-4	8 : 1	3.5 x 2.7 = 9.5
9	R-4	1 : 1.5	3.5 / 2.7 = 1.3

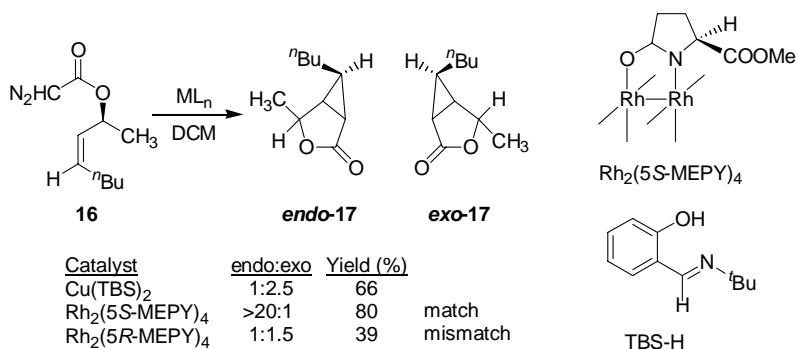
The results found in Table 2.1 show that if the ratio of diastereoisomers for the reaction of a chiral substrate with an achiral compound are multiplied, the value is approximately that expected for the matched reaction with both chiral substrates, whereas division of the diastereoisomer ratios affords the approximate value obtained for the case of mismatched chiral substrates. The prediction of diastereoselectivities in double diastereoselective homogeneous catalytic hydrogenation, epoxidation of allylic alcohols with the Katsuki-Sharpless reagent, and Diels-Alder reactions have

also been reviewed.² Use of either matched or mismatched pairs of chiral substrates in each of these types of reactions also afforded products with diastereoselectivities that were predictable based on the analogous control reactions using only one chiral reactant.

2.3 Application of Dirhodium(II) Carboxamidates to Match/Mismatch Reactions

Double asymmetric induction in intramolecular carbene addition reactions has been examined using chiral dirhodium(II) carboxamidates to catalyze the diazo decomposition of chiral diazoacetates.⁵ One example reported by Martin and co-workers described a match/mismatch relationship using $\text{Rh}_2(\text{MEPY})_4$ as a chiral catalyst in intramolecular cyclopropanation reactions of several chiral diazoacetates including **16** (Scheme 2.3).^{5a} Achiral bis-(*N*-*tert*-butylsalicylamidinato)copper(II) $[\text{Cu}(\text{TBS})_2]$ catalyzed diazo decomposition of **16** yielded a 1:2.5 *endo:exo* ratio in the formation of **17**, with the preference for the *exo* isomer originating from the conformational bias created by the innate chirality of **16**. The diazo decomposition of **16** catalyzed by the *R* and *S* enantiomers of $\text{Rh}_2(\text{MEPY})_4$ produced **17** with differential diastereoselectivity. Decomposition of **16** by $\text{Rh}_2(5S\text{-MEPY})_4$, favors the formation of *endo*-**17** in a greater than 20:1 ratio, which is an enhancement of the diastereoselectivity seen in diazo decomposition of **16** by $\text{Cu}(\text{TBS})_2$, making $\text{Rh}_2(5S\text{-MEPY})_4$ the matched catalyst for diazo decomposition of **16**. However, the mismatched catalyst for diazo decomposition of **16**, $\text{Rh}_2(5R\text{-MEPY})_4$, leads to the formation of *exo*-**17** preferentially with lower diastereoselectivity than that seen with achiral $\text{Cu}(\text{TBS})_2$.

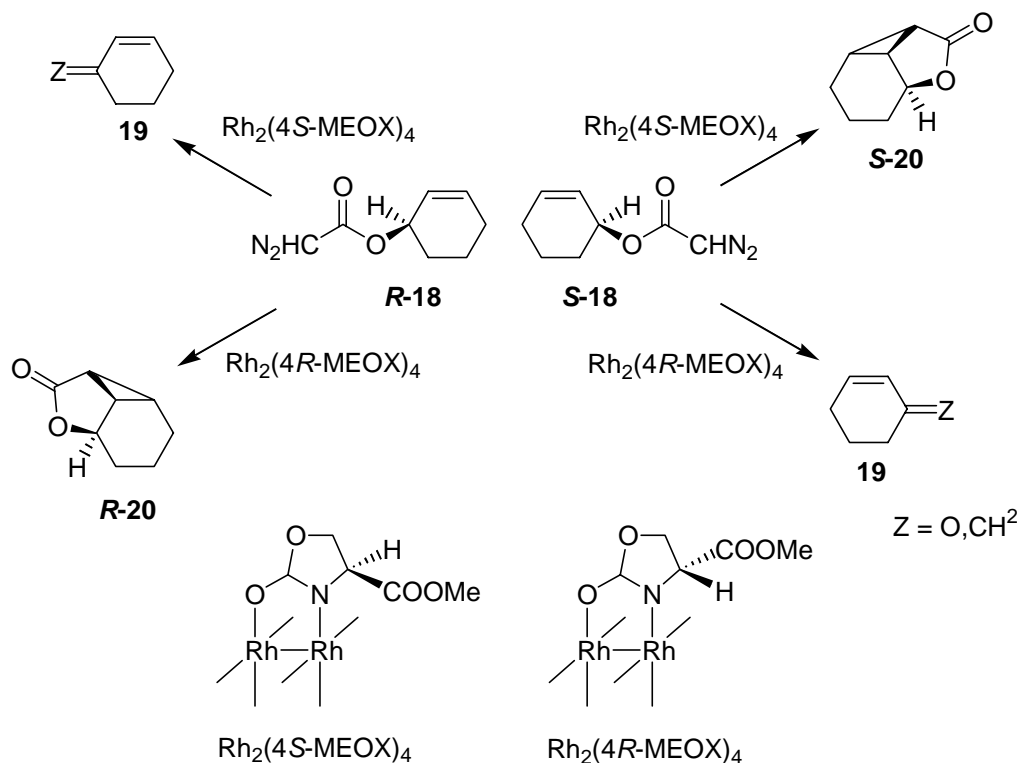
Scheme 2.3 Decomposition of Chiral Diazoacetate **16**



Dirhodium(II) carboxamidate catalyzed diazo decomposition reactions are known to proceed through several reaction pathways, including carbene addition, C-H insertion, ylide formation, and hydride abstraction.⁵ In several examples, more than one reaction pathway may occur from the diazo decomposition of a single substrate (i.e. cyclopropanation and C-H insertion).¹¹ One example of this was reported in which diazo decomposition resulted in the resolution of a racemic mixture of secondary allylic diazoacetate **18** (Scheme 2.4).⁵ Diazo decomposition of **R-18** with Rh₂(4R-MEOX)₄ yielded the bridged tricyclic compound **R-20**. However, diazo decomposition of **R-18** with Rh₂(4S-MEOX)₄ yielded **19**, which resulted from hydride abstraction from the 1-position.¹⁸

¹⁸ Hydride abstraction is a process known to occur with dirhodium carboxamidate catalysts and was described in : Doyle, M.P.; Dyatkin, A.B.; Autry, C.L.J. *J. Chem. Soc., Perkin Trans. 1* **1995**, 619.

Scheme 2.4 Match and Mismatch Decompositions of 18 with Rh₂(MEOX)₄



Diazo decomposition of **S-18** catalyzed by Rh₂(4S-MEOX)₄ results in carbene addition to the allylic carbon-carbon double bond, yielding **S-20**. However, formation of the opposite diastereoisomer, **R-20**, resulting from carbene addition to the opposite face of the carbon-carbon double bond is restricted by the conformational mismatch with the catalyst. Instead, diazo decomposition of **R-18** using Rh₂(4S-MEOX)₄ results in a different reaction pathway - that of hydride abstraction. The example of diazo decomposition of **18** could be used to extend the definition of the terms “match” and “mismatch” to reflect more than diastereoselectivity in metal carbene chemistry, as in this case it could be used to reflect the chemoselectivity seen in the reaction. The diazo decomposition of **R-18** catalyzed by Rh₂(4S-MEOX)₄ results in a metal carbene intermediate in which the

interaction between the chiral catalyst and the chiral diazoacetate does not afford a favorable conformation for carbene addition, as is described for a mismatched pair.² The result is not a diminished diastereoselectivity, but rather a change in the reaction pathway to hydride abstraction. In comparison, diazo decomposition of **S-18** catalyzed by Rh₂(4*S*-MEOX)₄ results in carbene addition to the olefin to yield the desired product **S-20**, and is the reaction of matched substrate and catalyst.

The examples described in Schemes 2.3 and 2.4 illustrate the excellent diastereoselectivity and chemoselectivity that chiral dirhodium(II) carboxamidate catalysts can provide in double asymmetric induction. However, the investigation of double asymmetric induction in carbene addition reactions has not been extended to include intramolecular reactions with remote conformational bias.

2.4 Formation of Ten-membered Rings by Carbene Addition Reactions

The formation of macrolides has been accomplished using select dirhodium(II) and copper(I) catalysts¹⁹ to mediate intramolecular carbene addition to both alkenes^{12a-b,20} and alkynes.¹² Several of these reactions use diazoacetates appropriate for the formation of ten-membered rings, including diazo decomposition reactions catalyzed by chiral dirhodium(II) carboxamidates, resulting in enantioselective formation of [8.1.0]-bicyclic compounds from asymmetric carbene addition to the allyl or propargyl functional group. In the examples found in Schemes 2.5 and 2.6, a chiral catalyst is used in conjunction with an achiral substrate. These reactions involving a

¹⁹ Doyle, M.P.; Hu, W. *Synlett* **2000**,

²⁰ Doyle, M.P.; Hu, W. *J. Org. Chem.* **2000**, 65, 8839.

chiral catalyst and an achiral substrate are an important part of evaluation, providing one of the control reactions described by Masamune and co-workers,² to compare to when using chiral diazoacetates and chiral catalysts to form ten-membered lactones. These reactions also provide general guidelines for the relative stereoselectivity with each catalyst and a comparison of the enantioselectivity differences between allyl and propargyl functional groups.

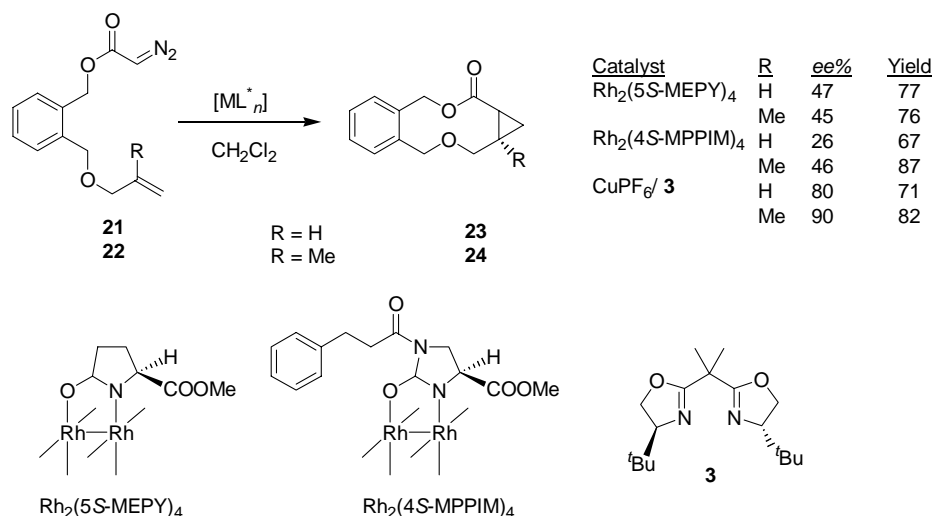
2.4.1 Intramolecular Cyclopropanation of Olefins

The first diazoacetate decomposition to yield a macrocycle formed a thirteen membered ring.²¹ Subsequently, the first reported ten-membered ring formation from metal mediated carbene addition was the diazo decomposition of diazoacetates **21** and **22**,^{12a} which represent two olefin substitution patterns (Scheme 2.5).^{12a} Diazo decomposition of **21** and **22** by Rh₂(5*S*-MEPY)₄, Rh₂(4*S*-MPPIM)₄, or the Cu(CH₃CN)₄PF₆/**3** complex results in formation of *cis* cyclopropanes **23** and **24** respectively, which contrasts with the intermolecular reactions of diazo esters, in which both *cis* and *trans* diastereoisomers are obtained.²² Enantioselectivity in these reactions is highest when catalyzed by the Cu(CH₃CN)₄PF₆/**3** complex, while the yields are similar with all catalysts.

²¹ For further discussion of this see section 1.2.5.

²² (a) Pfaltz, A. *Acc. Chem Res.* **1993**, 26, 339; (b) Müller, P.; Baud, C.; Ene, D.; Motallebi, S.; Doyle, M.P.; Brandes, B.D.; Dyatkin, A.B.; See, M.M. *Helv. Chim. Acta* **1995**, 78, 459; (c) Nishiyama, H. Itoh, Y.; Sugawara, Y.; Matsumoto, Aoki, K.; Itoh, K. *Bull. Chem. Soc. Jpn.* **1995**, 68, 1247.

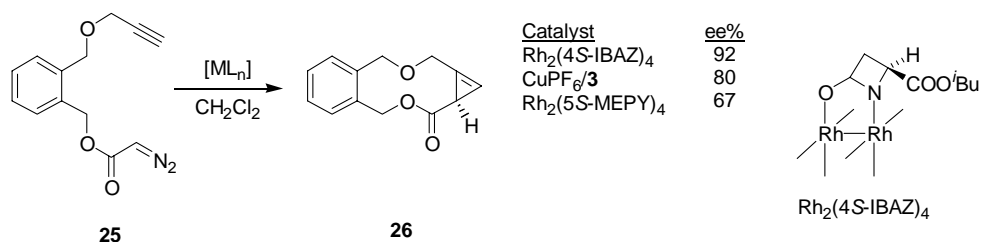
Scheme 2.5. 1,2-Benzenedimethanol Linked Cyclopropanation



2.4.2 Intramolecular Cyclopropanation in Macrocycles

Asymmetric synthesis of ten-membered rings by carbene addition to a terminal alkyne has also been reported.²² Diazo decomposition of diazoacetate **24** with a propargyl functional group affords cyclopropene **25** in high enantiomeric excess (56 to 92%) (Scheme 2.6). The chiral dirhodium(II) carboxamidate catalyst $\text{Rh}_2(4\text{S-IBAZ})_4$ affords the highest reported enantiomeric excess in diazo decomposition of **25** (Scheme 2.5).

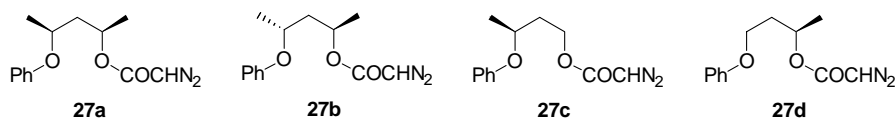
Scheme 2.6 Asymmetric Cyclopropanation Forming Ten-membered Rings



2.5 Linking a Diazoacetate to the Functional Group with a Chiral Tether

The dirhodium(II) tetraacetate catalyzed diazo decomposition of a diazoacetate linked to an aryl group through a chiral tether results in stereoselective carbene addition to the aryl ring.²³ Diazoacetates with chiral 2,4-pentanediol tethers connecting them to a phenyl group (Figure 2.1) were selected to evaluate the influence of the chiral tether on the enantioselectivity of the resulting products **28** (Scheme 2.7).²⁴

Figure 2.1 Chiral-Tethered Diazoacetates



Substrates bearing a single stereocenter adjacent to the diazoacetate (**27d**) or a single stereocenter adjacent to the aryl ring (**27c**) were decomposed using dirhodium(II) tetraacetate to evaluate the facial selectivity of carbene addition to the aryl ring. Two diazoacetates with stereocenters adjacent to both the aryl ring and the diazoacetate (**27a** and **27b**) were also subjected to diazo decomposition conditions with a dirhodium(II) tetraacetate catalyst, providing diastereoisomer ratios (*S*-**28**:*R*-**28**) used in the evaluation of how two stereocenters in a single substrate can interact with each other to influence the facial selectivity of carbene addition to the aryl ring.

²³ Tei, T.; Sato, Y.; Hagiya, K.; Tai, A.; Okuyama, T.; Sugimura, T. *J. Org. Chem.* **2002**, 67, 6593.

Scheme 2.7 Diazo Decomposition of 27

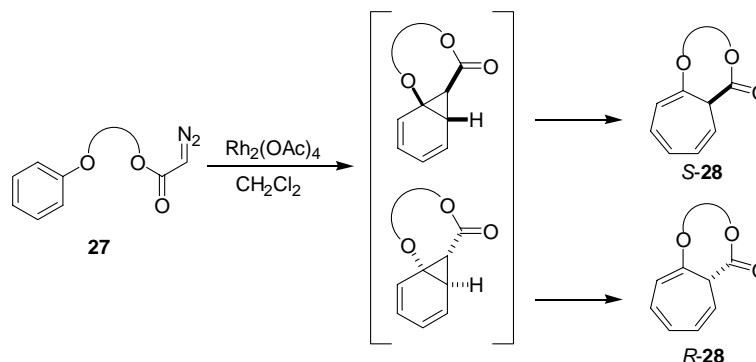


Table 2.2 Enantiomeric Ratios for Diazo Decomposition of 27 at 40° C^a

Substrate	<i>S</i> - 28 / <i>R</i> - 28
27d	36.1 ^b
27c	3.7 ^b
27b	19.1 ^b
27a	>500

a) Reproduced from the supporting information of: Tei, T.; Sato, Y.; Hagiya, K.; Tai, A.; Okuyama, T.; Sugimura, T. *J. Org. Chem.* **2002**, 67, 6593.

b) Average of the ratios obtained from two runs.

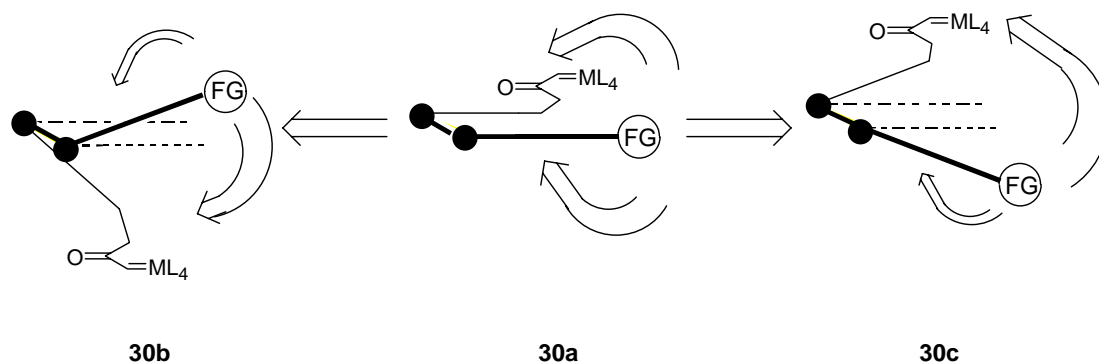
The ratio between isomers *S*-**28** and *R*-**28** listed in Table 2.2 reflects the conformational bias of each of the diazoacetate compounds resulting from the chiral tether in each substrate. Diazo decomposition of both **27c** and **27d** affords some degree of facial selectivity in the dirhodium(II) tetraacetate catalyzed carbene addition to the aryl functional group of **27**. The use of a chiral 2,4-pentanediol tether, with a chiral center adjacent to the diazoacetate and a chiral center adjacent to the aryl ring of the substrate, combines the influence of both chiral centers to form the conformational bias of the substrate. The combined influence of both stereocenters may result in higher facial selectivity (diastereoselectivity) of carbene addition to the aryl ring (**27a**) than either stereocenter alone. However, inversion of one tether stereocenter (**27b**) results in diastereoselectivity that falls between the

diastereoisomer ratios seen for **27c** and **27d**. The enhancement of diastereoselectivity (**27a**) versus moderation of diastereoselectivity (**27b**) with two stereocenters interaction together demonstrates how reaction selectivity in carbene addition reactions may be enhanced or diminished by multiple stereocenters.

2.6 Conformationally Biased Diazoacetate Substrates

In the diazo decomposition of an achiral substrate, both faces of the metal carbene intermediate **30a** are approached equally through two identical trajectories of the functional group (FG) (Figure 2.2). A macrocycle precursor in which both faces of the metal carbene can be approached through identical trajectories of the functional group has already been synthesized (i.e. **21** in Scheme 2.5), and diazo decomposition using chiral catalysts leads to the formation of **23** enantioselectively. However, by modifying the dihedral angle between the metal carbene and the functional group to be set at a value other than 180° or 0°, a conformational bias is created within the substrate in which approach of the reacting center to one face of the metal carbene is preferred over the other, as illustrated in **30b**. Changing the dihedral angle set in **30b** to the mirror image (enantiomer) structure of **30c** also changes the side of the metal carbene the functional group will prefer to approach, and will result in the enantiomeric product.

Figure 2.2 Impact of a Conformational Bias

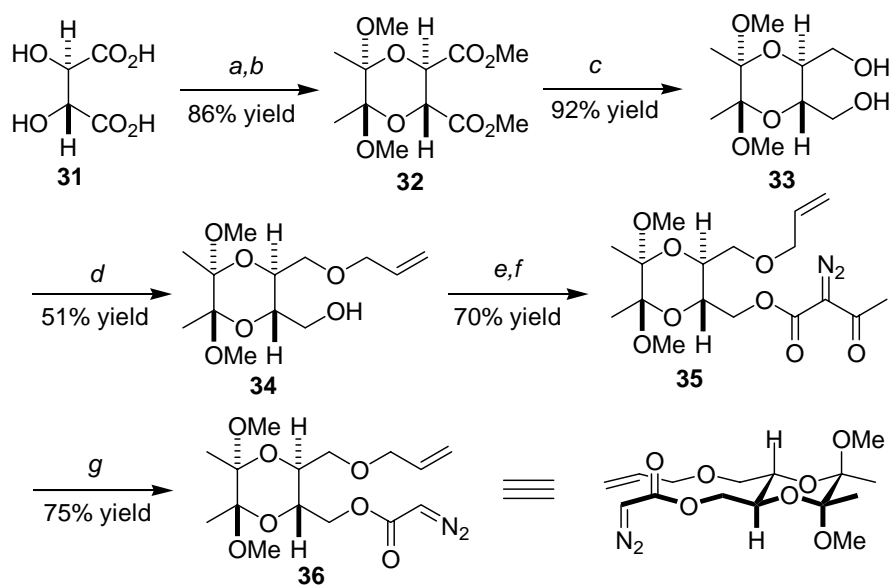


2.6.1 Synthesis Conformationally Biased Diazoacetates

To begin this study, a deliberately designed diazoacetate was synthesized. Work by Ley and co-workers reported that starting from (L)-tartaric acid, the highly crystalline 2,3-diacetal of threitol (**33**) was obtained in good yields (Scheme 2.8).²⁴ We were interested in using **33** for two reasons: (1) it has a set dihedral angle to provide a conformationally biased variant of the previously described non-biased 1,2-benzenedimethanol tether of **21** and (2) both enantiomers of tartaric acid are commercially available. Starting from **33**, the diol was mono-alkylated using allyl bromide, followed by formation of the diazoacetate using diketene addition, then diazo transfer from methanesulfonyl azide, and completed by hydrolysis with LiOH to afford **36** as a yellow oil. Diazoacetate **36** has a conformational bias originating from the dihedral angle set by the rigid six membered ring of the di-acetal of threitol (**36**) that is remote (more than one atom removed)⁸ in relationship to both the alkene and the diazoacetate.

²⁴ (a) Douglas, N. L.; Ley, S.V.; Osborn, H.M.I.; Owen, D.R.; Priepke, H.W.M.; Warriner, S.L. *Synlett* **1996**, 793-5 (b) Montchamp, J.-L.; Tian, F.; Hart, M.E.; Frost, J.W. *J. Org. Chem.* **1996**, 61, 3897-9.

Scheme 2.8 Synthesis of a Conformationally Biased Diazoacetate



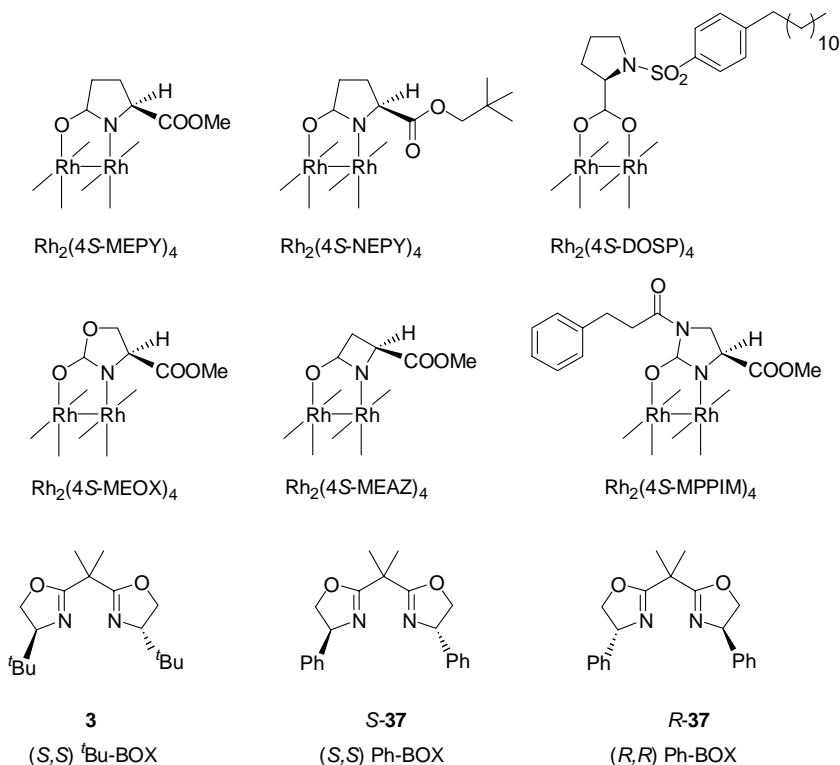
(a) MeOH, H₂SO₄(cat.), (CH₃O)₃CH, reflux; (b) butanedione, CSA, (CH₃O)₃CH, reflux; (c) LAH, THF; (d) NaH, allyl bromide, NaI, THF; (e) diketene, Et₃N, THF (f) MsN₃, Et₃N, THF; (g) LiOH, THF, H₂O

2.6.2 Cyclopropane Diastereoselectivity with Chiral Di-acetal Substrates

With the conformationally biased substrate **36** in hand, the chiral catalysts to be used were taken from available dirhodium(II) carboxamidates based on the classes of ligands available (see section 1.3). The catalysts Rh₂(MEPY)₄, Rh₂(MEOX)₄, Rh₂(MEAZ)₄, and Rh₂(MPPIM)₄ (Figure 2.3) were each selected because both enantiomers of each catalyst are known and well characterized. In addition, each of these catalysts has been used in previous work involving conformationally biased substrates⁴ or in the formation of ten-membered rings.^{11,12} The use of Rh₂(4*S*-DOSP)₄ provided a chiral dirhodium(II) carboxylate catalyst and Rh₂(5*S*-NEPY)₄ afforded a means of assessing the role of the ester group on diastereoselectivity. The C₂-symmetric chiral bis-oxazoline ligands in combination with copper(I) have also been used previously in comparison to dirhodium(II) carboxamidate catalysts in

carbene addition reactions to form ten-membered rings,^{11,12} and they were selected as catalysts for the diazo decomposition of conformationally biased diazoacetates.

Figure 2.3 Chiral Catalysts and Ligands Used in Diazo Decomposition of Conformationally Biased Diazoacetates



Diazo decomposition of **36** was achieved by syringe pump addition of a methylene chloride solution of **36** over one hour to a refluxing methylene chloride solution containing 1 mol% of dirhodium(II) tetraacetate (Scheme 2.9), affording two cyclopropane diastereoisomers (**39a** and **39b**) from carbene addition to the allyl carbon-carbon double bond, and **40**, from C-H insertion (Table 2.3). Analysis of both **39a** and **39b** by ^1H NMR allowed for determination that both compounds were *cis*-cyclopropanes based on the *J*-coupling values of the signals correlating to the cyclopropane protons (dt, *J* = 5.1, 8.2 Hz and dt, *J* = 5.2, 8.0 Hz) and on crystallographic data. The formation of **40** was inferred from the IR absorbance at

3458 cm^{-1} , which is consistent with an O-H stretch. Further justification for this compound is found in the peak area integration values of the ^1H NMR spectrum, which suggest that an additional proton is present, though the compound could not be isolated, and therefore could not be fully characterized. A fourth material was also detected, but could not be isolated. The C=O stretching frequency for the compound is 1734 cm^{-1} , which is consistent with six-membered or larger lactones. The ^1H NMR spectrum shows the olefinic protons of the allyl ether have not changed its chemical shift or J-coupling values. In addition, the signals for each methyl group of the starting diazoacetate **36** are present in the spectrum. No signals consistent with maleate or fumarate esters (singlet at 6.9 or 6.3 ppm), which would result from “carbene dimerization,” are observed. Further information could not be obtained, as the additional ^1H signals were overlapping and convoluted by remaining impurities that could not be removed. Based on the ^1H spectrum, and the IR spectrum obtained, the fourth material is believed to be **41**, resulting from C-H insertion. The product ratios of **39a**, **39b**, **40**, and **41** were obtained by GC analysis using an SPB-5 column.

Scheme 2.9 Diazo Decomposition of **36**

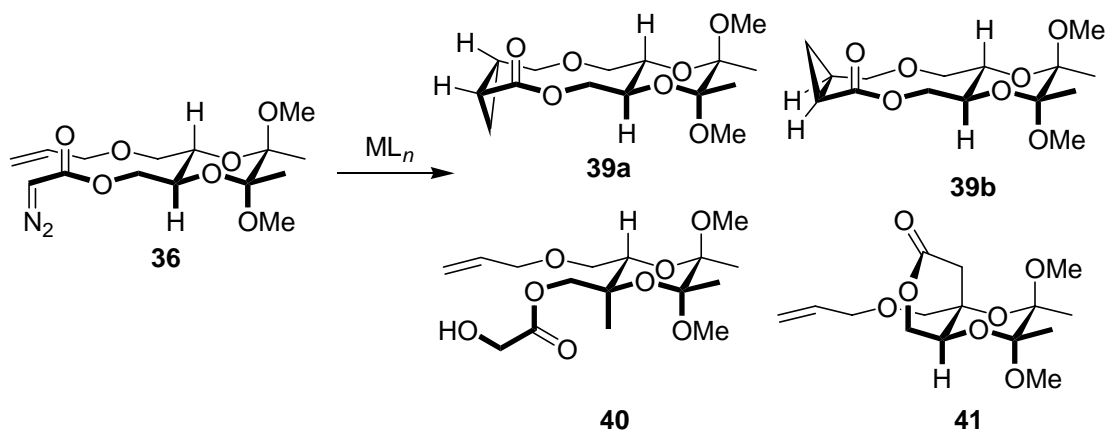


Table 2.3 Selectivity in Diazo Decomposition Reactions of **36^a**

Catalyst	39a ^b	39b ^b	40 ^b	41 ^b	d.r.(39a : 39b) ^b	Yield (39a + 39b) (%) ^c
Rh ₂ (OAc) ₄	64	29	3	4	70:30	72
Rh ₂ (5 <i>R</i> -MEPY) ₄	85	8	3	4	91:9	77
Rh ₂ (5 <i>S</i> -MEPY) ₄	43	26	6	25	63:37	47
Rh ₂ (5 <i>R</i> -MEAZ) ₄	85	11	3	1	88:12	69
Rh ₂ (5 <i>S</i> -MEAZ) ₄	60	35	3	2	63:37	70
Rh ₂ (5 <i>R</i> -MPPIM) ₄	74	15	5	6	83:17	75
Rh ₂ (5 <i>S</i> -MPPIM) ₄	55	30	8	7	64:36	62
Rh ₂ (5 <i>R</i> -MEOX) ₄	67	11	12	10	86:14	59
Rh ₂ (5 <i>S</i> -MEOX) ₄	40	24	13	23	63:37	45
Rh ₂ (5 <i>S</i> -DOSP) ₄	62	35	2	1	64:36	62
Rh ₂ (5 <i>S</i> -NEPY) ₄	40	23	21	16	64:36	39
[Cu(CH ₃ CN) ₄](PF ₆)	63	35	1	1	64:36	57
Cu(CH ₃ CN) ₄ PF ₆ / 3 ^d	67	15	2	16	81:19	69

(a) Decomposition of diazoacetate **36** was accomplished by addition over 2 h to a refluxing catalyst/DCM solution; (b) All product ratios were obtained by GC analysis on an SPB-5 column; (c) Yields determined by crude mass and ¹H NMR integration; (d) **3** is the (*S,S*)-^tBu-BOX ligand found in Figure 2.3.

During work-up of the crude reaction mixture from diazo decomposition of **36** with Rh₂(5*S*-MEPY)₄, it was noted that as the crude reaction was concentrated in

preparation for product analysis a solid material precipitated out of diethyl ether. The highly crystalline material was removed by filtration, and determined by ^1H NMR to be **39a** with less than 10% of **39b** present. This fortunate occurrence allowed us to obtain crystals to determine the absolute conformation of **39a** by elucidation of the single crystal X-ray structure (Figure 2.4). The dihedral angle of C(2)-C(1)-C(11)-C(10) is found to be -69.4° (Table 2.4), which reflects the conformation of the 1,4-dioxane ring that creates the conformational bias of diazoacetate **36**. The bond angles and bond distances of C(5), C(6), and C(7) conclusively show that the compound does have a cyclopropane ring, whereas the dihedral angles of the cyclopropane ring listed in Table 2.4 reflect the assigned stereochemistry of the cyclopropane ring.

Figure 2.4 ORTEP Diagram of 39a with Absolute Stereochemical Structure

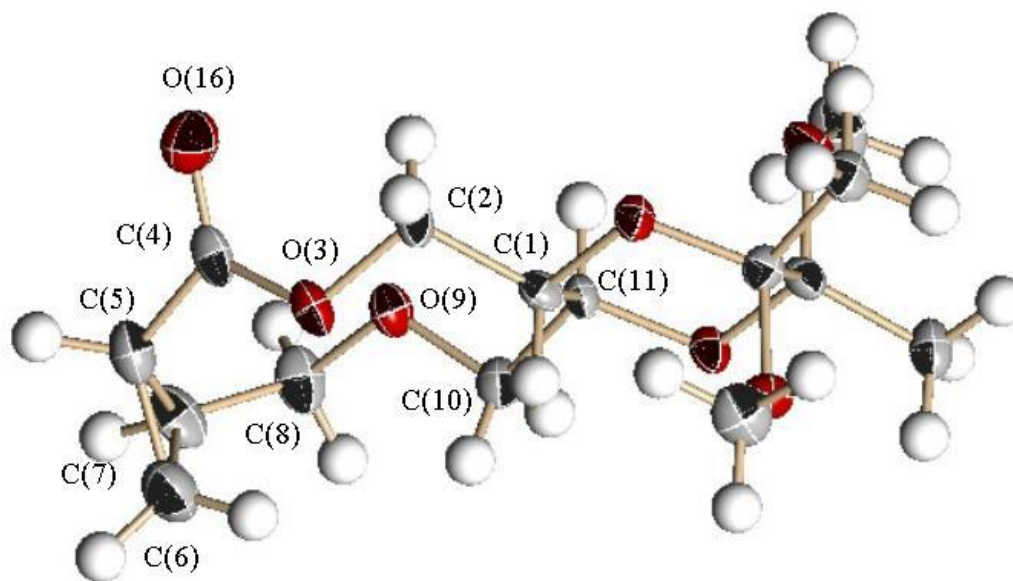


Table 2.4 Select Bond Angles and Bond Distances

Bond	Distance (Å)	Atoms	Angle [°]
C (4) – O (16)	1.200	C (6) – C (5) – C (7)	58.3
C (5) – C (7)	1.524	C (6) – C (7) – C (5)	59.5
C (5) – C (6)	1.483	C (7) – C (6) – C (5)	62.3
C (6) – C (7)	1.464		
Atoms		Torsion Angle [°]	
O (3) – C (4) – C (5) – C (7)		-78.0	
C (6) – C (7) – C (8) – O (9)		-55.2	
C (2) – C (1) – C (11) – C (10)		-69.4	

The diazo decomposition of **36** catalyzed by dirhodium(II) tetraacetate shows preferential formation of one diastereoisomer (**39a**) over the other (**39b**) due to the influence of the conformational bias of the diazoacetate precursor (Table 2.3). Decomposition of **36** using the chiral catalyst Rh₂(5*S*-MEPY)₄ affords slightly lower diastereoselectivity (63:37) in the formation of cyclopropanes **39a** and **39b** than that

seen using achiral dirhodium(II) tetraacetate. Decomposition of **36** catalyzed by $\text{Rh}_2(5R\text{-MEPY})_4$ affords **39a** and **39b** in a 91:9 ratio. Additional decomposition reactions using the *R* enantiomers of other chiral dirhodium(II) carboxamidate catalysts show a ratio between **39a** and **39b** of greater than 82:18 (Table 2.3), and using the *S* enantiomers of each catalyst, a 63:37 ratio (**39a:39b**) is obtained. The formation of **40** and **41** tends to be greater in diazo decomposition of **36** by the *S* enantiomers of each catalyst than for the *R* enantiomers. Decomposition of **36** catalyzed by achiral copper(I) hexafluorophosphate yielded similar diastereoselectivity and chemoselectivity to that seen in the dirhodium(II) tetraacetate catalyzed decomposition of **36**, whereas the chiral $\text{Cu}(\text{CH}_3\text{CN})_4\text{PF}_6/\mathbf{3}$ complex appeared to be the match catalyst for diazo decomposition of **36**, enhancing diastereoselectivity to 81:19.

Diazo decomposition of **36** by the *R* enantiomers of the dirhodium(II) carboxamidate catalysts affords the ten-membered lactone **39** with higher diastereoselectivity and chemoselectivity than is observed for the diazo decomposition of **36** by the *S* enantiomer or by achiral dirhodium(II) tetraacetate. Conversely, the diazo decomposition of **36** by the *S* enantiomer of the dirhodium(II) carboxamidate catalysts affords the ten-membered lactone **39** with lower diastereoselectivity and chemoselectivity than that seen for dirhodium(II) tetraacetate catalyzed decomposition of **36**. As previously defined,² the increase in diastereoselectivity (as compared to dirhodium(II) tetraacetate) in diazo decomposition of **36** by the *R* enantiomer of each catalyst makes these the matched reactions, whereas the reduction

in diastereoselectivity for diazo decomposition of **36** by the *S* enantiomer makes these reactions the mismatched reactions.

To verify the selectivity seen in the diazo decomposition of **36**, the enantiomer of **36** was also prepared (**42**). This also provided a means to complete the investigation of double diastereoselectivity with those catalysts, such as $\text{Rh}_2(4S\text{-DOSP})_4$, for which only one enantiomer is available. Starting from D-tartaric acid, and using the synthetic procedure described in Scheme 2.8, diazoacetate **42** was obtained with the same yields as those reported in the synthesis of **36**, from compounds having the opposite optical rotations of those compounds obtained using L-tartaric acid as the starting compound. Diazo decomposition of **42** catalyzed by dirhodium(II) tetraacetate (Scheme 2.14) yielded cyclopropane diastereoisomers **43a** and **43b** in the ratio of 70:30, and nearly identical chemoselectivity to that seen in the dirhodium(II) tetraacetate catalyzed diazo decomposition of **36**. Product ratios were determined by peak area integration of the GC trace obtained from an aliquot of the crude sample mixture injected onto an SPB-5 column (Table 2.5). The subtle difference in chemoselectivity seen in diazo decomposition of **36** and **42** was also observed in comparison of the results of several of the dirhodium(II) carboxamidate catalysts. Several of these reactions were repeated, including that of dirhodium(II) tetraacetate and **36**. The resulting product ratios obtained from GC analysis in these reactions showed that the peak area ratios varied by 1-3% in three runs of the same reaction, which was concluded to be due to experimental error.

Scheme 2.10 Diazo Decomposition of 41

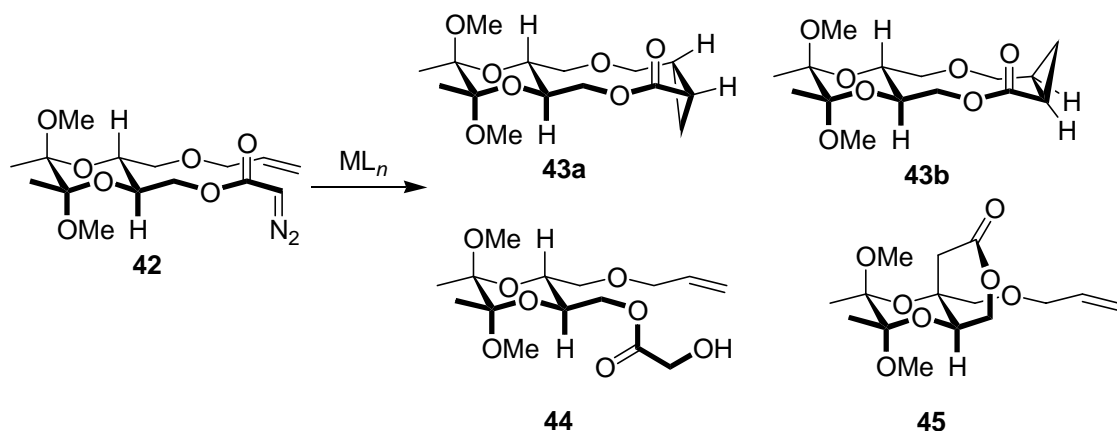


Table 2.5 Product Selectivity in Diazo Decomposition of 42^a

Catalyst	43a	43b	44	45	d.r. (43a:43b)	Yield (43a + 43b) (%)
Rh ₂ (OAc) ₄	67	29	2	2	70:30	66
Rh ₂ (5 <i>R</i> -MEPY) ₄	48	23	4	25	67:33	54
Rh ₂ (5 <i>S</i> -MEPY) ₄	85	9	2	4	90:10	67
Rh ₂ (5 <i>R</i> -MEAZ) ₄	60	35	2	3	63:37	74
Rh ₂ (5 <i>S</i> -MEAZ) ₄	86	12	1	1	88:12	71
Rh ₂ (5 <i>R</i> -MPPIM) ₄ ^d	42	28	8	22	60:40	60
Rh ₂ (5 <i>S</i> -MPPIM) ₄ ^d	73	14	5	8	84:16	69
Rh ₂ (5 <i>R</i> -MEOX) ₄	52	32	4	12	62:38	50
Rh ₂ (5 <i>S</i> -MEOX) ₄	81	10	4	5	89:11	73
Rh ₂ (5 <i>S</i> -NEPY) ₄	75	13	5	7	86:14	49
Rh ₂ (4 <i>S</i> -DOSP) ₄	59	33	7	1	64:36	64
Cu(CH ₃ CN) ₄ PF ₆ / 3 ^d	10	44	40	6	19:81	42

(a) Decomposition of diazoacetate **42** was accomplished by addition over 2 h to a refluxing catalyst/DCM solution; (b) All product ratios were obtained by GC analysis on an SPB-5 column; (c) Yields determined by crude mass and ¹H NMR integration; (d) Product ratios are the average of three separate runs; (d) **3** is the (*S,S*)-ⁱBu-BOX ligand found in Figure 2.3.

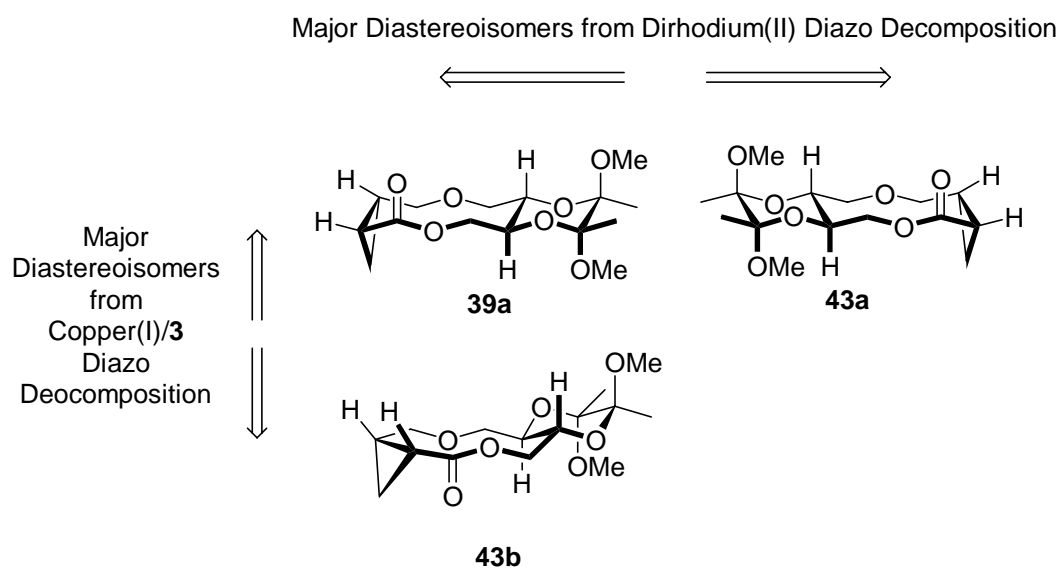
Diazo decomposition of **42** by Rh₂(5*R*-MEPY)₄ yielded **43a** and **43b** in the ratio of 67:33, making it the mismatched catalyst for **42**, whereas decomposition by match

catalyst $\text{Rh}_2(5S\text{-MEPY})_4$ afforded a 90:10 ratio of **43a** and **43b**, making it the matched catalyst. This same trend in match and mismatch was found with $\text{Rh}_2(\text{MEOX})_4$, $\text{Rh}_2(\text{MEAZ})_4$, and $\text{Rh}_2(\text{MPPIM})_4$ catalysts. The product ratios observed for $\text{Rh}_2(\text{MPPIM})_4$ catalyzed reactions were not reproducible within the 1-3% error margins, so each reaction was run three times, and the average data is reported. The comparison of diastereoselectivity in the diazo decomposition of **36** and **42** by $\text{Rh}_2(5S\text{-NEPY})_4$ also exhibits matched selectivity with **42** and mismatch selectivity with **36**. Decomposition of **36** and **42** by $\text{Rh}_2(4S\text{-DOSP})_4$ does not show diastereoselectivity or chemoselectivity differences consistent with match or mismatch selectivity. The $\text{Cu}(\text{CH}_3\text{CN})_4\text{PF}_6/\mathbf{3}$ complex exhibits complete reversal in diastereoselectivity (81:19 to 19:81) in the diazo decomposition of **36** and **42**, though comparison of the chemoselectivity in each reaction would suggest that this catalyst forms a matched pair with **36**, if one exists, as the percentage of C-H insertion products observed is much lower in this reaction.

The diastereoselectivity seen in dirhodium(II) carboxamidate catalyzed reactions shows that both matched and mismatched pairs of substrate and catalyst exist in the diazo decomposition of **36** and **42**. As expected, changing from the matched pair of **36** and $\text{Rh}_2(5R\text{-MEPY})_4$ to the enantiomer of each substrate (**42** and $\text{Rh}_2(5S\text{-MEPY})_4$) afforded the same diastereoselectivity and chemoselectivity ratios within the limits of experimental error. Diastereoselectivity in the dirhodium(II) carboxamidate catalyzed diazo decomposition of **36** and **42** is favored in the order of: $\text{Rh}_2(\text{MEPY})_4 > \text{Rh}_2(\text{MEOX})_4 > \text{Rh}_2(\text{MEAZ})_4 > \text{Rh}_2(\text{MPPIM})_4$. The difference in diastereoselectivity

seen in dirhodium(II) carboxamidate catalyzed reactions between matched and mismatched pairs was not observed in the $\text{Cu}(\text{CH}_3\text{CN})_4\text{PF}_6/\mathbf{3}$ catalyzed diazo decomposition of **36** and **42**. Rather, complete reversal of the diastereoisomer ratio formed from diazo decomposition of **36** and **42** was observed. The cyclopropane stereochemistry of the major isomer (**39a** and **43b**) formed from diazo decomposition of both **36** and **42** is identical (Figure 2.5). The remote conformational bias of the diazoacetate does not yield an enhancement or reduction of diastereoisomer ratios in $\text{Cu}(\text{CH}_3\text{CN})_4\text{PF}_6/\mathbf{3}$ catalyzed diazo decomposition of **36** and **42**, and match and mismatch pairs cannot be assigned based on diastereoselectivity. The remote conformational bias of **36** and **42** does affect chemoselectivity, and using the chemoselectivity as a means of assigning match and mismatch pairs (see section 2.3) the more chemoselective diazo decomposition of **36** by $\text{Cu}(\text{CH}_3\text{CN})_4\text{PF}_6/\mathbf{3}$ is a matched pair of substrates.

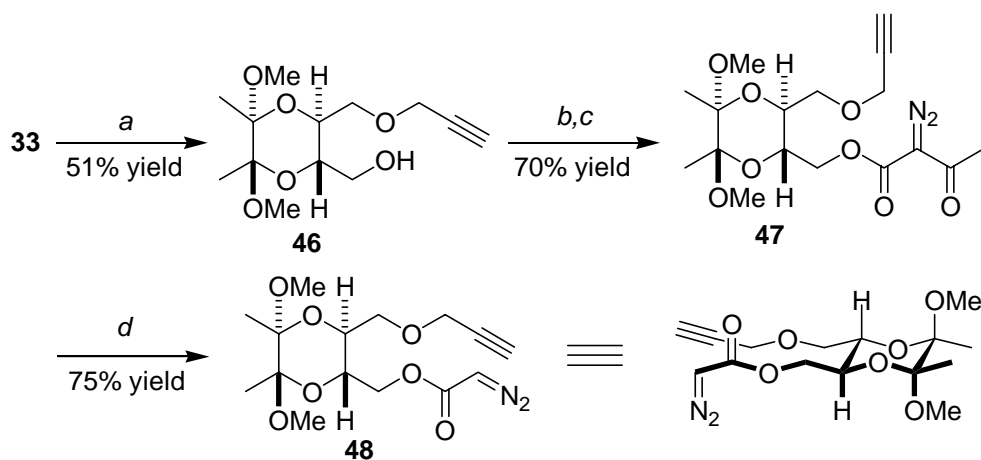
Figure 2.5 Major Diastereoisomer Selectivity



2.6.3 Cyclopropene Diastereoselectivity with Chiral Di-acetal Substrates

A previous study^{12c} describing the formation of ten-membered rings from carbene addition to a propargyl group (Scheme 2.8) showed that diazo decomposition afforded cyclopropenes with high enantioselectivity. To evaluate the effect of remote conformational bias on reaction selectivity in cyclopropene formation, diazoacetate **48** was prepared using the procedures described in Scheme 2.8 and replacing allyl bromide with propargyl bromide in the mono-alkylation of diol **36** (Scheme 2.11). Diazo decomposition of **48** was accomplished in the same manner as the decomposition of **36** (Scheme 2.12), and product evaluation of the resultant material was accomplished using GC and ¹H NMR spectroscopy as well as hydrogenation of one enantiomer of the cyclopropene to afford a cyclopropane that could be compared to known compounds **39a** and **39b**.

Scheme 2.11 Synthesis of 48



(a) NaH, allyl bromide, NaI, THF; (b) diketene, Et₃N, THF (c) MsN₃, Et₃N, THF;
(d) LiOH, THF, H₂O

The achiral dirhodium(II) tetraacetate catalyzed decomposition of **48** afforded cyclopropene diastereoisomers **49a** and **49b** in a ratio of 83:17 respectively, with the

diastereoselectivity attributed to the conformational bias in **48** (Table 2.6). Diazo decomposition of **48** catalyzed by $\text{Rh}_2(5S\text{-MEPY})_4$ afforded an increased degree of diastereoselectivity compared to the dirhodium(II) tetraacetate catalyzed reaction, with a 99:1 ratio (**49a**:**49b**), whereas $\text{Rh}_2(5R\text{-MEPY})_4$ yielded lower diastereoselectivity with a 71:29 product ratio (**49a**:**49b**). Based on the increase in diastereoisomer ratio obtained from diazo decomposition of **48** by $\text{Rh}_2(5S\text{-MEPY})_4$ compared to the diastereoisomer ratio obtained for diazo decomposition of **48** by dirhodium(II) tetraacetate, $\text{Rh}_2(5S\text{-MEPY})_4$ is the matched catalyst for **48**. The lower diastereoisomer ratio obtained from diazo decomposition of **48** by $\text{Rh}_2(5R\text{-MEPY})_4$ compared to the diastereoisomer ratio obtained for diazo decomposition of **48** by dirhodium(II) tetraacetate makes $\text{Rh}_2(5R\text{-MEPY})_4$ the mismatched catalyst for **48**. Similar diastereoselectivity, in which the *S* enantiomer was the match catalyst, was seen using $\text{Rh}_2(\text{MEAZ})_4$, $\text{Rh}_2(\text{MEOX})_4$, and $\text{Rh}_2(\text{MPPIM})_4$. The order of catalyst diastereoselectivity is: $\text{Rh}_2(5S\text{-MEPY})_4 > \text{Rh}_2(4S\text{-MEOX})_4 > \text{Rh}_2(4S\text{-MEAZ})_4 > \text{Rh}_2(4S\text{-MPPIM})_4$. The use of achiral copper(I) hexafluorophosphate in the diazo decomposition of **48** showed diastereoselectivity similar to that seen with dirhodium(II) tetraacetate, whereas catalysis by the $\text{Cu}(\text{CH}_3\text{CN})_4\text{PF}_6/\mathbf{3}$ complex afforded 69:31 diastereoselectivity that favored **49b** over **49a**. The formation of **49b** in preference to **49a** is the opposite diastereoselectivity of that seen for all dirhodium(II) catalyst *S*-enantiomers.

Scheme 2.12 Diazo Decomposition of 48

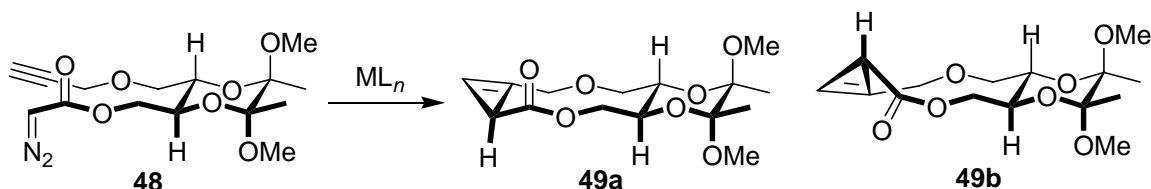


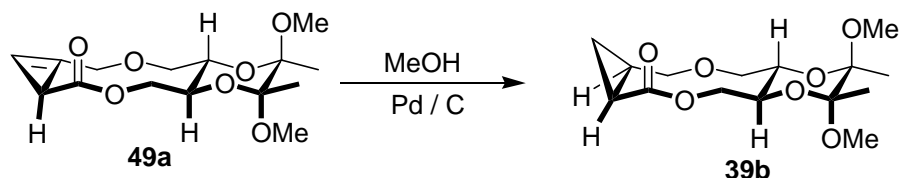
Table 2.6 Reaction Selectivity in Diazo Decomposition of 48^a

Catalyst	d.r. (49a:49b)	Yield (%)
Rh ₂ (OAc) ₄	83:17	83
Rh ₂ (5 <i>R</i> -MEPY) ₄	71:29	71
Rh ₂ (5 <i>S</i> -MEPY) ₄	99:1	80
Rh ₂ (5 <i>R</i> -MEAZ) ₄	81:19	71
Rh ₂ (5 <i>S</i> -MEAZ) ₄	91:9	79
Rh ₂ (5 <i>R</i> -MPPIM) ₄	96:4	78
Rh ₂ (5 <i>S</i> -MPPIM) ₄	89:11	75
Rh ₂ (5 <i>R</i> -MEOX) ₄	82:18	35
Rh ₂ (5 <i>S</i> -MEOX) ₄	98:2	73
Cu(CH ₃ CN) ₄ PF ₆	82:18	70
Cu(CH ₃ CN) ₄ PF ₆ / 3	39:61	72

(a) Decomposition of diazoacetate **48** was accomplished by addition over 2 h to a refluxing catalyst/DCM solution; (b) All product ratios were obtained by GC analysis on an SPB-5 column; (c) Yields determined by crude mass and ¹H NMR integration; (d) **3** is the (*S,S*)-*t*-Bu-BOX ligand found in Figure 2.3.

To determine the absolute configuration of **49a**, the substrate was derivatized by hydrogenation of the cyclopropene double bond with palladium on carbon (Scheme 2.16).^{12c} Stereochemistry of the hydrogenated material was then confirmed to be **39b** by comparison with the ¹H NMR spectrum of the authentic material isolated from diazo decomposition of **36**, and verified by GC analysis on an SPB-5 column to show an identical retention time to authentic **39**.

Scheme 2.13 Hydrogenation of 49a



To continue the evaluation of match and mismatch of conformationally biased diazoacetates with chiral catalysts, the enantiomer of **48** was needed. The synthesis of **50** was accomplished by starting with D-tartaric acid, and using the method described for preparation of **48** (Scheme 2.11), **50** was obtained as a yellow oil. Each intermediate in the synthesis of **50** was compared to that from the synthesis of **48** to verify that they had equal and opposite values of optical rotation. Diazo decomposition and product evaluation were both accomplished in the same manner as that described in the decomposition of **48** (Scheme 2.14), and the results are found in Table 2.7. The achiral dirhodium(II) tetraacetate catalyzed decomposition of **50** afforded cyclopropene diastereoisomers **51a** and **51b** in a ratio of 83:17, which is consistent with the diastereoselectivity seen in dirhodium(II) tetraacetate catalyzed decomposition of **48**. $\text{Cu}(\text{CH}_3\text{CN})_4\text{PF}_6/\mathbf{3}$ catalyzed diazo decomposition affords a 97:3 ratio (**51a**:**51b**), which is an increase over the diastereoselectivity for diazo decomposition catalyzed by copper(I) hexafluorophosphate, making it a matched catalyst with **50**, whereas the reduction in selectivity in diazo decomposition of **48** by $\text{Cu}(\text{CH}_3\text{CN})_4\text{PF}_6/\mathbf{3}$ makes it a mismatched catalyst with **48**.

Scheme 2.14 Diazo Decomposition of 49

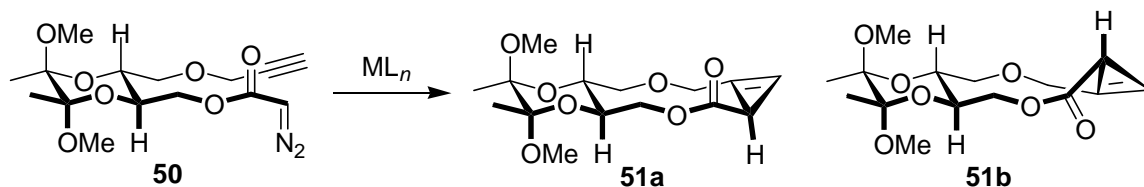


Table 2.7 Selectivity in Diazo Decomposition of 49 with Select Catalysts

Catalyst	d.r. (51a : 51b)	Yield (%)
Rh ₂ (OAc) ₄	83:17	78
Cu(CH ₃ CN) ₄ PF ₆ / 3	97:3	73

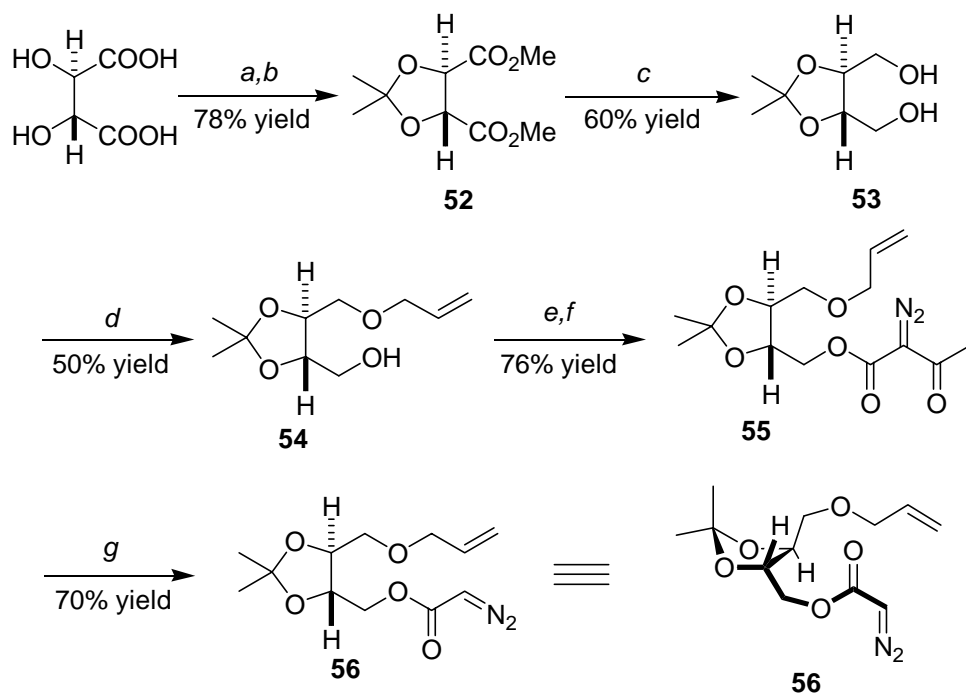
(a) Decomposition of diazoacetate was accomplished by addition over 2 h to a refluxing catalyst/DCM solution; (b) All product ratios were obtained by GC analysis on an SPB-5 column; (c) Yields determined by crude mass and ¹H NMR integration; (d) **3** is the (*S,S*)-^tBu-BOX ligand found in Figure 2.3.

Comparison of carbene addition to an allyl (**36**) versus a propargyl (**48**) shows that the conformational bias of the substrate influences cyclopropene diastereoselectivity to a greater extent than it influences cyclopropane diastereoselectivity. However, each matched dirhodium(II) carboxamidate catalyst for decomposition of **48** was the *S* enantiomer, whereas in decomposition of **36**, the matched catalyst was the *R* enantiomer. The difference in which enantiomer is the matched catalyst suggests that the remote conformational bias influences the olefin approach to the metal carbene intermediate and the propargyl approach to the metal carbene intermediate in different ways. This difference between allyl and propargyl groups is also seen in the diazo decompositions of **36** and **50** catalyzed by the Cu(CH₃CN)₄PF₆/**3** complex, where diastereoselectivity is greater for the matched propargyl substrate (**50**) than the matched allyl substrate (**36**), but the dihedral angle of the dioxane ring leading to the conformational bias of the diazoacetate is inverted between **50** and **36**.

2.6.4 Modification of the Conformational Bias

Having designed diazoacetates with a remote conformational bias that originates from the dihedral angle between carbon-1 and carbon-4 of threitol, assessment of the relationship between the dihedral angle and diastereoselectivity in carbene addition reactions is also important. By forming five-membered dioxolane **52** from tartaric acid instead of the six-membered diacetal **32** used previously, the dihedral angle between the methyl esters of the substrate was modified (Scheme 2.15). Dioxolane **52** was then mono-alkylated using allyl bromide, and the synthesis of diazoacetate **56** was completed using diketene, then methanesulfonyl azide, followed by hydrolysis with LiOH.

Scheme 2.15 Dimethyldioxolane Formation



2.6.5 Cyclopropane Diastereoselectivity with Chiral Dioxolane Substrates

With diazoacetate **56** in hand, the effect of the conformational bias on diastereoselectivity was evaluated. Diazoacetate **56** was decomposed by syringe pump addition of a solution of **56** in methylene chloride to a refluxing solution of the catalyst dissolved in methylene chloride over one hour. The product mixture was then analyzed by ¹H NMR and diastereoisomer ratios were determined by integration of peak areas for the doublet-doublet signal from **57b** at 4.79 ppm and the triplet signal from **57a** at 4.68 ppm, and the results are described in Table 2.8. Product ratios could not be determined by GC analysis on an SPB-5 column or a chiral B-PH column, as conditions for separation were not found. In addition, other product materials present could not be isolated, as no conditions could be found under which

multiple compounds were fully isolated in column chromatography or by thin layer chromatography on silica gel. This negated the evaluation of products formed from other reaction pathways, such as δ -lactone formation resulting from C-H insertion. Absolute stereochemistry of the major isomer of **57** was assigned based on the assumption that the stereochemistry of the major isomer formed from diazo decomposition of **56** by $\text{Rh}_2(5R\text{-MEPY})_4$ would match the stereochemistry found for the major isomer of **39**, which was determined by single crystal X-ray diffraction to be **39a** (Figure 2.4).

Scheme 2.16 Product Selectivity in Diazo Decomposition of **56**

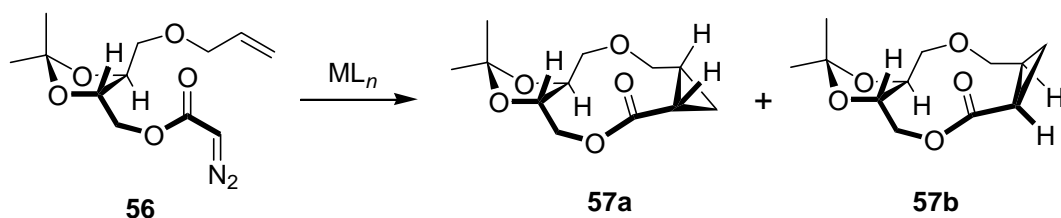


Table 2.8 Product Selectivity in Diazo Decomposition of **56^a**

Catalyst	d.r. (57a : 57b) ^b	Yield (%) ^c
Rh ₂ (OAc) ₄	52:48	78
Rh ₂ (5 <i>R</i> -MEPY) ₄	72:28	50
Rh ₂ (5 <i>S</i> -MEPY) ₄	38:62	21
Rh ₂ (5 <i>R</i> -MEAZ) ₄	74:26	70
Rh ₂ (5 <i>S</i> -MEAZ) ₄	30:70	68
Rh ₂ (5 <i>R</i> -MPPIM) ₄	58:42	26
Rh ₂ (5 <i>S</i> -MPPIM) ₄	43:57	41
Rh ₂ (5 <i>R</i> -MEOX) ₄	63:37	36
Rh ₂ (5 <i>S</i> -MEOX) ₄	52:48	38
Cu(CH ₃ CN) ₄ PF ₆	50:50	60
Cu(CH ₃ CN) ₄ PF ₆ / 3 ^d	50:50	72
Cu(CH ₃ CN) ₄ PF ₆ / <i>S,S</i> - 37 ^d	40:60	55
Cu(CH ₃ CN) ₄ PF ₆ / <i>R,R</i> - 37 ^d	79:21	52

(a) Decomposition of diazoacetate **56** was accomplished by addition over 2 h to a refluxing catalyst/DCM solution; (b) All product ratios were obtained by ¹H NMR integration values; (c) Yields determined by crude mass and ¹H NMR integration; (d) **3** is the (*S,S*)-*t*-Bu-BOX ligand and **37** are the Ph-BOX ligands found in Figure 2.3.

Diazo decomposition of **56** by achiral dirhodium(II) tetraacetate afforded cyclopropanes **57a** and **57b** in a ratio of 52:48, demonstrating very low diastereoselectivity resulting from the conformational bias of the diazoacetate (Scheme 2.16). Decomposition of **56** by Rh₂(5*R*-MEPY)₄ yielded a 72:28 ratio of **57a**:**57b**, whereas Rh₂(5*S*-MEPY)₄ afforded cyclopropanes **57a** and **57b** in a ratio of 38:62 (Table 2.8). Rh₂(5*R*-MEPY)₄ afforded higher diastereoselectivity than the Rh₂(5*S*-MEPY)₄ catalyst, but, because diastereoisomer ratios from both reactions are

greater than the diastereoisomer ratio obtained using dirhodium(II) tetraacetate as a catalyst, this is not a case of match/mismatch interactions. Rather, the conformational bias of **56** can only be described as influencing the diastereoselectivity of $\text{Rh}_2(5S\text{-MEPY})_4$ and $\text{Rh}_2(5R\text{-MEPY})_4$ differently. Copper(I) hexafluorophosphate catalyzed decomposition of **56** afforded a 50:50 mixture of diastereoisomers of **57**, and catalysis by the $\text{Cu}(\text{CH}_3\text{CN})_4\text{PF}_6/\mathbf{3}$ complex also yielded a 50:50 mixture of diastereoisomers.

To continue evaluating the relationship between the dihedral angle in the diazoacetate and diastereoselectivity in carbene addition reactions, the enantiomer of **56**, diazoacetate **58**, was synthesized by starting from D-tartaric acid and following the synthetic procedure described in Scheme 2.15. Diazo decomposition of diazoacetate **58** by dirhodium(II) tetraacetate (Scheme 2.18) afforded cyclopropanes **59a** and **59b** in a ratio of 53:47, demonstrating nearly identical diastereoselective control seen in dirhodium(II) tetraacetate decomposition of **56** (Table 2.9). As these ratios were determined by ^1H NMR peak area integration, the 1% difference was considered to be within error limits. Decomposition of **58** by $\text{Rh}_2(5R\text{-MEPY})_4$ yielded a 34:66 ratio of **59a** and **59b** respectively, whereas the catalyst $\text{Rh}_2(5S\text{-MEPY})_4$ afforded cyclopropanes **59a** and **59b** in a ratio of 72:28. Similar results were obtained using other chiral dirhodium(II) carboxamidates. The use of the $\text{Cu}(\text{CH}_3\text{CN})_4\text{PF}_6/\mathbf{3}$ complex to catalyze decomposition of **58** afforded mixture of the diastereoisomers of **59** of <5:95, providing the highest diastereoselectivity in the diazo decomposition of diazoacetates **56** and **58**.

Scheme 2.17 Diazo Decomposition of **58**

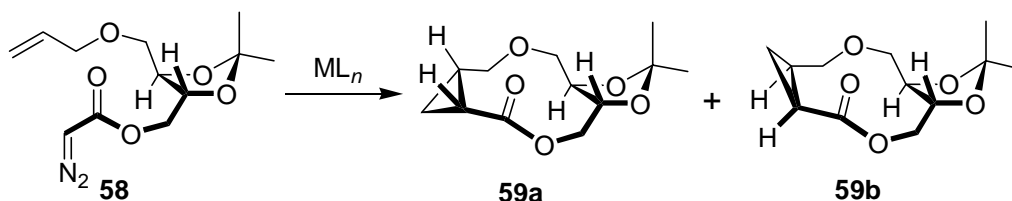


Table 2.9 Product Selectivity in Diazo Decomposition of **58^a**

Catalyst	d.r. (59a : 59b) ^b	Yield (%) ^c
$Rh_2(OAc)_4$	53:47	78
$Rh_2(5R-MEPY)_4$	34:66	42
$Rh_2(5S-MEPY)_4$	72:28	43
$Rh_2(5R-MEAZ)_4$	30:70	47
$Rh_2(5S-MEAZ)_4$	73:27	57
$Rh_2(5R-MPPIM)_4$	43:57	67
$Rh_2(5S-MPPIM)_4$	60:40	57
$Rh_2(5R-MEOX)_4$	43:57	55
$Rh_2(5S-MEOX)_4$	64:36	44
$Cu(CH_3CN)_4PF_6/3^d$	<5:95	42
$Cu(CH_3CN)_4PF_6/S,S-37^d$	35:65	53
$Cu(CH_3CN)_4PF_6/R,R-37^d$	81:19	50

(a) Decomposition of diazoacetate **58** was accomplished by addition over 2 h to a refluxing catalyst/DCM solution; (b) All product ratios were obtained by 1H NMR integration values; (c) Yields determined by crude mass and 1H NMR integration; (d) **3** is the (*S,S*)-*t*Bu-BOX ligand and **37** are the Ph-BOX ligands found in Figure 2.3.

The results from diazo decomposition of **56** and **58** provide a different picture of diastereoselectivity from that seen in decomposition of diazoacetates **36** and **42**. Results using achiral dirhodium(II) tetraacetate and copper(I) hexafluorophosphate catalysts both show that the conformational bias of the diazoacetate provides no greater than 53:47 diastereoselectivity in the formation of cyclopropanes **57** and **59**. The use of all chiral dirhodium(II) carboxamidate catalysts in the decomposition of **56** and **58** affords greater diastereoselectivity than the decomposition catalyzed by dirhodium(II) tetraacetate. These diazo decomposition reactions also demonstrate a

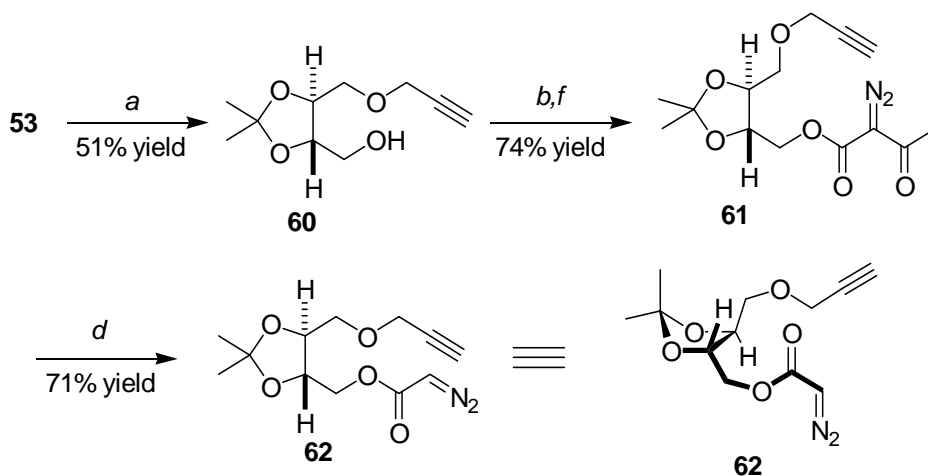
difference in the major diastereoisomer obtained from diazo decomposition using the *S*-enantiomer of a catalyst versus the major diastereoisomer obtained using the *R*-enantiomer of a catalyst. Whereas diazo decomposition of **36** with chiral dirhodium(II) carboxamidate catalysts would yield **39a** as the major diastereoisomer for both match and mismatch cases, decomposition of **56** will afford **57a** as the major diastereoisomer with Rh₂(*5R*-MEPY)₄, but **57b** as the major diastereoisomer with Rh₂(*5S*-MEPY)₄. Diastereoselectivity in the dirhodium(II) carboxamidate catalyzed reactions is favored in the order of: Rh₂(MEAZ)₄ > Rh₂(MEPY)₄ > Rh₂(MEOX)₄ > Rh₂(MPPIM)₄.

Diazo decomposition of **58** by Cu(CH₃CN)₄PF₆/**3** yields the diastereoisomer **59b** almost exclusively (<5:95), while decomposition of **56** catalyzed by the Cu(CH₃CN)₄PF₆/**3** complex formed both **57a** and **57b** in almost identical quantities, suggesting that Cu(CH₃CN)₄PF₆/**3** is the matched catalysts for **58** and the mismatched catalyst for **56**. However, the diastereoselectivity for diazo decomposition by copper(I) hexafluorophosphate is so small that the mismatch case cannot be verified. The constrained dihedral angle of **56** is only slightly different from that of **36**, yet the difference in diastereoselectivity in diazo decomposition catalyzed by Cu(CH₃CN)₄PF₆/**3** is very pronounced. Prompted by the unexpectedly high degree of diastereoselectivity seen using Cu(CH₃CN)₄PF₆/**3**, the effect of changing the chiral bis-oxazoline ligand was explored. The use of *S,S*-**37** and *R,R*-**37** as chiral ligands in copper(I) catalyzed diazo decomposition of **56** and **58** did not further enhance diastereoselectivity, and ligand modification was not pursued further.

2.6.6 Cyclopropene Diastereoselectivity with Chiral Dioxolane Substrates

Diazoacetate **62** was synthesized from the previously described precursor **53** by mono-alkylation with propargyl bromide to yield **60** (Scheme 2.18). The diazoacetate **62** was then synthesized by acylation of **60** using diketene, diazo transfer from methanesulfonyl azide, and hydrolysis using LiOH.

Scheme 2.18 Synthesis of **62**



(a) NaH, allyl bromide, NaI, THF; (b) diketene, Et₃N, THF (c) MsN₃, Et₃N, THF; (d) LiOH, THF, H₂O

The dirhodium(II) tetraacetate catalyzed diazo decomposition of **62** (Scheme 2.21) afforded cyclopropene **63** as two diastereoisomers in a 52:48 ratio (**63a**:**63b**), showing that the conformational bias of **63** does not innately promote high diastereoselectivity (Table 2.10). Diazo decomposition of **62** by Rh₂(5*R*-MEPY)₄ yields a 91:9 ratio of **63a** to **63b**, while a 13:87 ratio (**63a** to **63b**) is obtained using Rh₂(5*S*-MEPY)₄, and other chiral dirhodium(II) carboxamidate catalysts show similar reflective outcomes. In these reactions there does not appear to be a match/mismatch relationship between substrate and catalyst. The stereochemical assignments for **63a** and **63b** are based on the known major isomer **49a** formed from diazo decomposition

of **48** by $\text{Rh}_2(5S\text{-MEPY})_4$, and the assumption that the major isomer from this reaction is the same as that in diazo decomposition of **62**. The decomposition of **62** by all other dirhodium(II) carboxamidate catalysts afforded lower diastereoselectivity than $\text{Rh}_2(5R\text{-MEPY})_4$. The $\text{Cu}(\text{CH}_3\text{CN})_4\text{PF}_6/\mathbf{3}$ catalyzed decomposition of **62** afforded a 26:74 ratio (**63a**:**63b**).

Scheme 2.19 Diazo decomposition of **62**

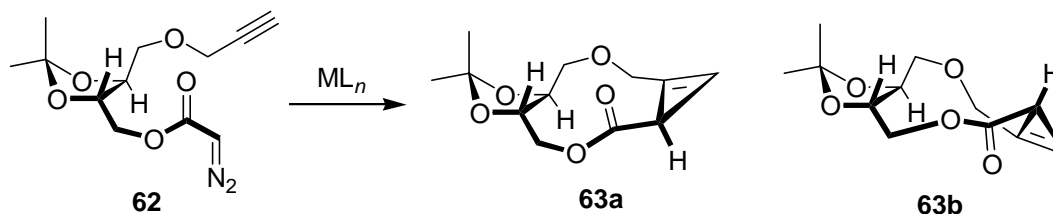


Table 2.10 Product Selectivity in Diazo Decomposition of **62**

Catalyst	d.r. (63a : 63b)	Yield (%)
$\text{Rh}_2(\text{OAc})_4$	52:48	42
$\text{Rh}_2(5R\text{-MEPY})_4$	91:9	91
$\text{Rh}_2(5S\text{-MEPY})_4$	13:87	64
$\text{Rh}_2(5R\text{-MEAZ})_4$	75:25	48
$\text{Rh}_2(5S\text{-MEAZ})_4$	33:67	33
$\text{Rh}_2(5R\text{-MPPIM})_4$	60:40	49
$\text{Rh}_2(5S\text{-MPPIM})_4$	52:48	50
$\text{Rh}_2(5R\text{-MEOX})_4$	76:24	28
$\text{Rh}_2(5S\text{-MEOX})_4$	36:64	40
$\text{Cu}(\text{I})\text{PF}_6$	50:50	56
$\text{Cu}(\text{CH}_3\text{CN})_4\text{PF}_6/\mathbf{3}$	26:74	25

(a) Decomposition of diazoacetate **62** was accomplished by addition over 2 h to a refluxing catalyst/DCM solution; (b) All product ratios were obtained by ^1H NMR integration values; (c) Yields determined by crude mass and ^1H NMR integration; (d) **3** is the (*S,S*)-*t*-Bu-BOX ligand found in Figure 2.3.

Diazoacetate **64** was synthesized starting from D-tartaric acid following the synthetic procedure used for the synthesis of **62** (Scheme 2.18). The dirhodium(II) tetraacetate

catalyzed diazo decomposition of **64** (Scheme 2.20) affords a 52:48 ratio of cyclopropenes **65a** and **65b** respectively, which is identical to the previous results obtained in the dirhodium(II) tetraacetate catalyzed diazo decomposition of **62** (Table 2.11). Diazo decomposition of **64** by Rh₂(5*S*-MEPY)₄ yields a 91:9 ratio of **65a** to **65b**, while, using Rh₂(5*R*-MEPY)₄, a 13:87 ratio (**65a** to **65b**) is obtained. Based on the higher diastereoselectivity in the diazo decomposition of **64** by Rh₂(5*S*-MEPY)₄ and Rh₂(5*R*-MEPY)₄ versus the diastereoselectivity in the diazo decomposition of **64** by Rh₂(OAc)₄, match and mismatch do not exist. Instead, the interaction between Rh₂(5*S*-MEPY)₄ and **64** affords a higher degree of diastereoselectivity than that observed for Rh₂(5*R*-MEPY)₄ and **64**, and each enantiomer of the catalyst favors a different diastereoisomer of **65**. The Cu(CH₃CN)₄PF₆/**3** catalyzed decomposition of **64** afforded a 61:39 ratio of **65a**:**65b**, which is lower diastereoselectivity compared to diazo decomposition of **62** by Cu(CH₃CN)₄PF₆/**3**.

Scheme 2.20 Diazo Decomposition of **64**

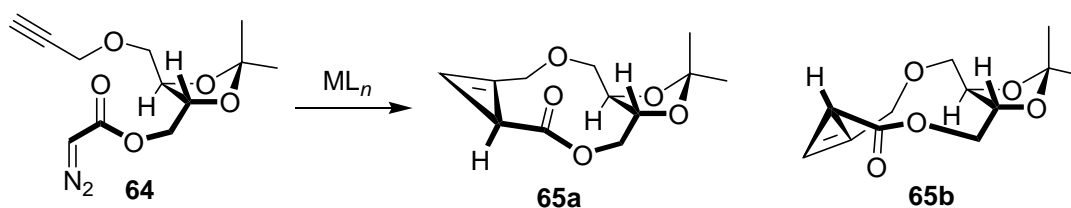


Table 2.11 Diazo Decomposition of **64**

Catalyst	d.r. (65a : 65b)	Yield (%)
Rh ₂ (OAc) ₄	52:48	42
Rh ₂ (5- <i>R</i> -MEPY) ₄	13:87	64
Rh ₂ (5- <i>S</i> -MEPY) ₄	91:9	91
Cu(CH ₃ CN) ₄ PF ₆ / 3	61:39	72

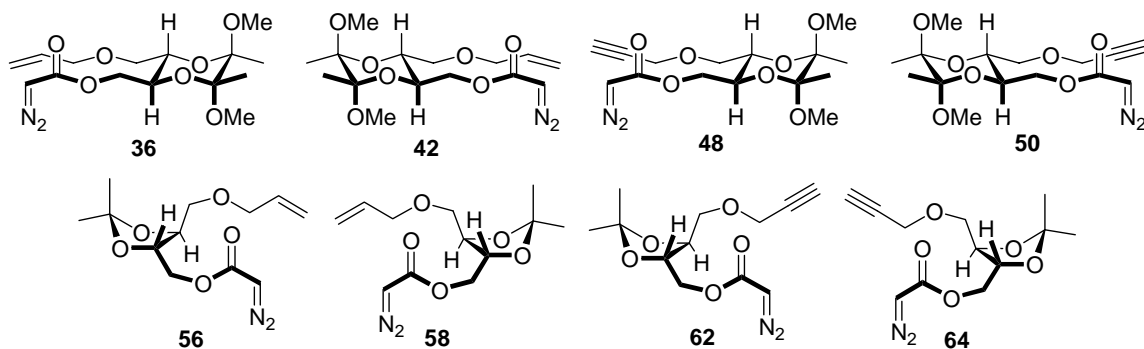
(a) Decomposition of diazoacetate **64** was accomplished by addition over 2 h to a refluxing catalyst/DCM solution; (b) All product ratios were obtained by ¹H NMR integration values; (c) Yields determined by crude mass and ¹H NMR integration; (d) **3** is the (*S,S*)-*t*-Bu-BOX ligand found in Figure 2.3.

Diazo decomposition of **62** and **64** by achiral dirhodium(II) tetraacetate or copper(I) hexafluorophosphate affords cyclopropenes with only 52:48 diastereoselectivity. The diastereoselectivities seen in the diazo decomposition of **62** using chiral dirhodium(II) carboxamidates are lower than those seen in the decomposition of **48**, which has a propargyl functional group but a different conformational bias. This suggests that the conformational bias from the five-membered dioxolane configurational constraint is less favorable for enhancement of diastereoselectivity in double asymmetric induction using the catalysts described. It should also be noted that yields in these reactions are also lower than those seen in the diazo decomposition of **48**. The most striking observation is that, whereas diazo decomposition of **48** by chiral dirhodium(II) carboxamidates provides a match/mismatch interaction, the diazo decomposition of **62** does not provide a match/mismatch relationship between catalyst and substrate.

2.7 Discussion and Conclusions

In this investigation eight different diazoacetates were decomposed by dirhodium(II) tetraacetate, dirhodium(II) carboxamides, copper(I) hexafluorophosphate, and copper(I) complexed by chiral bis-oxazoline ligands. The diazoacetates can be divided into sub-groups based on the functional group or the conformational bias in the substrate. The conformational bias in diazoacetates **36**, **42**, **48**, and **50** (Figure 2.6) affords greater than 2:1 ratios of diastereoisomers from diazo decomposition by achiral catalysts, whereas diazo decomposition of chiral dioxolane diazoacetates **56**, **58**, **62**, and **64** by achiral catalysts shows almost no diastereoselectivity in ten-membered ring formation. The subtle change in the dihedral angle by changing from a five-membered dioxolane ring to a six-membered di-acetal ring increases the diastereoselectivity from just 52:48 (**63a:63b**) to 83:17 (**49a:49b**).

Figure 2.6 Diazoacetate Structures



Diazo decomposition of the conformationally biased diazoacetates **36**, **42**, **48**, and **50** by chiral dirhodium(II) carboxamidate catalysts forms a matched pair between diazoacetate and catalyst yielding chiral ten-membered ring lactones with increased diastereoselectivity, or a mismatched pair between diazoacetate and catalyst with

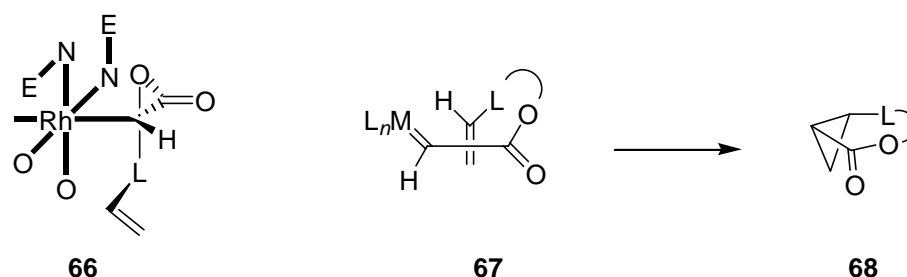
lower diastereoselectivity than the match pair. However, diazo decomposition of **56**, **58**, **62**, and **68** by chiral dirhodium(II) carboxamides does not afford a match/mismatch relationship between catalyst and substrate.

The diazo decomposition of **36** catalyzed by a $\text{Cu}(\text{CH}_3\text{CN})_4\text{PF}_6/\mathbf{3}$ complex yields cyclopropane **39** in an 81:19 ratio (**39a:39b**) of diastereoisomers and decomposition of **42** catalyzed by the $\text{Cu}(\text{CH}_3\text{CN})_4\text{PF}_6/\mathbf{3}$ complex yields **43** in a 19:81 ratio (**43a:43b**), which is not consistent with the match/mismatch behavior seen using dirhodium(II) carboxamides. Only chemoselectivity allows for possible differentiation between match and mismatch interactions, where diazo decomposition of **36** by $\text{Cu}(\text{CH}_3\text{CN})_4\text{PF}_6/\mathbf{3}$ affords just two percent of **40**, while diazo decomposition of **42** yields forty-four percent of **44**, making **42**/($\text{Cu}(\text{CH}_3\text{CN})_4\text{PF}_6/\mathbf{3}$) the mismatch pair. In contrast, decomposition of diazoacetate **56** exhibits a mismatch with the $\text{Cu}(\text{CH}_3\text{CN})_4\text{PF}_6/\mathbf{3}$ catalyst, giving a 50:50 mixture (**57a:57b**), while diazo decomposition of **58** and $\text{Cu}(\text{CH}_3\text{CN})_4\text{PF}_6/\mathbf{3}$ demonstrates match diastereoselectivity, forming **59b:59a** in a ratio of 95:5. These match/mismatch results are not identical to the results of dirhodium(II) carboxamide catalyzed decomposition of the same diazoacetates, but they are consistent with the mechanism of addition described by Doyle and Hu,²⁵ further illustrating the differences between chiral copper(I) and dirhodium(II) carboxamide catalysts.

²⁵ Doyle, M.P., Hu, W. *J. Org. Chem.* **2000**, 65, 8839.

Doyle and co-workers have reported computational work that describes the conformational minima of $\text{Rh}_2(5R\text{-MEPY})_4$ bonded to a carbomethoxy carbene,²⁶ and subsequent work²⁵ that described the trajectory of an olefin to the reactive carbene carbon (**66**).²⁷ The olefin trajectory was described using a metal carbene intermediate (**67**) with the tethered olefin (L = linker) rotating clockwise to avoid steric repulsion from the chiral esters of the (*S*) configured dirhodium(II) carboxamidate (E = ester), leading to the observed cyclopropane stereochemistry of **68** (Scheme 2.21).

Scheme 2.21 Influence of Dirhodium(II) Carboxamidate on Olefin Trajectory

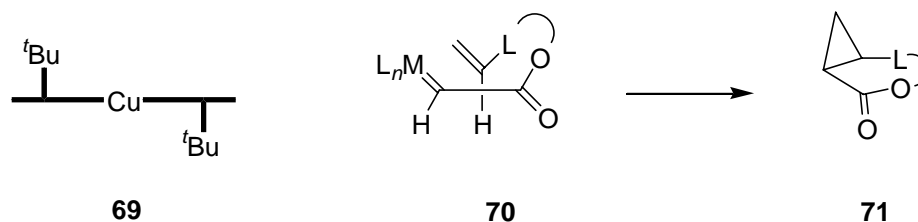


From product analysis, it was determined that the chiral $\text{Cu}(\text{CH}_3\text{CN})_4\text{PF}_6/\mathbf{3}$ complex, which is also the *S* enantiomer, favors the same clockwise rotation of the tethered olefin (L = linker) about the metal carbene, but a different olefin orientation in its approach to the metal carbene intermediate (**69**). The result of the change in olefin orientation from **67** to **70** is the formation of **71**, the enantiomer of **68** that was formed using chiral dirhodium(II) carboxamidate catalysts (Scheme 2.22).

²⁶ Doyle, M.P.; Winchester, W.R.; Hoorn, J.A.A.; Lynch, V.; Simonsen, S.H.; Ghosh, R. *J. Am. Chem. Soc.* **1993**, *115*, 9968.

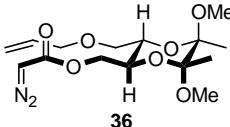
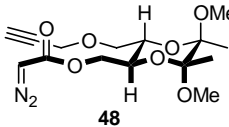
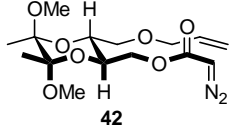
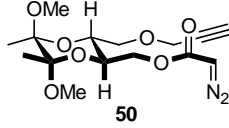
²⁷ For further discussion see section 1.3.

Scheme 2.22 Chiral Influence of Copper(I)/3 Complex on Olefin Trajectory



The diastereoselectivity seen in the diazo decomposition of conformationally biased diazoacetates with chiral dirhodium(II) carboxamidates is very different from that seen using the same diazoacetates and the chiral copper(I) catalysts described (Table 2.12). Whereas the representative carboxamidate $\text{Rh}_2(5R\text{-MEPY})_4$ affords the same relative stereochemistry for the major isomer from diazo decomposition of **36** and **42** or of **48** and **50**, the $\text{Cu}(\text{CH}_3\text{CN})_4\text{PF}_6/\mathbf{3}$ catalyzed reaction affords major isomers in which the relative stereochemistry is not the same, as the stereocenter(s) of the major isomer created from carbene addition are the same regardless of the conformational bias.

Table 2.12 Comparison of Diastereoselectivity Between Copper(I) and $\text{Rh}_2(5R\text{-MEPY})_4$

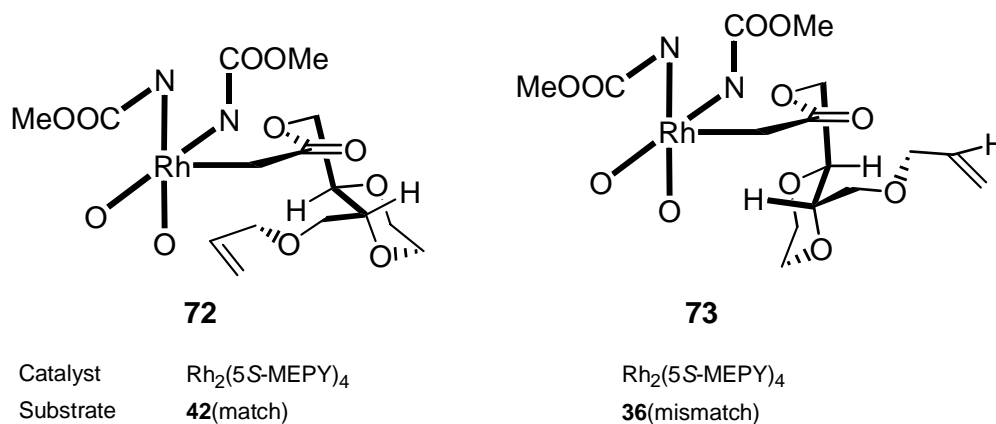
$\text{Rh}_2(5R\text{-MEPY})_4$ d.r.	Substrate	$\text{Cu}(\text{CH}_3\text{CN})_4\text{PF}_6/\mathbf{3}$ d.r.	Substrate	$\text{Rh}_2(5R\text{-MEPY})_4$ d.r.
91:9	 36	81:19	 48	71:29
67:33	 42	19:81	 50	99:1 ^a

(a) diastereoisomer ratio obtained from $\text{Rh}_2(5S\text{-MEPY})_4$ and **48**

Taking the model conformations **67** and **70** described in Schemes 2.21 and 2.22, the influence of the conformational bias in the substrate, which is the linker in **67** and **70**,

on the approach of the olefin to the metal carbene intermediate was evaluated using molecular models. Knowing that the remote conformational bias of **36** and **42** influences the facial selectivity in olefin approach to the metal carbene, the orientation of the linker in relationship to the metal center was considered. The 1,4-dioxane linker in **72** is repelled from the face of the dirhodium(II) catalyst, orienting the substrate such that the conformational bias derived from the 1,4-dioxane ring directs the olefin toward the chiral metal center in the matched reaction between $\text{Rh}_2(5S\text{-MEPY})_4$ and **42** (Figure 2.7). The olefin orientation in relation to the catalyst face caused by the conformational bias of the substrate favors the formation of **43a**. Conversely, in the formation of metal carbene intermediate **77** from diazo decomposition of **36**, the conformational bias creates a mismatch between catalyst and substrate, extending the olefin away from the catalyst, reducing the facial selectivity in carbene addition to the olefin. Intermediate **73** also shows that the C-H bond that must undergo insertion to form a six-membered lactone is favorably oriented in relationship to the metal carbene intermediate.

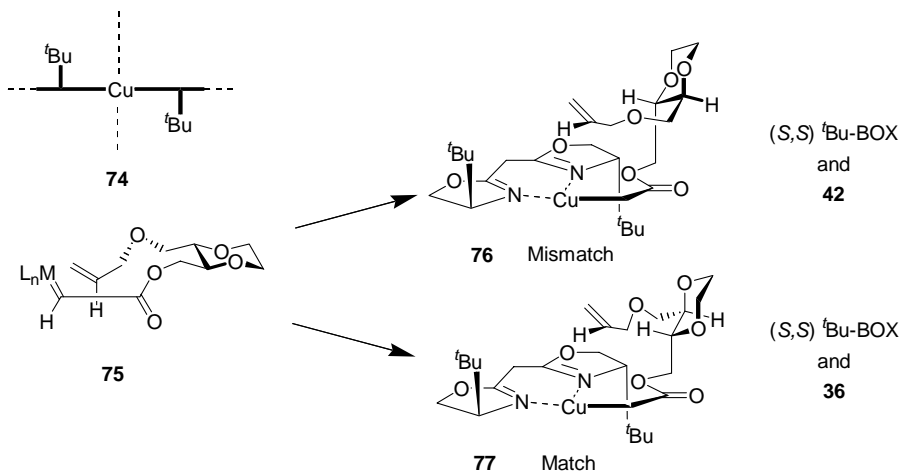
Figure 2.7 Rhodium-Carbene Intermediate



Copper(I) catalyzed diazo decomposition of **36** is different from dirhodium(II) catalyzed diazo decomposition, because of the C_2 -symmetry of chiral ligand **3** and the difference in preferred olefin orientation to the metal carbene intermediate. The $\text{Cu}(\text{CH}_3\text{CN})_4\text{PF}_6/\mathbf{3}$ complex viewed in the plane of the bis-oxazoline can be divided into quadrants in which bulky chiral *tert*-butyl groups occupy the upper left and lower right quadrants, while the remaining two quadrants are open (**74**). The metal-carbene intermediate **76**, formed from diazo decomposition of **36**, orients itself so that the remote conformational bias is placed in an open quadrant, allowing the trajectory of the olefin to the carbene to form the major diastereoisomer **39a** observed in this reaction (Figure 2.8). Diazo decomposition of **42** provides a metal carbene intermediate (**77**) that also places the remote conformational bias in an open quadrant of the chiral bis-oxazoline ligand, even though the conformational bias of the substrate is reversed. The conformation of **77** also favors the trajectory of the olefin to the carbene that is illustrated in **76**. The result is that the chiral bis-oxazoline

ligand plays a more significant role in diastereoselectivity than the conformational bias of diazoacetate compounds **36** and **42**.

Figure 2.8 Copper Catalyzed Diastereoselectivity



Changing the conformational bias by substrate modification from six-membered diacetal **36** to the five-membered dioxolane **56** also influences diastereoselectivity seen in the dirhodium(II) and copper(I) catalyzed carbene addition reactions. The configuration of the dioxolane alters the conformational bias of **56** in a way that affords only minimal diastereoselectivity (52:48 d.r.) in dirhodium(II) tetraacetate or copper(I) hexafluorophosphate catalyzed diazo decomposition. Comparison of the data for decomposition of diazoacetates **36** and **56** shows that modifying the conformational bias by increasing the dihedral angle between carbon-1 and carbon-4 of the threitol based linker does not automatically enhance the conformational bias and lead to increased diastereoselectivity in the reaction.

The semi-empirical method Masamune *et al* described to predict the outcome of double asymmetric induction reactions used multiplication of the diastereoisomer

ratios obtained independently using each chiral reactant with an achiral reactant (Section 2.2).² As a comparable reaction related to the conformationally biased diazoacetates used herein, previously described work using achiral diazoacetate **21** showed that diazo decomposition by $\text{Rh}_2(5S\text{-MEPY})_4$ yielded **23** with 47% ee (74:26 e.r.) (Scheme 2.5). The diastereomeric ratio obtained using achiral dirhodium(II) tetraacetate in the diazo decomposition of **36** is 70:30. Based on the method described by Masemune *et al*, multiplication of the ratios obtained from the two reactions using one chiral reagent and one achiral reagent should give an approximate ratio to be expected for the matched pair of chiral reagents, while division of these same ratios should give the approximate ratio for the mismatched pair of chiral reagents. However, there is no way of factoring in additional products that can form from competitive reaction pathways such as C-H insertion. The comparison of the data obtained with conformationally biased diazoacetates and chiral catalysts to the diastereoisomers ratios predicted by the Masamune method should show if reactions that compete with carbene addition are a contributing factor to the diastereoselectivity seen in diazo decomposition of chiral diazoacetates.

The enantiomeric ratio for diazo decomposition of **21** by $\text{Rh}_2(5S\text{-MEPY})_4$ multiplied by the diastereomeric ratio obtained using achiral dirhodium(II) tetraacetate in the diazo decomposition of **36** (74:26 x 70:30) gives the ratio 87:13, which is slightly lower than the 91:9 ratio obtained by diazo decomposition of **36** using $\text{Rh}_2(5S\text{-MEPY})_4$ as a catalyst. Division of enantiomeric ratio for diazo decomposition of **21** by $\text{Rh}_2(5S\text{-MEPY})_4$ multiplied by the diastereomeric ratio obtained using achiral

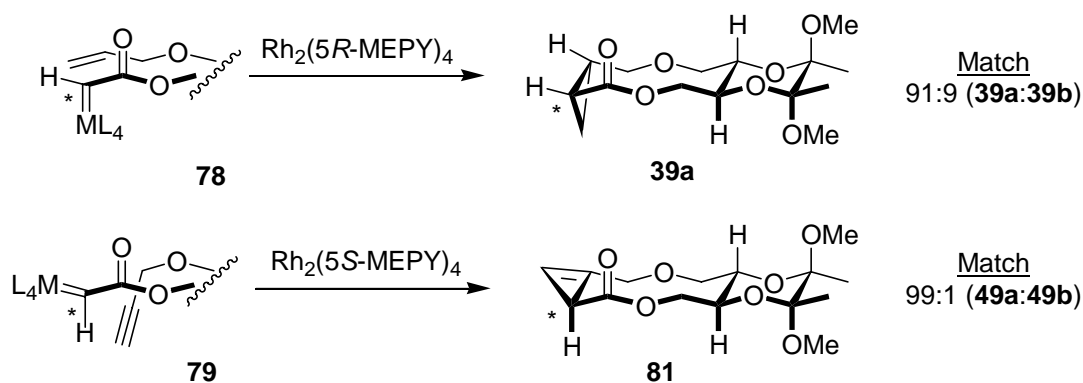
dirhodium(II) tetraacetate in the diazo decomposition of **36** (74:26/70:30) gives the ratio 55:45, which is lower than the 63:37 ratio obtained by diazo decomposition of **36** using $\text{Rh}_2(5S\text{-MEPY})_4$ as a catalyst. These results appear to agree with the diastereoselectivity predictions described by Masamune for matched catalysts and substrates, but are not as closely in agreement with the predictions in the mismatched cases, which may be due to the alternate reaction pathways such as C-H insertion that are available to dirhodium(II) metal carbene intermediates.

Diazo decomposition of **59** by achiral copper(I) hexafluorophosphate yields only a 50:50 diastereoisomer ratio. Using the multiplication of control reactions, the predicted ratio for matched catalyst and diazoacetate is 90:10, while the observed ratio is <5:95. The corresponding division of ratios for the mismatched reaction is 90:10, while the observed ratio is 50:50. This striking change in diastereoselectivity does not agree with the semi-empirical method that Masamune described² but may be partially explained with the previously discussed quadrant analogy (Figure 2.6). In each case the mismatched pair of catalyst and substrate was in a conformation that had the possibility to result in C-H insertion or reaction pathways other than carbene addition. In addition, materials not consistent with carbene addition were observed in other cases, but could not be isolated. There is no way to factor other reaction pathways such as insertion into the predictions for diastereoselectivity, but the alternate reaction pathways must be playing a role in influencing observed diastereoselectivity as material from the alternate reaction pathways is observed.

Results presented here have described the use of a remote conformational bias in the diazo decomposition of **36**, **42**, **56**, and **58** with chiral dirhodium(II) carboxamidate and $\text{Cu}(\text{CH}_3\text{CN})_4\text{PF}_6$ /**3** catalysts, in double asymmetric induction reactions that yield chiral ten-membered lactones via diastereoselective carbene addition to an allyl functional group. The diazo decomposition of **48**, **50**, **62**, and **64**, which have a propargyl functional group, also yields chiral ten-membered lactones with diastereoselectivity in the formation of cyclopropenes. The match and mismatch interactions between catalyst and substrates **48** and **50** may be explained in much the same way as the explanation given for allyl substrates, with the conformational bias influencing the trajectory of the alkyne to the carbene. However, the stereochemistry of the observed major diastereoisomer as well as the enantiomer of a catalyst that is the match to the substrate is different.

The previously referred to the work of Doyle and Hu described the trajectory of an olefin to the carbene of a dirhodium(II) carboxamidate/carbene complex (Scheme 2.21).²⁰ However, the trajectory of an alkyne to the carbene of a dirhodium(II) carboxamidate/carbene complex was not described in that discussion. The diazo decomposition of **36** and **48**, which have the same conformational bias, shows the match catalyst for **48** is the enantiomer of the match catalyst for **36**, resulting in formation of the opposite stereochemistry at the carbene center (*) of the preferred diastereoisomer (Scheme 2.23). This change in the stereochemistry is explained by considering the conformation of the alkene or alkyne relative to the metal carbene intermediate, as depicted in **78** and **79**.

Scheme 2.23 Stereochemistry by Conformation



The results of this investigation describe the impact a remote conformational bias in a diazoacetate has on diastereoselectivity in the formation of ten-membered lactones from metal carbene intermediates. This influence is then extended to double asymmetric induction with chiral dirhodium(II) carboxamidate catalysts and the $\text{Cu}(\text{CH}_3\text{CN})_4\text{PF}_6/\mathbf{3}$ complex to afford ten-membered lactones with match or mismatch interaction between substrate and catalyst. The diastereoselectivity seen in the products resulting from these diazo decomposition reactions is consistent with the semi-empirical method of evaluation described by Masamune² for other double asymmetric induction reactions, but shows that when other competitive reactions such as C-H insertion occur, the prediction of product selectivity may become more complex. However, by modifying the substrate from a dioxane to a dioxolane and modifying the conformational bias, diastereoselectivity changes from a match/mismatch interaction between catalyst and substrate to diastereoselectivity based on catalyst and modestly impacted by the chiral diazoacetate.

As a result of these studies, a methodical approach may be taken to predicting the effect of remote conformational bias on diastereoselectivity using metal carbene

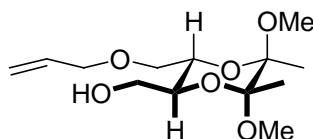
intermediates. The desired stereochemical outcome can be obtained through selection of both the catalyst and the reactive functional group on the diazoacetate. While the relative stereochemistry expected for carbene addition to allyl and propargyl functional groups is described, the degree of diastereoselectivity in double asymmetric induction reactions is not completely predictable using the Masamune method, as illustrated in the diazo decomposition of **59** catalyzed by the $\text{Cu}(\text{CH}_3\text{CN})_4\text{PF}_6/\mathbf{3}$ complex, in which diastereoselectivity is much greater than predicted by the Masamune method. In addition, the reason for the difference in trajectory of an allyl group and a propargyl group awaits discovery.

2.8 Experimental Procedures

General Methods. ^1H and ^{13}C spectra were obtained as solutions in CDCl_3 using a Bruker AM250, DRX400, DRX500, or DRX600 spectrometer; ^1H chemical shifts are reported as parts per million (ppm, δ) downfield from Me_4Si (TMS); ^{13}C chemical shifts are reported as parts per million (ppm, δ) relative to CDCl_3 (77.0 ppm). Mass spectra were obtained from the University of Arizona Mass Spectrometry Facility or the University of Maryland Mass Spectrometry Facility. Diastereoisomer ratios (d.r.) were measured on an HP5890A workstation with an HP3392 integrator with an SPB-5 column (Supelco 5% diphenylsilane / 95% dimethylsilane bonded, 30 m x 0.25 mm ID) programmed initially at 100 °C for 2 minutes then 7 °C/min heating rate to 275 °C, then maintained at that temperature for 25 minutes unless otherwise noted. Optical rotations were obtained as an average of five runs using a Jasco DIP1000 with a Na 589 nm filter. Infrared spectra were obtained using a Nicolet 560 EXC or Nicolet Impact 400D spectrophotometer as films on KBr plates with absorptions recorded in wavenumbers (cm^{-1}). All reagents were obtained from commercial sources and used as received unless otherwise noted. Anhydrous tetrahydrofuran (THF) was distilled over Na^0 /benzophenone ketyl, and anhydrous dichloromethane (DCM) was distilled over CaH_2 prior to use. Thin layer chromatography was performed on EM Scientific Silica Gel 60 F_{254} glass-backed plates with visualization by aqueous cerium molybdate solution.²⁸ All syringe pump additions were performed using a Kazel syringe pump. Chromatographic purification was performed using Silicycle 40-63 μm , 60 Å silica gel. Sodium hydride was used as a 95% suspension

²⁸ *Handbook of Thin-Layer Chromatography* J. Sherman and B. Fried, Eds., Marcel Dekker, New York, NY, 1991.

in mineral oil. Methanesulfonyl azide was prepared from methanesulfonyl chloride and sodium azide and was used without distillation.²⁹ Preparation of copper(I) hexafluorophosphate,³⁰ 2,2-bis[2-[4(*S*)-*tert*-butyl-1,3-oxazolinyl]] propane ((*S,S*)-*t*Bu-BOX),³¹ Rh₂(4*S*-MEPY)₄,³² Rh₂(4*S*-MPPIM)₄,³³ Rh₂(4*S*-MEOX)₄,³⁴ and Rh₂(4*S*-MEAZ)₄,³⁵ and Rh₂(4*S*-DOSP)₄³⁶ have been previously reported. All reactions were performed under an atmosphere of argon unless otherwise noted.



(2*S*,3*S*,5*R*,6*R*)-5,6-Dimethoxy-5,6-dimethyl-2-allyloxymethyl-3-(hydroxy)methyl-[1,4]-dioxane (34). To a stirred solution of (2*S*,3*S*,5*R*,6*R*)-5,6-dimethoxy-5,6-dimethyl-2,3-di(hydroxy)methyl-[1,4]-dioxane³⁷ (4.0 g, 17 mmol, 1.0 eq), and NaI (0.076 g, 0.51 mmol, 0.030 eq) in THF (125 mL) was added NaH (0.45 g, 18 mmol, 1.1 eq) as one portion. The solution instantly began to evolve gas and over five minutes produced a cloudy white suspension. After gas evolution had subsided, allyl bromide (1.9 mL, 22 mmol, 1.3 eq) was added as one aliquot. The solution was stirred for 12 h, then diluted with ethyl ether (125 mL) and washed with 2.5 M

²⁹ Danheiser, R.L.; Miller, R.F.; Brisbois, R.G.; Park, S.Z. *J. Org. Chem.* **1990**, *55*, 1959-64.

³⁰ Kubas, G.J. *Inorg. Synth.* **1979**, *19*, 90.

³¹ Evans, D.A.; Peterson, G.S.; Johnson, J.S.; Barnes, D.M.; Campos, K.R.; Woerpel, K.A. *J. Org. Chem.* **1998**, *63*, 4541-44.

³² Doyle, M.P.; Winchester, W.R.; Hoorn, J.A.; Lynch, V.; Simonson, S.H.; Ghosh, R.J. *J. Am. Chem. Soc.* **1993**, *115*, 9968-78.

³³ Doyle, M.P.; Zhou, Q.-L.; Raab, C.E.; Roos, G.H.P.; Simonsen, S.H.; Lynch, V. *Inorg. Chem.*, **1996**, *35*, 6064-73.

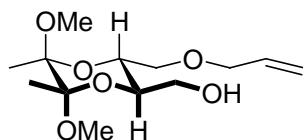
³⁴ Doyle, M.P.; Dyatkin, A.B.; Protopopova, M.N.; Yang, C.I.; Miertschin, C.S.; Winchester, W.R.; Simonsen, S.I.; Lynch, V.; Ghosh, R. *Recueil Trav. Chim. Pays-Bas*, **1995**, *114*, 163.

³⁵ Doyle, M.P.; Davies, S.B.; Hu, W.H. *J. Org. Chem.*, **2000**, *65*, 8839.

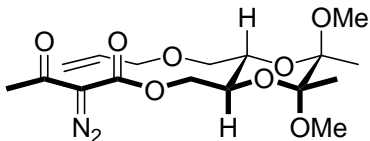
³⁶ Davies, H.M.L.; Bruzinski, P.R.; Lake, D.H.; Kong, N.; Fall, M.J. *J. Am. Chem. Soc.* **1996**, *118*, 6897.

³⁷ This compound was prepared as described in: Douglas, N. L.; Ley, S.V.; Osborn, H.M.I.; Owen, D.R.; Priepke, H.W.M.; Warriner, S.L. *Synlett* **1996**, 793-5.

aqueous NH_4Cl solution (3 x 100 mL). The yellow solution was dried over anhydrous magnesium sulfate, filtered through glass wool, and concentrated under reduced pressure. The resultant brown oil was purified by flash chromatography on silica gel (65:35 petroleum ether:ethyl ether) to afford alcohol **34** as a colorless oil (3.13 g, 11.3 mmol, 67% yield). ^1H NMR (250 MHz) δ 5.89 (ddt, $J = 17.2, 10.4, 5.7$ Hz, 1 H), 5.25 (ddd, $J = 17.2, 1.8, 1.3$ Hz, 1 H), 5.18 (ddd, $J = 10.4, 1.8, 1.3$ Hz, 1 H), 4.02 (dt, $J = 5.7, 1.3$ Hz, 2 H), 3.90-3.60 (comp, 4 H), 3.54 (dd, $J = 5.2, 1.7$ Hz, 2 H), 3.26 (s, 6 H), 2.65 (s, broad, 1 H), 1.31 (s, 3 H), 1.30 (s, 3 H); ^{13}C NMR (62.5 MHz) δ 134.0, 117.1, 98.4, 98.3, 72.1, 70.6, 69.7, 67.9, 62.0, 47.52, 47.49, 17.2, 17.1; $[\alpha]_{\text{D}}^{30} = -142.8^\circ$ ($c = 1.09$, CH_2Cl_2).

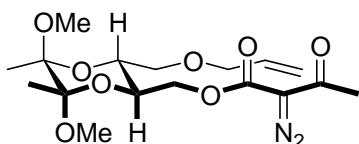


(2R,3R,5S,6S)-5,6-Dimethoxy-5,6-dimethyl-2-allyloxymethyl-3-(hydroxy)methyl-[1,4]-dioxane. ^1H NMR (250 MHz) δ 5.89 (ddt, $J = 17.2, 10.4, 5.7$ Hz, 1 H), 5.25 (ddd, $J = 17.2, 1.8, 1.3$ Hz, 1 H), 5.18 (ddd, $J = 10.4, 1.8, 1.3$ Hz, 1 H), 4.02 (dt, $J = 5.7, 1.3$ Hz, 2 H), 3.90-3.60 (comp, 4 H), 3.54 (dd, $J = 5.2, 1.7$ Hz, 2 H), 3.26 (s, 6 H), 2.65 (s, broad, 1 H), 1.31 (s, 3 H), 1.30 (s, 3 H); ^{13}C NMR (62.5 MHz) δ 134.0, 117.1, 98.4, 98.3, 72.1, 70.6, 69.7, 67.9, 62.0, 47.52, 47.49, 17.2, 17.1; $[\alpha]_{\text{D}}^{30} = +143.7^\circ$ ($c = 0.67$, CH_2Cl_2).



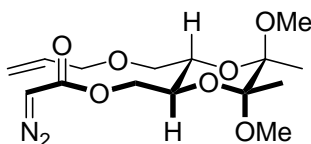
(2*S*,3*S*,5*R*,6*R*)-5,6-Dimethoxy-5,6-dimethyl-2-allyloxymethyl-3-

(diazoacetoacetoxy)methyl-[1,4]-dioxane (35). To a stirred solution of **34** (0.46 g, 1.7 mmol, 1.0 eq) in THF (20 mL) cooled in an ice bath was added Et₃N (0.050 mL, 0.30 mmol, 0.20 eq) followed by addition of diketene (0.16 mL, 2.0 mmol, 1.2 eq). The resulting brown solution was stirred for 12 h during which the solution was allowed to warm to ambient temperature. Then, Et₃N (0.27 mL 1.8 mmol, 1.1 eq) was added, followed by addition of methanesulfonyl azide (0.25 g, 2.0 mmol, 1.2 eq) and the resulting solution was stirred for an additional 18 h. Concentration under reduced pressure afforded a brown oil that was subjected to flash chromatography on silica gel (67:33 petroleum ether:ethyl ether) to yield diazoacetoacetate **35** as a pale yellow oil (0.44 g, 1.1 mmol, 69% yield). ¹H NMR (500 MHz) δ 5.89 (ddt, *J* = 17.2, 10.4, 5.6 Hz, 1 H), 5.25 (ddd, *J* = 17.2, 1.8, 1.2, Hz, 1 H), 5.18 (d, *J* = 10.4, 1.8, 1.2 Hz, 1 H), 4.45 (dd, *J* = 11.8, 2.6 Hz, 1 H), 4.26 (dd, *J* = 11.8, 6.3 Hz, 1 H), 4.05-3.96 (comp, 3 H), 3.82 (dt, *J* = 9.4, 4.9 Hz, 1 H), 3.52 (d, *J* = 4.5 Hz, 2 H), 3.25 (s, 3 H), 3.24 (s, 3 H), 2.48 (s, 3 H), 1.29 (s, 3 H), 1.28 (s, 3 H); ¹³C NMR (125 MHz) δ 189.8, 161.0, 134.2, 117.2, 98.7, 98.6, 72.3, 69.8, 68.4, 67.5, 64.3, 47.8, 47.7, 42.6, 28.0, 17.31, 17.29; IR: (C=N₂) 2140 cm⁻¹, (C=O) 1718, 1656 cm⁻¹; [α]_D³⁰ = -100.1° (*c* = 1.08, CH₂Cl₂).



(2R,3R,5S,6S)-5,6-Dimethoxy-5,6-dimethyl-2-allyloxymethyl-3-

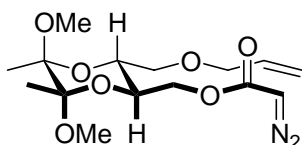
(diazoacetoacetoxy)methyl-[1,4]-dioxane. ^1H NMR (500 MHz) δ 5.89 (ddt, J = 17.2, 10.4, 5.6 Hz, 1 H), 5.25 (ddd, J = 17.2, 1.8, 1.2, Hz, 1 H), 5.18 (d, J = 10.4, 1.8, 1.2 Hz, 1 H), 4.45 (dd, J = 11.8, 2.6 Hz, 1 H), 4.26 (dd, J = 11.8, 6.3 Hz, 1 H), 4.05-3.96 (comp, 3 H), 3.82 (dt, J = 9.4, 4.9 Hz, 1 H), 3.52 (d, J = 4.5 Hz, 2 H), 3.25 (s, 3 H), 3.24 (s, 3 H), 2.48 (s, 3 H), 1.29 (s, 3 H), 1.28 (s, 3 H); ^{13}C NMR (125 MHz) δ 189.8, 161.0, 134.2, 117.2, 98.7, 98.6, 72.3, 69.8, 68.4, 67.5, 64.3, 47.8, 47.7, 42.6, 28.0, 17.31, 17.29; **IR:** (C=N₂) 2140 cm⁻¹, (C=O) 1718, 1656 cm⁻¹; $[\alpha]_D^{30}$ = +101.3° (c = 0.88, CH₂Cl₂).



(2S,3S,5R,6R)-5,6-Dimethoxy-5,6-dimethyl-2-allyloxymethyl-3-

(diazoacetoxy)methyl-[1,4]-dioxane (36). To a stirred solution of **35** (1.23 g, 3.17 mmol, 1.00 eq) in THF (25 mL) was added LiOH•H₂O (0.541g, 12.7 mmol, 4.0 eq) dissolved in deionized water (25 mL). The resulting yellow solution was allowed to stir fast enough to disrupt the liquid/liquid interface for 45 min. and monitored by ^1H NMR until complete disappearance of the singlet at 2.48 ppm was achieved. The reaction mixture was diluted with ethyl ether (30 mL) and washed with 2.5 M aqueous NH₄Cl (3 x 30 mL). The organic layer was dried over anhydrous magnesium sulfate, filtered through glass wool, and concentrated under reduced

pressure. The resulting yellow oil was subjected to flash chromatography on silica gel (75:25 petroleum ether:ethyl ether), yielding diazoacetate **36** as a yellow oil (0.731 g, 2.12 mmol, 67% yield). ^1H NMR (250 MHz) δ 5.83 (ddt, J = 17.2, 10.5, 5.7 Hz, 1 H), 5.18 (ddd, J = 17.2, 3.1, 1.5 Hz, 1 H), 5.12 (ddd, J = 10.5, 3.1, 1.5 Hz, 1 H), 4.74 (broad s, 1 H), 4.26 (dd, J = 11.9, 3.1 Hz, 1 H), 4.11 (dd, J = 11.9, 6.2 Hz, 1 H), 3.96-3.91 (comp, 2 H), 3.87 (ddd, J = 9.7, 6.2, 3.1 Hz, 1 H), 3.71 (dt, J = 9.7, 4.7 Hz, 1 H), 3.43 (d, J = 4.7 Hz, 2 H), 3.17 (s, 3 H), 3.16 (s, 3 H), 1.21 (s, 6 H); ^{13}C NMR (62.5 MHz) δ 134.3, 117.1, 99.6, 99.5, 72.3, 69.5, 68.4, 67.9, 63.8, 47.8, 47.6, 46.1, 17.4, 17.3 (the signal consistent with a carbonyl carbon was not observed, but was verified by IR); IR: (C=N₂) 2112 cm⁻¹, (C=O) 1699 cm⁻¹; $[\alpha]_{\text{D}}^{30}$ = -131.8° (c = 0.604, CH₂Cl₂).



(2R,3R,5S,6S)-5,6-Dimethoxy-5,6-dimethyl-2-allyloxymethyl-3-

(diazoacetoxy)methyl-[1,4]-dioxane (42). ^1H NMR (250 MHz) δ 5.83 (ddt, J = 17.2, 10.5, 5.7 Hz, 1 H), 5.18 (ddd, J = 17.2, 3.1, 1.5 Hz, 1 H), 5.12 (ddd, J = 10.5, 3.1, 1.5 Hz, 1 H), 4.74 (broad s, 1 H), 4.26 (dd, J = 11.9, 3.1 Hz, 1 H), 4.11 (dd, J = 11.9, 6.2 Hz, 1 H), 3.96-3.91 (comp, 2 H), 3.87 (ddd, J = 9.7, 6.2, 3.1 Hz, 1 H), 3.71 (dt, J = 9.7, 4.7 Hz, 1 H), 3.43 (d, J = 4.7 Hz, 2 H), 3.17 (s, 3 H), 3.16 (s, 3 H), 1.21 (s, 6 H); ^{13}C NMR (62.5 MHz) δ 134.3, 117.1, 99.6, 99.5, 72.3, 69.5, 68.4, 67.9, 63.8, 47.8, 47.6, 46.1, 17.4, 17.3 (the signal consistent with a carbonyl carbon was not

observed, but was verified by IR spectroscopy); **IR**: (C=N₂) 2112 cm⁻¹, (C=O) 1699 cm⁻¹; [α]_D³⁰ = +130.9° (*c* = 0.802, CH₂Cl₂).

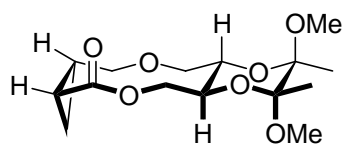
General Procedure for diazo decomposition of 36 and 42 by dirhodium(II)

catalysts: The procedure for diazo decomposition of **36** catalyzed by Rh₂(5*S*-MEPY)₄ is representative. To a refluxing solution of Rh₂(5*S*-MEPY)₄ (6.0 mg, 0.0070 mmol, 0.010 eq) in DCM (5.0 mL) was added a solution of **36** (0.24 g, 0.70 mmol, 1.0 eq) dissolved in DCM (5 mL) via syringe pump at a rate of 5 mL/h. The resulting solution was heated at reflux for an additional 1 h before filtration through a silica gel plug, which was rinsed with ethyl ether (20 mL). The resulting crude solution was concentrated under reduced pressure to afford **39a**, **39b**, **40**, and **41**. A small aliquot was then removed for GC analysis on an SPB-5 column, and the ratio of the products was determined by comparison of retention times versus previously isolated samples [retention times: (**41**) 18.4 min., (**40**) 22.9 min., (**39b**) 25.3 min., (**39a**) 25.5 min.]. Isolation of **39a**, **39b**, and **40** was accomplished by flash chromatography on silica gel (66:34 petroleum ether:ethyl ether): (**39a**) R_f = 0.48, (**39b**) R_f = 0.40, (**40**) R_f = 0.25, (**41**) R_f = 0.18.

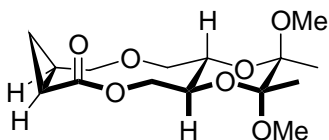
General Procedure for diazo decomposition of 36, 42 by copper(I) catalysts:

The procedure for diazo decomposition of **36** catalyzed by Cu(CH₃CN)₄PF₆/**3** is representative. A round bottom flask charged with copper(I) hexafluorophosphate (21 mg, 0.058 mmol, 0.10 eq) and bis-oxazoline **3** (21 mg, 0.070 mmol, 0.12 eq) in DCM (5.0 mL) was heated at reflux for 30 min. (heating at reflux for 30 min was

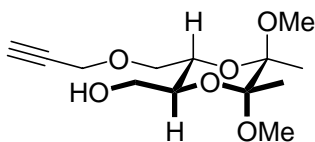
skipped if the bis-oxazoline ligand was not employed in the reaction). After 30 min, a solution of **36** (0.20 g, 0.58 mmol, 1.0 eq) dissolved in DCM (5 mL) was added via syringe pump at a rate of 5 mL/h. The resulting solution was heated at reflux for an additional 1 h before filtration through a silica gel plug, which was rinsed with ethyl ether (20 mL). The resulting crude solution was concentrated under reduced pressure to afford **39a**, **39b**, **40**, and **41**. A small aliquot was then removed for GC analysis on an SPB-5 column, and the ratio of the products was determined by comparison of retention times versus previously isolated samples.



(1S,5R,7S,11S,13R,14R)-13,14-Dimethoxy-13,14-dimethyl-3,9,12,15-tetraoxatricyclo[9.4.0.0^{5,7}]pentadecan-4-one (39a). ¹H NMR (600 MHz) δ 4.33 (dd, J = 11.4, 9.7 Hz, 1 H), 4.21 (dd, J = 11.4, 4.2 Hz, 1 H), 4.12 (dt, J = 9.7, 4.2 Hz, 1 H), 4.02 (dd, J = 12.0, 6.3 Hz, 1 H), 3.86 (dd, J = 10.6, 4.2 Hz, 1 H), 3.73 (dt, J = 9.7, 4.2 Hz, 1 H), 3.55 (dd, J = 12.0, 6.3 Hz, 1 H), 3.36 (dd, J = 10.6, 4.6 Hz, 1 H), 3.26 (s, 3 H), 3.23 (s, 3 H), 1.84 (ddd, J = 9.5, 8.0, 6.3 Hz, 1 H), 1.46 (ddq, J = 9.5, 8.2, 6.3 Hz, 1 H), 1.28-1.21 (mult, 1 H), 1.26 (s, 3 H), 1.25 (s, 3 H), 1.03 (dt, J = 8.2, 5.1 Hz, 1 H); ¹³C NMR (150 MHz, CDCl₃) δ 171.7, 98.8, 98.4, 71.4, 70.8, 70.0, 66.3, 63.3, 48.0, 47.9, 18.8, 18.7, 17.4, 17.3, 12.1; IR (solid deposition on KBr plate): (C=O) 1727 cm⁻¹

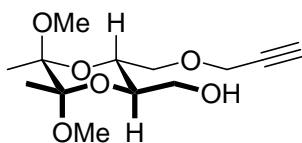


(1S,5S,7R,11S,13R,14R)-13,14-Dimethoxy-13,14-dimethyl-3,9,12,15-tetraoxatricyclo[9.4.0.0^{5,7}] pentadecan-4-one (39b). ¹H NMR (600 MHz) δ 4.56 (dd, J = 11.8, 10.0 Hz, 1 H), 4.08 (dd, J = 11.8, 5.9 Hz, 1 H), 4.05-3.99 (comp, 2 H), 3.77 (dd, J = 10.7, 4.1 Hz, 1 H), 3.69 (dt, J = 9.1, 3.9 Hz, 1 H), 3.43 (dd, J = 10.7, 3.9 Hz, 1 H), 3.29 (s, 3 H), 3.22 (s, 3 H), 3.20 (dd, J = 11.8, 8.2 Hz, 1 H), 1.88 (ddd, J = 9.4, 8.0, 6.1 Hz, 1 H), 1.57 (dddt, J = 9.4, 8.2, 8.0, 6.3 Hz, 1 H), 1.28 (s, 3 H), 1.27 (s, 3 H), 1.24 (ddd, J = 7.7, 6.1, 5.2 Hz, 1 H), 1.03 (ddd, J = 8.2, 8.0, 5.2 Hz, 1 H); ¹³C NMR (150 MHz) δ 172.5, 99.0, 98.9, 71.3, 70.5, 69.6, 67.6, 64.1, 48.1, 48.0, 19.5, 19.1, 17.5, 17.4, 12.4; IR (solid deposition on KBr plate): (C=O) 1727 cm⁻¹



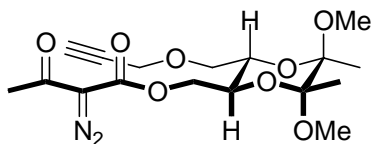
(2S,3S,5R,6R)-5,6-Dimethoxy-5,6-dimethyl-2-propargyloxymethyl-3-(hydroxy)methyl-[1,4]-dioxane (46). To a stirred solution of (2S,3S,5R,6R)-5,6-dimethoxy-5,6-dimethyl-2,3-di(hydroxy)methyl-[1,4]-dioxane¹⁰ (2.50 g, 10.7 mmol, 1.00 eq) in THF (125 mL) was added NaH (0.300 g, 11.6 mmol, 1.10 eq) as one portion. The solution instantly began to evolve gas, and over five minutes produced a cloudy white suspension. After gas evolution had subsided, a solution of 80% (w/w) propargyl bromide in toluene (1.87 g, 12.7 mmol, 1.20 eq) was added as one aliquot. The cloudy solution was stirred for 12 h at room temperature, diluted with ethyl ether (125 mL) and washed with 2.5 M aqueous NH₄Cl (3 x 100 mL). The resultant

solution was dried over anhydrous magnesium sulfate, filtered through glass wool, and concentrated under reduced pressure. The crude residue was purified by flash chromatography on silica gel (60:40 petroleum ether:ethyl ether) to yield alcohol **46** as a white crystalline solid (1.79 g, 6.53 mmol, 61% yield): ^1H NMR (250 MHz) δ 4.18 (dd, $J = 16.0, 2.3$ Hz, 1 H), 4.08 (dd, $J = 16.0, 2.3$ Hz, 1 H), 3.87-3.71 (comp, 2 H), 3.67-3.52 (comp, 4 H), 3.20 (s, 6 H), 2.43-2.37 (comp, 2 H), 1.24 (s, 6 H); ^{13}C NMR (62.5 MHz) δ 98.9, 98.8, 79.1, 70.1, 69.3, 67.8, 62.1, 58.5, 47.9, 47.8, 17.4, 17.3; $[\alpha]_{\text{D}}^{25} = -76.7^\circ$ ($c = 0.430$, CH_2Cl_2).



(2R,3R,5S,6S)-5,6-Dimethoxy-5,6-dimethyl-2-propargyloxymethyl-3-

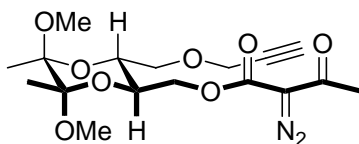
(hydroxymethyl)-[1,4]-dioxane. ^1H NMR (250 MHz) δ 4.18 (dd, $J = 16.0, 2.3$ Hz, 1 H), 4.08 (dd, $J = 16.0, 2.3$ Hz, 1 H), 3.87-3.71 (comp, 2 H), 3.67-3.52 (comp, 4 H), 3.20 (s, 6 H), 2.43-2.37 (comp, 2 H), 1.24 (s, 6 H); ^{13}C NMR (62.5 MHz) δ 98.9, 98.8, 79.1, 70.1, 69.3, 67.8, 62.1, 58.5, 47.9, 47.8, 17.4, 17.3; $[\alpha]_{\text{D}}^{25} = +77.3^\circ$ ($c = 0.760$, CH_2Cl_2).



(2S,3S,5R,6R)-5,6-Dimethoxy-5,6-dimethyl-2-propargyloxymethyl-3-

(diazoacetoacetoxy)methyl-[1,4]-dioxane (47). To a stirred solution of **46** (1.4 g, 5.3 mmol, 1.0 eq) in THF (20 mL) cooled in an ice bath was added Et_3N (0.15 mL, 1.1 mmol, 0.20 eq) followed by addition of diketene (0.49 mL, 6.3 mmol, 1.2 eq). The resulting brown solution was stirred 12 h, during which time the solution was allowed

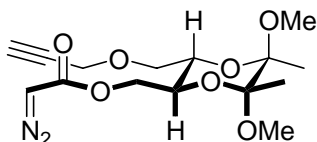
to warm to ambient temperature. Then Et₃N (0.88 mL, 6.3 mmol, 1.2 eq) was added, followed by addition of methanesulfonyl azide (0.76 g, 6.3 mmol, 1.2 eq), and the reaction was allowed to stir for an additional 24 h. The resulting brown solution was concentrated under reduced pressure and purified by flash chromatography on silica gel (67:33 petroleum ether:ethyl ether) to afford diazoacetoacetate **47** as a pale yellow oil (1.54 g, 4.00 mmol, 74% yield). ¹H NMR (500 MHz) δ 4.43 (dd, *J* = 11.7, 2.9 Hz, 1 H), 4.28 (dd, *J* = 11.7, 6.0 Hz, 1 H), 4.19 (dd, *J* = 10.7, 2.3 Hz, 2 H), 4.03 (ddd, *J* = 9.8, 6.0, 2.9 Hz, 1 H), 3.85 (dt, *J* = 9.8, 4.0 Hz, 1 H), 3.68 (dd, *J* = 10.7, 4.0 Hz, 1 H), 3.61 (dd, *J* = 10.7, 4.0 Hz, 1 H), 3.25 (s, 6 H), 2.49 (s, 3 H), 2.45 (t, *J* = 2.3 Hz, 1 H), 1.31 (s, 3 H), 1.29 (s, 3 H); ¹³C NMR (125 MHz) δ 161.2, 98.9, 98.8, 79.1, 75.0, 69.3, 67.7, 67.6, 64.3, 47.9, 47.8, 42.8, 28.2, 17.4 (the signal consistent with a ketone carbonyl carbon was not observed, but was verified by IR spectroscopy, other missing carbon signals are believed to be due to overlap of carbon signals); IR : (C=N₂) 2137 cm⁻¹, (C=O) 1716, 1651 cm⁻¹; [α]_D²⁵ = -57.6° (*c* = 0.254, CH₂Cl₂).



(2*R*,3*R*,5*S*,6*S*)-5,6-Dimethoxy-5,6-dimethyl-2-propargyloxymethyl-3-

(diazoacetoacetoxy)methyl-[1,4]-dioxane. ¹H NMR (500 MHz) δ 4.43 (dd, *J* = 11.7, 2.9 Hz, 1 H), 4.28 (dd, *J* = 11.7, 6.0 Hz, 1 H), 4.19 (dd, *J* = 10.7, 2.3 Hz, 2 H), 4.03 (ddd, *J* = 9.8, 6.0, 2.9 Hz, 1 H), 3.85 (dt, *J* = 9.8, 4.0 Hz, 1 H), 3.68 (dd, *J* = 10.7, 4.0 Hz, 1 H), 3.61 (dd, *J* = 10.7, 4.0 Hz, 1 H), 3.25 (s, 6 H), 2.49 (s, 3 H), 2.45 (t, *J* = 2.3 Hz, 1 H), 1.31 (s, 3 H), 1.29 (s, 3 H); ¹³C NMR (125 MHz) δ 161.2, 98.9,

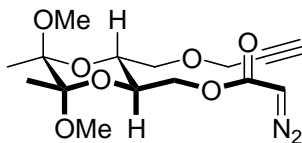
98.8, 79.1, 75.0, 69.3, 67.7, 67.6, 64.3, 47.9, 47.8, 42.8, 28.2, 17.4 (the signal consistent with one carbonyl carbon was not observed, but was verified by IR spectroscopy, other missing carbon signals are believed to be due to overlap of carbon signals); **IR** : (C=N₂) 2137 cm⁻¹, (C=O) 1716, 1651 cm⁻¹; [α]_D²⁵ = +58.5° (*c* = 0.470, CH₂Cl₂).



(2*S*,3*S*,5*R*,6*R*)-5,6-Dimethoxy-5,6-dimethyl-2-propargyloxymethyl-3-

(diazoacetoxy)methyl-[1,4]-dioxane (48). To a stirred solution of **47** (1.48 g, 3.86 mmol, 1.00 eq) in THF (25 mL) was added LiOH•H₂O (0.541g, 19.3 mmol, 5.00 eq) dissolved in deionized water (25 mL). The resultant yellow solution was allowed to stir fast enough to disrupt the liquid/liquid interface for 40 min and monitored by ¹H NMR until disappearance of the peak at 2.49 ppm was achieved. The solution was then washed with 2.5 M aqueous NH₄Cl (3 x 40 mL), dried over anhydrous magnesium sulfate, filtered through glass wool, and concentrated under reduced pressure. The resulting yellow oil was subjected to flash chromatography on silica gel (67:33 petroleum ether/ethyl ether) to afford diazoacetate **48** as a yellow oil (0.885 g, 2.59 mmol, 67% yield). **¹H NMR** (250 MHz) δ 4.82 (s, broad, 1 H), 4.34-4.24 (comp, 2 H), 4.19 (dd, *J* = 9.0, 2.4 Hz, 2 H), 3.99 (ddd, *J* = 9.8, 5.8, 3.3 Hz, 1 H), 3.83 (dt, *J* = 9.8, 4.0 Hz, 1 H), 3.67 (dd, *J* = 10.7, 4.0 Hz, 1 H), 3.61 (dd, *J* = 10.7, 4.0 Hz, 1 H), 3.26 (s, 3 H), 3.25 (s, 3 H), 2.46 (t, *J* = 2.4 Hz, 1 H), 1.31 (s, 3 H), 1.30 (s, 3 H); **¹³C NMR** (62.5 MHz) δ 98.9, 98.7, 79.2, 74.9, 69.1, 68.0, 67.8, 63.8, 58.5, 47.9, 47.7, 46.2, 17.5, 17.4 (the signal consistent with a carbonyl carbon was not

observed, but was verified by IR spectroscopy). **IR** (C=N₂) 2111 cm⁻¹, (C=O) 1698 cm⁻¹; **HRMS** Calculated for C₁₅H₂₂O₇N₂: 343.1505; found: 343.1495. [α]_D²⁵ = -60.9° (*c* = 0.860, CH₂Cl₂).



(2*R*,3*R*,5*S*,6*S*)-5,6-Dimethoxy-5,6-dimethyl-2-propargyloxymethyl-3-

(diazoacetoxy)methyl-[1,4]-dioxane (50). ¹H NMR (250 MHz) δ 4.82 (s, broad, 1 H), 4.34-4.24 (comp, 2 H), 4.19 (dd, *J* = 9.0, 2.4 Hz, 2 H), 3.99 (ddd, *J* = 9.8, 5.8, 3.3 Hz, 1 H), 3.83 (dt, *J* = 9.8, 4.0 Hz, 1 H), 3.67 (dd, *J* = 10.7, 4.0 Hz, 1 H), 3.61 (dd, *J* = 10.7, 4.0 Hz, 1 H), 3.26 (s, 3 H), 3.25 (s, 3 H), 2.46 (t, *J* = 2.4 Hz, 1 H), 1.31 (s, 3 H), 1.30 (s, 3 H); ¹³C NMR (62.5 MHz) δ 98.9, 98.7, 79.2, 74.9, 69.1, 68.0, 67.8, 63.8, 58.5, 47.9, 47.7, 46.2, 17.5, 17.4; **IR** (C=N₂) 2111 cm⁻¹, (C=O) 1698 cm⁻¹; [α]_D²⁵ = +60.8° (*c* = 1.04, CH₂Cl₂).

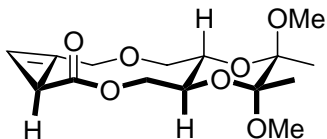
General Procedure for diazo decomposition of 48 and 50 by dirhodium(II)

catalysts: The procedure for diazo decomposition of **48** with Rh₂(4*S*-MEAZ)₄ is representative. To a refluxing solution of Rh₂(4*S*-MEAZ)₄ (3.4 mg, 0.0044 mmol, 0.010 eq) in DCM (5.0 mL) was added a solution of **48** (0.12 g, 0.44 mmol, 1.0 eq) dissolved in DCM (5 mL) via syringe pump at a rate of 5 mL/h. The resulting solution was heated at reflux for an additional 1 h before filtration through a silica gel plug, which was rinsed with ethyl ether (20 mL). The resulting crude solution was concentrated under reduced pressure to afford a mixture of **49a** and **49b**. A small

aliquot was then removed for GC analysis on an SPB-5 column, and the ratio of the products was determined by comparison of retention times versus previously isolated samples (retention times: (**49b**) 25.7 min., (**49a**) 25.9 min.). Isolation of **49a** and **49b** was accomplished by flash chromatography on silica gel (66:34 petroleum ether:ethyl ether).

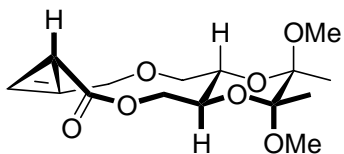
General Procedure for diazo decomposition of 48 and 50 by copper(I) catalysts:

The procedure for diazo decomposition of **48** catalyzed by $\text{Cu}(\text{CH}_3\text{CN})_4\text{PF}_6/\mathbf{3}$ is representative. A round bottom flask charged with copper(I) hexafluorophosphate (27.1 mg, 0.0730 mmol, 0.100 eq) and bis-oxazoline **3** (25.6 mg, 0.0860 mmol, 0.120 eq) in DCM (5.0 mL) was heated at reflux for 30 min. (heating at reflux for 30 min was skipped if the bis-oxazoline ligand was not employed in the reaction). After 30 min, a solution of **48** (0.250 g, 0.730 mmol, 1.00 eq) in DCM (5 mL) was added via syringe pump at a rate of 5 mL/h. The resulting solution was then heated at reflux for an additional 1 h before filtration through a silica gel plug, which was rinsed with ethyl ether (20 mL). Concentration under reduced pressure afforded a mixture of **49a** and **49b**. A small aliquot was then removed for GC analysis on an SPB-5 column, and the ratio of the products was determined by comparison of retention times versus previously isolated samples.



(1S,5S,11S,13R,14R)-13,14-Dimethoxy-13,14-dimethyl-3,9,12,15-tetraoxatricyclo[9.4.0.0^{5,7}]pentadec-6-en-4-one (49a).

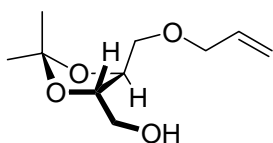
¹H NMR (500 MHz) δ 6.67 (s, 1 H), 4.80 (dd, J = 11.0, 3.4 Hz, 1 H), 4.54 (d, J = 13.9 Hz, 1 H), 4.34 (d, J = 13.9 Hz, 1 H), 4.02 (dt, J = 3.4, 10.0 Hz, 1 H), 3.79 (dd, J = 10.4, 2.0 Hz, 1 H), 3.69 (d, J = 10.4 Hz, 1 H), 3.61 (d, J = 10.0 Hz, 1 H), 3.54 (t, J = 11.0 Hz, 1 H), 3.26 (s, 3 H), 3.24 (s, 3 H), 2.23 (s, 1 H), 1.33 (s, 3 H), 1.26 (s, 3 H); **¹³C NMR** (125 MHz, CDCl₃) δ 179.3, 112.9, 99.5, 99.2, 98.7, 71.8, 68.6, 63.4, 62.7, 61.9, 48.0, 47.9, 20.2, 17.5, 17.4; **HRMS** (FAB+) Calculated for C₁₅H₂₂O₇Li: 321.1526; found: 321.1552.



(1S,5R,11S,13R,14R)-13,14-Dimethoxy-13,14-dimethyl-3,9,12,15-tetraoxatricyclo[9.4.0.0^{5,7}]pentadec-6-en-4-one (49b). **¹H NMR** (400 MHz) δ 6.74 (t, J = 1.4 Hz, 1 H), 4.50 (d, J = 13.7 Hz, 1 H), 4.36 (t, J = 10.8 Hz, 1 H), 4.32 (dt, J = 13.7, 1.4 Hz, 1 H), 3.99 (ddd, J = 10.8, 9.6, 3.8 Hz, 1 H), 3.89 (dd, J = 10.8, 3.8 Hz, 1 H), 3.75 (dd, J = 9.9, 4.9 Hz, 1 H), 3.65 (dd, J = 9.9, 1.3 Hz, 1 H), 3.60 (ddd, J = 9.6, 4.9, 1.3 Hz, 1 H), 3.28 (s, 3 H), 3.27 (s, 3 H), 2.25 (d, J = 1.4 Hz, 1 H), 1.31 (s, 3 H), 1.28 (s, 3 H); **¹³C NMR** (100 MHz, CDCl₃) δ 174.4, 112.6, 99.1, 98.9, 98.5, 71.8, 71.3, 67.2,

64.1, 61.5, 48.06, 48.03, 20.1, 17.5, 17.3; **HRMS** (FAB+) Calculated for C₁₅H₂₂O₇Li: 321.1526; found: 321.1530.

Hydrogenation of 49a: A round bottom flask charged with **49a** (0.90 g, 0.29 mmol, 1.0 eq), anhydrous methanol (20 mL) and palladium on carbon (10%) was sealed under an atmosphere of nitrogen and a rubber balloon containing hydrogen gas was introduced. The reaction was allowed to stir rapidly for 1 h and the balloon was removed. After evacuation of the flask and addition of nitrogen to equilibrate the pressure in the flask, the solution was filtered through a pad of Celite that was rinsed with ethyl ether (3 x 25 mL). The filtrate was concentrated under reduced pressure, and the resultant solid was subjected to flash chromatography on silica gel (petroleum ether: ethyl ether, 67:33) to afford cyclopropane **39b** (0.067 g, 0.23 mmol, 80 %). The resultant solid was analyzed by ¹H NMR spectroscopy to identify the product as **39b**, and confirmed by GC on an SPB-5 column to give the same retention time as authentic **39b**.

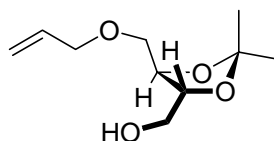


(1S,2S)-4,4-Dimethyl-1-allyloxymethyl-2-hydroxymethyl-[1,3]-dioxolane (54).

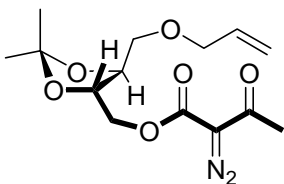
To a stirred solution of (1S,2S)-4,4-dimethyl-1,2-(hydroxy)methyl-[1,3]-dioxolane³⁸ (5.02 g, 31.0 mmol, 1.00 eq) and NaI (0.162g, 1.10 mmol, 0.0300 eq) in THF (150 mL) was added NaH (0.839 g, 35.0 mmol, 1.10 eq) as one portion. The solution

³⁸ This compound was prepared as described in Goldberg, I.; Stein, Z.; Weber, E.; Doerpinghaus, N.; Franklin, S. *J. Chem. Soc., Perkin II* **1990**, 953.

instantly began to evolve gas, and over five minutes produced a cloudy white suspension. After gas evolution had subsided, allyl bromide (3.50 mL, 40.4 mmol, 1.30 eq) was added in one aliquot. The resulting cloudy yellow solution was stirred for 12 h, diluted with ethyl ether (125 mL), washed with 2.5 M aqueous NH_4Cl (3 x 120 mL), dried over anhydrous magnesium sulfate, filtered through glass wool, and concentrated under reduced pressure. The resultant yellow oil was purified by flash chromatography on silica gel (60:40 petroleum ether:ethyl ether) to afford alcohol **54** as a colorless oil (3.13 g, 15.5 mmol, 50% yield). ^1H NMR (250 MHz) δ 5.79 (ddt, J = 17.2, 10.5, 5.6 Hz, 1 H), 5.19 (ddd, J = 17.2, 1.5, 1.0 Hz, 1 H), 5.14 (ddd, J = 10.5, 1.5, 1.0 Hz, 1 H), 3.97 (dt, J = 5.6, 1.5 Hz, 2 H), 3.98-3.82 (comp, 2 H), 3.74-3.38 (comp, 4 H), 2.65 (s, broad, 1 H), 1.36 (s, 6 H); ^{13}C NMR (62.5 Hz, CDCl_3) δ 134.0, 117.4, 109.2, 79.4, 76.5, 72.4, 70.2, 62.3, 26.83, 26.79; $[\alpha]_{\text{D}}^{30}$ = -11.9° (c = 1.19, MeOH).

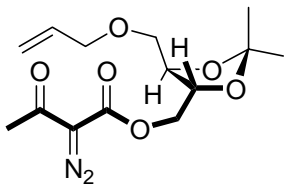


(1*R*,2*R*)-4,4-Dimethyl-1-allyloxymethyl-2-hydroxymethyl-[1,3]-dioxolane. ^1H NMR (250 MHz) δ 5.79 (ddt, J = 17.2, 10.5, 5.6 Hz, 1 H), 5.19 (ddd, J = 17.2, 1.5, 1.0 Hz, 1 H), 5.14 (ddd, J = 10.5, 1.5, 1.0 Hz, 1 H), 3.97 (dt, J = 5.6, 1.5 Hz, 2 H), 3.98-3.82 (comp, 2 H), 3.74-3.38 (comp, 4 H), 2.65 (s, broad, 1 H), 1.36 (s, 6 H); ^{13}C NMR (62.5 Hz, CDCl_3) δ 134.0, 117.4, 109.2, 79.4, 76.5, 72.4, 70.2, 62.3, 26.83, 26.79; $[\alpha]_{\text{D}}^{30}$ = +12.0° (c = 1.03, MeOH).



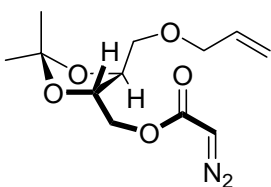
(1*S*,2*S*)-4,4-Dimethyl-2-allyloxymethane-1-(diazoacetoacetoxy)methyl-[1,3]-

dioxolane (55). To a stirred solution of **54** (3.2 g, 16 mmol, 1.0 eq) in THF (40 mL) cooled in an ice bath was added diketene (1.5 mL, 19 mmol, 1.2 eq) followed by Et₃N (0.45 mL, 3.1 mmol, 0.20 eq). The resulting brown solution was stirred for 12 h and allowed to warm to ambient temperature, followed by addition of Et₃N (2.6 mL, 19 mmol, 1.2 eq) then addition of methanesulfonyl azide (2.3 g, 19 mmol, 1.2 eq). The solution was allowed to stir for an additional 18 h, and the resultant brown solution was concentrated under reduced pressure. Purification by flash chromatography on silica gel (60:40 petroleum ether:ethyl ether) afforded diazoacetoacetate **55** as a pale yellow oil (3.70 g, 11.8 mmol, 76% yield). ¹H NMR (250 MHz) δ 5.89 (ddt, *J* = 17.2, 10.5, 5.6 Hz, 1 H), 5.28 (ddd, *J* = 17.2, 2.9, 1.5 Hz, 1 H), 5.21 (ddd, *J* = 10.5, 2.9, 1.5 Hz, 1 H), 4.47 (dd, *J* = 11.8, 3.5 Hz, 1H), 4.33 (dd, *J* = 11.8, 5.2 Hz, 1 H), 4.12 (ddd, *J* = 8.1, 5.1, 3.5 Hz, 1 H), 4.05 (dd, *J* = 5.6, 1.5 Hz, 2 H), 4.01 (ddd, *J* = 8.1, 5.1, 3.5 Hz, 1 H), 3.65 (dd, *J* = 10.0, 5.4 Hz, 1 H), 3.55 (dd, *J* = 10.0, 5.4 Hz, 1 H), 2.50 (s, 3 H), 1.44 (s, 3 H), 1.42 (s, 3 H); ¹³C NMR (62.5 Hz) δ 185.0, 160.9, 134.0, 117.3, 109.9, 76.5, 76.2, 72.5, 70.2, 64.5, 28.1, 26.8, 26.7; IR: (C=N₂) 2141 cm⁻¹, (C=O) 1722, 1660 cm⁻¹; [α]_D²⁵ = -10.7° (c = 1.09, MeOH).



(1*R*,2*R*)-4,4-Dimethyl-2-allyloxymethane-1-(diazoacetoacetoxy)methyl-[1,3]-

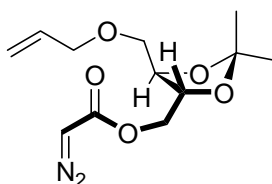
dioxolane. ^1H NMR (250 MHz) δ 5.89 (ddt, $J = 17.2, 10.5, 5.6$ Hz, 1 H), 5.28 (ddd, $J = 17.2, 2.9, 1.5$ Hz, 1 H), 5.21 (ddd, $J = 10.5, 2.9, 1.5$ Hz, 1 H), 4.47 (dd, $J = 11.8, 3.5$ Hz, 1H), 4.33 (dd, $J = 11.8, 5.2$ Hz, 1 H), 4.12 (ddd, $J = 8.1, 5.1, 3.5$ Hz, 1 H), 4.05 (dd, $J = 5.6, 1.5$ Hz, 2 H), 4.01 (ddd, $J = 8.1, 5.1, 3.5$ Hz, 1 H), 3.65 (dd, $J = 10.0, 5.4$ Hz, 1 H), 3.55 (dd, $J = 10.0, 5.4$ Hz, 1 H), 2.50 (s, 3 H), 1.44 (s, 3 H), 1.42 (s, 3 H); ^{13}C NMR (62.5 Hz) δ 185.0, 160.9, 134.0, 117.3, 109.9, 76.5, 76.2, 72.5, 70.2, 64.5, 28.1, 26.8, 26.7; IR: (C=N₂) 2141 cm⁻¹, (C=O) 1722, 1660 cm⁻¹; [α]_D²⁵ = 10.5° ($c = 1.11$, MeOH).



(1*S*,2*S*)-4,4-Dimethyl-2-allyloxymethyl-1-(diazoacetoxy)methyl-[1,3]dioxolane

(56). To a stirred solution of **55** (5.01g, 16.0 mmol, 1.00 eq) in THF (40 mL) was added LiOH·H₂O (3.37 g, 80.0 mmol, 5.00 eq) dissolved in deionized water (45 mL). The resultant yellow solution was then allowed to stir fast enough to disrupt the liquid/liquid interface for 45 min. and monitored by ^1H NMR until complete disappearance of the singlet at 2.48 ppm was achieved. The yellow solution was diluted with ethyl ether (45 mL) followed by washing with 2.5 M aqueous NH₄Cl (3 x

100 mL). The organic layer was dried over anhydrous magnesium sulfate, filtered through glass wool, and concentrated under reduced pressure. The resultant yellow oil was purified by flash chromatography on silica gel (67:33 petroleum ether:ethyl ether) to afford diazoacetate **56** as a yellow oil (3.45 g, 12.8 mmol, 80% yield). **¹H NMR** (250 MHz) δ 5.88 (ddt, J = 17.2, 10.4, 5.6 Hz, 1 H), 5.28 (ddd, J = 17.2, 3.1, 1.4 Hz, 1 H), 5.20 (ddd, J = 10.4, 3.1, 1.4 Hz, 1 H), 4.85 (s, broad, 1 H), 4.41 (dd, J = 11.7, 3.0 Hz, 1 H), 4.21 (dd, J = 11.7, 5.1 Hz, 1 H), 4.07-3.99 (comp, 4 H), 3.61 (dd, J = 10.2, 5.1 Hz, 1 H), 3.55 (dd, J = 10.2, 4.4 Hz, 1 H), 1.43 (s, 3 H), 1.42 (s, 3 H); **¹³C NMR** (75 Hz) δ 134.2, 117.3, 109.9, 76.5, 72.5, 70.1, 64.3, 46.2, 26.9, 26.8 (the signal consistent with a carbonyl carbon was not observed, but was verified by IR); **IR**: (C=N₂) 2113 cm⁻¹, (C=O) 1701 cm⁻¹; **HRMS** (FAB +) Calculated for C₁₂H₁₈O₅N₂: 271.1294; found: 271.1294; [α]_D³⁰ = -18.7° (c = 0.834, MeOH).



(1R,2R)-4,4-Dimethyl-2-allyloxymethyl-1-(diazoacetoxy)methyl-[1,3]-dioxolane.

¹H NMR (250 MHz) δ 5.88 (ddt, J = 17.2, 10.4, 5.6 Hz, 1 H), 5.28 (dt, J = 17.2, 1.4 Hz, 1 H), 5.20 (dd, J = 10.4, 1.4 Hz, 1 H), 4.85 (broad s, 1 H), 4.41 (dd, J = 11.7, 3.0 Hz, 1 H), 4.21 (dd, J = 11.7, 5.1 Hz, 1 H), 4.07-3.99 (comp, 4 H), 3.61 (dd, J = 10.2, 5.1 Hz, 1 H), 3.55 (dd, J = 10.2, 4.4 Hz, 1 H), 1.43 (s, 3 H), 1.42 (s, 3 H); **¹³C NMR** (75 Hz) δ 134.2, 117.3, 109.9, 76.5, 72.5, 70.1, 64.3, 46.2, 26.9, 26.8 (the signal consistent with a carbonyl carbon was not observed, but was verified by IR

spectroscopy); **IR**: (C=N₂) 2113 cm⁻¹, (C=O) 1701 cm⁻¹; [α]_D³⁰ = +18.7° (*c* = 0.786, MeOH).

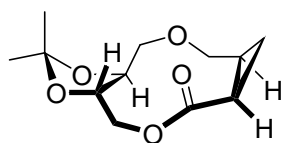
General Procedure for diazo decomposition of 56 and 58 by dirhodium(II)

catalysts: The procedure for diazo decomposition of **56** with Rh₂(5*S*-MPPIM)₄ is representative. To a refluxing solution of Rh₂(5*S*-MPPIM)₄ (9.3 mg, 0.0074 mmol, 0.010 eq) in DCM (5.0 mL) a solution of **56** (0.21 g, 0.74 mmol, 1.0 eq) dissolved in DCM (5 mL) was added via syringe pump at a rate of 5 mL/h. The resulting solution was then heated at reflux for an additional 1 h before filtration through a silica gel plug, which was rinsed with ethyl ether (20 mL). The resulting crude solution was concentrated under reduced pressure to afford a mixture of **57a** and **57b**. An aliquot was removed and the diastereoisomer ratio of the products was determined by comparison of ¹H NMR integration at defined chemical shifts of previously isolated **57** (chemical shifts: (**57a**) 4.72 ppm (dd), (**57b**) 4.61 ppm (t)).

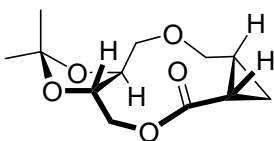
General Procedure for diazo decomposition of 56 and 58 by copper(I) catalysts:

The procedure for diazo decomposition of **56** catalyzed by Cu(CH₃CN)₄PF₆/**3** is representative. A round bottom flask charged with copper(I) hexafluorophosphate (27.1 mg, 0.0740 mmol, 0.100 eq) and bis-oxazoline **3** (26.6 mg, 0.0890 mmol, 0.120 eq) in DCM (5.0 mL) was heated at reflux for 30 min. (heating at reflux for 30 min. was skipped if the bis-oxazoline ligand was not employed in the reaction). After 30 min., a solution of **56** (0.200 g, 0.740 mmol, 1.00 eq) dissolved in DCM (5 mL) was added via syringe pump at a rate of 5 mL/h. The resulting solution was then heated at

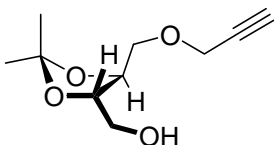
reflux for an additional 1 h before filtration through a silica gel plug, which was rinsed with ethyl ether (20 mL). The resulting crude solution was concentrated under reduced pressure to afford a mixture of **57a** and **57b**. An aliquot was removed and the diastereoisomer ratio of the products was determined by comparison of ^1H NMR integration at defined chemical shifts of previously isolated **57** [chemical shifts: (**57a**) 4.72 ppm (dd), (**57b**) 4.61 ppm (t)]. Separation of **57** from the crude reaction mixture was accomplished by flash chromatography on silica gel (petroleum ether: ethyl ether, 67:33)



(1S, 5R, 7S, 11S)-13-Dimethyl-3,9,12,14-tetraoxa-tricyclo[9.3.0.0^{5,7}] tetradecan-4-one (25a). ^1H NMR (600 MHz) δ 4.68 (t, J = 10.6 Hz, 1 H), 4.23-4.15 (comp, 2 H), 4.06 (ddd, J = 10.6, 7.7, 4.2 Hz, 1 H), 3.87 (ddd, J = 9.7, 7.7, 3.2 Hz, 1 H), 3.18 (t, J = 9.3 Hz, 1 H), 3.15 (dd, J = 11.6, 9.7 Hz, 1 H), 1.83 (ddd, J = 9.7, 8.0, 5.8 Hz, 1 H), 1.72-1.61 (mult, 1 H), 1.38 (s, 3 H), 1.35 (s, 3 H), 1.28 (dt, J = 6.0, 5.8, 5.1 Hz, 1 H), 1.09 (ddd, J = 10.2, 8.0, 5.1 Hz, 1 H); ^{13}C NMR (75 Hz) δ 171.4, 108.2, 79.1, 78.3, 75.6, 71.6, 71.4, 63.6, 26.3, 19.6, 18.3, 12.5; **HRMS** (FAB+) Calculated for $\text{C}_{12}\text{H}_{18}\text{O}_5$: 243.1232; found: 243.1238.

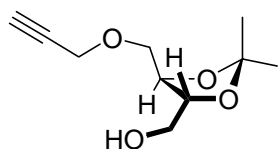


(1S, 5S, 7R, 11S)-13-Dimethyl-3,9,12,14-tetraoxa-tricyclo[9.3.0.0^{5,7}] tetradecan-4-one (25b). ¹H NMR (600 MHz) δ 4.77 (dd, J = 10.4, 4.5 Hz, 1 H), 4.26 (ddd, J = 10.4, 7.0, 4.7 Hz, 1 H), 4.19 (ddd, J = 10.4, 7.0, 4.5 Hz, 1 H), 4.02 (dd, J = 9.5, 6.3 Hz, 1 H), 3.92 (t, J = 10.4 Hz, 1 H), 3.68 (dd, J = 11.9, 4.7 Hz, 1 H), 3.41 (dd, J = 11.9, 10.4 Hz, 1 H), 3.28 (t, J = 9.5 Hz, 1 H), 1.82 (ddd, J = 9.1, 8.0, 5.8 Hz, 1 H), 1.67 (dddt, J = 9.5, 9.1, 8.0, 6.3 Hz, 1 H), 1.40 (s, 3 H), 1.37 (s, 3 H), 1.29 (dt, J = 6.3, 5.8 Hz, 1 H), 1.11 (ddd, J = 8.0, 6.3, 5.8 Hz, 1 H); ¹³C NMR (150 Hz) δ ; 171.6, 109.6, 75.6, 75.4, 70.2, 68.9, 64.8, 26.58, 26.54, 19.3, 18.5, 13.3; HRMS (FAB+) Calculated for C₁₂H₁₈O₅: 243.1232; found: 243.1238.



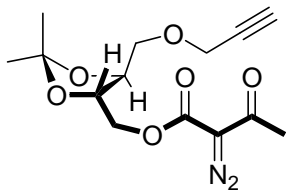
(1S,2S)-4,4-Dimethyl-1-propargyloxymethyl-2-hydroxymethyl-[1,3]dioxolane (60). To a stirred solution of (1S,2S)-4,4-dimethyl-1,2-(hydroxy)methyl-[1,3]dioxolane¹¹ (8.00 g, 49.3 mmol, 1.00 eq) and NaI (0.0729 g, 0.490 mmol, 0.0100 eq) in THF (250 mL) was added NaH (1.30 g, 51.8 mmol, 1.05 eq) as one portion, resulting in immediate gas evolution and a cloudy white suspension emerged over five minutes. After gas had subsided an 80% (w/w) solution of propargyl

bromide in toluene (9.35 g, 64.0 mmol, 1.30 eq) was added as one aliquot. The resultant brown solution was stirred for 12 h while warming to ambient temperature, then diluted with ethyl ether (250 mL), washed with 2.5 M aqueous NH_4Cl (3 x 250 mL), dried over anhydrous magnesium sulfate, filtered through glass wool, and concentrated under reduced pressure. The resultant brown crude residue was purified by flash chromatography on silica gel (50:50 petroleum ether:ethyl ether) to afford alcohol **60** as a colorless oil (5.03 g, 25.1 mmol, 51% yield). ^1H NMR (500 MHz) δ 4.16 (d, $J = 2.4$, 2 H), 4.01 (ddd, $J = 10.2$, 8.2, 5.1 Hz, 1 H), 3.89 (ddd, $J = 12.3$, 8.2, 4.1 Hz, 1 H), 3.72 (ddd, $J = 11.8$, 5.0, 3.8 Hz, 1 H), 3.69-3.56 (comp, 3 H), 2.41 (t, $J = 2.4$ Hz, 1 H), 2.32 (s, 1 H), 1.37 (s, 6 H); ^{13}C NMR (125 Hz) δ 109.4, 79.1, 79.0, 76.0, 75.0, 69.9, 62.2, 58.6, 26.9, 26.8; $[\alpha]_{\text{D}}^{33} = -9.5^\circ$ ($c = 0.860$, CH_2Cl_2).



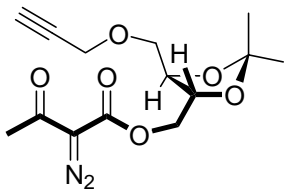
(1*R*,2*R*)-4,4-Dimethyl-1-propargyloxymethyl-2-hydroxymethyl-[1,3]dioxolane.

^1H NMR (500 MHz) δ 4.16 (d, $J = 2.4$, 2 H), 4.01 (ddd, $J = 10.2$, 8.2, 5.1 Hz, 1 H), 3.89 (ddd, $J = 12.3$, 8.2, 4.1 Hz, 1 H), 3.72 (ddd, $J = 11.8$, 5.0, 3.8 Hz, 1 H), 3.69-3.56 (comp, 3 H), 2.41 (t, $J = 2.4$ Hz, 1 H), 2.32 (s, 1 H), 1.37 (s, 6 H); ^{13}C NMR (125 Hz) δ 109.4, 79.1, 79.0, 76.0, 75.0, 69.9, 62.2, 58.6, 26.9, 26.8; $[\alpha]_{\text{D}}^{33} = +9.5^\circ$ ($c = 0.578$, CH_2Cl_2).



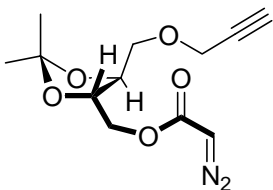
(1*S*,2*S*)-4,4-Dimethyl-1-propargyloxymethyl-2-(diazoacetoacetoxy)methyl-

[1,3]dioxolane (61). To a stirred solution of **60** (5.0 g, 25 mmol, 1.0 eq) and THF (30 mL) cooled in an ice bath was added diketene (2.3 mL, 30 mmol, 1.2 eq) followed by Et₃N (0.70 mL, 5.0 mmol, 0.20 eq). The resulting brown solution was stirred for 12 h during which time the solution was allowed to warm to ambient temperature. Next, methanesulfonyl azide (3.7 g, 30 mmol, 1.2 eq) was added as one aliquot, followed by addition of Et₃N (4.2 mL, 30 mmol, 1.2 eq) as one aliquot, and the solution was stirred for an additional 18 h. The brown reaction solution was concentrated under reduced pressure and the resultant brown oil was purified by flash chromatography on silica gel (60:40 petroleum ether:ethyl ether) to afford diazoacetoacetate **61** as a pale yellow oil (5.76 g, 18.6 mmol, 74% yield). **¹H NMR** (250 MHz) δ 4.42 (ddd, J = 11.7, 3.6, 1.1 Hz, 1 H), 4.30 (dd, J = 11.7, 5.1 Hz, 1 H), 4.20 (d, J = 2.4 Hz, 2 H), 4.09 (dt, J = 8.0, 4.2 Hz, 1 H), 4.01 (dt, J = 8.0, 5.0 Hz, 1 H), 3.69 (dd, J = 5.7, 2.4 Hz, 1 H), 3.64 (dd, J = 5.7, 2.4 Hz, 1 H), 2.46 (s, 3 H), 2.43 (t, J = 2.4 Hz, 1 H), 1.40 (s, 3 H), 1.38 (s, 3 H); **¹³C NMR** (125 Hz) δ 189.8, 161.0, 110.1, 78.9, 76.4, 76.2, 75.0, 69.9, 64.4, 58.8, 42.8, 28.2, 26.9, 26.8; **IR**: (C=N₂) 2146 cm⁻¹, (C=O) 1719, 1656 cm⁻¹; [α]_D³³ = -12.6° (c = 0.708, CH₂Cl₂).



(1R,2R)-4,4-Dimethyl-1-propargyloxymethyl-2-(diazoacetoacetoxy)methyl-

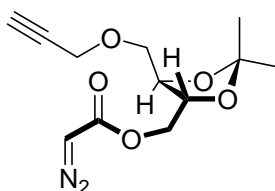
[1,3]dioxolane. ^1H NMR (250 MHz) δ 4.42 (ddd, $J = 11.7, 3.6, 1.1$ Hz, 1 H), 4.30 (dd, $J = 11.7, 5.1$ Hz, 1 H), 4.20 (d, $J = 1.4$ Hz, 2 H), 4.09 (dt, $J = 8.0, 4.2$ Hz, 1 H), 4.01 (dt, $J = 8.0, 5.0$ Hz, 1 H), 3.69 (dd, $J = 5.7, 2.4$ Hz, 1 H), 3.64 (dd, $J = 5.7, 2.4$ Hz, 1 H), 2.46 (s, 3 H), 2.43 (t, $J = 2.4$ Hz, 1 H), 1.40 (s, 3 H), 1.38 (s, 3 H); ^{13}C NMR (125 Hz) δ 189.8, 161.0, 110.1, 78.9, 76.4, 76.2, 75.0, 69.9, 64.4, 58.8, 42.8, 28.2, 26.9, 26.8; **IR:** (C=N₂) 2146 cm⁻¹, (C=O) 1719, 1656 cm⁻¹; $[\alpha]_D^{33} = +12.7^\circ$ ($c = 0.680$, CH₂Cl₂).



(1S,2S)-4,4-Dimethyl-1-propargyloxymethyl-2-(diazoacetoxy)methyl-

[1,3]dioxolane (62). To a stirred solution of **61** (5.77 g, 18.6 mmol, 1.00 eq) in THF (40 mL) was added a solution of LiOH•H₂O (3.90 g, 92.9 mmol, 5.00 eq) dissolved in deionized water (60 mL). The resultant yellow solution was allowed to stir fast enough to disrupt the liquid/liquid interface for 30 min. and monitored by ^1H NMR until complete disappearance of the singlet at 2.46 ppm was achieved. The reaction mixture was diluted with ethyl ether (45 mL) and washed with 2.5 M aqueous NH₄Cl (3 x 50 mL). The resultant organic layer was dried over anhydrous magnesium sulfate, filtered through glass wool and concentrated under reduced pressure, then

subjected to flash chromatography on silica gel (60:40 petroleum ether/ethyl ether) to afford diazoacetate **62** as a yellow oil (3.04 g, 11.3 mmol, 61% yield). ^1H NMR (250 MHz) δ 4.84 (s, broad, 1 H), 4.40 (dd, $J = 11.7, 3.2$ Hz, 1 H), 4.26-4.19 (comp, 3 H), 4.11-3.99 (comp, 2 H), 3.69 (d, $J = 4.6$ Hz, 2 H), 2.51 (t, $J = 2.4$ Hz, 1 H), 1.44 (s, 3 H), 1.42 (s, 3 H); ^{13}C NMR (125 Hz) δ 110.0, 79.1, 76.4, 76.3, 74.9, 69.8, 64.2, 58.7, 46.2, 26.9, 26.7 (the signal consistent with a carbonyl carbon was not observed, but was verified by IR spectroscopy); IR: (C=N₂) 2115 cm⁻¹, (C=O) 1728 cm⁻¹; $[\alpha]_{\text{D}}^{33} = -18.5^\circ$ ($c = 0.860$, CH₂Cl₂).



(1S,2S)-4,4-Dimethyl-1-propargyloxymethyl-2-(diazoacetoxy)methyl-

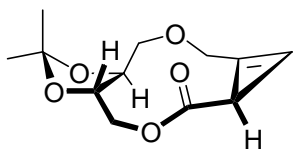
[1,3]dioxolane. ^1H NMR (250 MHz) δ 4.84 (broad s, 1 H), 4.40 (dd, $J = 11.7, 3.2$ Hz, 1 H), 4.26-4.19 (comp, 3 H), 4.11-3.99 (comp, 2 H), 3.69 (d, $J = 4.6$ Hz, 2 H), 2.51 (t, $J = 2.4$ Hz, 1 H), 1.44 (s, 3 H), 1.42 (s, 3 H); ^{13}C NMR (125 Hz) δ 110.0, 79.1, 76.4, 76.3, 74.9, 69.8, 64.2, 58.7, 46.2, 26.9, 26.7 (the signal consistent with a carbonyl carbon was not observed, but was verified by IR spectroscopy); IR: (C=N₂) 2115 cm⁻¹, (C=O) 1728 cm⁻¹; HRMS (FAB +) Calculated for C₁₂H₁₆O₇N₂: 269.1137; found: 269.1128; $[\alpha]_{\text{D}}^{33} = +18.4^\circ$ ($c = 0.702$, CH₂Cl₂).

General Procedure for diazo decomposition of 62 and 63 by dirhodium(II) catalysts: The procedure for diazo decomposition of **62** with Rh₂(5*R*-MEPY)₄ is

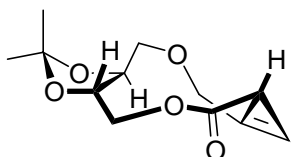
representative. To a refluxing solution of $\text{Rh}_2(5R\text{-MEPY})_4$ (6.5 mg, 0.0075 mmol, 0.010 eq) in DCM (5.0 mL) was added a solution of **62** (0.20 g, 0.75 mmol, 1.0 eq) dissolved in DCM (5 mL) via syringe pump at a rate of 5 mL/h. The resulting solution was heated at reflux for an additional 1 h before filtration through a silica gel plug, which was rinsed with ethyl ether (20 mL). The resulting crude solution was concentrated under reduced pressure to afford a mixture of **63a** and **63b**. An aliquot was removed and the diastereoisomer ratio of the products was determined by comparison of ^1H NMR integration at defined chemical shifts of previously isolated samples (chemical shifts: (**63a**) 6.76 ppm (d), (**63b**) 6.67 ppm (t)).

General Procedure for diazo decomposition of 62 and 64 by copper(I) catalysts:

The procedure for diazo decomposition of **62** catalyzed by $\text{Cu}(\text{CH}_3\text{CN})_4\text{PF}_6/\mathbf{3}$ is representative. A round bottom flask charged with copper(I) hexafluorophosphate (27.1 mg, 0.0730 mmol, 0.100 eq) and bis-oxazoline **3** (25.6 mg, 0.0860 mmol, 0.120 eq) in DCM (5.0 mL) was heated at reflux for 30 min. (heating at reflux for 30 min. was skipped if the bis-oxazoline ligand was not employed in the reaction). After 30 min. a solution of **62** (0.250 g, 0.730 mmol, 1.00 eq) in DCM (5 mL) was added via syringe pump at a rate of 5 mL/h. The resulting solution was then heated at reflux for an additional 1 h before filtration through a silica gel plug, which was rinsed with ethyl ether (20 mL). The resulting crude solution was concentrated under reduced pressure to afford a mixture of **63a** and **63b**. An aliquot was removed and the diastereoisomer ratio of the products was determined by ^1H NMR integration of the cyclopropene peaks at 6.73 (**63a**) and 6.66 (**63b**).



(1R,5S,11R)-13-Dimethyl-3,9,12,14-tetraoxa-tricyclo[9.3.0.0^{5,7}] tetradeca-6-en-4-one (63a). ¹H NMR (400 MHz) δ 6.73 (t, J = 1.3 Hz, 1 H), 5.14 (dd, J = 10.3, 3.7 Hz, 1 H), 4.45 (d, J = 13.7 Hz, 1 H), 4.37 (d, J = 13.7 Hz, 1 H), 3.95 (dd, J = 11.4, 1.3 Hz, 1 H), 3.89 (ddd, J = 10.6, 8.4, 3.7 Hz, 1 H), 3.69 (ddd, J = 8.4, 3.1, 1.3 Hz, 1 H), 3.63 (dd, J = 11.4, 3.1 Hz, 1 H), 3.50 (dd, J = 10.6, 10.3 Hz, 1 H), 2.25 (d, J = 1.3 Hz, 1 H), 1.37 (s, 3 H), 1.33 (s, 3 H); ¹³C NMR (100 Hz) δ 174.5, 112.9, 108.7, 100.5, 80.9, 70.6, 66.2, 62.7, 62.1, 26.7, 26.6, 20.7; **HRMS** (FAB+) Calculated for



C₁₂H₁₆O₇Li: 247.1158; found: 247.1149.

(1R,5S,11S)-13-Dimethyl-3,9,12,14-tetraoxa-tricyclo[9.3.0.0^{5,7}] tetradeca-6-en-4-one (63b). ¹H NMR (400 MHz) δ 6.66 (t, J = 1.3 Hz, 1 H), 4.49 (d, J = 14.5 Hz, 1 H), 4.42 (t, J = 10.3 Hz, 1 H), 4.34 (dd, J = 14.5, 1.6 Hz, 1 H), 4.12 (dd, J = 10.3, 4.4 Hz, 1 H), 3.96 (dd, J = 10.7, 1.6 Hz, 1 H), 3.85 (ddd, J = 10.3, 8.6, 4.4 Hz, 1 H), 3.65 (ddd, J = 8.6, 4.2, 1.6 Hz, 1 H), 3.57 (dd, J = 10.7, 4.2 Hz, 1 H), 2.44 (d, J = 1.3 Hz, 1 H), 1.33 (s, 3 H), 1.31 (s, 3 H); ¹³C NMR (100 Hz) δ 174.1, 113.1, 109.1, 98.6, 82.1, 75.8, 70.7, 63.8, 62.7, 26.7, 26.4, 20.1; **HRMS** (FAB+) Calculated for C₁₂H₁₆O₇Li: 247.1158; found: 247.1154.

Chapter 3. Enhancing the Macrocyclization Reaction Pathway

3.1. Macrocycle Formation

Macrocycles are classified as twelve membered rings and larger.³⁹ They have been studied because of their unique physical properties and the synthetic challenges in their preparation.^{1,40} Over recent decades, macrocyclic compounds have been found to be more common in nature than previously realized, and they are recognized as important materials in natural products, pharmaceuticals, host-guest complexes, molecular machines, display technologies, and biocatalysis.⁴¹ The complexity and structural diversity of synthetic targets having core macrocycles continues to increase, and with it the need for macrocyclization reactions achieving high yields and selectivity.⁴²

Macrocycles are synthesized by ring expansion, cleavage of internal bonds, and end-to-end cyclization of open, long-chain precursors.⁴³ End-to-end cyclization (macrocyclization) is the method of choice, but is entropically disfavored.⁴⁴ Increasing the distance between reacting termini brings increased degrees of freedom, lowering the probability of two distant termini meeting to react. To increase reaction

³⁹ Eliel, E.L. *Stereochemistry of Carbon Compounds*; McGraw-Hill: New York, 1962, pp 188-203.

⁴⁰ Prelog, V. *J. Chem. Soc.* **1950**, 420.

⁴¹ For representative examples see: (a) Roxburgh, C.J. *Tetrahedron* **1995**, *51*, 9767; (b) Gokel, G.W.; Leevy, W.M.; Weber, M.E. *Chem. Rev.* **2004**, *104*, 2723; (c) Schalley, C.A.; Beizai, K.; Vögtle, F. *Acc. Chem. Res.* **2001**, *34*, 465; (d) Meunie, B.; de Visser, S.P.; Shaik, S. *Chem. Rev.* **2004**, *104*, 3947; (e) Rychnovsky, S.D. *Chem. Rev.* **1995**, *95*, 2021; (f) Jedlinski, Z. *Acc. Chem. Res.* **1998**, *31*, 55; (g) Kovbasyuk, I.; Krämer, R. *Chem. Rev.* **2004**, *104*, 3161.

⁴² Yeung, K.-S.; Paterson, I. *Angew. Chem. Int. Ed.* **2002**, *41*, 4632.

⁴³ Deitrich, B.; Viout, P.; Lehn, J.-M. *Macrocyclic Chemistry*, VCH Publishers: New York, 1993.

⁴⁴ Illuminati, G.; Mandolini, L. *Acc. Chem. Res.* **1981**, *14*, 95.

selectivity and yields, high dilution and large solvent volumes are traditionally used in macrocyclization reactions.⁴⁵

As described in Chapter 1, the development of metal mediated carbene reactions has provided an effective methodology for macrocyclization. Ring sizes of 10 to 23 members were found in reactions catalyzed by dirhodium(II) and copper(I) species.⁴⁶ One example even reports the formation of a 52 membered ring using copper(II) acetoacetate.⁴⁷ However, in substrates having a C-H bond four atoms removed from the carbene, γ -butyrolactone formation from C-H insertion has been a severe limitation to macrocyclization reactions using dirhodium(II) carboxamidate catalysts.⁴⁸ Because of the general preference of intramolecular C-H insertion for the γ -position, we considered that blocking that position would improve macrocyclization yields.⁴⁹ We have found a simple substrate modification inhibiting this competitive C-H insertion pathway, enabling a broader range of catalysts to be used in macrocyclic carbene addition reactions.

3.1.1 The Dilution Principle

The “dilution principle”, requiring low substrate concentration and large solvent volumes, was a proposed solution to resolving competitive processes between

⁴⁵ Knops, P.; Sendhoff, N.; Mekelbirger, H.-B.; Vögtle, F. High Dilution Reactions- New Synthetic Applications In Topics in Current Chemistry: Macrocycles ed. Dewar, M.J.S.; Dunitz, J.D.; Hafner, K.; Ito, S.; Lehn, J.-M.; Niedenzu, K.; Raymond, K.N.; Rees, C.W.; Vögtle, F. Springer-Verlag:Berlin, 1992, pp.1-106.

⁴⁶ Doyle, M.P.; McKervey, M.A.; Ye, T. *Modern Catalytic Methods for Organic Synthesis with Diazo Compounds: from Cyclopropanes to Ylides*, Wiley-Interscience:New York, 1998.

⁴⁷ Kulkowit, S.; McKervey, M.A. *J. Chem. Soc., Chem. Commun.* **1981**, 616.

⁴⁸ (a) Doyle, M.P.; Hu, W. *J. Org. Chem.* **2000**, 65, 8839; (b) Doyle, M.P.; Phillips, I.M. *Tetrahedron Lett.* **2001**, 42, 3155

⁴⁹(a) Taber, D.F.; Petty, E.H. *J. Org. Chem.* **1982**, 47, 4808; (b) Taber, D.F.; Ruckle, R.E., Jr. *J. Am. Chem. Soc.* **1986**, 108, 7686.

intramolecular and intermolecular reactions, promoting intramolecular macrocyclization over competitive intermolecular polymerization.⁵⁰ Since its initial use by Ruggli, high dilution has become the standard technique for general macrocyclization.⁵¹ Intramolecular reactions, defined by equation 3.1a, are substrate concentration dependent to the first power, while intermolecular reactions, defined by rate equation 3.1b, are substrate concentration dependant to the second power. As concentration decreases, the intermolecular reaction rate will decrease exponentially in comparison to the intramolecular rate. Thus, under very dilute conditions, the rate of the intermolecular reaction becomes inconsequential in comparison to the intramolecular reaction rate.

Equation 3.1 Rate Equations for Intramolecular and Intermolecular Reactions

$$\text{Intramolecular reaction rate} \quad \text{rate}_{\text{intra}} = k_{\text{intra}} [\text{substrate}] \quad (3.1a)$$

$$\text{Intermolecular reaction rate} \quad \text{rate}_{\text{inter}} = k_{\text{inter}} [\text{substrate}]^2 \quad (3.1b)$$

Development of the dilution principle has led to discussion of cyclization in terms of effective molarity (EM), defined as the concentration at which the intramolecular reaction rate is equal to the intermolecular reaction rate ($1 = \text{rate}_{\text{intra}}/\text{rate}_{\text{inter}}$). This measurement of effective rate of cyclization has been investigated using lactonization by intramolecular S_N2 displacement, and EM values for various ring sizes have been reported (e.g., Table 3.1).⁵² The EM values for thirteen membered rings and larger

⁵⁰ Ruggli, P. *Ann.* **1912**, 392, 92.

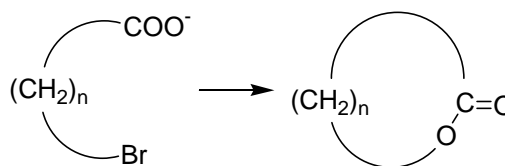
⁵¹ Meng, Q.; Hesse, M. Ring Closure Methods in the Synthesis of Macrocyclic Natural Products In *Topics in Current Chemistry: Macrocycles*, 161; Dewar, M.J.S., Dunitz, J.D., Hafner, K., Ito, S., Lehn, J.-M., Niedenzu, K.; Raymond, K.N.; Rees, C.W.; Vögtle, F. Springer-Verlag:Berlin, 1992 , pp.108-176.

⁵² Illuminati, G.; Mandolini, L.; Masci, B. *J. Am. Chem. Soc.* **1977**, 99, 6308.

formed by lactonization of ω -bromoalkanoate ions remain virtually unchanged, regardless of the number of atoms placed between reacting termini. This means that at a reactant concentration of approximately 1×10^{-2} M half of the material resulting from the reaction will be macrocycles resulting from the intramolecular reaction and the other half of the material will be the result of intermolecular reaction.

Table 3.1 Effective Molarity of Lactonization of ω -Bromoalkanoate ions

n	EM (M)	n	EM (M)
3	1.23×10^{-2}	11	4.82×10^{-3}
4	13.5	12	6.02×10^{-3}
5	1.6×10^3	13	1.82×10^{-2}
6	14.5	14	2.37×10^{-2}
7	5.51×10^{-2}	15	2.56×10^{-2}
8	5.66×10^{-4}	16	2.94×10^{-2}
9	6.33×10^{-4}	18	2.90×10^{-2}
10	1.90×10^{-3}	23	3.42×10^{-2}



As a means of overcoming large solvent volume requirements, dilution by time and dilution by solid phase supported synthesis are also successful dilution techniques applied to macrocyclization.^{5,53} Dilution by time requires substrate addition to a reaction solution over an extended period of time, using, for example, addition controlled by a syringe pump, keeping the substrate concentration very low at any point in time while the total solvent volume required for the complete reaction is reduced. Metal carbene intermediates formed from diazoacetates react rapidly and irreversibly, making diazoacetates ideal substrates for dilution by time.

Dilution by solid supported synthesis is another technology that makes use of the "dilution principle". Here, the reactive substrate is attached to a solid support, preventing it from reacting intermolecularly with another immobilized substrate.

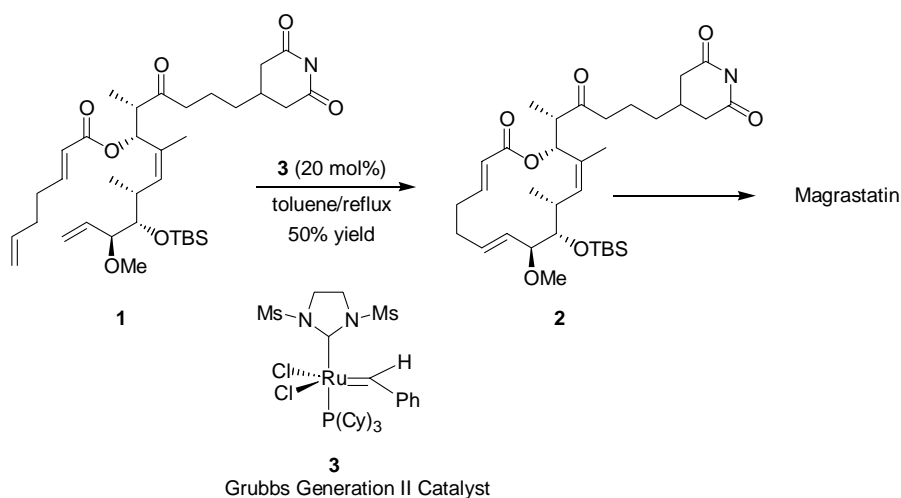
⁵³ Wilson, L.J. Recent Advances in Solid-Phase Synthesis of Natural Products. In *Solid-Phase Organic Synthesis*, Burgess, K. Ed.; Wiley:New York, 2000; pp. 247-367.

However, dilution by solid support is not considered a general method for synthesis in large quantities, as solid supports are costly, and they are not generally recyclable.⁵⁴

3.1.2 Carbene Addition Reactions in Macrocycle Formation

Ring closure to form lactone-containing macrocycles (“macrolides”)⁵⁵ has been extensively developed. A variety of synthetic reactions including esterification, carbon-carbon bond formation, and alkylation of heteroatoms have been reported as effective for macrocyclization.^{3a,13} The most commonly used macrocycle forming reaction using a metal carbene intermediate is ring closing metathesis (RCM).⁵⁶ As an example, the ring closure step in the recently reported total synthesis of mygrastatin⁵⁷ illustrates ring formation through RCM (Scheme 3.1).

Scheme 3.1 Ring Closing Metathesis in the Synthesis of Mygrastatin



Metal carbene intermediates generated from diazo compounds have also been utilized in the synthesis of a variety of macrolides via carbene insertion and addition

⁵⁴ Dörwald, F.Z. *Organic Synthesis on Solid Phase*, Wiley:New York, 2002; pp.18-38.

⁵⁵ Woodward, R.B. *Angew. Chem.*, **1957**, 69, 50.

⁵⁶ Trnka, T.M.; Grubbs, R.H. *Acc. Chem. Res.* **2001**, 34, 18.

⁵⁷ Gaul, C.; Njardarson, J.T.; Shan, D.; Dom, D.C.; Wu, K.-D.; Tong, W.P.; Huang, X.-Y.; Moore, M.A.S.; Danishefsky, S.J. *J. Am. Chem. Soc.*, **2004**, 126, 11326.

reactions. Transformations include addition to olefins,^{10,58} acetylenes,⁵⁹ furans,⁶⁰ and arenes,⁶¹ association with heteroatoms (ylide formation),^{10,20,21} alkene formation ("carbene dimerization"),⁶² and insertion into C-H^{20a} and O-H^{9,63} bonds. These reactions proceed in moderate to good yields, and they demonstrate regio-, stereo-, and chemoselectivity, producing 10 to 23 membered rings. Catalytic diazo decomposition relies on dilution by time instead of by substrate concentration as metathesis, lactonization, and almost all macrocyclization reactions do, reducing the required solvent volume. Dilution by time is not possible with many other macrocyclization reactions, as the reactions are reversible. As concentration increases in a reversible reaction, intermolecular reactions will become increasingly favored, reducing the yield of macrocyclization products. The selectivity and yields reported in the synthesis of macrolides via carbene addition reactions show that metal catalyzed carbene addition reactions are a reasonable means of achieving macrocycle formation.

⁵⁸ (a) Doyle, M.P.; Protopopova, M.N.; Poulter, C.D.; Rogers, D.H. *J. Am. Chem. Soc.*, **1995**, *117*, 7281; (b) Doyle, M.P.; Peterson, C.S.; Parker, D.L., Jr. *Angew. Chem. Int. Ed. Engl.* **1996**, *35*, 1334; (c) Doyle, M.P.; Peterson, C.S.; Protopopova, M.N.; Marnett, A.B.; Parker, D.L., Jr.; Ene, D.G.; Lynch, V. *J. Am. Chem. Soc.* **1997**, *119*, 8826; (d) Doyle, M.P.; Hu, W.; Chapman, B.; Marnett, A.B.; Peterson, C.S.; Vitale, J.P.; Stanley, S.A. *J. Am. Chem. Soc.* **2000**, *122*, 5718.

⁵⁹ (a) Doyle, M.P.; Ene, D.G.; Peterson, C.S.; Lynch, V. *Angew. Chem. Int. Ed. Engl.* **1999**, *38*, 700; (b) Doyle, M.P.; Hu, W. *Tetrahedron Lett.* **2000**, *41*, 6265.

⁶⁰ Doyle, M.P.; Chapman, B.J.; Hu, W.; Peterson, C.S.; McKervey, M.A.; Garcia, C.F. *Org. Lett.* **1999**, *1*, 1327.

⁶¹ Doyle, M.P.; Protopopova, M.N.; Peterson, C.S.; Vitale, J.P. *J. Am. Chem. Soc.*, **1996**, *118*, 7865

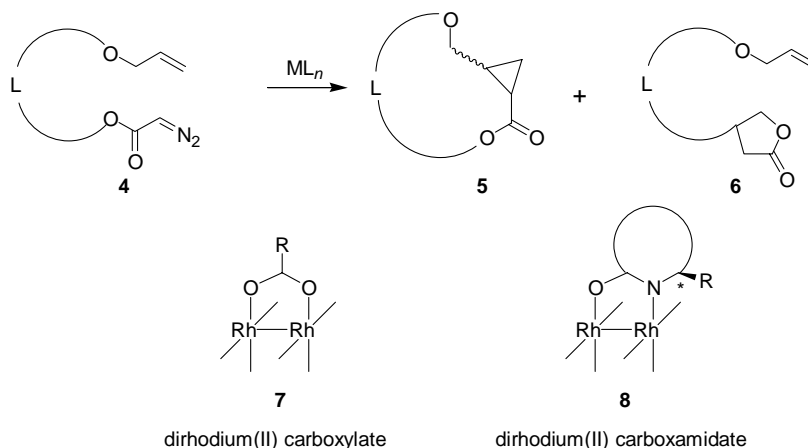
⁶² Doyle, M.P.; Hu, W.; Phillips, I.M. *Org. Lett.* **2000**, *2*, 1777.

⁶³ Helsin, J.C.; Moody, C.J. *J. Chem. Soc., Perkin Trans. 1* **1988**, 1417.

3.1.2.1 Competitive C-H Insertion Reaction Pathways

The most widely investigated catalytic metal carbene addition reactions forming macrocycles use diazoacetates connected by any suitable organic substrate (linker = L)⁶⁴ to an olefin (Scheme 3.2). Macrocyclization occurs by metal catalyzed carbene addition to the olefin (**5**).⁶⁵ Chiral dirhodium(II) carboxylates and copper(I) catalysts are more suitable for macrocyclization than the highly enantioselective chiral dirhodium(II) carboxamides,¹⁰ because chiral dirhodium(II) carboxamides prefer intramolecular carbon-hydrogen insertion resulting in **6**.

Scheme 3.2 Intramolecular Reaction Pathways of Diazo Decomposition



The unique geometry and rigid structure of dirhodium(II) carboxamidates (**8**) makes them excellent catalysts for enantioselective intramolecular cyclopropanation.⁸ Unlike chiral carboxylates, the characteristic geometry of chiral dirhodium(II) carboxamidates is the projection of a chiral ester from the plane formed by the ligand bridging both rhodium atoms, which is the source of the enantiocontrol that these

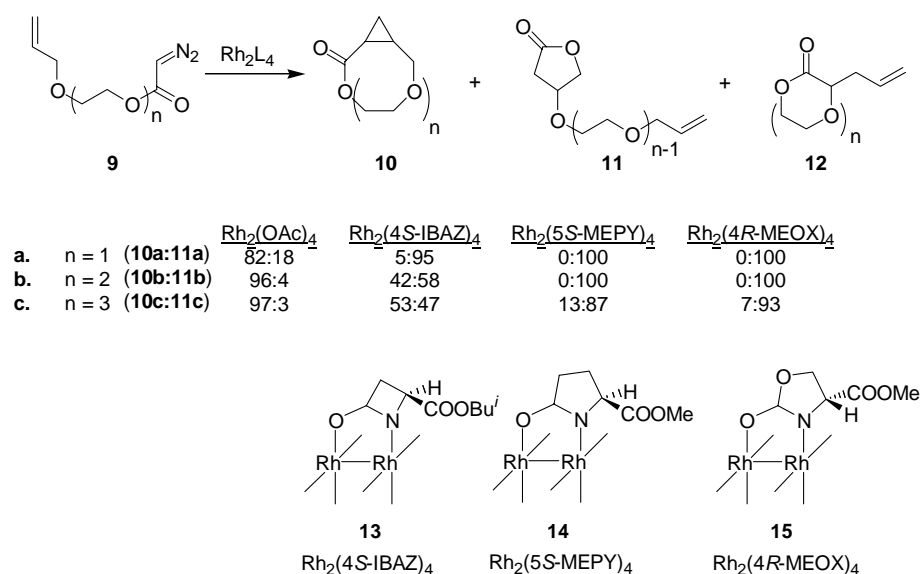
⁶⁴ A linker in this context is any organic compound that connects the diazoacetate to the allyl group through bonds and provides the conformational freedom required for the formation of **5**.

⁶⁵ Doyle, M.P.; Hu, W. *Synlett*, **2001**, 9, 1364.

catalysts exhibit (see section 1.3). Finding a way to disfavor γ -butyrolactone formation would enable chiral dirhodium(II) carboxamides to be utilized as catalysts in asymmetric carbene addition to form macrocycles.

A study using ethylene glycol based linkers of various lengths showed that dirhodium carboxamides were less likely to undergo cyclopropanation (**10**) than dirhodium tetraacetate, instead preferring C-H insertion to form γ -butyrolactones (**11**) (Scheme 3.3).^{10a} Each of these reactions was performed with 1.0 mol% catalyst at a final substrate concentration of 0.10 M.

Scheme 3.3 Carboxamidate versus Carboxylate Catalysts



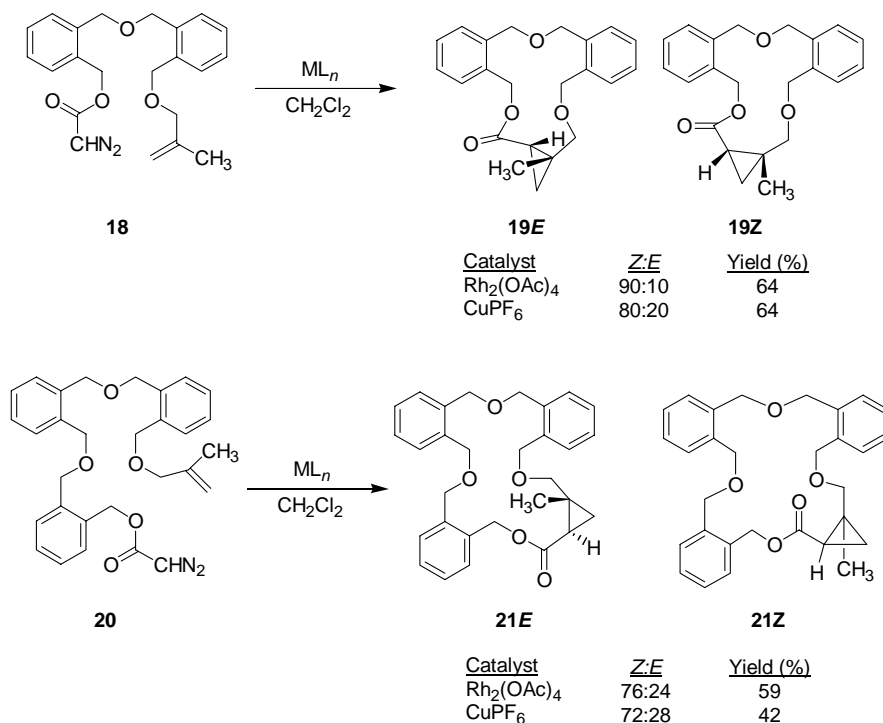
Competitive formation of γ -butyrolactones (**11**) reduced the macrocyclization pathway to the point of exclusion in several reactions. For example, in reactions using $\text{Rh}_2(5S\text{-MEPY})_4$ and $\text{Rh}_2(4R\text{-MEOX})_4$ for catalytic decomposition of **9**, C-H insertion product **11** is the major product formed. With the activated dirhodium(II) carboxamidate catalyst $\text{Rh}_2(4S\text{-IBAZ})_4$, on the other hand, diazoacetates **9b** and **9c**

undergo cyclopropanation (**10**) much more readily than when catalyzed by Rh₂(4*R*-MEOX)₄, but still do not overcome competitive C-H insertion as compared to decomposition of the same compounds with dirhodium(II) tetraacetate. Diazo decomposition of **6a** and **6b** also produced a small amount of **12** ($\leq 6\%$), which originates from ylide formation on the allyl ether oxygen, followed by [2,3]-sigmatropic rearrangement. The relative yield of **12** is not included in the product ratios (**10:11**) in Scheme 3.2 for simplicity.

3.2 Macrocycle Ring Size Limits

The largest rings formed via cyclopropanation used repeating units of 1,2-benzenedimethanol as a linker.^{20c} Successful use of 1,2-benzenedimethanol as an unreactive linker has been demonstrated in the formation of macrocycles **19** and **21** with yields exceeding fifty percent (Scheme 3.4).^{20c} Noteworthy is the observation that C-H insertion, which must occur into a C-H bond that would form a 4- or 7-membered ring, is not reported, though such insertion reactions are known and aromatic cycloaddition, which is readily detected by ¹H NMR absorptions between 6 and 7 ppm, is not observed. We have previously discussed the low susceptibility of 1,2-benzenedimethanol to carbene addition and insertion reactions (section 1.4). By selecting a linker derived from 1,2-benzenedimethanol, compounds **18** and **20** are substrates in which a macrocyclization pathway is far more facile than any other pathway, driving the reaction to form macrocycles in good yields and high chemoselectivity.

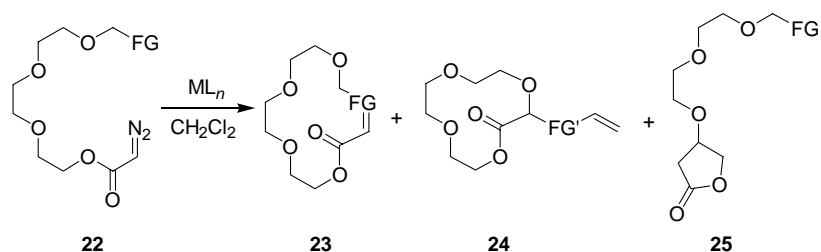
Scheme 3.4. Large ring cyclopropanation



3.2.1 Functional Group Variants

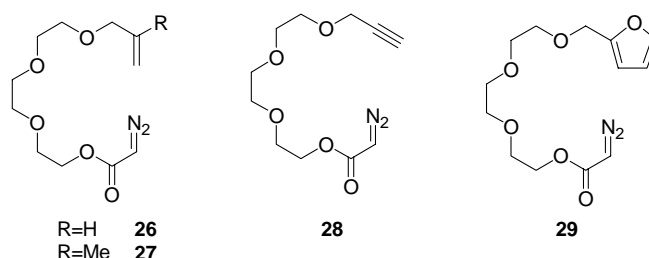
The effects functional groups have on regioselectivity and chemoselectivity in macrocycle formation have also been investigated and were discussed in section 1.4.4.1 (Scheme 3.5).^{21b} Diazo decomposition of these substrates using dirhodium(II) and copper(I) catalysts resulted in a mixture of products from carbene addition (**23**) and C-H insertion to form γ -butyrolactones (**25**) and ylide formation followed by [2,3]-sigmatropic rearrangement (**24**). The resulting regioselectivity, diastereoselectivity, and chemoselectivity using each functional group were then reviewed and compared.^{21b}

Scheme 3.5 Macrocyclization with Various Functional Groups



In the diazo decomposition of substrates having an allyl (**26**), methallyl (**27**), propargyl (**28**), or furfuryl (**29**) functional group tethered by tri(ethylene glycol) to a diazoacetate (Figure 3.1), the more reactive catalysts, dirhodium(II) tetraacetate and copper(I) catalysts, preferred carbene addition (**23**) over C-H insertion (**24**). Dirhodium(II) carboxamidate decomposition of the same compounds produced γ -butyrolactones resulting from C-H insertion. γ -Butyrolactone formation was dependent on both the catalyst employed and the functional group available to undergo carbene addition. The relative preference for C-H insertion was allyl > methallyl > furfuryl > propargyl.

Figure 3.1 Diazoacetates



3.2.2 Linker Modification

The previous examples utilized ethylene glycol based linkers in synthesis of the diazoacetates **26**, **27**, **28**, and **29**. However, Doyle and Phillips reported synthesis and decomposition of diazoacetates having aliphatic linkers (Scheme 3.6).^{10b}

Scheme 3.6 Ring Formation with Alkane Linkers

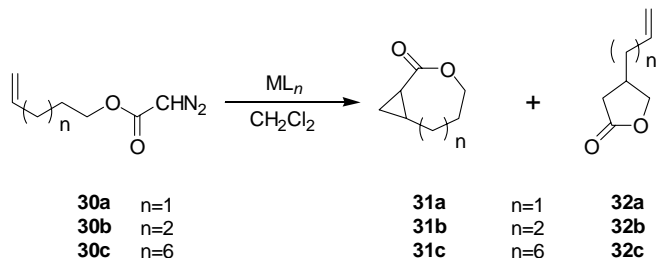


Table 3.2 Selectivity in the Diazo Decomposition of **30^a**

Catalyst	Substrate	31:32 ^b
$Rh_2(OAc)_4$	30a	>99:<1
	30b	84:16
	30c	68:32
$Rh_2(5S-TBPRO)_4$	30a	>99:<1
	30b	82:18
	30c	79:21
$Rh_2(4S-IBAZ)_4$	30a	92:8
	30b	50:50
	30c	18:82
$Rh_2(4S-MEOX)_4$	30a	19:81
	30b	9:91
	30c	1:99

(a) Reactions performed in 15 mL total volume refluxing dichloromethane with 1.0 mol% of catalyst with 1.0 mmol of diazo ester.

(b) Ratios obtained by GC (SPB-5 column).

The results show that dirhodium(II) carboxamidate catalysts exhibit greater chemoselectivity for C-H insertion (**32**) than dirhodium(II) carboxylate catalysts in the diazo decomposition reactions of **30**. In addition, the longer the linker between diazoacetate and olefin (**30a-c**), the greater the preference of C-H insertion over cyclopropanation, regardless of the catalyst used. Both of these observations are consistent with macrocyclic cyclopropanation to γ -butyrolactone ratios in the diazo

decomposition of diazoacetate compounds using ethylene glycol based linkers.^{10a,21b,22}

3.3 Inhibition of γ -Lactone Formation

To enhance chemoselectivity in macrocyclic cyclopropanation, C-H insertion at the γ -position of the diazoacetate must be inhibited. Previous work demonstrates that the 1,2-benzenedimethanol ester of a diazoacetate effectively blocks C-H insertion at the γ -position, favoring macrocycle formation.^{20c,66} In order to enhance macrocyclic cyclopropanation in reactions of polyether tethered diazoacetates we have blocked C-H insertion at the γ -position using a 1,2-benzenedimethanol linker, and we find significantly enhanced macrocyclization yields and unexpectedly high selectivity for macrocycle formation.

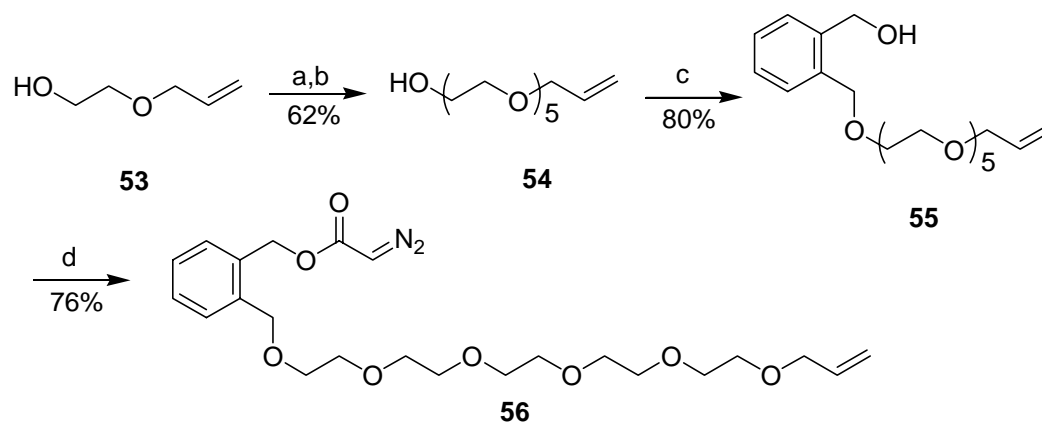
3.3.1 γ -Position C-H Insertion Inhibited Diazoacetates: Synthesis of Diazoacetates

Modification of our previously reported polyether tethered diazoacetates (**26**, **27**, **28**) was easily accomplished by addition of 1,2-benzenedimethanol between the diazoacetate and the ethylene glycol based linker. The synthesis of diazoacetate **56** was accomplished linearly, starting from the olefin terminus (Scheme 3.7), allowing for straightforward modification of the length of the ethylene glycol linker. Product **54** from alkylation of tetra(ethylene glycol) initially proved difficult to purify as flash chromatography did not provide complete separation between **54** and tetra(ethylene

⁶⁶The following reports nucleophilic aromatic addition to 1,2-benzenedimethanol in a unique case with no other reaction possible: Doyle, M.P.; Protopopova, M.N.; Peterson, C.S.; Vitale, J.P. *J. Am. Chem. Soc.* **1996**, *118*, 7865.

glycol). This was resolved by distillation of the crude reaction mixture to remove approximately ninety percent (as determined by recovered volume) of the remaining tetra(ethylene glycol) under reduced pressure, followed by flash chromatography of the remaining mixture of **54** and tetra(ethylene glycol) to achieve isolation of **54**. Residual 1,2-benzenedimethanol from the formation of **55** was also removed by distillation, with nearly quantitative recovery of the excess 1,2-benzenedimethanol used in the reaction.⁶⁷ The Corey-Myers diazoacetate transfer protocol⁶⁸ was used in preference to other diazo transfer methods because it is a single step process in an organic solvent, avoiding aqueous extraction as well as difficulties that are associated with water removal.

Scheme 3.7 Synthesis of Diazo Precursors



(a) MsCl, Et₃N, THF; (b) NaH, tetra(ethylene glycol), THF, reflux; (c) NaH, 1,2-benzenedimethanol, THF, reflux; (d) glyoxylic acid chloride p-toluenesulfonylhydrazone, *N,N*-dimethylaniline, Et₃N, CH₂Cl₂, 0 °C.

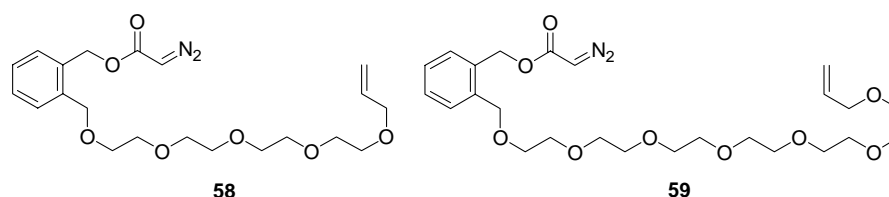
Synthesis of **58** and **59** was accomplished using the procedures described for the synthesis of **56** with the modification of using allyl bromide in place of 2-allyloxy-

⁶⁷ Recovery percentage was based on the mass of 1,2-benzenedimethanol material recovered.

⁶⁸ Corey, E.J.; Myers, A.G. *Tetrahedron Lett.* **1984**, 25, 3359.

ethyl methansulfonyl ester or penta(ethylene glycol) in place of tetra(ethylene glycol) respectively in step (b) (Scheme 3.7). The substrates were synthesized in anticipation of investigating the effectiveness of macrocyclization with changes in tether length between allyl and diazoacetate (Figure 3.2). Isolation of intermediate substrates was accomplished using distillation and flash chromatography procedures identical to those used in the synthesis of **56**, and reaction yields were similar.

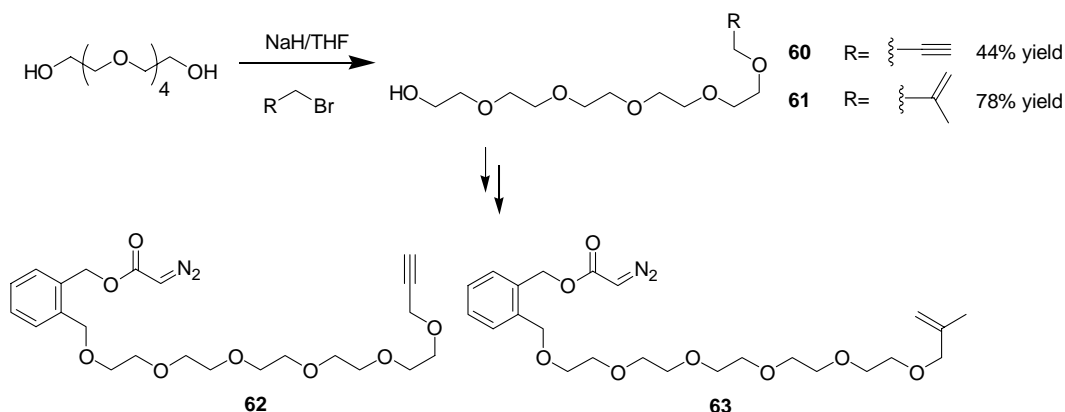
Figure 3.2 Diazoacetate Precursors



Chemoselectivity based on functional group differences, as discussed in section 3.2.3, prompted us to evaluate both propargyl (**62**) and methallyl (**63**) functional groups in substrates that inhibit γ -lactone formation. Synthesis of these compounds was achieved using the synthetic procedure developed to prepare **56** (Scheme 3.11). Initial alkylation of penta(ethylene glycol) was accomplished using the bromide leaving group of the alkylating reagent⁶⁹ instead of the mesylate leaving group used in synthesis of **56**, **58**, and **59** (Scheme 3.8). This led to improved yields in the formation of **61**, but reduced yields in the formation of **60**. Subsequent steps to complete the synthesis of diazoacetates **62** and **63** were carried out using the procedures described in the synthesis and isolation of **56**.

⁶⁹ Propargyl bromide was used in the synthesis of **60**, and methallyl bromide was used in the synthesis of **61**.

Scheme 3.8 Synthesis of Macrocycle Precursors with Functional Group Diversity



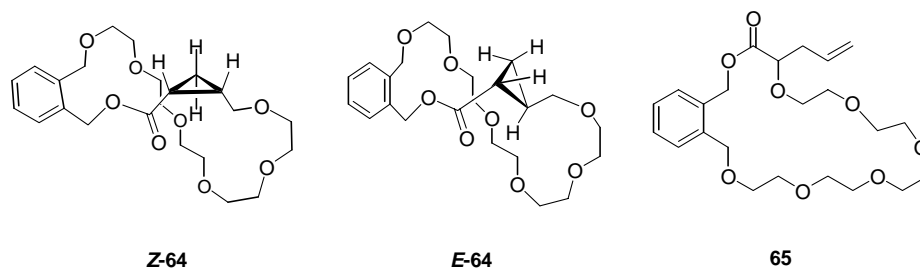
3.3.2 Diazoacetates where γ -C-H Insertion is Inhibited: Selectivity

Based on the chemoselectivity seen in earlier studies,^{10,20-22} catalyst selection in this investigation is important. Dirhodium tetraacetate was selected as a catalyst due to its excellent chemoselectivity previously reported in macrocycle formation from carbene addition. The high preference for γ -butyrolactone formation exhibited by $\text{Rh}_2(4R\text{-MEOX})_4$ made it an excellent catalyst for this investigation. $\text{Rh}_2(4S\text{-MEAZ})_4$ was selected for the aforementioned increased reactivity of dirhodium(II) carboxamides having azetidinone based ligands. Copper(I) hexafluorophosphate was selected as a metal species having reactivity similar to that of dirhodium tetraacetate and for its ability to promote oxonium ylide formation with subsequent [2,3]-sigmatropic rearrangement.

Only the 25-membered macrocycle **64** was isolated from diazo decomposition of **56** catalyzed by dirhodium(II) tetraacetate. Macrocycle **64** was formed as a composite of two geometrical isomers that were structurally characterized by ^1H NMR chemical shifts, and coupling constants consistent with those seen for *E* ($J = 9.1, 4.6$ Hz) and *Z*

($J = 8.5, 7.7, 5.9$ Hz) isomers of previously characterized cyclopropanes.^{10a} Products were analyzed for the geometrical preference of the cyclopropane by integration of the signals observed at 0.89 ppm and 1.10 ppm in the ^1H NMR spectrum of the reaction mixture; these signals correspond to the *E* and *Z* isomers respectively. Integration of UV absorbance spectra from HPLC separation of the isomers agreed with the *E* and *Z* isomer ratios obtained by ^1H NMR signal integration. ^1H NMR spectra of the crude decomposition mixtures do not reveal any doublet-doublet or triplet coupled protons between the chemical shifts of 2.5 and 3.3 ppm, which would correlate to an intramolecular C-H insertion product, and no other monomeric product could be identified. This is important to note, as it means that C-H insertion is not a significant reaction pathway in the decomposition of **56**. Other materials were observed, but their origins were not determined.

Figure 3.2 Macrocycles formed from Catalytic Diazo Decomposition of **56**

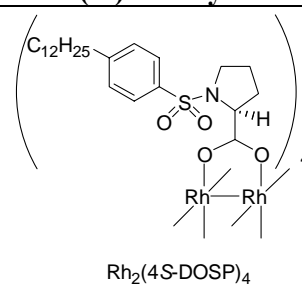


Cyclopropanation product **64** was also obtained with other dirhodium(II) catalysts (Table 3.3), showing modest variation in the diastereomer ratio (**64E:64Z**). The chiral carboxamidate catalysts $\text{Rh}_2(4S\text{-MEOX})_4$ and $\text{Rh}_2(4S\text{-MEAZ})_4$ formed **64** in good yields, but enantioselectivity of the products formed from these reactions was not measured due to the unavailability of means of separation. Dirhodium(II) caprolactamate ($\text{Rh}_2(\text{cap})_4$) was used as an achiral carboxamidate for comparison.

Surprisingly, $\text{Rh}_2(\text{cap})_4$ formed **64** in only trace quantities, and the only additional products that could be identified were those resulting from carbene dimerization, which were identified by the singlet peaks at 6.3 and 6.9 ppm for the maleate and fumarate esters, respectively. With use of the highly reactive $\text{Rh}_2(\text{pfb})_4$ a new product (**65**), consistent with that that from intramolecular oxonium ylide formation and subsequent [2,3]-sigmatropic rearrangement, was observed in minor amounts (Figure 3.2). In each reaction the recovered crude mass was approximately ninety percent of the theoretical mass.

Table 3.3 Diazo Decomposition^a of **56 with Selected Dirhodium(II) Catalysts**

Catalyst	64:65^b	<i>E:Z</i> (64) ^a	Yield (64 + 65) ^c
$\text{Rh}_2(\text{pfb})_4$	94:6	52:48	41
$\text{Rh}_2(\text{OAc})_4$	100:0	36:64	71
$\text{Rh}_2(\text{oct})_4$	100:0	44:56	70
$\text{Rh}_2(4S\text{-DOSP})_4$	100:0	40:60	62
$\text{Rh}_2(4S\text{-MEAZ})_4$	100:0	50:50	50
$\text{Rh}_2(4S\text{-MEOX})_4$	100:0	75:25	41
$\text{Rh}_2(\text{cap})_4$	100:0	n.d.	trace



a) reactions carried out as 2 h addition of **56** to refluxing solution of 1 mol% catalyst in 10 mL methylene chloride b) Ratios of products obtained by ^1H NMR c) yields obtained by crude mass and ^1H NMR ratios.

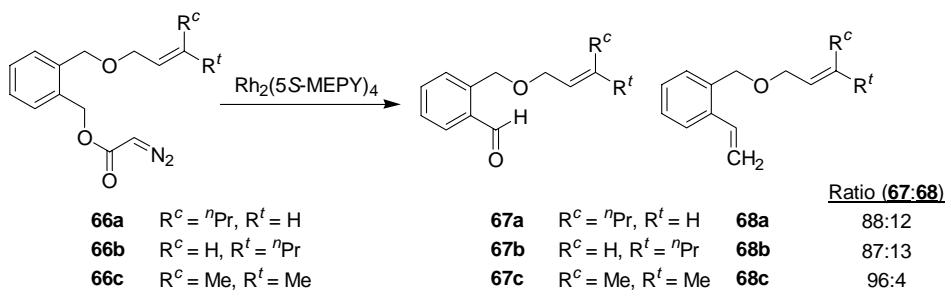
The results found in Table 3.3 show that **64** can be formed through dirhodium(II) mediated carbene addition to an allylic olefin in moderate to good yields, and that inhibition of carbene insertion into the γ position C-H of the diazoacetate enhances the effectiveness of dirhodium(II) catalysts for macrocycle formation. The chemoselectivity gained by blocking γ -butyrolactone formation from C-H insertion is best illustrated in the results seen in diazo decomposition of **56** catalyzed by $\text{Rh}_2(4S\text{-DOSP})_4$ and by the chiral carboxamidates $\text{Rh}_2(4S\text{-MEAZ})_4$ and $\text{Rh}_2(4S\text{-MEOX})_4$. Each catalyst is known to effectively activate C-H insertion reactions in competition

with cyclopropanation.²⁴ Diazo decompositions of **56** catalyzed by $\text{Rh}_2(4S\text{-DOSP})_4$, $\text{Rh}_2(4S\text{-MEAZ})_4$ or $\text{Rh}_2(4S\text{-MEOX})_4$ yield macrocycle **64** in moderate yields, and there is no indication of products resulting from C-H insertion in the ^1H NMR spectra of the crude reaction mixtures. Effective blocking of C-H insertion in the γ position opens the door for a much larger range of dirhodium(II) catalysts to be utilized in macrocycle forming carbene addition reactions.

Hydride abstraction has been reported in the decomposition of 1,2-benzenedimethanol diazoacetate esters (**66**) using three different dirhodium(II) carboxamidate catalysts (Scheme 3.9).^{20d,70} The resulting products are an aryl aldehyde (**67**) and an aryl olefin (**68**), which is formed formally from the β -lactone insertion product.³⁴ A singlet was observed at δ 10.23 in the ^1H NMR of crude material from the $\text{Rh}_2(4S\text{-MEOX})_4$ catalyzed decomposition of **56**, which is consistent with the chemical shift of an aldehyde. However, the integrated area of this peak corresponded to less than 10% of the crude product material, and an aldehyde was not isolated. Evidence for the formation of an accompanying olefin was not found.

⁷⁰ Doyle, M.P.; Dyatkin, A.B.; Autry, C.L. *J. Chem. Soc., Perkin Trans I* **1995**, 619.

Scheme 3.9 Hydride Abstraction in 1,2-Benzenedimethanol Diazoacetates



Singlet peaks at δ 6.3 and 6.9 consistent with maleate and fumarate esters from "carbene dimerization" were also observed in the ^1H NMR of crude material from the $\text{Rh}_2(\text{cap})_4$ catalyzed decomposition of **56**. Integration of the peak areas showed that the materials were approximately 20% of the crude reaction material, but attempts to isolate the products by reverse phase chromatography failed to separate the products from other unidentified materials completely. The infrequent occurrence of products from "carbene dimerization" with 0.25 mmol of diazoacetate compound and 10 mL of methylene chloride illustrates just 0.025 M concentration is needed to keep intermolecular reactions from occurring using metal mediated carbene addition reactions for macrocycle formation.

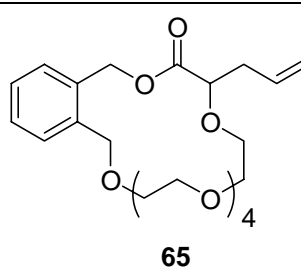
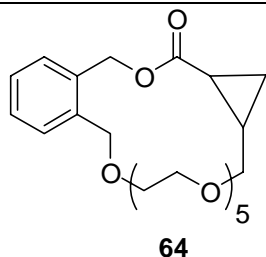
Copper catalysts also exhibit good conversion of **56** to macrocyclic products **64** and **65**. The competitive reaction pathway of oxonium ylide formation leads to production of **64** and **65** in nearly equal quantities (Table 3.4). Reported investigations of copper catalyzed oxonium ylide formation showed that copper ligand and counter-ion modifications resulted in improved yields and selectivity.⁷¹ However, in our hands, diazo decomposition of **56** with three different copper

⁷¹ Clark, J.S.; Krowiak, S.A. *Tetrahedron Lett.* **1993**, 34, 4385.

catalysts resulted in virtually no change in chemoselectivity between substrates **64** and **65**. Diazo decomposition was also attempted using copper(II) acetylacetonate [Cu(acac)₂], but decomposition only occurred in refluxing dichloroethane (DCE) without formation of macrocycles **64** or **65**, and no ¹H NMR signals consistent with C-H insertion, carbene dimerization, or ylide formation were observed.

Table 3.4 Diazo Decomposition^a of **56 with Selected Copper(I) Catalysts**

Catalyst	64 : 65	<i>E</i> : <i>Z</i> (64) ^a	Yield (64 + 65) ^b
[Cu(OTf)] ₂ C ₆ H ₆	62:38	57:43	76
Cu(CH ₃ CN) ₄ PF ₆	51:49	57:43	82
Cu(hfacac) ₂ ^d	52:48	60:40	75
CuPF ₆ / 34	N/A	N/A	0



a) reactions carried out as 2 h addition of **45** to refluxing solution of 10 mol% catalyst in 10 mL methylene chloride b) Ratios of products obtained by ¹H NMR c) yields obtained by crude mass and ¹H NMR ratios d) hfacac = hexafluoroacetoacetate

Diazo decomposition of **56** by copper(I) hexafluorophosphate incubated with 2,2'-isopropylidene-bis[(4*S*)-4-*tert*-butyl-2-oxazoline] (**34**) yielded an unexpected result. Coordination of an external ligand to the copper catalyst appears to impede the formation of macrocycles by both the cyclopropanation and ylide reaction pathways. ¹H NMR spectra of the resultant reaction crude displayed no identifiable monomeric products. Copper coordination of **34** appears to change the catalyst reactivity in a manner that disfavors macrocycle formation, though the exact reason for this change is not apparent at this time.

The effect of the length of the linker between the diazoacetate and the allyl group on chemoselectivity and yield was investigated using diazoacetates **56**, **58**, and **59**. Decomposition of these compounds with dirhodium(II) tetraacetate or copper(I) hexafluorophosphate led to cyclopropanes **64**, **69**, and **70** from carbene addition as well as **65**, **71**, and **72**, resulting from oxonium ylide formation followed by [2,3]-sigmatropic rearrangement (Scheme 3.10). Products **65**, **71**, and **72** could not be isolated, but were assigned based on the ^1H NMR signal observed at 5.85 ppm that has a ddt splitting pattern. This signal is consistent with the signal observed for previously isolated macrocycles formed from oxonium ylide formation followed by [2,3]-sigmatropic rearrangement.^{10a}

Scheme 3.10 Diazo Decomposition of Substrates with Variable Linker Lengths

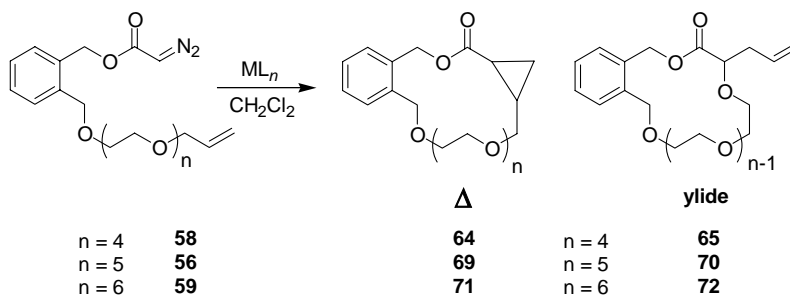


Table 3.5 Synthesis of Cyclopropanes with Varying Ring Size^a

Catalyst	substrate	Δ :ylide	<i>E:Z</i> ^b	% yield ^c
$\text{Rh}_2(\text{OAc})_4$	58	100:0	40:60	69
	56	100:0	36:64	71
	59	100:0	35:65	68
$\text{Rh}_2(4S\text{-MEAZ})_4$	58	100:0	34:66	42
	56	100:0	50:50	50
	59	100:0	44:56	46
$\text{Rh}_2(4S\text{-MEOX})_4$	58	100:0	44:56	39
	56	100:0	65:35	46
	59	100:0	n.d.	<5
$\text{Cu}(\text{CH}_3\text{CN})_4\text{PF}_6$	58	56:44	61:39	84
	56	51:49	57:43	82
	59	55:45	47:53	76
$\text{Cu}(\text{hfacac})_2$	58	47:53	54:46	63
	56	52:48	60:40	75
	59	51:49	54:46	66

a) reactions carried out as 2 h addition of diazo substrate to refluxing solution of catalyst in 10 mL methylene chloride b) Ratios of products obtained by ¹H NMR c) yields obtained by Crude mass and ¹H NMR ratios.

Diazo decomposition of **59** with $\text{Rh}_2(4S\text{-MEOX})_4$ did not yield cyclopropanation products in significant quantities in spite of several attempts (Table 3.5). ¹H NMR spectral analysis of the $\text{Rh}_2(4S\text{-MEOX})_4$ catalyzed crude reaction mixture showed only trace amounts of macrocyclic compounds resulting from cyclopropanation. Though $\text{Rh}_2(4S\text{-MEOX})_4$ catalyzed diazo decomposition of **59** was complete, no

additional products could be identified in the ^1H NMR spectrum. Copper(II) hexafluoroacetoacetate $[\text{Cu}(\text{hfacac})_2]$ was employed because previous work had described the favorable chemoselectivity of this catalyst in oxonium ylide formation followed by [2,3]-sigmatropic rearrangement.³⁵ However, chemoselectivity in the diazo decompositions of **56**, **58**, and **59** does not significantly differ from that observed when using copper(I) hexafluorophosphate. The cyclopropanes formed from **56**, **58**, and **59** using dirhodium(II) tetraacetate exhibit low diastereoselectivity, with *E* to *Z* ratios consistent with those seen in intermolecular cyclopropanation using ethyl diazoacetate.⁷² This same trend of low diastereoselectivity is also seen in the decompositions of **56**, **58**, and **59** using copper(I) catalysts. Each reaction was run with 0.25 mmol of diazoacetate compound and 10 mL of methylene chloride, yet the preference for an intramolecular reaction pathway over an intermolecular pathway was not affected by the length of the linker between the diazoacetate and the allyl group at this concentration.

Investigation of the role of the functional group in effecting chemoselectivity was accomplished using dirhodium(II) tetraacetate, dirhodium(II) perfluorobutyrate, copper(I) hexafluorophosphate, and copper(I) triflate to decompose **56**, **62**, and **63** (Scheme 3.11). The decomposition of **62** by dirhodium(II) catalysts affords cyclopropene **73**, while copper(I) catalyzed decomposition of **62** yields **74** (Table 3.6). Diastereoselectivity in the dirhodium(II) catalyzed diazo decomposition of **63** favors the *Z* diastereoisomer, while copper(I) catalyzed diazo decomposition favors

⁷² Doyle, M.P.; Bagheri, V.; Wandless, T.J.; Harn, N.K.; Brinker, D.A.; Eagle, C.T.; Loh, K.-L. *J. Am. Chem. Soc.*, **1990**, *112*, 1906.

the *E* diastereoisomer. Fortunately, both **73** and **75** were isolated, confirming that oxonium ylide formation followed by [2,3]-sigmatropic rearrangement occurs with these substrates, and lending support to the previous assumption that products **65**, **70** and **72** were also formed.

Scheme 3.11 Macrocyclization with Allyl, Methallyl, and Propargyl Functional Groups

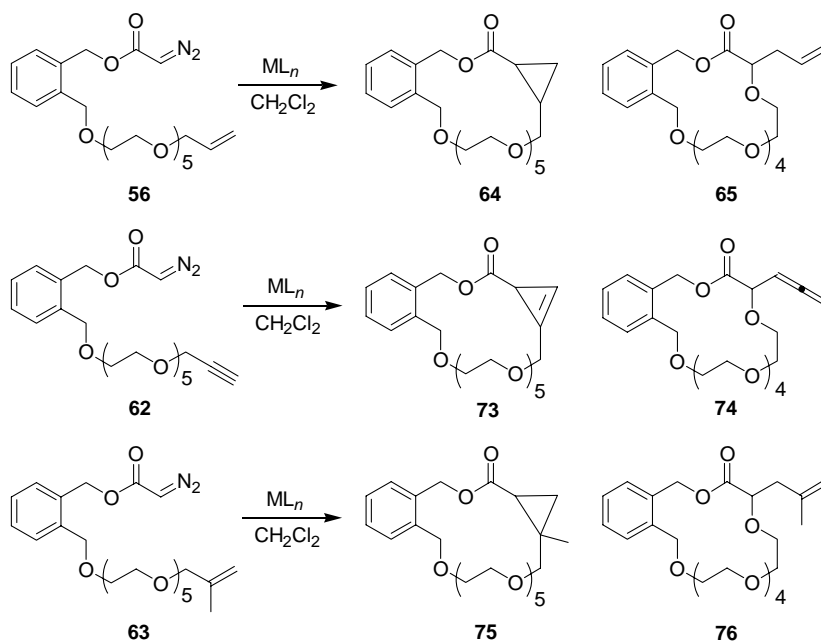
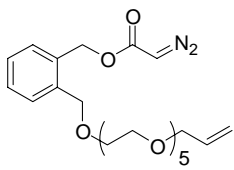
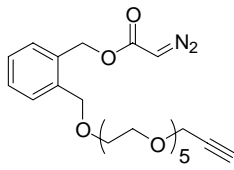
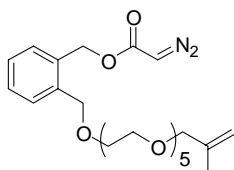


Table 3.6 Diazo Decomposition of Substrates with Selected Functional Groups^a

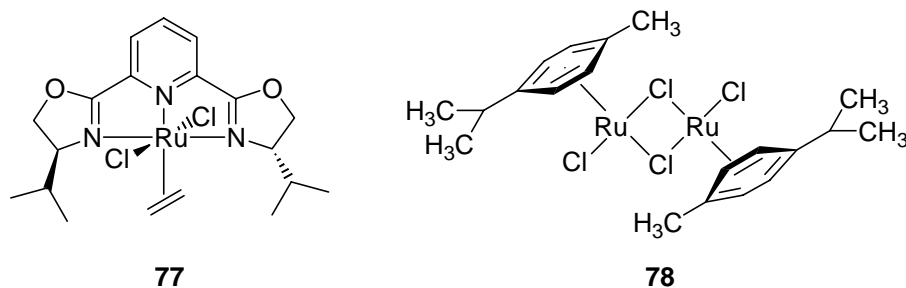
Substrate	Catalyst	64:65	<i>E:Z</i> ^b	% yield ^c
 56	Rh ₂ (OAc) ₄	100:0	36:64	71
	Rh ₂ (pfb) ₄	94:6	52:48	41
	Cu(CH ₃ CN) ₄ PF ₆	51:49	57:43	82
	[Cu(OTf)] ₂ C ₆ H ₆	62:38	57:43	76
 62	(73:74)			
	Rh ₂ (OAc) ₄	100:0	N/A	70
	Rh ₂ (pfb) ₄	100:0	N/A	3
	Cu(CH ₃ CN) ₄ PF ₆	0:100	N/A	70
 63	(75:76)			
	Rh ₂ (OAc) ₄	100:0	34:66	38
	Rh ₂ (pfb) ₄	100:0	29:71	24
	Cu(CH ₃ CN) ₄ PF ₆	34:66	81:19	69
	[Cu(OTf)] ₂ C ₆ H ₆	63:37	72:28	80

- a) reactions carried out as 2 h addition of diazo substrate to refluxing solution of catalyst in 10 mL methylene chloride
b) Ratios of products obtained by ¹H NMR integration
c) yields obtained by crude mass and ¹H NMR ratios.

Use of [RuCl₂(*p*-cymene)]₂ (**78**), Nishiyama's RuCl₂(*S,S*)^{*i*}Pr-pybox catalyst (**77**),⁷³ boron trifluoride etherate, silver(I) hexafluorophosphate, and silver(I) triflate to decompose **56** showed complete diazo decomposition without macrocycle formation or identifiable monomeric products (Figure 3.3). From this we conclude that the catalyst species that promotes diazo decomposition must also facilitate the carbene addition or ylide formation to undergo macrocycle formation.

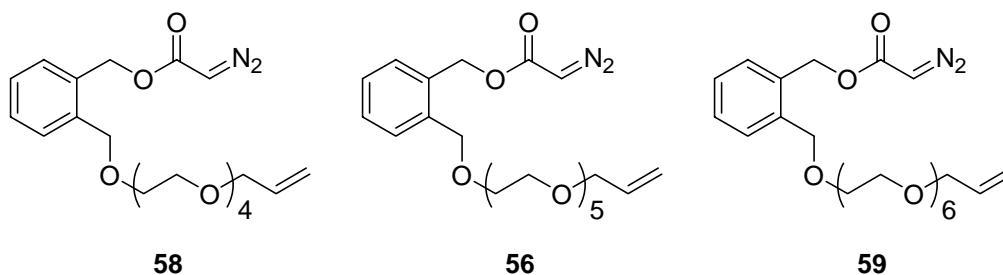
⁷³ Nishiyama, H.; Itoh, Y.; Matsumoto, H.; Park, S.-B.; Itoh, K. *J. Am. Chem. Soc.* **1994**, *116*, 2223.

Figure 3.3 Additional Catalysts Used in the Decomposition of 56



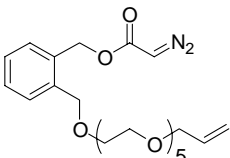
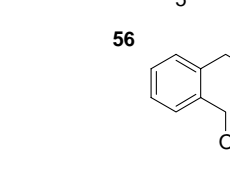
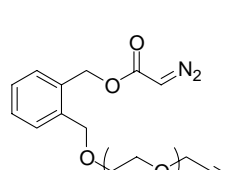
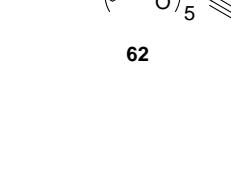
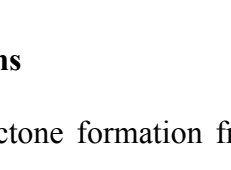
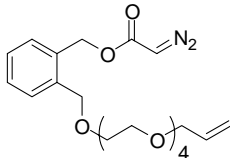
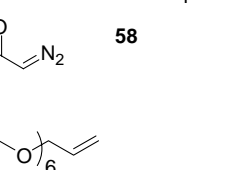
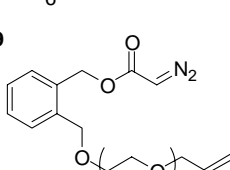
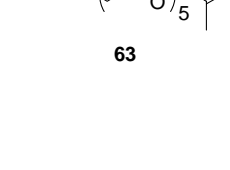
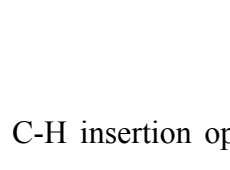
The importance of catalyst reactivity may be seen by comparing results of diazo decomposition of **56**, **58**, and **59** (Figure 3.4) by dirhodium(II) tetraacetate and $\text{Rh}_2(4S\text{-MEOX})_4$ (Table 3.5). Decomposition by dirhodium(II) tetraacetate is characterized by virtually unchanged yields and selectivities seen regardless of ring size. Diazo decomposition by $\text{Rh}_2(4S\text{-MEOX})_4$ provides lower product yields than does dirhodium(II) tetraacetate, and decomposition of **59** with $\text{Rh}_2(4S\text{-MEOX})_4$ fails to produce macrocyclic products. The reason for this unique result requires further investigation. In general, more reactive dirhodium(II) carboxylates and copper(I) catalysts afford higher yields of macrocyclic compounds than dirhodium(II) carboxamides. $\text{Rh}_2(\text{cap})_4$ catalyzed diazo decomposition of **56** yields only a trace amount of macrocyclic compounds, while decomposition of **56** by $\text{Rh}_2(4S\text{-MEOX})_4$ and $\text{Rh}_2(4S\text{-MEAZ})_4$ affords higher product yields, and dirhodium(II) tetraacetate produces the highest product yields of the catalysts surveyed.

Figure 3.4 Diazoacetates **56, **58**, and **59****



The exception to the relationship between catalyst reactivity and the yield of macrocyclic compounds is dirhodium(II) perfluorobutyrate, which has the most electron withdrawing ligands of all of the catalysts screened. Contrary to the general trend between catalyst reactivity and the yield of cyclopropanation products seen with other dirhodium(II) catalysts, product yields from dirhodium(II) perfluorobutyrate catalyzed diazo decompositions are diminished in comparison to those catalyzed by dirhodium(II) tetraacetate (Table 3.7). The reactivity of dirhodium(II) perfluorobutyrate makes it the only dirhodium(II) catalyst promoting oxonium ylide formation in the diazo decomposition of **56**, **59**, and **59**. Data obtained from HPLC analysis of dirhodium(II) perfluorobutyrate catalyzed decomposition of **56** shows several additional compounds not consistent with products **64** or **65** that could not be fully characterized, but ¹H NMR analysis shows that the allyl group is still intact. This lack of reaction selectivity is a reflection of the high reactivity of the metal carbene intermediate.

Table 3.7 Yields of Reactions Catalyzed by Rh₂(pfb)₄ versus Rh₂(OAc)₄

Catalyst	Substrate	Yield (%)	
Rh ₂ (OAc) ₄	58	69	
	56	71	
	59	68	
	62	70	
	63	38	
Rh ₂ (pfb) ₄	58	31	
	56	44	
	59	31	
	62	3	
	63	24	

3.4 Conclusions and Future Directions

Substrate design inhibiting γ -butyrolactone formation from C-H insertion opens up new avenues for the use of carbene addition reactions in macrocycle formation. This inhibition further increases the chemoselectivity of dirhodium(II) catalysts and permits the use of catalysts, such as Rh₂(MEOX)₄, not previously viable for macrocycle formation. Diazo decomposition of **56**, **58**, **59**, **62**, and **63** by select dirhodium(II) and copper(I) catalysts results in the formation of macrocycles ranging in size from 20 to 28-membered rings in yields that exceeded 80% in some cases.

This study inhibiting γ -butyrolactone formation enables chiral dirhodium(II) carboxamidate catalysts to be used in macrocyclization, which may now be carried on to investigate enantioselectivity and diastereoselectivity in carbene addition reactions to form new macrocycles. Inhibition of γ -butyrolactones formation also allows for

investigation of new substrates. Tethers between the diazoacetate and the reactive functional group can now be prepared using aliphatic compounds to provide diversified substrates. Finally, reaction rates and the effective molarity (EM) of diazoacetates may be investigated for macrocyclic substrates with dirhodium(II) and copper(I) catalysts.

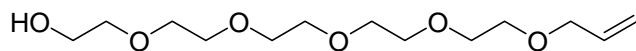
3.5 Experimental Procedures

General Methods. ^1H and ^{13}C spectra were obtained as solutions in CDCl_3 using a Bruker DRX400 workstation; ^1H chemical shifts are reported as parts per million (ppm, δ) downfield from Me_4Si (TMS); ^{13}C chemical shifts are reported as parts per million (ppm, δ) relative to CDCl_3 (77.0 ppm). Mass spectra were obtained from the University of Maryland Department of Chemistry and Biochemistry Mass Spectrometry Facility. Infrared spectra were obtained from thin film depositions on KBr plates using a Nicolet 560 EXC spectrophotometer with absorptions recorded in wavenumbers (cm^{-1}). All reagents were obtained from Aldrich and used as received unless otherwise noted. All reactions were carried out under an atmosphere of nitrogen. Anhydrous tetrahydrofuran (THF) and dichloromethane (DCM) were obtained from nitrogen forced flow of Baker HPLC grade solvents over activated alumina prior to use.⁷⁴ Thin layer chromatography was performed on EM Scientific Silica Gel 60 F₂₅₄ glass-backed plates. Flash chromatographic purification was performed using Silicycle 40-63 μm , 60 Å silica gel. Reverse phase (HPLC) chromatographic analyses were performed on a Varian Prostar instrument with dual wavelength detection at 220 and 254 nm employing a Varian Dynamax 250x10mm microsorb C18 column. Reverse phase solvents were 18M Ω water and HPLC grade acetonitrile which was obtained from Pharmco and used as received. Sodium hydride was used as a 60% suspension in mineral oil. Glyoxylic acid chloride *p*-tolusulphonylhydrazone was prepared as previously reported.⁷⁵ Preparation of

⁷⁴ Panghonr, A.B.; Giardello, M.A.; Grubbs, R.H.; Rosen, R.K.; Timmers, F.J. *Organometallics*, **1996**, *15*, 1518.

⁷⁵ (a) House, H.O.; Blankley, C.J. *J. Org. Chem.* **1968**, *33*, 53; (b) Blankely, C.J.; Sauter, F.J.; House, H.O. *Org. Synth.* **1969**, *49*, 22.

copper(I) hexfluorophosphate,⁷⁶ 2,2-bis[2-[4(*S*)-*tert*-butyl-1,3-oxazolinyl]]propane [(*S,S'*)*t*Bu-BOX],⁷⁷ Rh₂(4*S*-MEOX)₄,⁷⁸ and Rh₂(4*S*-MEAZ)₄⁷⁹ have been previously reported.



(2-(2-(2-(2-(2-Allyloxy-ethoxy)-ethoxy)-ethoxy)-ethoxy)-ethanol (54).

To a 100 mL round bottom flask charged with allyloxyethanol (5.00 g, 49.0 mmol) dissolved in THF (50 ml) was added methanesulfonyl chloride (4.2 ml, 54 mmol) all at once followed by triethylamine (7.6 ml, 54 mmol) at ambient temperature. The resulting suspension was stirred for 1.5 h then filtered, followed by washing the filter cake with diethyl ether (3 x 25 mL). The combined filtrates were concentrated under reduced pressure yielding 2-allyloxy-ethyl-1-methanesulfonate ester as a colorless oil (6.48 g, 36.0 mmol, 73.5%): ¹H NMR (300 MHz) δ 5.90 (ddt, *J* = 17.3, 10.3, 5.7 Hz, 1 H), 5.32 (ddd, *J* = 17.3, 3.3, 1.7 Hz, 1 H), 5.20 (ddt, *J* = 10.3, 1.7, 1.3 Hz, 1 H), 4.38 (dt, *J* = 2.7, 4.5 Hz, 2H), 4.04 (dt, *J* = 5.7, 1.3 Hz, 2 H), 3.73 (dt, *J* = 2.7, 4.5 Hz, 2H), 3.07 (s, 3H); ¹³C NMR (75 MHz) δ 133.90, 117.62, 72.10, 69.14, 67.66, 37.58; HRMS (FAB+): calculated for C₆H₁₂SO₄: 181.0535; found 181.0536.

To a flame-dried round bottom flask charged with tetra(ethylene glycol) (9.9 mL, 57 mmol, 1.0 eq) and THF (500 mL) was added NaH (2.40 g, 60 mmol, 1.1 eq.) in one portion. After gas evolution subsided, the solution was brought to reflux and 2-

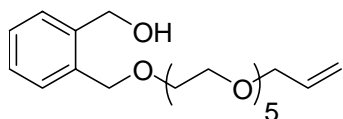
⁷⁶ Kubas, G.J. *Inorg. Synth.* **1979**, *19*, 90.

⁷⁷ Evans, D.A.; Peterson, G.S.; Johnson, J.S.; Barnes, D.M.; Campos, K.R.; Woerpel, K.A. *J. Org. Chem.* **1998**, *63*, 4541.

⁷⁸ Doyle, M.P.; Dyatkin, A.B.; Protopopova, M.N.; Yang, C.I.; Miertschin, C.S.; Winchester, W.R.; Simonsen, S.I.; Lynch, V.; Ghosh, R. *Recueil Trav. Chim. Pays-Bas*, **1995**, *114*, 163.

⁷⁹ Doyle, M.P.; Davies, S.B.; Hu, W.H. *J. Org. Chem.*, **2000**, *65*, 8839.

allyloxy-1-ethyl methanesulfonate (13 g, 74 mmol, 1.3 eq) was added in one aliquot, after which the reaction mixture was heated with stirring at reflux for 12 h. The resulting cloudy solution was filtered through a pad of Celite, and the solid residue was rinsed with ethyl ether (3 x 150 mL). The filtrate was concentrated under reduced pressure, and the resultant yellow oil was purified by flash chromatography on silica gel (EtOAc:hexanes:Et₂O, 55:35:10), yielding alcohol **1** as a clear oil (9.71 g, 34.8 mmol, 61 %): TLC R_f = 0.11 (88:10:2 EtOAc:Et₂O:MeOH) visualized using cerium molybdate (Hanessian's Stain);⁸⁰ ¹H NMR (400 MHz) δ 5.93 (ddt, J = 17.3, 10.3, 5.7 Hz, 1 H), 5.29 (ddd, J = 17.3, 3.3, 1.7 Hz, 1 H), 5.19 (ddt, J = 10.3, 1.7, 1.3 Hz, 1 H), 4.04 (dt, J = 5.7, 1.3 Hz, 2 H), 3.76-3.60 (comp, 20 H), 2.59 (s, broad, 1 H); ¹³C NMR (100 MHz) δ 134.7, 117.1, 72.5, 72.2, 70.6, 70.56, 70.54, 70.3, 69.4, 61.7; HRMS (FAB+) calculated for C₁₃H₂₆O₇: 279.1808; found: 279.1821.



(2-(2-(2-(2-(2-(2-Allyloxy-ethoxy)-ethoxy)-ethoxy)-ethoxy)-ethoxymethyl)-phenyl)-methanol (55). To a 250 mL round bottom flask charged with **54** (3.90 g, 14.0 mmol, 1.00 eq) in THF (100 mL) was added methanesulfonyl chloride (1.14 mL, 14.7 mmol, 1.05 eq) followed by triethylamine (2.05 mL, 14.7 mmol, 1.05 eq). The reaction solution was stirred for 1 h at ambient temperature. The resultant cloudy white solution was filtered, and the collected solid was washed with diethyl ether (3 x 25 mL). The combined filtrates were concentrated under reduced pressure, resulting in a clear oil. To a second flame-dried 1000 mL flask charged with 1,2-

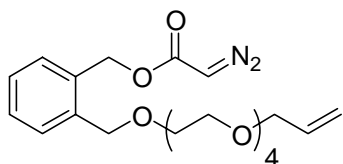
⁸⁰ *Handbook of Thin-Layer Chromatography* J. Sherman and B. Fried, Eds., Marcel Dekker, New York, NY, 1991.

benzenedimethanol⁸¹ (2.89 g, 21.0 mmol, 1.50 eq) in THF (500 mL) was added NaH (0.870 g, 21.7 mmol, 1.55 eq) in one portion. After gas evolution subsided the suspension was brought to reflux, and the resultant oil from the initial flask was added in one aliquot. After refluxing for 12 h, the solution was cooled to room temperature, then filtered through a pad of Celite, and the pad was washed with diethyl ether (3 x 150 mL). The combined filtrates were concentrated under reduced pressure to provide a pale yellow oil, from which residual 1,2-benzenedimethanol (bp = 140 °C @ 0.8 torr)⁸² was removed by kugelrohr distillation (160 °C @ 0.7 torr). The remaining viscous oil was purified by flash chromatography on silica gel (EtOAc:hexanes:Et₂O 55:35:10) to yield alcohol **55** as a clear, viscous oil (4.47 g, 11.2 mmol, 80 %): TLC *R*_f = 0.16 (88:10:2 EtOAc:Et₂O:MeOH) visualized using a solution of KMnO₄; ¹H NMR (400 MHz) δ 7.41 (d, *J* = 7.6 Hz, 1 H), 7.34 (dt, *J* = 2.8, 6.8 Hz, 1 H), 7.30-7.25 (comp, 2 H), 5.91 (ddt, *J* = 17.2, 10.4, 5.7 Hz, 1 H), 5.26 (ddd, *J* = 17.2, 3.1, 1.5 Hz, 1 H), 5.17 (ddd, *J* = 10.4, 1.5, 1.2 Hz, 1 H), 4.66 (s, 2 H), 4.65 (d, *J* = 6.4 Hz, 2 H), 4.01 (dt, *J* = 5.7, 1.2 Hz, 2 H), 3.65-3.57 (comp, 20 H), 3.48 (t, *J* = 6.4 Hz, 1 H); ¹³C NMR (100 MHz) δ 140.7, 135.8, 134.6, 129.9, 129.7, 128.7, 127.6, 116.9, 72.3, 72.1, 70.46, 70.43, 70.40, 70.3, 70.2, 69.3, 69.0, 63.2; HRMS (FAB+) calculated for C₂₁H₃₄O₇: 399.2383; found: 399.2377.

⁸¹ 1,2-Benzendimethanol prepared by the following method method: Doyle, M.P.; Peterson, C.S.; Protopopova, M.N.; Marnett, A.B.; Parker, D.L., Jr.; Ene, D.G.; Lynch, V. *J. Am. Chem. Soc.* **1997**, *119*, 8826.

⁸² Entel, J; Ruof, C.F; Howar, H.C, *J. Am. Chem. Soc.* **1952**, *74*, 441.

(ddd, $J = 10.4, 3.1, 1.3$ Hz, 1 H), 4.81 (s, broad, 1 H), 4.62 (s, 2 H), 4.02 (dt, $J = 1.3, 5.7$ Hz, 2 H), 3.67-3.58 (comp, 20 H); ^{13}C NMR (100 MHz) δ 136.5, 134.7, 134.3, 129.2, 129.1, 128.4, 128.0, 117.0, 72.2, 70.9, 70.6, 70.5, 69.6, 69.4, 64.0, 46.2; IR (neat oil): (C=N₂) 2111cm⁻¹, (C=O) 1692cm⁻¹; HRMS (FAB+) calculated for C₂₃H₃₄O₈N₂Li: 473.2475; found: 473.2481.



(2-(2-(2-(2-(2-Allyloxy-ethoxy)-ethoxy)-ethoxy)-ethoxymethyl)-phenyl)methyl diazoacetate (58). To a flame-dried 500 mL round bottom flask charged with tetra(ethylene glycol) (5.01 g, 25.7 mmol, 1.00 eq) in THF (300 mL) was added NaH (1.08 g, 27.0 mmol, 1.05 eq) in one portion, and the resulting mixture was stirred vigorously until gas evolution subsided and a clear solution was obtained. Allyl bromide (3.20 mL, 36.0 mmol, 1.40 eq) was then added in one aliquot, and the resultant yellow solution was stirred for 12 h at ambient temperature, filtered through a pad of Celite, which was subsequently washed with ethyl ether (3 x 75 mL), and the combined filtrates were concentrated under reduced pressure to yield a clear oil. The oil was purified by flash chromatography on silica gel (EtOAc:hexanes:Et₂O, 55:35:10) and (2-(2-(2-(2-allyloxy-ethoxy)-ethoxy)-ethoxy)-ethoxy)-ethan-1-ol was isolated as a clear, viscous oil (3.98 g, 17.0 mmol, 66 %): TLC $R_f = 0.15$ (88:10:2 EtOAc:Et₂O:MeOH) visualized using cerium molybdate. ^1H NMR (400 MHz) δ 5.92 (ddt, $J = 17.2, 10.4, 5.7$ Hz, 1 H), 5.29 (ddd, $J = 17.2, 3.2, 1.3$ Hz, 1 H), 5.19 (ddd, $J = 10.4, 3.2, 1.3$ Hz, 1 H), 4.04 (dt, $J = 5.7, 1.3$ Hz, 2 H), 3.77-3.61 (comp, 16 H), 2.56

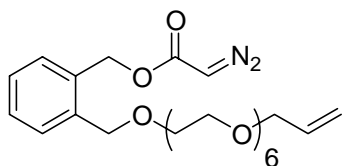
(t, $J = 6.0$ Hz, 1 H); ^{13}C NMR (100 MHz) δ 135.1, 117.6, 72.9, 72.8, 72.7, 71.1, 71.02, 71.00, 70.8, 69.8, 62.2; HRMS (FAB+) calculated for $\text{C}_{11}\text{H}_{22}\text{O}_5$: 235.1545; found: 235.1563.

To a 250 mL round bottom flask charged with (2-(2-(2-(2-allyloxy-ethoxy)-ethoxy)-ethoxy)-ethan-1-ol (1.59 g, 6.77 mmol, 1.00 eq) in THF (100 mL) was added methanesulfonyl chloride (0.550 mL, 7.11 mmol, 1.05 eq) followed by triethylamine (0.991 mL, 7.11 mmol, 1.05 eq). The reaction solution was stirred for 1 h at ambient temperature. The resultant cloudy white solution was filtered, and the collected solid was rinsed with diethyl ether (3 x 25 mL). The combined filtrates were concentrated under reduced pressure, resulting in a clear oil. To a second flame-dried flask charged with 1,2-benzenedimethanol (1.41 g, 10.2 mmol, 1.50 eq) in THF (300 mL) was added NaH (0.408 g, 10.2 mmol, 1.50 eq) in one portion. After gas evolution had subsided, the suspension was brought to reflux, and the resultant oil from the initial flask was added as one aliquot. After refluxing for 12 h, the solution was cooled to room temperature, then filtered through a pad of Celite, which was rinsed with diethyl ether (3 x 100 mL). The combined filtrates were concentrated under reduced pressure to afford a pale yellow oil, from which residual 1,2-benzenedimethanol was removed by kugelrohr distillation (160 °C @ 0.7 torr). The remaining viscous oil was purified by flash chromatography on silica gel (EtOAc:hexanes:Et₂O 55:35:10) to yield (2-(2-(2-(2-(2-allyloxy-ethoxy)-ethoxy)-ethoxy)-ethoxymethyl)-phenyl)-methanol as a clear, viscous oil (1.77 g, 4.99 mmol, 74 %): TLC $R_f = 0.16$ (88:10:2 EtOAc:Et₂O:MeOH) visualized using a solution of KMnO_4 ; ^1H NMR (400 MHz) δ 7.42 (d, $J = 7.3$ Hz, 1 H), 7.34 (td, $J = 6.7, 2.8$ Hz, 1

H), 7.30-7.25 (comp, 2 H), 5.91 (ddt, $J = 17.3, 10.4, 5.6$ Hz, 1 H), 5.27 (ddd, $J = 17.3, 3.2, 1.3$ Hz, 1 H), 5.17 (ddd, $J = 10.4, 3.2, 1.3$ Hz, 1 H), 4.67 (s, 2 H), 4.66 (d, $J = 6.7$ Hz, 2 H), 4.02 (dt, $J = 5.6, 1.3$ Hz, 2 H), 3.66-3.57 (comp, 16 H), 3.46 (t, $J = 6.7$ Hz, 1 H); ^{13}C NMR (100 MHz) δ 141.3, 136.3, 135.2, 130.7, 130.4, 129.4, 128.2, 117.5, 73.0, 72.7, 71.1, 71.0, 70.9, 70.8, 69.8, 69.6, 63.9; HRMS (FAB+) calculated for $\text{C}_{19}\text{H}_{30}\text{O}_6$: 355.2121; found: 355.2115.

To a flame-dried 100 mL round bottom flask was added (2-(2-(2-(2-(2-allyloxy-ethoxy)-ethoxy)-ethoxy)-ethoxymethyl)-phenyl)-methanol (1.60 g, 4.51 mmol, 1.00 eq) and DCM (10.0 mL). The stirred solution was cooled to 0 °C and glyoxylic acid chloride *p*-tolusulphonylhydrazone (1.77 g, 6.77 mmol, 1.50 eq) was added in one portion followed by addition of *N,N*-dimethylaniline (0.858 mL, 6.77 mmol, 1.50 eq) as one aliquot, producing a clear, yellow solution. After stirring for 1 h, during which time the solution changed to a deep green color, triethylamine (3.14 mL, 22.6 mmol, 5.00 eq) was added as one aliquot, instantly changing the solution color to deep red, and the reaction mixture was stirred for an additional hour, then concentrated under reduced pressure. Concentration produced a heterogeneous mixture which was dissolved in a minimal amount of methanol and subjected to flash chromatography on silica gel (Et_2O :petroleum ether:MeOH 50:50:0 to 48:48:4), yielding diazoacetate 58 as a viscous yellow oil (1.39 g, 3.29 mmol, 73 %): ^1H NMR (400 MHz) δ 7.40-7.27 (comp, 4 H), 5.91 (ddt, $J = 17.3, 10.4, 5.7$ Hz, 1 H), 5.31 (s, 2 H), 5.26 (ddd, $J = 17.3, 3.1, 1.3$ Hz, 1 H), 5.17 (ddd, $J = 10.4, 3.1, 1.3$ Hz, 1 H), 4.81 (s, broad, 1 H), 4.62 (s, 2 H), 4.02 (td, $J = 5.7, 1.3$ Hz, 2 H), 3.67-3.58 (comp, 16 H); ^{13}C NMR (100 MHz) δ 136.5, 134.7, 134.3, 129.2, 129.1, 128.3, 128.0, 117.0, 72.2, 70.9, 70.6, 69.6, 69.4,

64.0, 46.2; **IR** (neat oil): (C=N₂) 2112 cm⁻¹, (C=O) 1694 cm⁻¹; **HRMS** (FAB+) calculated for C₂₁H₃₁O₇N₂: 423.2131; found: 423.2116.



(2-(2-(2-(2-(2-(2-Allyloxy-ethoxy))-ethoxy)-ethoxy)-ethoxy)-ethoxy)-

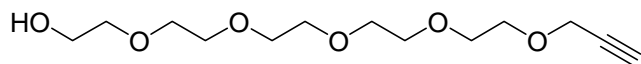
ethoxymethyl)-phenyl)methyl diazoacetate (59). To a 250 mL round bottom flask charged with penta(ethylene glycol) (1.00 mL, 4.73 mmol, 1.00 eq) and THF (75 mL) was added NaH (0.199 g, 4.97 mmol, 1.05 eq) in one portion. After gas evolution subsided, the solution was brought to reflux, and 2-allyloxy-1-ethyl methanesulfonate (1.11 g, 6.14 mmol, 1.30 eq) was added in one aliquot, after which the reaction mixture was heated at reflux for 12 h. The resulting cloudy solution was filtered through a pad of Celite, and the pad was washed with ethyl ether (3 x 25 mL). The combined filtrates were concentrated under reduced pressure, and the resultant yellow oil was purified by flash chromatography on silica gel (EtOAc:hexanes:Et₂O, 55:35:10) yielding (2-(2-(2-(2-(2-(2-allyloxy-ethoxy))-ethoxy)-ethoxy)-ethoxy)-ethoxy)ethan-1-ol as a clear oil (1.18 g, 3.66 mmol, 60 %): **¹H NMR** (400 MHz) δ 5.91 (ddt, *J* = 17.3, 10.4, 5.6 Hz, 1 H), 5.28 (ddd, *J* = 17.3, 3.1, 1.4 Hz, 1 H), 5.18 (ddd, *J* = 10.4, 3.1, 1.4 Hz, 1 H), 4.02 (dt, *J* = 5.6, 1.4 Hz, 2 H), 3.75-3.59 (comp, 24 H), 2.53 (t, *J* = 4.9 Hz, 1 H); **¹³C NMR** (100 MHz) δ 134.7, 116.9, 72.4, 72.1, 70.51, 70.48, 70.3, 69.3, 63.3; **HRMS** (FAB+) calculated for C₁₅H₃₁O₇: 323.2070; found: 323.2089.

To a round bottom flask charged with (2-(2-(2-(2-(2-(2-allyloxy-ethoxy)-ethoxy)-ethoxy)-ethoxy)-ethoxy)ethan-1-ol (2.75 g, 8.53 mmol, 1.00 eq) in THF (250 mL) was added methanesulfonyl chloride (0.693 mL, 8.96 mmol, 1.05 eq) followed by triethylamine (1.25 mL, 8.96 mmol, 1.05 eq). The reaction solution was stirred for 1 h at ambient temperature. The resultant cloudy white solution was filtered, and the filter cake was rinsed with diethyl ether (3 x 50 mL). The combined filtrate was concentrated under reduced pressure, resulting in a clear oil. To a second flame-dried flask charged with 1,2-benzenedimethanol (1.77 g, 12.8 mmol, 1.50 eq) in THF (300 mL) was added NaH (0.544 g, 13.6 mmol, 1.60 eq) in one portion. After gas evolution had subsided, the suspension was brought to reflux, and the resultant oil from the initial flask was added as one aliquot. After refluxing for 12 h, the solution was cooled, then filtered through a pad of Celite, which was rinsed with diethyl ether (3 x 100 mL). The combined filtrate was concentrated under reduced pressure to afford a cloudy, yellow oil from which the residual 1,2-benzenedimethanol was removed by kugelrohr distillation (160 °C @ 0.7 torr). The remaining viscous oil was purified by flash chromatography on silica gel (EtOAc:hexanes:Et₂O 55:35:10) to yield (2-(2-(2-(2-(2-(2-(2-allyloxy-ethoxy)-ethoxy)-ethoxy)-ethoxy)-ethoxy)-ethoxymethyl)-phenyl)-methanol as a clear, viscous oil (2.79 g, 6.30 mmol, 74 %):

¹H NMR (400MHz) δ 7.41 (d, *J* = 7.3 Hz, 1H), 7.32 (dt, *J* = 2.8, 6.7 Hz, 1H), 7.30-7.25 (comp, 2H), 5.90 (ddt, *J* = 17.3, 10.4, 5.6 Hz, 1H), 5.26 (ddd, *J* = 17.3, 3.2, 1.3 Hz, 1H), 5.17 (ddd, *J* = 10.4, 3.2, 1.3 Hz, 1H), 4.66 (s, 2H), 4.65 (d, *J* = 6.7 Hz, 2H), 4.02 (dt, *J* = 5.6, 1.3 Hz, 2H), 3.68-3.59 (comp, 24H), 3.46 (t, *J* = 6.7 Hz, 1H); **¹³C NMR** (100 MHz) δ 140.8, 135.8, 134.7, 129.9, 129.8, 128.7, 127.6, 116.9, 72.4, 72.1,

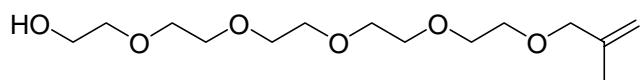
70.5, 70.47, 70.44, 70.38, 70.3, 69.3, 69.0, 63.3; **HRMS** (FAB+) calculated for $C_{23}H_{39}O_8$: 443.2645; found: 443.2631.

To a flame-dried 100 mL round bottom flask was added (2-(2-(2-(2-(2-(2-allyloxy-ethoxy)-ethoxy)-ethoxy)-ethoxy)-ethoxy)-ethoxymethyl)-phenyl)methanol (1.48 g, 3.34 mmol, 1.00 eq) and DCM (16.0 mL). The stirring solution was cooled to 0 °C, and glyoxylic acid chloride *p*-tolusulphonylhydrazone (1.30 g, 5.00 mmol, 1.50 eq) was added in one portion followed by dropwise addition of *N,N*-dimethylaniline (0.634 mL, 5.00 mmol, 1.50 eq) over 5 min., producing a clear, yellow solution. After stirring for 1.5 h, during which time the solution changed to a deep green color, triethylamine (2.33 mL, 16.7 mmol, 5.00 eq) was added as one aliquot, instantly changing the solution color to deep red, and the reaction mixture was stirred for an additional hour, then concentrated under reduced pressure. Concentration produced a heterogeneous mixture which was dissolved in a minimal amount of methanol and subjected to flash chromatography on silica gel (Et₂O:petroleum ether:MeOH 50:50:0 to 47:47:6) to afford the title compound as a viscous yellow oil (1.34 g, 2.62 mmol, 79 %): **¹H NMR** (400 MHz) δ 7.40-7.29 (comp, 4 H), 5.91 (ddt, J = 17.2, 10.4, 5.7 Hz, 1 H), 5.31 (s, 2 H), 5.26 (ddd, J = 17.2, 3.3, 1.5 Hz, 1 H), 5.17 (ddd, J = 10.4, 3.0, 1.5 Hz, 1 H), 4.81 (s, broad, 1 H), 4.62 (s, 2 H), 4.02 (dt, J = 5.7, 1.5 Hz, 2 H), 3.67-3.58 (comp, 24 H) **¹³C NMR** (100 MHz) δ 136.5, 134.8, 134.4, 129.2, 129.1, 128.4, 128.1, 117.1, 72.2, 71.0, 70.63, 70.61, 70.58, 70.56, 69.7, 69.4, 64.0, 46.3; **IR** (neat oil): (C=N₂) 2110cm⁻¹, (C=O) 1692cm⁻¹; **HRMS** (FAB+) calculated for $C_{25}H_{38}O_9N_2Li$: 517.2737; found: 517.2725.



(2-(2-(2-(2-(2-Propargyloxy-ethoxy)-ethoxy)-ethoxy)-ethoxy)-ethoxy)-ethan-1-ol (60).

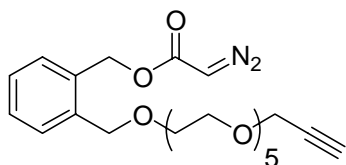
To a flame-dried round bottom flask charged with penta(ethylene glycol) (1.13 g, 4.73 mmol, 1.00 eq) in THF (25 mL) was added NaH (0.197 g, 4.96 mmol, 1.05 eq) in one portion, and the resultant mixture was stirred vigorously until gas evolution subsided. To the clear solution was added an 80% (w/w) solution of propargyl bromide in toluene (1.20 g, 10.1 mmol, 1.60 eq) in one aliquot, and the resultant yellow solution was stirred for 16 h at ambient temperature, filtered through a pad of Celite, which was subsequently washed with ethyl ether (3 x 25 mL), and the combined filtrate was concentrated under reduced pressure to yield a clear oil. The oil was purified by flash chromatography on silica gel (EtOAc:hexanes:Et₂O, 55:35:10), and the title compound was isolated as a clear, viscous oil (0.673g, 2.44 mmol, 44 %): TLC R_f = 0.21 (88:10:2 EtOAc:Et₂O:MeOH) visualized using cerium molybdate; ¹H NMR (400 MHz) δ 4.20 (d, J = 2.3 Hz, 2 H), 3.73-3.64 (comp, 18 H), 3.61 (t, J = 4.5 Hz, 2 H), 2.48 (s, broad, 1 H), 2.43 (t, J = 2.3 Hz, 1 H); ¹³C NMR (100 MHz) δ 79.6, 74.5, 72.4, 70.6, 70.5, 70.4, 70.3, 69.1, 61.7, 58.4; HRMS (FAB+) calculated for C₁₃H₂₄O₆: 277.1651; found: 277.1650.



(2-(2-(2-(2-(2-(2-Methyl-allyloxy)-ethoxy)-ethoxy)-ethoxy)-ethoxy)-ethoxy)ethan-1-ol

(61). To a flame-dried 100 mL round bottom flask charged with penta(ethylene glycol) (0.85 mL, 4.0 mmol, 1.00 eq) in THF (50 mL) was added NaH (0.17 g, 4.2

mmol, 1.05 eq) in one portion, and the resultant mixture was stirred vigorously until gas evolution subsided. To the clear solution was added methallyl bromide (0.51 mL, 5.0 mmol, 1.3 eq) in one aliquot, and the resultant yellow solution was stirred for 12 h at ambient temperature, filtered through a pad of Celite, which was subsequently washed with ethyl ether (3 x 25 mL), and the combined filtrate was concentrated under reduced pressure to yield a clear oil. The oil was purified by flash chromatography on silica gel (EtOAc:Et₂O:MeOH; 89:10:1), yielding alcohol 61 as a viscous, clear oil (0.57 g, 1.9 mmol, 49%): TLC R_f = 0.20 (88:10:2 EtOAc:Et₂O:MeOH) visualized using a solution of KMnO₄; **¹H NMR** (400 MHz) δ 4.96 (s, 1 H), 4.89 (s, 1 H), 3.92 (s, 2 H), 3.72 (t, J = 4.5 Hz, 2 H), 3.69-3.64 (comp, 14 H), 3.61 (t, J = 4.5 Hz, 2 H), 3.56 (t, J = 4.7 Hz, 2 H), 2.72 (s, broad, 1 H), 1.73 (s, 3 H); **¹³C NMR** (100 MHz) δ 142.1, 112.1, 75.0, 72.4, 70.6, 70.5, 70.4, 70.3, 69.0, 61.2, 19.3; **HRMS** (FAB+) calculated for C₁₄H₂₈O₆: 293.1964; found: 293.1954.

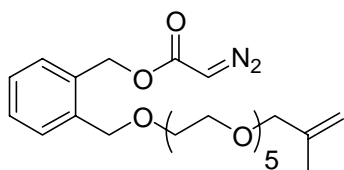


(2-(2-(2-(2-(2-(2-Propargyloxy-ethoxy)-ethoxy)-ethoxy)-ethoxy)-ethoxymethyl)-phenyl)-methyl diazoacetate (62). To a 100 mL round bottom flask charged with 60 (1.13 g, 4.08 mmol, 1.00 eq) in THF (50 mL) was added methanesulfonyl chloride (0.332 mL, 4.29 mmol, 1.05 eq) followed by triethylamine (0.600 mL, 4.29 mmol, 1.05 eq). The reaction solution was stirred for 0.5 h at ambient temperature. The resultant cloudy white solution was filtered and the collected solid was washed with diethyl ether (3 x 25 mL). The combined filtrate was concentrated under reduced

pressure, resulting in a clear oil. To a second flame-dried 250 mL flask charged with 1,2-benzenedimethanol (0.789 g, 5.71 mmol, 1.40 eq) in THF (125 mL) was added NaH (0.229 g, 5.71 mmol, 1.40 eq) in one portion. After gas evolution had subsided, the suspension was brought to reflux, and the resultant oil from the initial flask was added as one aliquot. After refluxing for 12 h, the solution was cooled, then filtered through a pad of Celite, and the pad was washed with diethyl ether (3 x 50 mL). The combined filtrates were concentrated under reduced pressure to afford a yellow oil, from which the residual 1,2-benzenedimethanol was removed by kugelrohr distillation (160 °C @ 0.7 torr). The remaining viscous oil was purified by flash chromatography on silica gel (EtOAc:hexanes:Et₂O 55:35:10) to yield (2-(2-(2-(2-(2-(2-propargyloxy-ethoxy)-ethoxy)-ethoxy)-ethoxy)-ethoxymethyl)-phenyl)-methanol as a clear, viscous oil (0.811 g, 2.05 mmol, 50 %): **¹H NMR** (400 MHz) δ 7.41 (d, *J* = 7.4 Hz, 1 H), 7.34 (dt, *J* = 2.7, 6.7 Hz, 1 H), 7.30-7.24 (comp, 2 H), 4.66 (s, 4 H), 4.20 (d, *J* = 2.4 Hz, 2 H), 3.72-3.59 (comp, 20 H), 3.22 (s, broad, 1 H), 2.43 (t, *J* = 2.4 Hz, 1 H); **¹³C NMR** (100 MHz) δ 141.3, 136.3, 130.6, 130.4, 129.4, 128.2, 80.1, 74.9, 73.0, 71.01, 70.99, 70.97, 70.94, 70.89, 70.81, 70.78, 69.6, 63.9.

To a round bottom flask was added (2-(2-(2-(2-(2-(2-propargyloxy-ethoxy)-ethoxy)-ethoxy)-ethoxy)-ethoxymethyl)-phenyl)-methanol (0.528 g, 1.33 mmol, 1.00 eq) and DCM (5.0 mL). The stirring solution was cooled to 0 °C, and glyoxylic acid chloride *p*-tolusulphonylhydrazide (0.519 g, 1.99 mmol, 1.50 eq) was added in one portion followed by addition of *N,N*-dimethylaniline (0.252 mL, 1.99 mmol, 1.50 eq) in, producing a clear, yellow solution. After stirring for 1 h, during which time the solution changed to a deep green color, triethylamine (0.927 mL, 6.65 mmol, 5.00 eq)

was added as one aliquot, instantly changing the solution color to deep red, and the reaction mixture was stirred for an additional hour, then concentrated under reduced pressure. Concentration produced a heterogeneous mixture which was dissolved in a minimal amount of methanol and subjected to flash chromatography on silica gel (Et₂O:petroleum ether:MeOH 50:50:0 to 48:48:4) to afford diazoacetate **63** as a viscous yellow oil (0.567 g, 1.22 mmol, 92 %): **¹H NMR** (400 MHz) δ 7.40-7.36 (comp, 2 H), 7.33-7.26 (comp, 2 H), 5.31 (s, 2 H), 4.81 (s, broad, 1 H), 4.63 (s, 2 H), 4.20 (d, J = 2.4 Hz, 2 H), 3.68-3.63 (comp, 20 H), 2.43 (t, J = 2.4 Hz, 1 H); **¹³C NMR** (100 MHz) δ 136.5, 134.3, 129.2, 129.1, 128.3, 128.0, 79.6, 74.5, 71.0, 70.9, 70.6, 70.52, 70.48, 70.3, 69.6, 69.5, 69.0, 63.9, 58.3, 46.2; **IR** (neat oil): (C=N₂) 2110cm⁻¹, (C=O) 1692cm⁻¹; **HRMS** (FAB⁺) calculated for C₂₃H₃₂O₈N₂Li: 471.2299; found: 471.2319.



(2-(2-(2-(2-(2-(2-(2-Methyl-allyloxy)-ethoxy)-ethoxy)-ethoxy)-ethoxy)-ethoxymethyl)-phenyl)-methyl diazoacetate (63**)**. To a 500 mL round bottom flask charged with **61** (3.00 g, 10.3 mmol, 1.00 eq) in THF (150 mL) was added methanesulfonyl chloride (0.836 mL, 10.8 mmol, 1.05 eq) followed by triethylamine (1.51 mL, 10.8 mmol, 1.05 eq). The reaction solution was stirred for 2 h at ambient temperature. The resultant cloudy white solution was filtered and the collected solid was washed with diethyl ether (3 x 50 mL). The combined filtrates were concentrated under reduced pressure, resulting in a clear oil. To a second flame-dried

flask charged with 1,2-benzenedimethanol (2.14 g, 15.5 mmol, 1.50 eq) in THF (250 mL) was added NaH (0.640 g, 16.0 mmol, 1.55 eq) in one portion. After gas evolution had subsided, the suspension was brought to reflux, and the resultant oil from the initial flask was added as one aliquot. After refluxing for 15 h, the solution was cooled, then filtered through a pad of Celite, and the pad was washed with diethyl ether (3 x 100 mL). The combined filtrates were concentrated under reduced pressure to afford a yellow oil, from which the residual 1,2-benzenedimethanol was removed by kugelrohr distillation (160 °C @ 0.7 torr). The remaining viscous oil was purified by flash chromatography on silica gel (EtOAc:hexanes:Et₂O 55:35:10, yielding (2-(2-(2-(2-(2-(2-methyl-allyloxy)-ethoxy)-ethoxy)-ethoxy)-ethoxy)-ethoxymethyl)-phenyl)-methanol as a clear, viscous oil (1.78 g, 4.32 mmol, 42 %): **¹H NMR** (400 MHz) δ 7.41 (d, J = 7.6 Hz, 1 H), 7.33 (td, J = 2.7, 6.8 Hz, 1 H), 7.30-7.25 (comp, 2 H), 4.95 (s, 1 H), 4.88 (s, 1 H), 4.66 (s, 4 H), 3.92 (s, 2 H), 3.65-3.59 (comp, 18 H), 3.55 (dd, J = 5.8, 3.8 Hz, 2 H), 3.20 (s, broad, 1 H), 1.73 (s, 3 H); **¹³C NMR** (100 MHz) δ 142.1, 140.9, 135.9, 130.2, 129.9, 128.9, 127.7, 112.188, 75.1, 72.6, 70.58, 70.56, 70.52, 70.4, 70.3, 69.3, 69.11, 69.09, 68.97, 69.4, 37.7, 19.4; **IR** (neat oil): (C=N₂) 2111 cm⁻¹, (C=O) 1692 cm⁻¹; **HRMS** (FAB+) calculated for C₂₂H₃₆O₇: 413.2539; found: 413.2528.

To a round bottom flask was added (2-(2-(2-(2-(2-(2-methyl-allyloxy)-ethoxy)-ethoxy)-ethoxy)-ethoxy)-ethoxymethyl)-phenyl)-methanol (0.694 g, 1.68 mmol, 1.00 eq) and DCM (7.0 mL). The stirring solution was cooled to 0 °C and glyoxylic acid chloride *p*-tolusulphonylhydrazone (0.657 g, 2.52 mmol, 1.50 eq) was added in one portion followed by addition of *N,N*-dimethylaniline (0.319 mL, 2.52 mmol, 1.50 eq)

in one aliquot, producing a clear, yellow solution. After stirring for 1 h, in which time the solution changed to a deep green color, triethylamine (1.17 mL, 8.40 mmol, 5.00 eq) was added as one aliquot, instantly changing the solution color to deep red, and the reaction mixture was stirred for an additional hour, then concentrated under reduced pressure. Concentration yielded a heterogeneous mixture, which was dissolved in a minimal amount of methanol and subjected to flash chromatography on silica gel (Et₂O:petroleum ether:MeOH 50:50:0 to 48:48:4) to afford diazoacetate **63** as a viscous yellow oil (0.619 g, 1.29 mmol, 77 %): ¹H NMR (400 MHz) δ 7.40-7.36 (comp, 2 H), 7.35-7.28 (comp, 2 H), 5.31 (s, 2 H), 4.95 (s, 1 H), 4.88 (s, 1 H), 4.81 (s, broad, 1 H), 4.62 (s, 2 H), 3.92 (s, 2 H), 3.69-3.54 (comp, 20 H), 1.73 (s, 3 H); ¹³C NMR (100 MHz) δ 142.1, 136.5, 134.3, 129.2, 129.1, 128.3, 128.0, 112.1, 75.0, 70.9, 70.6, 70.5, 69.6, 69.0, 63.9, 46.2, 19.3; IR (neat oil): (C=N₂) 2111 cm⁻¹, (C=O) 1693 cm⁻¹; HRMS (FAB+) calculated for C₂₄H₃₆O₈N₂Li: 487.2632; found: 487.2651.

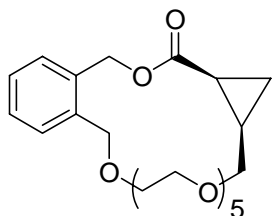
General Procedure for diazo decomposition of **56, **58**, **59**, **62**, and **63** with dirhodium(II) catalysts:** The following is an example procedure of diazo decomposition. An oven dried flask was charged with Rh₂(OAc)₄ (1.7 mg, 2.1 μmol, 0.010 eq) and DCM (5 mL) and brought to reflux. To the refluxing solution was added a solution of **56** (100 mg, 0.21 mmol, 1.0 eq) dissolved in anhydrous DCM (5 mL) over 2 h using a Kazel syringe pump. The resultant yellow solution was allowed to reflux for an additional 2 h after addition, cooled to room temperature, and concentrated under reduced pressure. The crude reaction mixture was filtered through a glass pipet loaded with 2 inches of silica gel with a solution of EtOAc:Et₂O

(3:1, 15 mL) to remove the catalyst. The filtrate was concentrated under reduced pressure, to yield a clear oil (82 mg, 91 %), and a ^1H NMR spectrum was obtained immediately.

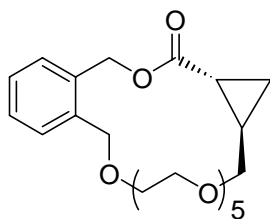
General Procedure for diazo decomposition of 56, 58, 59, 62, and 63 with copper(I) hexafluorophosphate: The following is an example procedure of diazo decomposition. An oven dried flask was charged with copper (I) hexafluorophosphate (7.8 mg, 22 μmol , 0.10 eq) and DCM (5 mL) and brought to reflux. To the refluxing solution was added a solution of **59** (120 mg, 0.22 mmol, 1.0 eq) dissolved in anhydrous DCM (5 mL) over 2 h using a Kazel syringe pump. The resultant yellow solution was allowed to reflux for an additional 2 h after addition, cooled to room temperature, and concentrated under reduced pressure. The crude reaction mixture was filtered through a glass pipet loaded with 2 inches of silica gel with a solution of EtOAc:Et₂O (3:1, 15 mL) to remove the catalyst. The filtrate was concentrated under reduced pressure, to yield a clear oil (88 mg, 84 % theoretical mass), and a ^1H NMR spectrum was obtained immediately.

General Procedure for diazo decomposition of 56, 58, and 59, with copper(I) hexafluorophosphate/34: The following is an example procedure of diazo decomposition. An oven dried flask was charged with copper(I) hexafluorophosphate (8.3 mg, 23.7 μmol , 0.10 eq), bis-oxazoline **34** (9.3 mg, 28.4 μmol , 0.12 eq) and DCM (5 mL) and brought to reflux. After the solution was at reflux for 30 min., a solution of **58** (111 mg, 0.24 mmol, 1.0 eq) dissolved in anhydrous DCM (5 mL) was

added over 2 h using a Kazel syringe pump. The resultant yellow solution was allowed to reflux for an additional 2 h after addition, cooled to room temperature, and concentrated under reduced pressure. The crude reaction mixture was filtered through a glass pipet loaded with 2 inches of silica gel with a solution of EtOAc:Et₂O (3:1, 15 mL) to remove the catalyst. The filtrate was concentrated under reduced pressure, to yield a clear oil (90 mg, 96 % theoretical mass), and a ¹H NMR spectrum was obtained immediately.

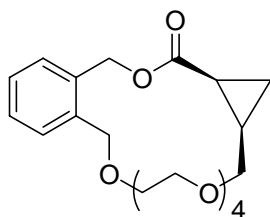


Z-3,9,12,15,18,21,24-Hepta-oxa-tricyclo[24.4.0.0^{5,7}]triaconta-1(26),27,29-trien-4-one (Z-64). ¹H NMR (400 MHz) δ 7.46 (dd, *J* = 9.0, 3.7 Hz, 1 H), 7.42 (dd, *J* = 9.0, 3.7 Hz, 1 H), 7.33 (dd, *J* = 9.0, 3.7 Hz, 2 H), 5.32 (d, *J* = 12.7 Hz, 1 H), 5.25 (d, *J* = 12.7 Hz, 1 H), 4.72 (d, *J* = 12.0, 1 H), 4.68 (d, *J* = 12.0 Hz, 1 H), 3.87 (dd, *J* = 10.6, 5.1 Hz, 1 H), 3.75-3.48 (comp, 21 H), 1.89 (ddd, *J* = 8.5, 7.7, 5.9 Hz, 1 H), 1.65 (dddt, *J* = 8.5, 8.4, 7.0, 5.1, 5.1 Hz, 1 H), 1.14-1.08 (comp, 2 H); ¹³C NMR (100 MHz) δ 172.3, 136.7, 134.8, 129.6, 129.3, 128.2, 128.0, 71.1, 70.7, 70.5, 70.0, 69.8, 68.6, 63.9, 21.2, 17.6, 11.5; HRMS(FAB⁺) calculated for C₂₃H₃₄O₈: 439.2332; found: 439.2338.

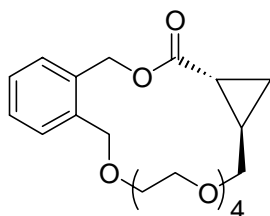


***E*-3,9,12,15,18,21,24-Hepta-oxa-tricyclo[24.4.0.0^{5,7}]triaconta-1(26),27,29-trien-4-one (*E*-64).** ¹H NMR (400 MHz) δ 7.43-7.36 (comp, 2 H), 7.33 (dt, *J* = 6.0, 2.7 Hz, 2 H), 5.29 (d, *J* = 12.5 Hz, 1 H), 5.25 (d, *J* = 12.5 Hz, 1 H), 4.71 (d, *J* = 12.5 Hz, 1 H), 4.68 (d, *J* = 12.5 Hz, 1 H), 3.74-3.61 (comp, 21 H), 3.23 (dd, *J* = 10.6, 7.5 Hz, 1 H), 1.76 (dddddd, *J* = 8.5, 7.5, 6.9, 4.6, 4.3 Hz, 1 H), 1.69 (dt, *J* = 8.3, 4.3 Hz, 1 H), 1.25 (ddd, *J* = 9.1, 4.6, 4.6 Hz, 1 H), 0.89 (ddd, *J* = 8.3, 6.3, 4.3 Hz, 1 H); ¹³C NMR (100 MHz) δ 173.6, 137.0, 134.6, 129.7, 129.2, 128.4, 128.0, 72.5, 71.2, 70.93, 70.85, 70.81, 70.78, 70.75, 70.72, 70.67, 70.1, 69.8, 64.3, 22.0, 18.9, 12.6; HRMS (FAB+) calculated for C₂₃H₃₄O₈: 439.2332; found: 439.2338.

Purification of the crude reaction mixture containing *Z*-69 and *E*-69 was achieved using semi-preparative reverse-phase chromatography at a flow rate of 3.0 mL/min with water:acetonitrile (60:40) for 18 min, ramped at 2.4 %/min to water:acetonitrile (0:100) and maintained 15 min. *Z*-69 was eluted at 23.1 min and *E*-69 eluted at 24.7 min. The collected fractions were concentrated under reduced pressure to remove acetonitrile, frozen, and residual water was sublimed under reduced pressure.

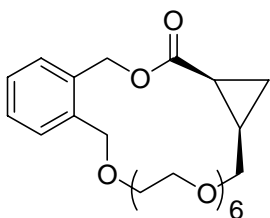


Z-3,9,12,15,18,21-Hexaoxa-tricyclo[21.4.0.0^{5,7}]heptacosan-4-one (Z-69). ¹H NMR (400MHz) δ 7.49-7.31 (comp, 4 H), 5.42 (d, *J* = 13.0 Hz, 1 H), 5.27 (d, *J* = 13.0 Hz, 1 H), 4.70 (s, 2 H), 3.88 (dd, *J* = 10.4, 4.8 Hz, 1 H), 3.74-3.64 (comp, 17 H), 1.90 (ddd, *J* = 8.5, 7.3, 6.1 Hz, 1 H), 1.69 (dddt, *J* = 12.7, 8.4, 7.6, 4.8 Hz, 1 H), 1.13-1.07 (comp, 2 H); ¹³C NMR (100 MHz) δ 172.2, 136.4, 135.4, 129.3, 129.2, 128.1, 128.0, 71.5, 71.1, 71.0, 70.72, 70.67, 70.5, 70.3, 69.9, 69.8, 68.6, 63.6, 21.2, 17.7, 11.4; **HRMS** (FAB+) calculated for C₂₁H₃₀O₇: 395.2070; found: 395.2077.

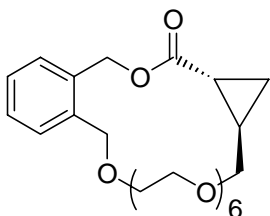


E-3,9,12,15,18,21-Hexaoxa-tricyclo[21.4.0.0^{5,7}]heptacosan-4-one (E-69). ¹H NMR (400 MHz) δ 7.45-7.30 (comp, 4 H), 5.28 (d, *J* = 12.4 Hz, 1 H), 5.24 (d, *J* = 12.4 Hz, 1 H), 4.70 (s, 2 H), 3.77 (dd, *J* = 10.8, 4.8 Hz, 1 H), 3.74-3.62 (comp, 16 H), 3.16 (dd, *J* = 10.8, 7.9 Hz, 1 H), 1.77 (dddd, *J* = 10.8, 7.0, 6.4, 4.6, 4.4 Hz, 1 H), 1.70 (dt, *J* = 8.3, 4.6 Hz, 1 H), 1.26 (dt, *J* = 10.8, 4.6 Hz, 1 H), 0.88 (ddd, *J* = 8.3, 6.3, 4.4 Hz, 1 H); ¹³C NMR (100 MHz) δ 173.7, 137.2, 134.4, 130.1, 129.3, 128.6, 128.0, 72.5, 71.2, 70.89, 70.84, 70.80, 70.78, 70.0, 69.9, 64.5, 22.2, 19.0, 12.4; **HRMS** (FAB+) calculated for C₂₁H₃₀O₇: 395.2070; found: 395.2077.

Purification of the crude reaction mixture containing **Z-71** and **E-71** was achieved using semi-preparative reverse phase chromatography at a flow rate of 2.7 mL/min with water:acetonitrile (62:48) for 36 min, ramped at 8.9 %/min to water:acetonitrile (0:100) and maintained 15 min, **Z-71** was eluted at 20.8 min and **E-71** eluted at 22.3 min. The collected fractions were concentrated under reduced pressure to remove acetonitrile, frozen, and residual water was sublimed under reduced pressure.

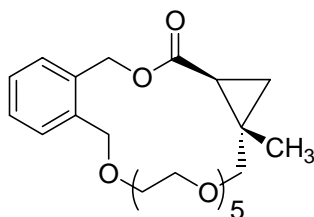


Z-3,9,12,15,18,21,24,27-Octaoxa-tricyclo[27.4.0.0^{5,7}]tritriaconta-1(29),30,32-trien-4-one (Z-71). ¹H NMR (400 MHz) δ 7.44 (dd, J = 8.9, 4.7 Hz, 2 H), 7.31 (comp, 2 H), 5.27 (d, J = 12.8 Hz, 1 H), 5.22 (d, J = 12.8 Hz, 1 H), 4.66 (s, 2 H), 3.82 (dd, J = 10.5, 5.4 Hz, 1 H), 3.71-3.45 (comp, 24 H), 1.86 (ddd, J = 8.6, 7.6, 5.8 Hz, 1 H), 1.64 (dddd, J = 8.6, 7.6, 5.4, 8.8 Hz, 1 H), 1.12-1.05 (comp, 2 H); ¹³C NMR (100 MHz) δ 172.2, 136.6, 134.7, 129.4, 129.2, 128.2, 128.0, 71.0, 70.8, 70.5, 69.9, 69.8, 68.7, 63.8, 21.1, 17.6, 11.7; **HRMS** (FAB +) calculated for C₂₅H₃₈O₉Li: 489.2676; found: 489.2681.



E-3,9,12,15,18,21,24,27-Octaoxa-tricyclo[27.4.0.0^{5,7}]tritriaconta-1(29),30,32-trien-4-one (E-71). ¹H NMR (400 MHz) δ 7.40-7.26 (comp, 4 H), 5.27 (d, J = 12.7

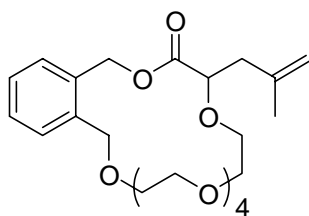
136.7, 134.9, 129.5, 129.2, 128.2, 128.0, 72.2, 71.1, 70.82, 70.76, 70.5, 69.9, 69.8, 63.7, 27.2, 25.7, 22.6, 19.4; **HRMS** (FAB+) calculated for C₂₄H₃₆O₈Li: 459.2570; found: 459.2570.



***E*-7-Methyl-3,9,12,15,18,21,24-hepta-oxa-tricyclo[24.4.0.0^{5,7}]triaconta-1(26),27,29-trien-4-one (*E*-75).** ¹H NMR (400 MHz) δ 7.44-7.38 (comp, 2 H), 7.36-7.30 (comp, 2 H), 5.30 (d, *J* = 13.1 Hz, 1 H), 5.27 (d, *J* = 13.1 Hz, 1 H), 4.71 (s, 2 H), 3.74-3.56 (comp, 21 H), 3.15 (d, *J* = 10.1 Hz, 1 H), 1.83 (dd, *J* = 8.2, 5.6 Hz, 1 H), 1.28 (s, 3 H), 1.12 (dd, *J* = 5.6, 4.5 Hz, 1 H), 1.01 (dd, *J* = 8.2, 4.5 Hz, 1 H); ¹³C NMR (100 MHz) δ 172.2, 137.0, 134.8, 129.7, 129.1, 128.3, 128.0, 71.2, 71.0, 70.9, 70.7, 70.6, 70.4, 69.7, 64.2, 26.4, 24.3, 17.6, 14.7; **HRMS** (FAB+) calculated for C₂₄H₃₆O₈Li: 459.2570; found: 459.2570.

Purification of the crude reaction mixture containing **76** was achieved using semi-preparative reverse phase chromatography at a flow rate of 2.8 mL/min with water:acetonitrile (60:40) for 33 min, ramped at 0.36%/min to water:acetonitrile (55:45) then ramped at 4.5%/min to water:acetonitrile (55:45) and maintained 15 min. *Z*-**75** was eluted at 30.2 min, *E*-**75** was eluted at 31.6 min, and **76** was eluted at 37.9

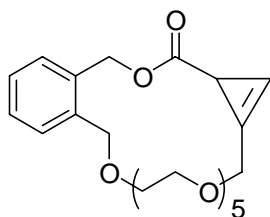
min. The collected fraction was concentrated under reduced pressure to remove acetonitrile, frozen, and residual water was sublimed under reduced pressure.



8-(2-Methyl-allyl)-5,10,11,13,14,16,17,19,20,22,23,25-dodecahydro-

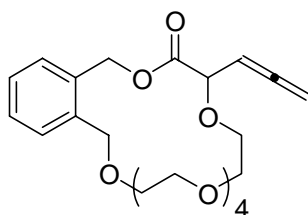
6,9,12,15,18,21,24-heptaioxabenzocyclotricosin-7-one (76). ^1H NMR (400 MHz) δ 7.43-7.39 (comp, 2 H), 7.38-7.32 (comp, 2 H), 5.38 (d, J = 12.7 Hz, 1 H), 5.33 (d, J = 12.7 Hz, 1 H), 4.80 (s, 1 H), 4.75 (s, 1 H), 4.71 (s, 2 H), 4.23 (t, J = 6.7 Hz, 1 H), 3.76-3.59 (comp, 20 H), 2.47 (d, J = 6.7 Hz, 2 H), 1.78 (s, 3 H); ^{13}C NMR (100 MHz) δ 172.4, 141.0, 136.7, 134.5, 129.5, 129.3, 128.4, 128.1, 113.4, 71.4, 70.83, 70.75, 70.71, 70.6, 70.0, 69.8, 64.2, 41.0, 22.6.

Purification of the crude reaction mixture containing **73** was achieved using semi-preparative reverse phase chromatography at a flow rate of 3.0 mL/min with water:acetonitrile (60:40) for 23 min, ramped at 3.0%/min to water:acetonitrile (0:100) and maintained 15 min. **73** was eluted at 16.0 min. The collected fractions were concentrated under reduced pressure to remove acetonitrile, frozen, and residual water was sublimed under reduced pressure.



3,9,12,15,18,21,24-Hepta-oxa-tricyclo[24.4.0.0^{5,7}]triaconta-1(26),6,27,29-tetraen-4-one (73). ¹H NMR (400 MHz) δ 7.41 (comp, 2 H), 7.34 (comp, 2 H), 6.75 (q, J = 1.5 Hz, 1 H), 5.30 (d, J = 12.6 Hz, 1 H), 5.24 (d, J = 12.6 Hz, 1 H), 4.68 (s, 2 H), 4.61 (t, J = 1.5 Hz, 2 H), 3.73-3.67 (comp, 20 H), 2.37 (d, J = 1.5 Hz, 1 H); ¹³C NMR (100 MHz) δ 175.3, 136.9, 134.7, 129.7, 129.2, 128.3, 128.0, 112.5, 97.6, 71.2, 70.75, 70.72, 70.6, 70.1, 69.8, 64.7, 64.1, 20.3.

Purification of the crude reaction mixture containing **74** was achieved using semi-preparative reverse phase chromatography at a flow rate of 3 mL/min with water:acetonitrile (60:40) for 18 min, ramped at 2.4%/min to water:acetonitrile (0:100) and maintained 15 min. **74** was eluted at 20.9 min. The collected fractions were concentrated under reduced pressure to remove acetonitrile, frozen, and residual water was sublimed under reduced pressure.



8-Propa-1,2dienyl-5,10,11,13,14,16,17,19,20,22,23,25-dodecahydro-6,9,12,15,18,21,24-hepta-oxabenzocyclotricosen-7-one (74). ¹H NMR (400 MHz) δ

7.40-7.36 (comp, 2 H), 7.36-7.27 (mult, 1 H), 7.30 (d, $J = 9.0$ Hz, 1 H), 5.38 (d, $J = 13.0$ Hz, 1 H), 5.36 (d, $J = 13.0$ Hz, 1 H), 5.30 (dt, $J = 7.5, 6.7$ Hz, 1 H), 4.86 (dd, $J = 6.6, 1.9$ Hz, 2 H), 4.68 (d, $J = 1.6$ Hz, 2 H), 4.63 (dt, $J = 7.7, 1.9$ Hz, 1 H), 3.78-3.61 (comp, 20 H); ^{13}C NMR (100 MHz) δ 209.3, 170.1, 136.6, 134.4, 129.3, 129.2, 128.3, 128.0, 88.0, 77.7, 71.4, 70.9, 70.73, 70.70, 70.67, 70.5, 69.8, 69.1, 64.5; HRMS (DEI+) calculated for $\text{C}_{23}\text{H}_{32}\text{O}_8$: 436.2097; found: 436.2084.

Chapter 4 – Templated Macrocycle Formation of Metal Carbenes

4.1 Introduction and Background

Macrocycle formation through end-to-end cyclization is governed by entropy associated with the number of degrees of conformational freedom in the substrate.¹ The probability of two ends of a substrate meeting decreases as the length between the ends increases, and entropy for ring closure increases. Therefore, decreasing the entropy of the substrate should favor ring closure.² One means of lowering internal entropy is the incorporation of a template that reduces conformational freedom in the substrate. A chemical template is defined as a material that "...organizes an assembly of atoms, with respect to one or more geometric loci, in order to achieve a particular linking of atoms."³ To phrase this more specifically for macrocycle formation, a template for macrocycle formation arranges an acyclic substrate in a conformation suitable for the ends to meet and react, thereby aiding macrocycle formation. While cations are known to form complexes with polyether substrates, assisting in macrocyclization reactions,² the use of a template to assist in macrocycle formation *for carbene addition* reactions has not been previously reported.

Metal mediated carbene addition has been used in the formation of 10 to 23 membered rings.⁴ Several examples have used a diazoacetate linked through a poly-

¹ Ruzicka, L.; Brugger, W.; Pfeiffer, M.; Sehin, H.; Stoll, M. *Helv. Chem. Act.* **1926**, 9, 499.

² Dietrich, B.; Viout, P. Lehn, J.-M. Macrocycle Synthesis. *Macrocyclic Chemistry*, Wiley-VCH:New York, 1993.

³ Busch, D.H. *J. Inclusion Phenom.* **1992**, 12, 389.

⁴ Doyle, M.P., Hu, W. *Synlett* **2001**, 9, 1364.

ether substrate to an allyl, methallyl, propargyl, or furfuryl functional group.⁵ However, diazo decomposition of these substrates has not been performed in the presence of a cationic template such as an alkali metal, alkaline earth metal, or lanthanide. To form a complex with a metal cation, a diazoacetate having multiple ether oxygen atoms must adopt a conformation conducive to complexation, influencing the geometric relationship between the olefin and the metal carbene, thus affecting the trajectory of the olefin to the metal carbene intermediate formed from diazo decomposition. Doyle and co-workers have demonstrated that the trajectory of an olefin to a metal carbene influences diastereoselectivity and enantioselectivity in macrocycle formation.^{5c,6} We now wish to report an investigation of the influence of a cation template on the reaction selectivity of diazoacetates coupled to select functional groups through a polyether tether.

4.1.1 Templates for Macrocycle Formation

Templates can enhance macrocycle formation or inhibit macrocycle formation with a substrate, directing the outcome of attempted macrocyclization, as graphically depicted below (Figure 4.1).⁷ A template that enhances macrocyclization brings together the reactive ends of a molecule. A template that inhibits macrocycle formation prevents the reactive ends of a molecule from coming together.^{7,8}

⁵ (a) Doyle, M.P., Hu, W. *Tetrahedron Lett.* **2000**, *41*, 6265; (b) Doyle, M.P.; Chapman, B.J.; Hu, W.; Peterson, C.S.; McKervy, M.A.; Garcia, C.F. *Org. Lett.* **1999**, *1*, 1327; (c) Doyle, M.P.; Hu, W. *J. Org. Chem.* **2000**, *65*, 8839; (d) Doyle, M.P.; Hu, W.; Phillips, I.M.; Wee, A.G.H. *Org. Lett.* **2000**, *2*, 1777.

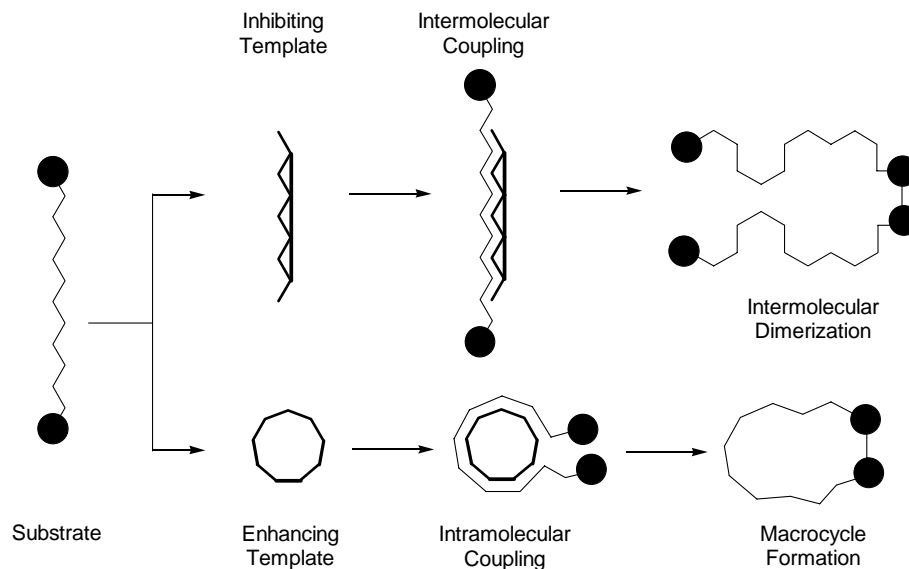
⁶ (a) Doyle, M.P. *Chem. Rev.* **1986**, *86*, 919; (b) Doyle, M.P.; Hu, W.; Chapman, B.; Marnett, A.B.; Peterson, C.S.; Vitale, J.P.; Stanley, S.A. *J. Am. Chem. Soc.* **2000**, *122*, 5717.

⁷ Gerbelet, N.V.; Arion, V.B.; Burgess, J. *Template Synthesis of Macrocyclic Compounds*, Wiley-VCH:New York, 1999.

⁸ Anderson, S., Anderson, H.L.; Sanders, J.K.M. *J. Chem. Soc., Perkin Trans. I* **1995**, 2247.

Templates that enhance macrocycle formation will promote and accelerate ring closure, while inhibiting templates retard or inhibit ring closure, often leading to dimerization products from intermolecular reactions.

Figure 4.1 Template Derived Reaction Control

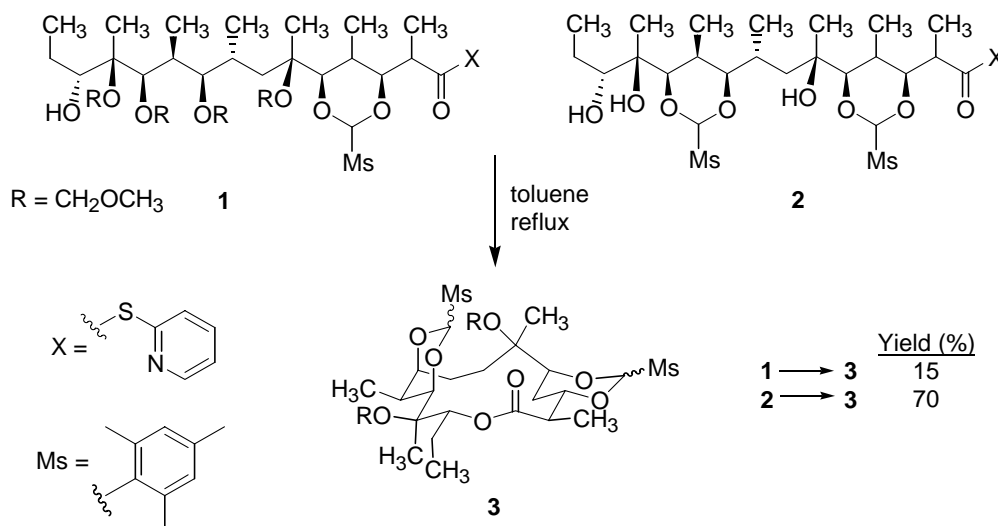


Woodward *et al.* demonstrated both ring closing enhancement and inhibition in macrocycle forming reactions.⁹ As shown in scheme 4.1, structures **1** and **2** use alcohol protecting groups that prevent esterification between these oxygen atoms and the activated ester (X), but also create conformational constraints. The configurational constraint of the acetal protecting groups on substrate **1** does not promote a conformation of **1** favorable for macrocyclic lactonization, and only poor

⁹ Woodward, R.B.; Logusch, E.; Nambar, K.P.; Sakan, K.; Ward, D.E.; Au-Yeung, B.-W.; Balaram, P.; Browne, L.J.; Card, P.J.; Chen, C.H.; Chênevert, R.B.; Fliri, A.; Frobel, F.K.; Gais, H.-J.; Garratt, D.G.; Hayakawa, K.; Heggie, W.; Hesson, D.P.; Hoppe, D.; Hoppe, I.; Hyatt, J.A.; Ikeda, D.; Jacobi, P.A.; Kim, K.S.; Kobuke, Y.; Kolima, K.; Krowicki, K.; Lee, V.J.; Leutert, T.; Malchenko, S.; Martens, J.; Matthews, R.S.; Ong, B.S.; Press, J.B.; Rajan Babu, T.V.; Rousseau, G.; Sauter, H.M.; Suzuki, M.; Tatsuta, K.; Tolbert, L.M.; Truesdale, E.A.; Uchida, I.; Ueda, Y.; Uyehara, T.; Vasalla, A.T.; Vladuchick, W.C.; Wade, P.A.; Williams, R.M.; Wong, H.N.-C. *J. Am. Chem. Soc.* **1981**, *103*, 3213.

yields of **3** are obtained (15% yield), making this a negative effect. However, as a result of the acetal groups, the conformation adopted by **2** works very well for macrocycle formation (70% yield), and the protecting group selection is a positive effect on the cyclization reactions.

Scheme 4.1 Erythromycin Lactonization with Configurational Constraints



4.1.2 Substrate Modifications

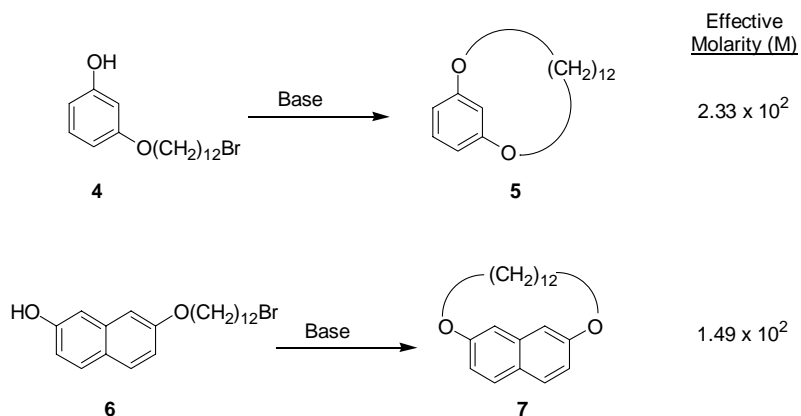
The addition of a rigid group (i.e., olefin, arene, acetylene, etc.) was proposed by Baker *et al.*¹⁰ as a method to reduce the degrees of freedom in an acyclic substrate, reducing the number of possible conformations the acyclic substrate can adopt. The use of rigid groups to enhance end-to-end macrocycle formation has been determined to be slight or non-existent.² Using a variety of aromatic substrates as rigid groups, Mandolini *et al.* showed that the effective molarity (EM)¹¹ of ring closure did not vary significantly with ring size, as illustrated in scheme 4.2.¹²

¹⁰ Baker, W.; McOmie, J.F.W.; Ollis, W.D. *J. Chem. Soc.* **1951**, 200.

¹¹ For a more detailed description of effective molarity see section 3.1.1.

¹² Mandolini, L.; Masci, B.; Roelens, S. *J. Org. Chem.* **1997**, *42*, 3733.

Scheme 4.2 Effective Molarity of Ring Closure with Select Phenol Compounds^a



Gem-dialkyl substitution and heteroatoms have also been used in attempts to enhance ring closure yields in the formation of macrocycles. These methods have been developed to promote ring closure by lowering ring strain and reducing transannular interactions, but they have not demonstrated general applicability for macrocycle formation.¹³ The lack of enhancement in ring closure as a result of gem-dialkyl or heteroatom substitution is attributed to the lack of ring strain or transannular interactions in macrocycles.

4.1.3 Template Cyclization

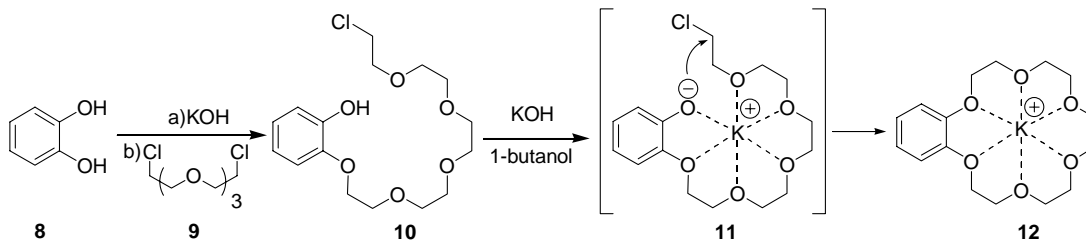
Template synthesis of crown ethers, as originally described by Pederson,¹⁴ is based on complex formation between a reactant substrate and an alkali metal cation, promoting the reactant to adopt a conformation amenable to macrocyclization (Scheme 4.1).

¹³ Eliel, E.L. *Stereochemistry of Carbon Compounds*; McGraw-Hill: New York, 1962, pp 188-203.

¹⁴ Pedersen, C.J. *J. Am. Chem. Soc.* **1967**, 89, 7071.

Substrate coordination to a template (**11**) reduces the degrees of freedom of **10**, lowering the internal entropy and facilitating macrocyclization.¹⁵

Scheme 4.3 Formation of Benzo-18-crown-6 Templated by Potassium^a



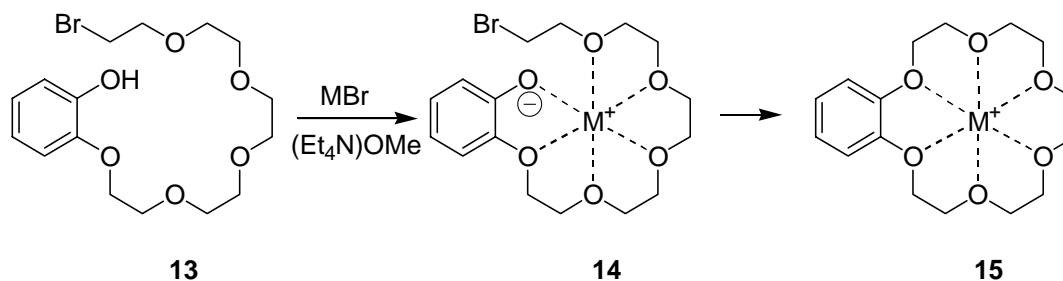
Effective templates for macrocyclization set a substrate conformation that increases the rate of ring closure, increasing the dominance of intramolecular cyclization over competitive intermolecular reactions (see section 3.1).¹⁶ Quantitative data for benzo-18-crown-6 ring closure by phenoxide displacement of a bromide in the presence of strontium salts (**14**) shows that the cationic template affects substrate conformation to dramatically accelerate the rate of reaction, accelerating the relative rate of ring closure 540-fold over the cationic metal free reaction (Scheme 4.4).¹⁷

¹⁵(a) Shaw, B.L. *J. Am. Chem. Soc.* **1975**, 97, 3856; (b) Ochiai, E.I. *Coord. Chem. Rev.* **1968**, 3, 49.

¹⁶ Mandolini, L.; Masci, B. *J. Am. Chem. Soc.* **1977**, 99, 7709.

¹⁷ Ercolani, G.; Mandolini, L.; Masci, B. *J. Am. Chem. Soc.* **1981**, 103, 2780.

Scheme 4.4 Template Macrocyclization

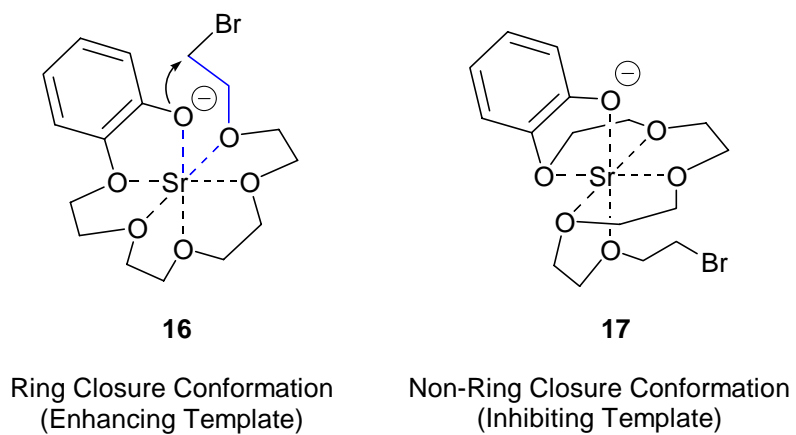


Added Cation (M^+)	$k (s^{-1})$	k_{rel}
none	8.73×10^{-6}	1.00
Na^+	3.83×10^{-4}	43.5
K^+	1.08×10^{-3}	124
Sr^{2+}	4.72×10^{-3}	540

These kinetics studies demonstrate the benefit of using cationic templates in the macrocyclization of polyether substrates. However, the structural drawing of **14** depicted in Scheme 4.4 does not portray the three dimensional conformation of **13** upon complex formation with a cationic metal template. The octahedral geometry about the metal center of crown ether complexes such as **15** has been previously described,^{14,18} and the conformation of acyclic complexes such as **14** is assumed to closely resemble the octahedral geometry as well. The conformation of an acyclic substrate complexing a cation (**16**) is important to macrocyclization because the conformation of the substrate controls the ability of the termini to meet and react. Assuming an octahedral geometry about the cation template, two reasonable geometries exist (**16**, **17**), and only one (**16**) is conducive to ring closure (Figure 4.2). Ring formation proves that the substrate conformation favorable for ring closure exists, but does not quantitate the relative population of this conformation, because interchange between conformations **16** and **17** occurs.

¹⁸ Dunitz, J.D.; Dobler, M.; Seiler, P.; Phizackerley, R.P. *Acta Crst. B* **1974**, *30*, 2733.

Figure 4.2 Cation Template Geometries

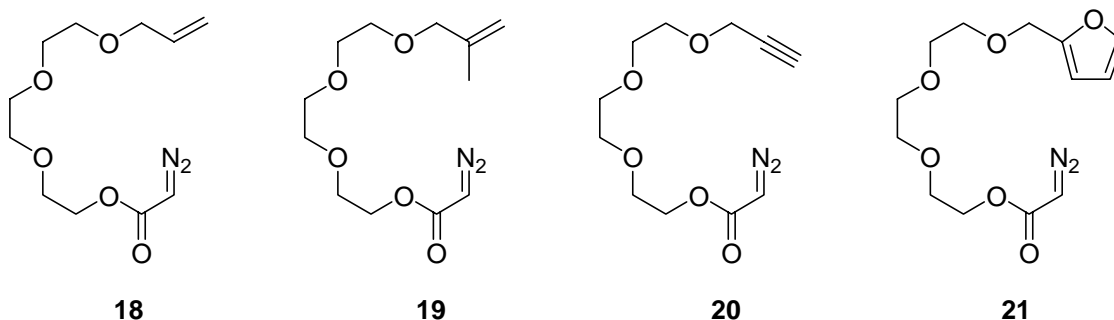


Noteworthy in structure **16** is that the substrate, which will close to form an eighteen membered ring, has the two oxygen atoms closest to each terminus of the substrate bridged by the strontium cation. The strontium cation bridge changes the separation between the termini to just three atoms (with bonds highlighted in blue) instead of sixteen atoms. The cationic metal template lowers the number of degrees of freedom of the poly-ether substrate, increasing the relative reaction rate in comparison the non-templated reaction. It should be pointed out that, as written, **16** is a chiral substrate, and a racemic mixture of **16** would exist in solution.

4.1.2 Selectivity Between Oxonium Ylide and Carbene Addition Pathways

Diazoacetates in which the reacting functional group is separated from the diazoacetate by ethylene glycol linkages have been synthesized.^{19,20,21} The copper(I) catalyzed diazo decomposition of **18**, **19**, or **20** (Figure 4.3) have yielded macrocyclic products resulting from oxonium ylide formation followed by [2,3]-sigmatropic rearrangement, whereas decomposition of these substrates by dirhodium(II) catalysts does not yield these products. Regioselectivity seen in the diazo decomposition of **21** is also catalyst dependent. Within the reported studies, the products formed from diazo decomposition of **20** and **21** best illustrate the unique chemoselectivity seen with copper(I) catalysts.

Figure 4.3 Diazoacetates with Ethylene Glycol Linkages to Functional Groups



Decomposition by copper(I) hexafluorophosphate of diazoacetate **20** linked by tri(ethylene glycol) to a propargyl functional group yielded the oxonium ylide derived **25** as the major product of the reaction (Scheme 4.5). The $\text{Cu}(\text{CH}_3\text{CN})_4\text{PF}_6$ /**26** complex catalyzed diazo decomposition of **20** afforded cyclopropene **23** resulting

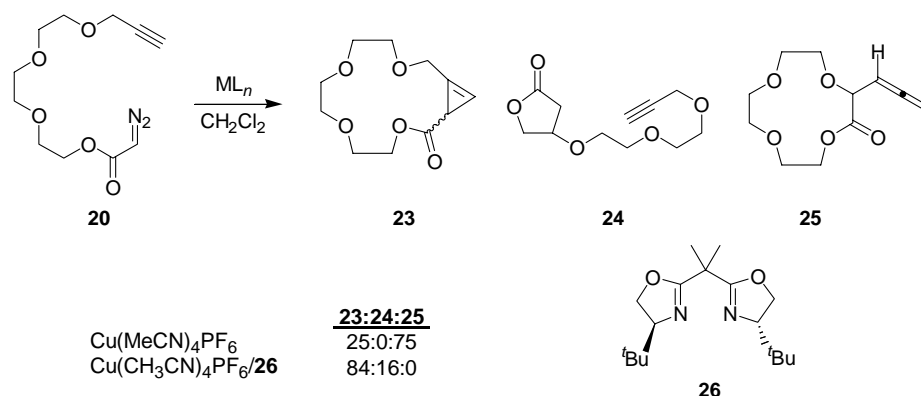
¹⁹ (a) Doyle, M.P.; Peterson, C.S.; Parker, D.L. *Angew. Chem. Int. Ed. Eng.* **1996**, 35, 1334. (b) Doyle, M.P.; Hu, W.; Chapman, B.; Marnett, A.B.; Peterson, C.S.; Vitale, J.P.; Stanley, S.A. *J. Am. Chem. Soc.* **2000**, 122, 5718.

²⁰ Doyle, M.P.; Ene, D.G.; Peterson, C.S.; Lynch, V. *Angew. Chem. Int. Ed.* **1996**, 38, 700.

²¹ Doyle, M.P.; Chapman, B.J.; Hu, W.; Peterson, C.S.; McKerver, M.A.; Garcia, C.F. *Org. Lett.* **1999**, 1, 1327.

from metal carbene addition to the alkyne.²² The report stated that the product formation of **23** and **25** based on the catalysts employed may reflect the ability of copper(I) hexafluorophosphate to initially coordinate the substrate through its ether oxygen atoms, and promote ylide formation followed by [2,3] sigmatropic rearrangement. Catalyst coordination to the substrate is not required for carbene addition reactions, as is shown in the dirhodium(II) tetraacetate catalyzed decomposition of **20**. However, how catalyst coordination to the substrate influenced reaction selectivity is not known.

Scheme 4.5 Decomposition of **20** Using Copper(I)

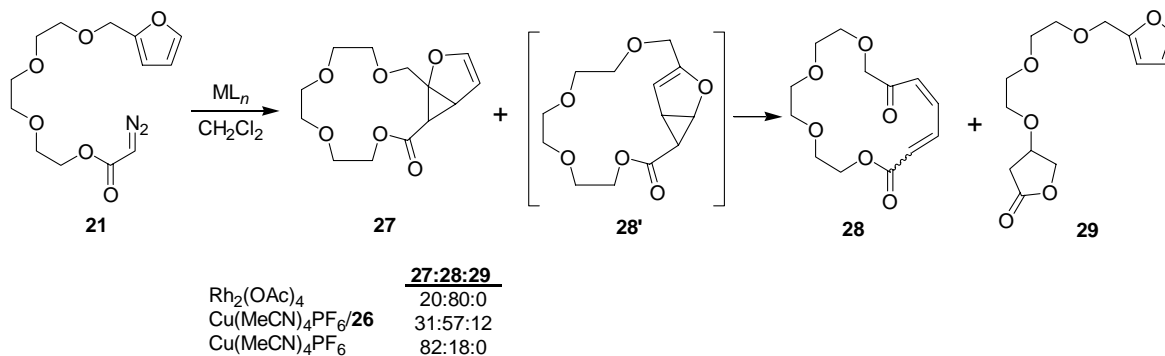


A second study reported the synthesis of a diazoacetate precursor coupling a furfuryl group to tri(ethylene glycol) to ultimately afford diazoacetate **21**.²⁰ Diazo decomposition catalyzed by dirhodium tetraacetate or $Cu(CH_3CN)_4PF_6/26$ favored carbene addition to the less substituted 2,3 position of the furan, while diazo decomposition catalyzed by copper(I) hexafluorophosphate without bis-oxazoline ligand **26** preferentially added to the more substituted 4,5 position (Scheme 4.6).²¹ The unique product formation seen with copper(I) hexafluorophosphate was

²² Doyle, M.P.; Hu, W. *Tetrahedron Lett.* **2000**, *41*, 6265.

suggested to be the result of copper(I) coordination to the ether framework of the substrate.

Scheme 4.6 Intramolecular Addition Reactions to Furans



Formation of γ -butyrolactones is competitive with macrocyclization, as discussed in Chapter 3. However, copper(I) hexafluorophosphate catalyzed diazo decomposition of both **20** and **21** yields no observable γ -butyrolactone product resulting from intramolecular C-H insertion. The Cu(CH₃CN)₄PF₆/26 catalyzed diazo decomposition of **20** and **21** resulted in 16% and 12% respectively of the observed product mixture attributed to γ -butyrolactone formation. From these results, it appears that the interaction between substrates **20** or **21** and copper(I) hexafluorophosphate also disfavors C-H insertion, and diazo decomposition results in the formation of other products. The examples illustrated in Schemes 4.5 and 4.6 both show that interaction between ether oxygen atoms and the copper(I) catalyst promotes a different reaction pathway from that of catalysts that do not interact with the substrate.

The reaction selectivity seen in the copper(I) hexafluorophosphate catalyzed diazo decomposition of **20** and **21** has been rationalized by the coordination of copper(I) to

the ether framework of the diazoacetate. If coordination of **20** or **21** with the copper catalyst occurs through their ether oxygen atoms, then the copper metal may also act as a template to direct macrocycle formation. To the best of our knowledge, such a templating influence has not been previously demonstrated in macrocycle formation via carbene addition reactions or oxonium ylide formation from a metal carbene intermediate. Based on the results illustrated in schemes 4.5 and 4.6, the use of a cationic template would provide regioselectivity and chemoselectivity in macrocycle formation via carbene addition and oxonium ylide formation from a metal carbene intermediate.

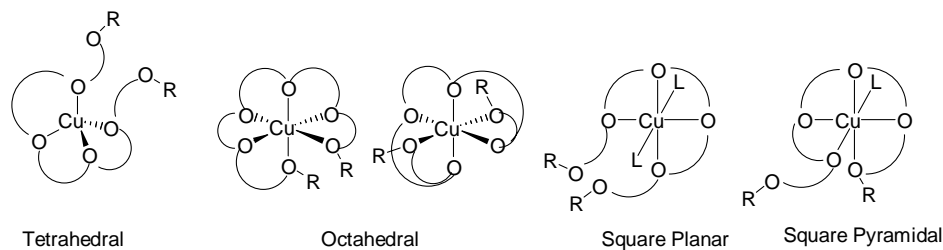
4.2 Template Macrocylic Cyclopropanation

The chemoselectivity seen in copper(I) hexafluorophosphate catalyzed diazo decomposition reactions discussed in section 4.2 prompted us to investigate the effect of cationic templates on reaction selectivity. Copper coordination to a substrate having six ether oxygen atoms can exist in two discrete geometries, a tetrahedral geometry, or an octahedral geometry (Figure 4.4).²³ Tetrahedral geometry would be expected for copper coordination to the substrate prior to diazo decomposition (as a copper(I) species),²³ while octahedral geometry would be expected for catalyst/substrate coordination subsequent to diazo decomposition, as carbene coordination is oxidative addition, resulting in a formal oxidation state of copper(III). Other geometries such as square planar or square pyramidal cannot be ruled out, as similar coordination geometries have been obtained from X-ray crystal structures of

²³ Cotton, F.A.; Wilkenson, G.; Murillo, C.A.; Bochmann, M. *Advanced Inorganic Chemistry*, 6th ed.; Wiley & Sons: New York, 1999; pp. 854-876.

copper(II) coordination to polyether macrocycles.²⁴ Square planar and square pyramidal geometries would be coordinatively unsaturated, or would have a second ligand such as a solvent molecule coordinated to the other coordination sites as illustrated in Figure 4.4.

Figure 4.4 Geometry of Copper Coordination



The formation of a complex between a copper(I) catalyst and a diazoacetate compound having multiple ether oxygen atoms would lower the degrees of freedom within the compound, affecting conformational freedom. By lowering the degrees of freedom within a substrate, the probability of the ends of the diazoacetate compound approaching each other would change. This lowering of the degrees of freedom within a substrate would be manifest in the diazo decomposition reaction selectivity.

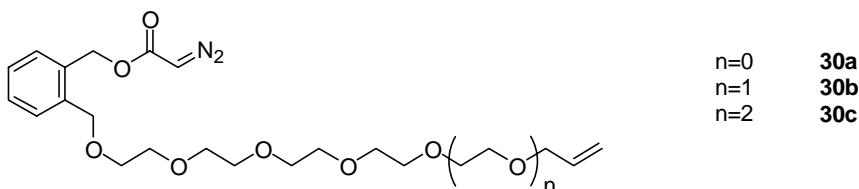
4.2.1 Copper Templating Effects

To investigate the interaction between a copper(I) catalyst and the ether oxygen atoms of a diazoacetate compound with multiple ether oxygen atoms we employed **30a-c**, whose synthesis was described in section 3.3 (Figure 4.5). These compounds have five (**30a**), six (**30b**), and seven (**30c**) ether oxygen atoms respectively. Each

²⁴ For examples see : (a) Comarmond, J.; Plumeré, P.; Lehn, J.-L.; Agnus, Y.; Louis, R.; Weiss, R.; Kahn, O.; Morgenstern-Badarau, O. *J. Am. Chem. Soc.* **1982**, *104*, 6330; (b) Beall, L.S.; Mani, N.S.; White, A.J.P.; Williams, D.J.; Barrett, A.J.M.; Hoffman, B.M. *J. Org. Chem.* **1998**, *63*, 5806; (c) Martens, C.F.; Gebbink, R.J.M.K.; Feiters, M.C.; Kooijman, G.H.; Smeets, W.J.J.; Spek, A.L.; Nolte, R.J.M. *Inorg. Chem.* **1994**, *33*, 5541.

substrate also has two ester oxygen atoms that are not expected to coordinate, as they will not be as electron donating as the ether oxygen atoms. The difference in available oxygen atoms is expected to produce a difference in the reaction selectivity for diazo decomposition, should copper be acting as a template. Substrate coordination in a tetrahedral geometry by copper(I) will involve all but one of the ether oxygen atoms of **30a**, while coordination of **30c** will leave three oxygen atoms uncoordinated, allowing for more freedom in the substrate. In addition, coordination to the allyl oxygen atom will inhibit ylide formation, and if copper(I) coordination occurs, the difference in selectivity between cyclopropanation and ylide formation with [2,3]-sigmatropic rearrangement for diazo decomposition of **30a-c** will show this.

Figure 4.5 Diazoacetate Compounds for Macrocyclization



Diazo decomposition of **30a-c** was accomplished by addition of the diazoacetate over two hours to a refluxing solution of dichloromethane with 10 mol% of catalyst. Reaction selectivity in each of the diazo decomposition reactions catalyzed by copper(I) hexafluorophosphate is low, with nearly 50:50 mixtures of **31:32** in each case (Table 4.1). Decomposition of **30a-c** catalyzed by the $\text{Cu}(\text{CH}_3\text{CN})_4\text{PF}_6$ /**26** complex was intended to provide a control reaction with a copper(I) catalyst that cannot coordinate to the diazoacetate compound. However, diazo decomposition in these reactions affords the macrocycle compound **31** in low yields. The formation of

32 could not be detected in any reaction catalyzed by the $\text{Cu}(\text{CH}_3\text{CN})_4\text{PF}_6/\mathbf{26}$ complex, and the diastereoselectivity for formation of **31** seen in the decomposition of **33a** is different than that seen using the $\text{Cu}(\text{CH}_3\text{CN})_4\text{PF}_6$ alone.

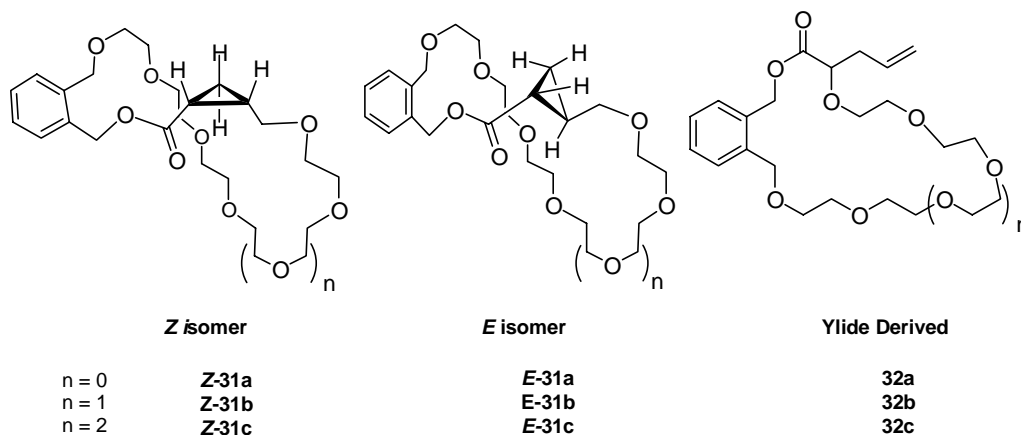
Table 4.1 Ring Size Product Ratios for Copper(I) Diazo Decomposition^a

Catalyst	Substrate	31 : 32 ^b	<i>E</i> : <i>Z</i> (31) ^b	Yield, (%) ^c
$\text{Cu}(\text{CH}_3\text{CN})_4\text{PF}_6$	30a	56:44	61:39	84
	30b	51:49	57:43	82
	30c	55:45	47:53	76
$\text{Cu}(\text{CH}_3\text{CN})_4\text{PF}_6/\mathbf{26}$	30a	100:0	50:50	13
	30b	N/A	N/A	0
	30c	100:0	n.d.	8

a) Reactions carried out as 2 h addition of **30** to refluxing solution of 10 mol% catalyst in 10 mL methylene chloride b) Ratios of products obtained by ¹H NMR c) yields obtained by crude mass and ¹H NMR ratios.

N/A = not applicable

n.d. = not determined



The results of diazo decomposition of **30a-c** by copper(I) hexafluorophosphate show that the number of oxygen atoms in the diazoacetate compounds available for coordination to copper does not affect the ability of **30a-c** to cyclize to form **31** and **32** or influence the ratio between them. However, diastereoselectivity in the diazo decomposition of **30a** is 61:39 in favor of the *E* isomer, and diminishes to 51:49 in the diazo decomposition of **30b**, while a 47:53 ratio in favor of the *Z* isomer is seen in the diazo decomposition of **30c**. Diastereoselectivity in cyclopropane formation is

indicative of the ability of the olefin to approach the metal carbene intermediate in a conformation conducive to the formation of *E* or *Z* cyclopropane isomers of **31**.^{6a} The change in diastereoselectivity seen in the diazo decomposition of **30a-c** catalyzed by Cu(CH₃CN)₄PF₆ may be related to the number of ether oxygens found in each substrate, suggesting that interactions between the ether oxygen atoms of diazoacetate and the copper cation are influencing the approach of the olefin to the metal carbene in the reaction.

In comparison, diazo decomposition of **30a-c** by the Cu(CH₃CN)₄PF₆/**26** complex yields only small quantities of macrocycles **31** and **32**. The Cu(CH₃CN)₄PF₆/**26** complex catalyzed decomposition of **30a** and **30c** only forms **31**. The poor yields and lack of formation of **32** seen using Cu(CH₃CN)₄PF₆/**26** complex as a catalyst also suggest that an interaction between the copper cation and the ether oxygen atoms of the diazoacetate influences the selectivity for macrocycle formation in diazo decomposition of **30a-c**. However, as the yields of the Cu(CH₃CN)₄PF₆/**26** complex catalyzed diazo decomposition of **30** are so low that the results may also be deceptive, as some factor other than interaction between the copper cation and ether oxygen atoms may be involved.

Reaction selectivity for diazo decomposition of **30** may be related to macrocyclic products **31** and **32** complexing the copper(I) catalyst, preventing further coordination between the copper(I) catalyst and the reactant. By varying the mol% of catalyst used in the reaction we were able to determine if the catalyst was forming a complex with

macrocyclic products **31** and **32**, and affecting reaction selectivity (Table 4.2). The chemoselectivity (**31:32**) seen in the copper(I) hexafluorophosphate catalyzed diazo decomposition of **30b** is nearly identical regardless of the catalyst loading used, but the difference in diastereoselectivity (*E*-**31b**:*Z*-**31b**) changes in a trend consistent with the change in catalyst loading.

Table 4.2 Catalyst Loading and Product Selectivity in Diazo Decomposition of **33b^a**

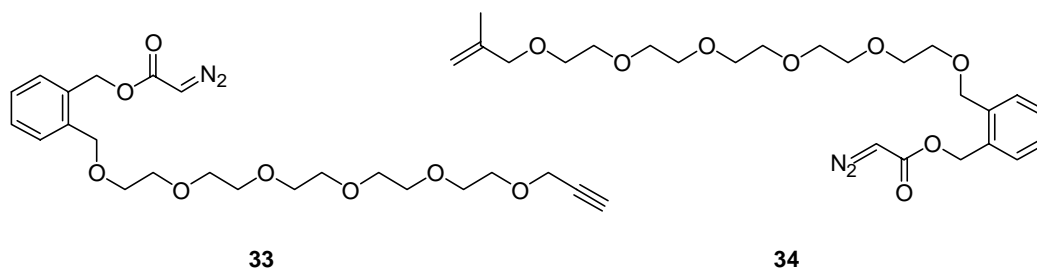
Catalyst (mol %)	31b:32b ^b	<i>E:Z</i> (31b) ^b	Yield, (%) ^c
110	62:38	66:34	62
80	63:37	63:37	54
10	51:49	57:43	82
1	61:39	48:52	76

a) reactions carried out as 2 h addition of **30b** to refluxing solution of 10 mol% catalyst in 10 mL methylene chloride b) Ratios of products obtained by ¹H NMR c) yields obtained by crude mass and ¹H NMR ratios.

The difference in copper(I) hexafluorophosphate loading does not make a difference in chemoselectivity (**31b:32b**) in the diazo decomposition of **30b**, but a trend is seen in the diastereoselectivity in the formation of **31b**. The chemoselectivity seen using 10 mol% catalyst is different from all other entries, and was repeated twice more with the same results each time. The continuous change in the *E:Z* ratio from 66:34 with 110 mol% catalyst loading to 48:52 with 1 mol% catalyst suggests that the catalyst interacts with the products of diazo decomposition of **30b**, modifying the catalyst reactivity in further catalytic cycles with **30b**. However, this trend is not conclusive evidence for copper coordination to ether oxygen atoms of **30b** as a single piece of data.

As previously discussed, interactions between a copper(I) catalyst and ether oxygen atoms of poly-ether esters of diazoacetate compounds were first proposed to affect reaction selectivity in the diazo decomposition of substrates having a propargyl or furfuryl functional group (section 4.1.2). To investigate how these observations relate to diazoacetate compounds with the diazoacetate of 1,2-benzenedimethanol derived compounds we used **33** and **34** having, respectively, a propargyl or a methallyl functional group (Figure 4.6).

Figure 4.6 Diazoacetate Precursors With Various Functional Groups



The chemoselectivity of copper(I) catalyzed diazo decomposition was examined using three different functional groups coupled through penta(ethylene glycol) and 1,2-benzenedimethanol to the diazoacetate (**30b**, **33**, **34**). Both copper(I) hexafluorophosphate and copper(I) triflate were used as catalysts to investigate the effect of the anion associated with the copper(I) cation on reaction selectivity. For comparison dirhodium(II) tetraacetate was also used, as it has only one open coordination site per rhodium atom and cannot coordinate to the substrate and decompose it simultaneously. The use of a $\text{Cu}(\text{CH}_3\text{CN})_4\text{PF}_6$ /**26** complex as a copper(I) catalyst to decompose **30b** was reported (Table 4.1), and the use of this catalyst as a non-coordinating copper(I) species did not yield macrocyclic products.

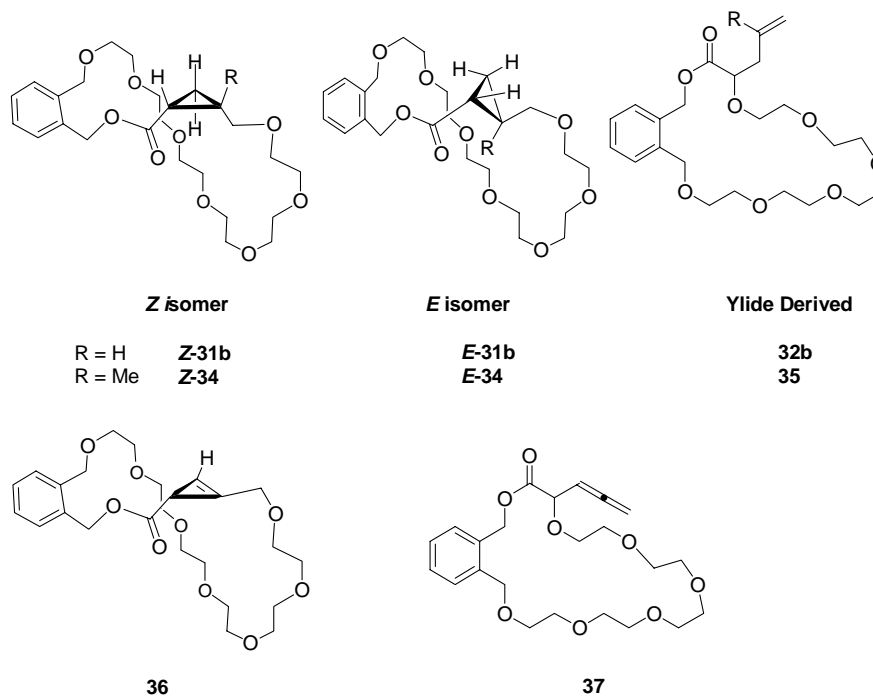
Diazo decomposition reactions catalyzed by dirhodium(II) tetraacetate uniformly showed exclusive chemoselectivity for cyclopropanation over ylide formation regardless of the functional group (Table 4.3). The diastereoselectivities for cyclopropanation seen in the dirhodium(II) tetraacetate catalyzed diazo decomposition of **30b** and **34** were nearly identical, though product yields varied significantly. Copper(I) catalyzed diazo decomposition of **30b** yielded cyclopropanation and ylide-derived **32b** with equal selectivities using both copper(I) catalysts, while chemoselectivity in the diazo decomposition of **34** was different from **30b**; copper(I) hexafluorophosphate catalyzed diazo decomposition of **34** favored ylide formation and subsequent [2,3]-sigmatropic rearrangement to cyclopropanation by a 2:1 ratio, and copper(I) triflate yielded the opposite chemoselectivity, favoring cyclopropanation by a 2:1 ratio. The copper(I) catalyzed diazo decomposition of **33** led to exclusive formation of **37** and no detectable amount of **36**, though the yield of **37** for copper(I) triflate catalyzed decomposition was low.

Table 4.3 Copper Decomposition with Various Functional Groups

Substrate	Catalyst	31b:32b	<i>E:Z</i> (31b)	Yield (%)
30b	Rh ₂ (OAc) ₄	100:0	36:64	71
	Cu(CH ₃ CN) ₄ PF ₆	51:49	57:43	82
	[Cu(OTf)] ₂ C ₆ H ₆	62:38	57:43	76
		34:35	<i>E:Z</i> (34)	
34	Rh ₂ (OAc) ₄	100:0	34:66	38
	Cu(CH ₃ CN) ₄ PF ₆	34:66	81:19	69
	[Cu(OTf)] ₂ C ₆ H ₆	63:37	72:28	80
		36:37		
33	Rh ₂ (OAc) ₄	100:0		70
	Cu(CH ₃ CN) ₄ PF ₆	0:100		70
	[Cu(OTf)] ₂ C ₆ H ₆	0:100		15

a) reactions carried out as 2 h addition of substrate to refluxing solution of catalyst in 10 mL methylene chloride b) Ratios of products obtained by ¹H NMR c) yields obtained by crude mass and ¹H NMR ratios.

N/A = not applicable



The preference of copper(I) catalysts to undergo oxonium ylide formation followed by [2,3]-sigmatropic rearrangement in the diazo decomposition of **33** is suggestive of an interaction between the ether oxygen atoms and the copper catalyst based on the

observed preference of ylide formation over cyclopropenation as was previously reported with a similar substrate (see section 4.1.2). Though coordination to the propargylic or allylic oxygen atom is unreasonable in ylide formation, other ether oxygen atoms may coordinate and influence reaction selectivity. It is apparent that the functional groups contribute significantly to the product selectivity seen in copper(I) catalyzed diazo decomposition, favoring ylide formation with [2,3]-sigmatropic rearrangement in the order of propargyl > methallyl > allyl.

The correlation between diastereoselectivity in the formation of **31a-c** and the number of ether oxygen atoms in **30a-c** is consistent with copper coordination to the diazoacetate. Coordination of bis-oxazoline **26** to copper(I) hexafluorophosphate prior to diazo decomposition of **30** inhibits the formation of both **31** and **32**, and suggests that the stronger binding bis-oxazoline ligand inhibits or prevents other coordination that facilitates macrocyclization and causes the formation of ylide derived products to be absent altogether. The investigation of catalysts loading in the diazo decomposition of **30b** shows that the use of stoichiometric copper(I) hexafluorophosphate affords a different ratio of diastereoisomers than that using catalytic copper(I) hexafluorophosphate, which is consistent with the copper cation interaction with the substrate to influence diastereoselectivity, but does not clearly support a conclusion. While these results do not prove that copper(I) coordinates to the ether oxygen atoms of the diazoacetate in diazo decomposition, they are consistent with this interaction.

4.2.2 Use of a Sodium Template

Crown ethers and polyether substrates are known to coordinate ions of alkali and alkaline earth metals.⁷ Additionally, diazoacetates are not known to be susceptible to decomposition by these ions.²⁵ The addition of an alkaline metal ion to diazoacetate compounds such as **30a-c** as a template allows coordination between the metal ion and the ether oxygen atoms to occur, ensuring that the substrate has formed a complex with the cation template prior to diazo decomposition. In addition, the use of an alkali metal ion establishes the geometry of the complex as octahedral with a maximum of six ether oxygen atoms coordinated to the metal ion.

We selected the sodium tetraphenylborate salt to provide a sodium cation template due to the solubility of the tetraphenylborate anion in organic solvents. We first obtained ¹H NMR spectra of both **30b** (Figure 4.7) and a solution containing a 1:1 mixture of NaBPh₄ and **30b** (Figure 4.8). The low solubility of sodium tetraphenylborate in CDCl₃ results in heterogeneous mixtures, but a CDCl₃ solution of **30b** readily dissolved one equivalent of sodium tetraphenyl borate. Coordination of the sodium ion to **30b** was confirmed by ¹H NMR chemical shifts of protons adjacent to ether oxygen atoms.

²⁵ Doyle, M.P.; McKervey, M.A.; Ye, T. Modern Catalytic Methods for Organic Synthesis with Diazo Compounds: from Cyclopropanes to Ylides, Wiley-Interscience: New York, 1998.

Figure 4.7 ^1H Spectra of 30b without NaBPh₄

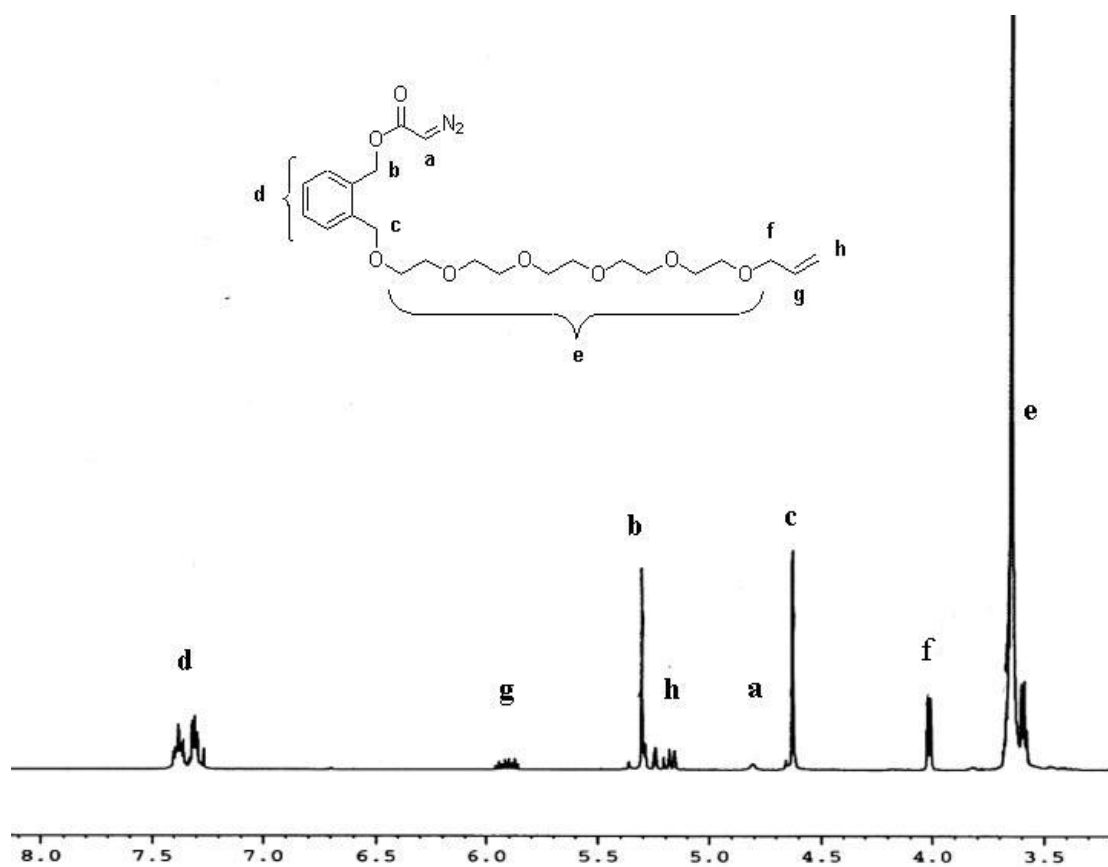
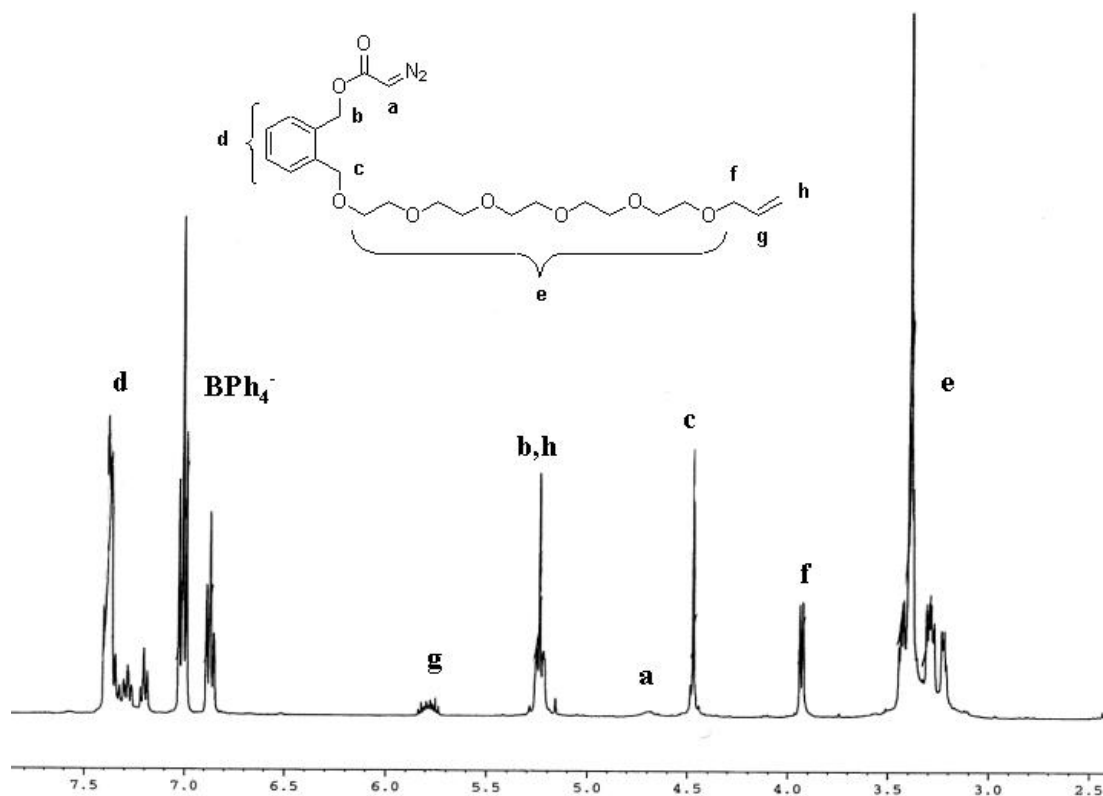


Figure 4.8 ^1H Spectra of **30b** with NaBPh_4



The addition of sodium tetraphenylborate to **30b** gives rise to several changes in the chemical shift of protons in **30b** (Table 4.4). Proton signals associated with the allyl functional group (peaks f and g in figures 4.7, 4.8) are shifted upfield by approximately 0.1 ppm, while the benzylic proton adjacent to an ether oxygen atom (peak c in figure 4.8) is shifted upfield approximately 0.2 ppm. The chemical shift region between 3.7 and 3.5 ppm is assigned as the absorbance frequency of the protons in the penta(ethylene glycol) portion of **30b**, but with the addition of NaBPh_4 the absorbance frequency of these protons is observed approximately 0.2 ppm upfield, and the chemical shift range of the protons broadens, so that discreet signals begin to emerge. This upfield chemical shift and broadening of the chemical shift

range is consistent with the sodium ion forming a complex with **33b**, and lowering the degrees of freedom within the substrate.

Table 4.4 Chemical Shifts in the ^1H NMR Spectra of **33b**

Substrate	Proton signals (ppm)							
	a	b	c	d	e	f	g	h
33b	4.81	5.31	4.62	7.40-7.29	3.67-3.58	4.02	5.91	5.26-5.15
33b /NaBPh ₄	4.68	5.27	4.48	7.43-7.30	3.48-3.10	3.94	5.79	5.28-5.19

Based on the complex between **30b** and NaBPh₄ observed in the ^1H NMR study of NaBPh₄/**30b** in solution, we have a sodium cation template coordinating a diazoacetate compound that is known to undergo diazo decomposition to yield macrocycle compounds **31b** and **32b**. The mixture of **30b** with sodium tetraphenylborate was dissolved in methylene chloride and allowed to equilibrate for thirty minutes, then subjected to diazo decomposition by slow addition to a refluxing solution of catalyst in methylene chloride (Scheme 4.7). Following diazo decomposition, integration of ^1H NMR spectra of the crude reaction mixture was used to determine relative yields (Table 4.4). These reactions proved difficult to analyze, as the sodium salt was not removed from the crude product mixture after flash chromatography of the crude reaction mixture through a silica gel plug. Because of this, a large error factor is associated with the mass of the crude reaction mixture, and quantitative yields could not be accurately determined.

Scheme 4.7 Diazo Decomposition of 30b with a Na Template

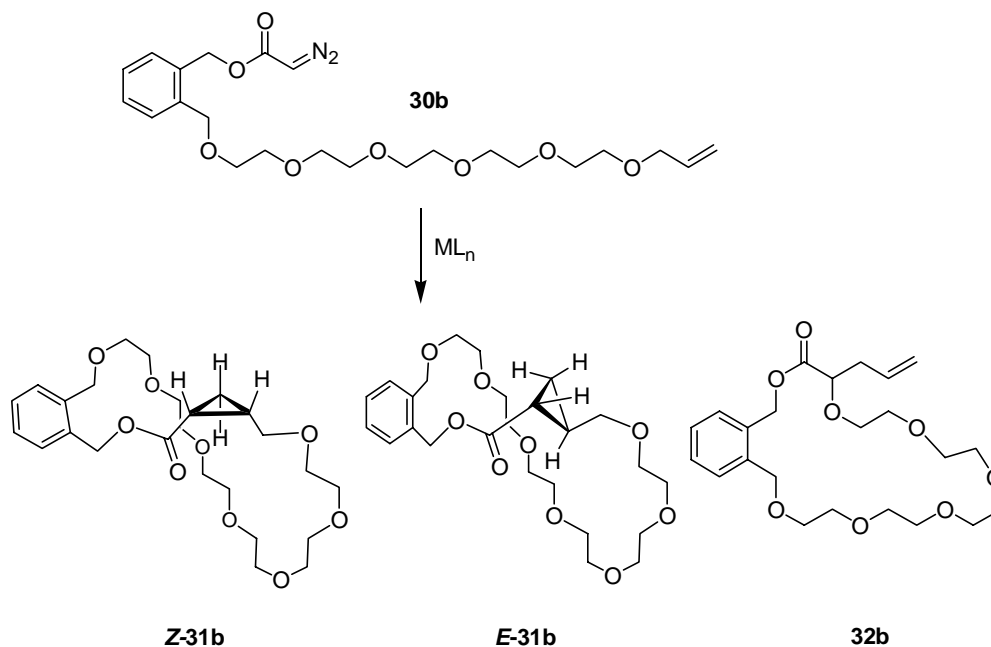


Table 4.4 Selectivity in Diazo Decomposition of 30b with a Na Template

Catalyst	NaBPh ₄ (mol %)	31b:32b	<i>E:Z</i> (31b)	Yields (%) ^d
Rh ₂ (OAc) ₄	110	100:0	35:65	45
	80	100:0	38:62	47
	10	100:0	35:65	61
	0	100:0	36:64	71
Cu(CH ₃ CN) ₄ PF ₆	110	100:0	n.d. ^e	49
	80	100:0	80:20	55
	10	63:37	72:38	73
	0	51:49	57:43	82

a) Decomposition carried out as 2 h addition of **31b** to refluxing solution of catalyst in methylene chloride b) Ratios of products obtained by ¹H NMR c) yields obtained by crude mass and ¹H NMR ratios (d) yields obtained are based on proton NMR data and assume complete mass recovery after filtration e) not determined

Relative yields of products from diazo decomposition were obtained by integration of ¹H NMR signals associated with materials related to the olefin of the starting material (i.e., cyclopropane, allyl, and the olefin resulting from [2,3]-sigmatropic

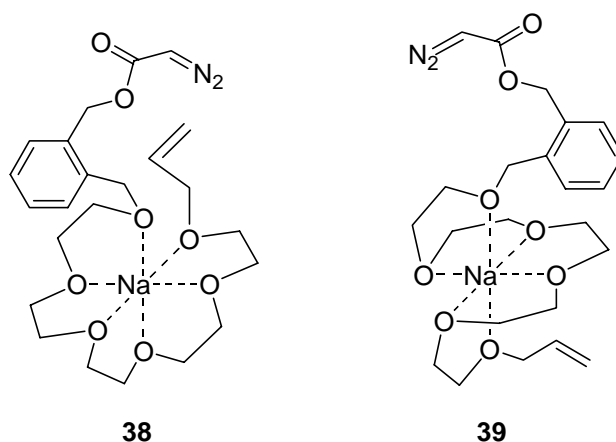
rearrangement²⁶). Reactions containing 110 mol% or 80 mol% of sodium tetraphenylborate had 15-30% lower yields of **31b** and **32b** than those with 10 mol% or no sodium tetraphenylborate. The ratios between *E* and *Z* diastereoisomers of **31** did not deviate with the change in mol% of NaBPh₄ for dirhodium(II) tetraacetate catalyzed reactions, but the ratios between *E* and *Z* diastereoisomers of **31** were substantially different in the copper(I) hexafluorophosphate catalyzed reactions. Formation of oxonium ylide derived product **32b** was not observed in the ¹H NMR spectrum of the crude reaction mixtures using 110 or 80 mol% of sodium tetraphenylborate, and even 10 mol% of the sodium template reagent impacted chemoselectivity, lowering the amount of **32b** seen.

Diastereoselectivity seen in the copper(I) hexafluorophosphate catalyzed diazo decomposition of the **30b**/NaBPh₄ complex is dependent on the mol% of NaBPh₄ used. The conformational constraint the sodium template places on **30b** affects the approach of the olefin to the metal carbene intermediate, enhancing the formation of the *Z* isomer of **31b**. Assuming that the sodium cation is coordinated to six oxygen atoms of **30b**, the complex formed would be arranged in one of two geometries (**38**, **39**), with only **38** allowing carbene addition to the allyl group (Figure 4.8). In **38**, the diazoacetate and the allyl group are constrained in close proximity to each other by the sodium template, resembling a diazoacetate that would form a smaller ring in which the *cis* isomer of the cyclopropane is preferred.^{6a} The lower yields seen in the diazo decomposition of **30b** using 110 mol% or 80 mol% NaBPh₄ can also be

²⁶ The signal is the unique proton signal for the olefin of the product formed from oxonium ylide formation followed by [2,3]-sigmatropic rearrangement observed at 5.65 ppm as a ddt.

rationalized by the conformational constraint placed on **30b** by the sodium template, as graphically illustrated in **39**. Sodium constraining **30b** in the geometric arrangement illustrated in **39** prohibits carbene addition to the allyl group, and an alternate reaction pathway must occur, affecting the yield of **31b** observed in the reaction. It is believed that the conformations described in **38** and **39** both exist, and that they influence the reaction selectivity in diazo decomposition of **30b**. Coordination by the sodium cation to all six ether oxygen atoms of **30b** would also affect the chemoselectivity seen in copper(I) catalyzed diazo decomposition of **30b**. When coordinated to sodium cation, the oxygen atoms are not able to form an oxonium ion as readily, and ylide formation is inhibited, which is manifest in the reported chemoselectivity for copper(I) catalyzed reactions in Table 4.6. Sodium cation coordination enhances chemoselectivity and diastereoselectivity in the diazo decomposition of **30b** and also enhances the yield of macrocyclic cyclopropanation product **31b**.

Figure 4.8 Configuration of 30b with Sodium Template

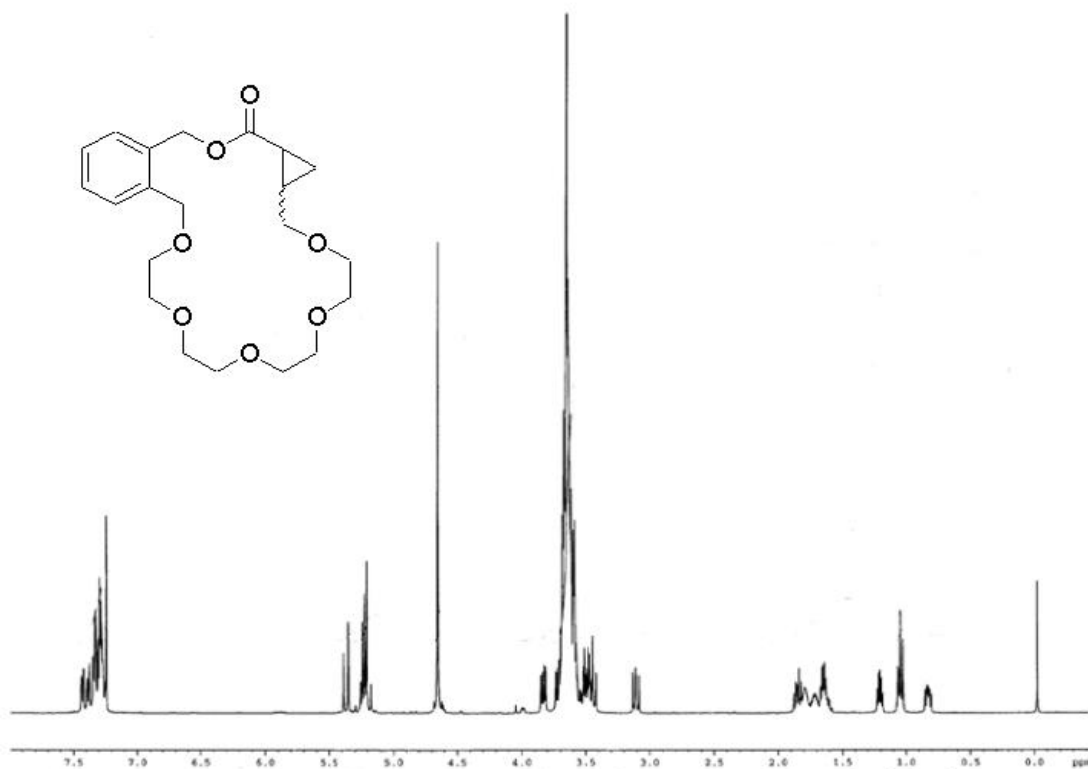


4.2.3 Product Complexes of Sodium

The sodium cation also forms complexes with macrocycles **E-31b** and **Z-31b**, and the complexes were recovered as a mixture of both diastereoisomers after reverse phase chromatography of the product mixture resulting from diazo decomposition of the **30b**/NaBPh₄ complex by dirhodium(II) tetraacetate. Integration of the peak area for both **31b** and NaBPh₄ in the ¹H NMR spectrum showed that the isolated complex of **31b** and sodium tetraphenylborate is a 1:1 complex. The large multiplet at 3.5 ppm that is associated with the protons of the ethylene glycol linker expands to 4.0 to 3.0 ppm with multiple doublets. This change in chemical shift of the ethylene glycol linker reflects the change in conformational freedom, as the sodium template restricts the rapid conformational interchange of **31b**.

Diazo decomposition of **30a** by dirhodium(II) tetraacetate was followed by HPLC analysis of the crude reaction mixture, providing a diastereomeric mixture of sodium free **31a**. Addition of one equivalent of sodium tetraphenylborate to sodium free **31a** affords a complex with 1:1 ratio between **31a** and sodium tetraphenylborate, observable by ¹H NMR. The chemical shifts seen in the ¹H NMR spectrum of the **31a**/NaBPh₄ complex are analogous to those obtained from the diazo decomposition of **31b** in the presence of one equivalent of NaBPh₄ (Figure 4.9). Additional characterization using IR spectroscopy shows a shift of the C=O stretch, and a broad range of C-H stretches (Table 4.5). From the ¹H NMR and IR spectral information it was concluded that the sodium ion coordinated to the substrate.

Figure 4.9 ^1H NMR Spectra of 31a with and without NaBPh_4



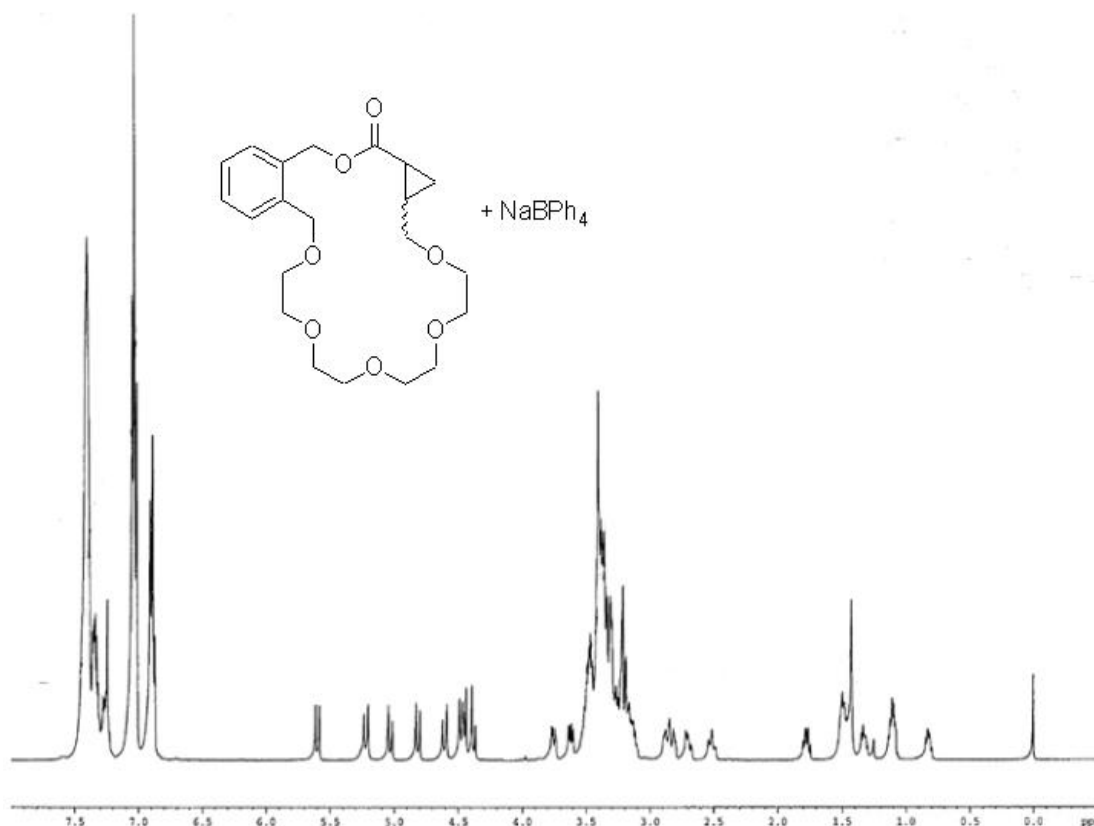


Table 4.5 IR Absorbances of 31a with and without a Na Template^a

Substrate	C-H stretch (cm ⁻¹)			C=O stretch (cm ⁻¹)	
31a	2943	2900	2865	1725	
31a/NaBPh₄	3056	3034	3003	1732	1715
	2981	2912	2973	1700	

a) IR spectra obtained in a solution of CDCl₃

Development of template assisted macrocycle formation using additional template reagents met with no success. Studies using either potassium tetraphenylborate or cesium tetraphenylborate as template reagents were not possible under the reaction conditions described for diazo decomposition using sodium tetraphenyl borate as a template reagent. The solubility of these salts in methylene chloride is lower than that of sodium tetraphenylborate, and no evidence for complex formation between these salts and **30b** was found. Use of a polar solvent such as nitromethane to

increase solubility of the salts was not investigated with potassium or cesium salts, but may be a means to promote complexation.

4.3 Conclusions and Future Work

The evaluation of reaction control using copper(I) catalysts has been performed using diazoacetates **30a-c**, **33**, and **34**. Chemoselectivity in the diazo decomposition of these substrates appears to directly correlate to the functional group used. The influence of the copper cation on diastereoselectivity in cyclopropanation of **30** correlates to the length of the tether of the diazoacetate compound. Copper catalyst loading also influences cyclopropanation diastereoselectivity, suggesting that the macrocycle products formed also associate with the copper cation during the course of the reaction. Attempts to run a control reaction with $\text{Cu}(\text{CH}_3\text{CN})_4\text{PF}_6$ /**26** failed to yield significant quantities of macrocyclic compounds for evaluation, and while the results are meaningful, the interpretation of them is subject to the enlistment of negative results.

Sodium tetraphenylborate has been shown to form a complex with **30b** in methylene chloride. The use of a sodium cation as a template in the copper(I) hexafluorophosphate catalyzed diazo decomposition of **30a-c** has been shown to influence both chemoselectivity and diastereoselectivity. The diastereoselectivity, chemoselectivity, and yields for diazo decomposition of **30b** are all consistent with a sodium/**30b** complex with an octahedral geometry. The use of NaBPh_4 as a template in copper(I) catalyzed diazo decomposition influences the diastereoselectivity in the

formation of **31b** and also impedes the formation of oxonium ylides. However, the use of NaBPh₄ as a template in dirhodium(II) tetraacetate catalyzed diazo decomposition does not influence diastereoselectivity.

The addition of a sodium template to direct ring closure has demonstrated the ability of the template to influence diastereoselectivity and chemoselectivity in metal carbene addition reactions. Challenges remain in improving the modest macrocycle yields and difficulties found in removing the ionic template. Further enhancement of template synthesis of macrocycles using metal carbene intermediates may optimize the template used based on charge and ionic radius of the cation. The range of catalysts and functional groups that are compatible with template synthesis and metal carbene intermediates is still open to further investigation, and the use of template control in asymmetric macrocyclic cyclopropanation has not been investigated.

4.4 Experimental Procedures

General Procedure for diazo decomposition of 56, 58, and 59, with NaBPh₄ by copper(I) hexafluorophosphate: The following is an example procedure of diazo decomposition. To a 1.5 dram vial with a Teflon cap liner was added **56** (0.101 g, 0.214 mmol, 1.00 eq), then DCM (1.0 mL), and finally NaBPh₄ (81.8 mg, 0.235 mmol, 1.10 eq). The solution was shaken for 1 min. and allowed to stand for 30 min. Next, an oven dried flask was charged with copper(I) hexafluorophosphate (8.3 mg, 23.7 μ mol, 0.10 eq), bis-oxazoline **34** (9.3 mg, 28.4 μ mol, 0.12 eq) and DCM (5 mL) and brought to reflux. To the refluxing solution was added the solution of **58** and NaBPh₄ diluted with DCM to a total volume of 5 mL over 2 h using a Kazel syringe pump. The resultant yellow/brown solution was allowed to reflux for an additional 2 h after addition, cooled to room temperature, and concentrated under reduced pressure. The crude reaction mixture was filtered through a glass pipet loaded with 2 inches of silica gel to remove the catalyst and washed with a solution of EtOAc:Et₂O (3:1, 15 mL). The filtrate was concentrated under reduced pressure, to yield a cloudy heterogeneous mixture, and a ¹H NMR spectrum was obtained immediately. Purification of the crude reaction mixture was achieved using semi-preparative reverse phase HPLC at a flow rate of 3.0 mL/min with water:acetonitrile (60:40) for 28 min, ramped at 2.7%/min to water:acetonitrile (0:100) and maintained 15 min. *Z*-**64** and *E*-**64** were eluted as a mixture at 20.5-22.8 min. along with the NaBPh₄ salts. The collected fractions were concentrated under reduced pressure to remove acetonitrile, frozen, and residual water was sublimed under reduced pressure.

General Procedure for diazo decomposition of 56, 58, and 59, with NaBPh₄ by dirhodium(II) tetraacetate: The following is an example procedure for diazo decomposition. To a 1.5 dram vial with a Teflon cap liner was added **56** (0.103 g, 0.214 mmol, 1.00 eq), then DCM (1.0 mL), and finally NaBPh₄ (80.6 mg, 0.235 mmol, 1.10 eq). The solution was shaken for 1 min. and allowed to stand for 30 min. Next, an oven dried flask was charged with dirhodium(II) tetraacetate (1.9 mg, 2.1 μ mol, 0.010 eq) and DCM (5 mL) and brought to reflux. To the refluxing solution was added the solution of **58** and NaBPh₄ diluted with DCM to a total volume of 5 mL over 2 h using a Kazel syringe pump. The resultant yellow/brown solution was allowed to reflux for an additional 2 h after addition, cooled to room temperature, and concentrated under reduced pressure. The crude reaction mixture was filtered through a glass pipet loaded with 2 inches of silica gel with a solution of EtOAc:Et₂O (3:1, 15 mL) to remove the catalyst. The filtrate was concentrated under reduced pressure, to yield a cloudy heterogeneous mixture, and a ¹H NMR spectrum was obtained immediately. Purification of the crude reaction mixture was achieved using semi-preparative reverse phase HPLC at a flow rate of 3.0 mL/min with water:acetonitrile (60:40) for 28 min, ramped at 2.7 %/min to water:acetonitrile (0:100) and maintained 15 min. *Z*-**64** and *E*-**64** were eluted as a mixture at 20.5-22.8 min. along with the NaBPh₄ salts. The collected fractions were concentrated under reduced pressure to remove acetonitrile, frozen, and residual water was sublimed under reduced pressure.

Chapter 5. Summary and Conclusions

The investigations reported herein have served to describe: how a remote conformational bias influences diastereoselectivity in carbene addition to allyl and propargyl ethers, the enhancement of macrocycle formation by eliminating competitive reaction pathway of γ -butyrolactone formation, and aiding ring closure using a sodium template. Results from these studies have advanced the understanding of metal carbene chemistry in various ways related to the mechanism of carbene addition and the substrate requirements for macrocycle formation via carbene addition. The 28-membered cyclopropane described in chapter 3 is the largest macrocycle formed via carbene addition to date and the results from diazo decomposition do not indicate any limitations in ring size for this class of diazoacetates. The use of a conformational bias is shown to enhance diastereoselectivity with both copper(I) and dirhodium(II) carboxamidate catalysts, and is highly dependent on the conformational bias. Incorporation of a sodium template reduces the formation of oxonium ylides in copper catalyzed diazo decomposition and enhances the selective formation of cis cyclopropanes over trans cyclopropanes.

Danishefsky and co-workers recently demonstrated that replacement of an epoxide by a cyclopropane in a macrocyclic compound did not significantly change the IC₅₀ values of the molecule in a screen against specific cancer cell lines.¹ This result suggests that many macrocycles containing a cyclopropane may be bioactive and that

¹ Yamamoto, K.; Garbaccio, R.M.; Stachel, S.J.; Solit, D.B.; Chiosis, G.; Rosen, N.; Danishefsky, S.J. *Angew. Chem. Int. Ed.* **2003**, *42*, 1280.

synthetic strategies using cyclopropanation as a means of macrocyclization in the synthesis of pharmacological targets are viable. The macrocycles formed in the investigations described here are applicable to the synthesis of bioactive macrocycles containing cyclopropanes in large ring formation and in the influence of a remote stereocenter on diastereoselectivity. With new leads in drug discovery that involve macrocycles containing a cyclopropane subunit, macrocyclic cyclopropanation and other carbene addition reactions hold potential to expand a new generation of drug development.

A second area in which macrocycles are a key component is that of display technologies rising from the demand for optoelectronic devices. Luminescent molecular architectures built from new molecular scaffolds provide a means to control and manipulate the electronic properties of the material. In many cases these new architectures are arising from novel macrocycles. Carbene addition reactions provide access to macrocycles from readily available starting materials with good yields in a macrocyclization method suitable for large scale reactions. The studies described herein provide a foundation for the use of templates and cations in macrocyclization by carbene addition reactions.

Appendix A

X-Ray Crystal Structure of **39a** (Chapter 2)

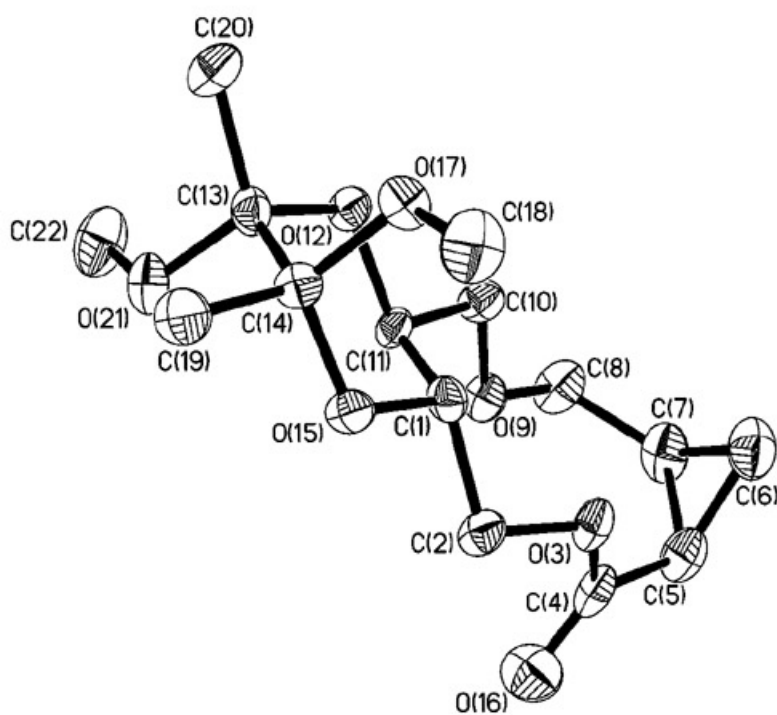
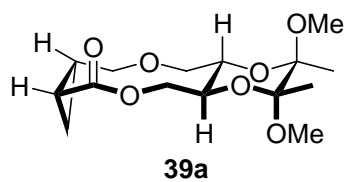


Table 1. Crystal data and structure refinement for TW01S.

Identification	code tw01s
Empirical formula	C15 H24 O7
Formula weight	316.34
Temperature	170(2) K
Wavelength	0.71073 Å
Crystal system	Monoclinic
Space group	P2(1)
Unit cell dimensions	a = 6.8596(12) Å $\alpha = 90^\circ$ b = 9.5668(16) Å $\beta = 95.413(3)^\circ$ c = 11.922(2) Å $\gamma = 90^\circ$
Volume, Z	778.9(2) Å ³ , 2
Density (calculated)	1.349 Mg/m ³
Absorption coefficient	0.107 mm ⁻¹
F(000)	340
Crystal size	0.3 x 0.15 x 0.025 mm
Theta range for data collection	1.72 to 26.08°
Limiting indices	-8 ≤ h ≤ 8, -11 ≤ k ≤ 11, -14 ≤ l ≤ 14
Reflections collected	7693
Independent reflections	3025 (R(int) = 0.0470)
Completeness to theta = 26.08°	98.9 %
Absorption correction	Semi-empirical from equivalents
Max. and min. transmission	1 and 0.799941
Refinement method	Full-matrix least-squares on F ²
Data / restraints / parameters	3025 / 1 / 203
Goodness-of-fit on F ²	1.023
Final R indices [I > 2sigma(I)]	R1 = 0.0471, wR2 = 0.1039
R indices (all data)	R1 = 0.0730, wR2 = 0.1147
Absolute structure parameter	1.3(13)
Largest diff. peak and hole	0.308 and -0.204 eÅ ⁻³

Table 2. Atomic coordinates [$\times 10^4$] and equivalent isotropic displacement parameters [$\text{\AA}^2 \times 10^3$] for TW01S. U(eq) is defined as one third of the trace of the orthogonalized U^{ij} Tensor.

	x	y	z	U (eq)
C(1)	7515(4)	8642(3)	8085(2)	22(1)
C(2)	9121(4)	8982(3)	7344(2)	26(1)
O(3)	9094(3)	10476(2)	7177(2)	28(1)
C(4)	9294(4)	10945(3)	6113(3)	29(1)

C(5)	8734(5)	12413(3)	5941(3)	36(1)
C(6)	7769(5)	13205(4)	6803(3)	45(1)
C(7)	6585(5)	12835(3)	5759(3)	39(1)
C(8)	4915(4)	11801(3)	5654(3)	36(1)
O(9)	5422(3)	10443(2)	6087(1)	27(1)
C(10)	4730(4)	10129(3)	7131(2)	26(1)
C(11)	5470(4)	8687(3)	7483(2)	20(1)
O(12)	4102(3)	8174(2)	8231(2)	23(1)
C(13)	4499(4)	6785(3)	8623(2)	24(1)
C(14)	6599(4)	6708(3)	9212(2)	21(1)
O(15)	7956(2)	7245(2)	8483(2)	23(1)
O(16)	9957(3)	10237(2)	5410(2)	47(1)
O(17)	6546(3)	7570(2)	10165(2)	26(1)
C(18)	8286(5)	7613(3)	10913(3)	38(1)
C(19)	7260(4)	5234(3)	9492(2)	30(1)
C(20)	2946(4)	6448(3)	9399(3)	31(1)
O(21)	4493(3)	5852(2)	7701(2)	30(1)
C(22)	2732(5)	5789(4)	6967(3)	44(1)

Table 3. Bond lengths [Å] and angles [°] for TW01S.

C(1)-O(15)	1.441(3)	C(14)-C(19)	1.509(4)
C(1)-C(2)	1.511(3)	O(17)-C(18)	1.421(3)
C(1)-C(11)	1.515(3)	C(18)-H(18A)	0.9800
C(1)-H(1A)	1.0000	C(18)-H(18B)	0.9800
C(2)-O(3)	1.442(3)	C(18)-H(18C)	0.9800
C(2)-H(2A)	0.9900	C(19)-H(19A)	0.9800
C(2)-H(2B)	0.9900	C(19)-H(19B)	0.9800
O(3)-C(4)	1.365(4)	C(19)-H(19C)	0.9800
C(4)-O(16)	1.200(4)	C(20)-H(20A)	0.9800
C(4)-C(5)	1.466(4)	C(20)-H(20B)	0.9800
C(5)-C(6)	1.483(5)	C(20)-H(20C)	0.9800
C(5)-C(7)	1.524(5)	O(21)-C(22)	1.424(3)
C(5)-H(5A)	1.0000	C(22)-H(22A)	0.9800
C(6)-C(7)	1.464(4)	C(22)-H(22B)	0.9800
C(6)-H(6A)	0.9900	C(22)-H(22C)	0.9800
C(6)-H(6B)	0.9900		
C(7)-C(8)	1.510(4)	O(15)-C(1)-C(2)	104.5(2)
C(7)-H(7A)	1.0000	O(15)-C(1)-C(11)	109.8(2)
C(8)-O(9)	1.429(3)	C(2)-C(1)-C(11)	114.3(2)
C(8)-H(8A)	0.9900	O(15)-C(1)-H(1A)	109.4
C(8)-H(8B)	0.9900	C(2)-C(1)-H(1A)	109.4
O(9)-C(10)	1.406(3)	C(11)-C(1)-H(1A)	109.4
C(10)-C(11)	1.516(4)	O(3)-C(2)-C(1)	107.1(2)
C(10)-H(10A)	0.9900	O(3)-C(2)-H(2A)	110.3
C(10)-H(10B)	0.9900	C(1)-C(2)-H(2A)	110.3
C(11)-O(12)	1.441(3)	O(3)-C(2)-H(2B)	110.3
C(11)-H(11A)	1.0000	C(1)-C(2)-H(2B)	110.3
O(12)-C(13)	1.426(3)	H(2A)-C(2)-H(2B)	108.6
C(13)-O(21)	1.416(3)	C(4)-O(3)-C(2)	116.9(2)
C(13)-C(20)	1.510(4)	O(16)-C(4)-O(3)	122.8(3)
C(13)-C(14)	1.544(4)	O(16)-C(4)-C(5)	123.7(3)
C(14)-O(17)	1.407(3)	O(3)-C(4)-C(5)	113.4(3)
C(14)-O(15)	1.428(3)	C(4)-C(5)-C(6)	121.4(3)

C(4)-C(5)-C(7)	120.8(3)	C(14)-C(19)-H(19A)	109.5
C(6)-C(5)-C(7)	58.3(2)	C(14)-C(19)-H(19B)	109.5
C(4)-C(5)-H(5A)	114.9	H(19A)-C(19)-H(19B)	109.5
C(6)-C(5)-H(5A)	114.9	C(14)-C(19)-H(19C)	109.5
C(7)-C(5)-H(5A)	114.9	H(19A)-C(19)-H(19C)	109.5
C(7)-C(6)-C(5)	62.3(2)	H(19B)-C(19)-H(19C)	109.5
C(7)-C(6)-H(6A)	117.5	C(13)-C(20)-H(20A)	109.5
C(5)-C(6)-H(6A)	117.5	C(13)-C(20)-H(20B)	109.5
C(7)-C(6)-H(6B)	117.5	H(20A)-C(20)-H(20B)	109.5
C(5)-C(6)-H(6B)	117.5	C(13)-C(20)-H(20C)	109.5
H(6A)-C(6)-H(6B)	114.6	H(20A)-C(20)-H(20C)	109.5
C(6)-C(7)-C(8)	125.7(3)	H(20B)-C(20)-H(20C)	109.5
C(6)-C(7)-C(5)	59.5(2)	C(13)-O(21)-C(22)	116.3(2)
C(8)-C(7)-C(5)	123.7(3)	O(21)-C(22)-H(22A)	109.5
C(6)-C(7)-H(7A)	112.7	O(21)-C(22)-H(22B)	109.5
C(8)-C(7)-H(7A)	112.7	H(22A)-C(22)-H(22B)	109.5
C(5)-C(7)-H(7A)	112.7	O(21)-C(22)-H(22C)	109.5
O(9)-C(8)-C(7)	114.1(2)	H(22A)-C(22)-H(22C)	109.5
O(9)-C(8)-H(8A)	108.7	H(22B)-C(22)-H(22C)	109.5
C(7)-C(8)-H(8A)	108.7		
O(9)-C(8)-H(8B)	108.7		
C(7)-C(8)-H(8B)	108.7		
H(8A)-C(8)-H(8B)	107.6		
C(10)-O(9)-C(8)	115.0(2)		
O(9)-C(10)-C(11)	107.9(2)		
O(9)-C(10)-H(10A)	110.1		
C(11)-C(10)-H(10A)	110.1		
O(9)-C(10)-H(10B)	110.1		
C(11)-C(10)-H(10B)	110.1		
H(10A)-C(10)-H(10B)	108.4		
O(12)-C(11)-C(1)	109.0(2)		
O(12)-C(11)-C(10)	105.1(2)		
C(1)-C(11)-C(10)	115.3(2)		
O(12)-C(11)-H(11A)	109.1		
C(1)-C(11)-H(11A)	109.1		
C(10)-C(11)-H(11A)	109.1		
C(13)-O(12)-C(11)	113.9(2)		
O(21)-C(13)-O(12)	110.3(2)		
O(21)-C(13)-C(20)	113.0(2)		
O(12)-C(13)-C(20)	106.0(2)		
O(21)-C(13)-C(14)	104.9(2)		
O(12)-C(13)-C(14)	109.6(2)		
C(20)-C(13)-C(14)	113.1(2)		
O(17)-C(14)-O(15)	110.4(2)		
O(17)-C(14)-C(19)	113.6(2)		
O(15)-C(14)-C(19)	105.7(2)		
O(17)-C(14)-C(13)	104.2(2)		
O(15)-C(14)-C(13)	109.84(19)		
C(19)-C(14)-C(13)	113.2(2)		
C(14)-O(15)-C(1)	113.94(19)		
C(14)-O(17)-C(18)	116.1(2)		
O(17)-C(18)-H(18A)	109.5		
O(17)-C(18)-H(18B)	109.5		
H(18A)-C(18)-H(18B)	109.5		
O(17)-C(18)-H(18C)	109.5		
H(18A)-C(18)-H(18C)	109.5		
H(18B)-C(18)-H(18C)	109.5		

Symmetry transformations used to generate equivalent atoms:
 #1 -x,-y+1,-z+1

Table 4. Anisotropic displacement parameters [$\text{\AA}^2 \times 10^3$] for TW01S. The anisotropic displacement factor exponent takes the form:
 $-2\pi^2[(ha^*)^2U^{11} + \dots + 2hka^*b^*U^{12}]$

	U11	U22	U33	U23	U13	U12
C(1)	24(2)	16(2)	25(1)	1(1)	1(1)	3(1)
C(2)	23(2)	19(2)	36(2)	9(1)	5(1)	1(1)
O(3)	26(1)	20(1)	36(1)	4(1)	-2(1)	-6(1)
C(4)	22(2)	24(2)	39(2)	8(2)	-6(1)	-7(1)
C(5)	37(2)	30(2)	42(2)	8(2)	1(2)	-8(2)
C(6)	58(2)	35(2)	43(2)	-2(2)	3(2)	-10(2)
C(7)	45(2)	23(2)	47(2)	10(2)	-7(2)	5(1)
C(8)	31(2)	32(2)	42(2)	16(2)	-5(1)	2(1)
O(9)	30(1)	22(1)	28(1)	8(1)	-1(1)	-1(1)
C(10)	22(1)	26(2)	32(2)	5(1)	3(1)	2(1)
C(11)	20(1)	16(2)	25(1)	3(1)	3(1)	-3(1)
O(12)	21(1)	17(1)	30(1)	5(1)	3(1)	3(1)
C(13)	29(2)	17(2)	25(2)	0(1)	3(1)	-1(1)
C(14)	22(2)	23(2)	19(1)	4(1)	1(1)	1(1)
O(15)	21(1)	18(1)	29(1)	7(1)	5(1)	5(1)
O(16)	57(2)	45(2)	40(1)	8(1)	13(1)	2(1)
O(17)	28(1)	26(1)	24(1)	-1(1)	-1(1)	4(1)
C(18)	40(2)	41(2)	31(2)	2(2)	-10(1)	-2(2)
C(19)	31(2)	26(2)	33(2)	7(1)	4(1)	5(1)
C(20)	23(2)	29(2)	40(2)	11(2)	3(1)	-2(1)
O(21)	36(1)	22(1)	31(1)	-1(1)	-6(1)	-4(1)
C(22)	48(2)	44(2)	39(2)	2(2)	-12(2)	-15(2)

Table 5. Hydrogen coordinates ($\times 10^4$) and isotropic displacement parameters ($\text{\AA}^2 \times 10^3$) for TW01S.

	x	y	z	U(eq)
H(1A)	7594	9300	8740	26
H(2A)	10407	8683	7712	31
H(2B)	8886	8494	6612	31
H(5A)	9636	12976	5508	43
H(6A)	7501	12702	7498	54
H(6B)	8135	14200	6917	54
H(7A)	6360	13647	5234	47
H(8A)	3832	12175	6060	43
H(8B)	4426	11713	4849	43
H(10A)	3281	10145	7063	31
H(10B)	5216	10830	7702	31
H(11A)	5420	8071	6803	24

H(18A)	8149	8320	11496	57
H(18B)	9399	7853	10492	57
H(18C)	8510	6696	11268	57
H(19A)	8641	5242	9790	45
H(19B)	7102	4659	8808	45
H(19C)	6466	4843	10057	45
H(20A)	1647	6560	8992	46
H(20B)	3075	7085	10046	46
H(20C)	3109	5482	9665	46
H(22A)	2919	5163	6335	67
H(22B)	2396	6726	6680	67
H(22C)	1668	5432	7382	67

Table 6. Torsion angles [°] for TW01S.

O(15)-C(1)-C(2)-O(3)	-164.2(2)
C(11)-C(1)-C(2)-O(3)	75.9(3)
C(1)-C(2)-O(3)-C(4)	-137.1(2)
C(2)-O(3)-C(4)-O(16)	-19.0(4)
C(2)-O(3)-C(4)-C(5)	164.5(2)
O(16)-C(4)-C(5)-C(6)	174.9(3)
O(3)-C(4)-C(5)-C(6)	-8.7(4)
O(16)-C(4)-C(5)-C(7)	105.6(4)
O(3)-C(4)-C(5)-C(7)	-78.0(3)
C(4)-C(5)-C(6)-C(7)	-109.1(3)
C(5)-C(6)-C(7)-C(8)	111.6(4)
C(4)-C(5)-C(7)-C(6)	110.2(3)
C(4)-C(5)-C(7)-C(8)	-4.8(5)
C(6)-C(5)-C(7)-C(8)	-114.9(4)
C(6)-C(7)-C(8)-O(9)	-55.2(4)
C(5)-C(7)-C(8)-O(9)	18.9(4)
C(7)-C(8)-O(9)-C(10)	104.8(3)
C(8)-O(9)-C(10)-C(11)	-177.6(2)
O(15)-C(1)-C(11)-O(12)	55.7(3)
C(2)-C(1)-C(11)-O(12)	172.7(2)
O(15)-C(1)-C(11)-C(10)	173.6(2)
C(2)-C(1)-C(11)-C(10)	-69.4(3)
O(9)-C(10)-C(11)-O(12)	-155.33(19)
O(9)-C(10)-C(11)-C(1)	84.6(3)
C(1)-C(11)-O(12)-C(13)	-58.4(3)
C(10)-C(11)-O(12)-C(13)	177.4(2)
C(11)-O(12)-C(13)-O(21)	-58.2(3)
C(11)-O(12)-C(13)-C(20)	179.1(2)
C(11)-O(12)-C(13)-C(14)	56.8(3)
O(21)-C(13)-C(14)-O(17)	-176.4(2)
O(12)-C(13)-C(14)-O(17)	65.2(2)
C(20)-C(13)-C(14)-O(17)	-52.8(3)
O(21)-C(13)-C(14)-O(15)	65.4(2)
O(12)-C(13)-C(14)-O(15)	-53.0(3)
C(20)-C(13)-C(14)-O(15)	-171.0(2)
O(21)-C(13)-C(14)-C(19)	-52.5(3)
O(12)-C(13)-C(14)-C(19)	-170.9(2)
C(20)-C(13)-C(14)-C(19)	71.1(3)
O(17)-C(14)-O(15)-C(1)	-59.1(3)

C(19)-C(14)-O(15)-C(1)	177.7(2)
C(13)-C(14)-O(15)-C(1)	55.3(3)
C(2)-C(1)-O(15)-C(14)	179.9(2)
C(11)-C(1)-O(15)-C(14)	-57.2(3)
O(15)-C(14)-O(17)-C(18)	-66.3(3)
C(19)-C(14)-O(17)-C(18)	52.2(3)
C(13)-C(14)-O(17)-C(18)	175.8(2)
O(12)-C(13)-O(21)-C(22)	-58.4(3)
C(20)-C(13)-O(21)-C(22)	60.0(3)
C(14)-C(13)-O(21)-C(22)	-176.3(2)

Symmetry transformations used to generate equivalent atoms:

#1 -x,-y+1,-z+1

Bibliography

- 1) Deitrich, B.; Viout, P.; Lehn, J.-M. Macrocyclic Chemistry, VCH Publishers: New York, 1993.
- 2) Zhang, X.X.; Bradshaw, J.S.; Izatt, R.M. *Chem. Rev.* **1997**, 97, 3313.
- 3) Gokel, G.W.; Leeve, W.M.; Weber, M.E. *Chem. Rev.* **2004**, 104, 2723.
- 4) Schalley, C.A.; Beizai, K.; Vögtle, F. *Acc. Chem. Res.* **2001**, 34, 465.
- 5) Meunie, B.; de Visser, S.P.; Shaik, S. *Chem. Rev.* **2004**, 104, 3947.
- 6) Takahashi, K. *Chem. Rev.* **1998**, 98, 2013.
- 7) Rychnovsky, S.D. *Chem. Rev.* **1995**, 95, 2021.
- 8) Kovbasyuk, L.; Krämer, R. *Chem. Rev.* **2004**, 104, 3161.
- 9) Balzani, V.; Credi, A.; Raymo, F.M.; Stoddart, J. F. *Angew. Chem. Int. Ed.* **2000**, 39, 3349.
- 10) Macrolides : Chemistry, Pharmacology, and Clinical Uses Bryskier, A.J. Ed.; Arnette Blackwell: Boston, 1993.
- 11) Roxborgh, C.J. *Tetrahedron* **1995**, 51, 1995.
- 12) Ruzieka, L.; Brugger, W.; Pfeiffer, M.; Sehin, H.; Stoll, M. *Helv. Chem. Act.* **1926**, 9, 499.
- 13) Meng, Q.; Hesse, M. Ring Closure Methods in the Synthesis of Macrocyclic Natural Products. In *Topics in Current Chemistry: Macrocycles*, 161; Dewar, M.J.S., Dunitz, J.D., Hafner, K., Ito, S., Lehn, J.-M., Niedenzu, K.; Raymond, K.N.; Rees, C.W.; Vögtle, F. Springer-Verlag:Berlin, 1992.
- 14) V. Prelog and H.C. Brown as cited in : Brown, H.C.; Fletcher, R.S.; Johannesen, R.B. *J. Am. Chem. Soc.* **73**, 212.
- 15) Illuminati, G.; Mandolini, L. *Acct. Chem. Res.* **1981**, 14, 95.
- 16) Eliel, E.L. Stereochemistry of Carbon Compounds McGraw-Hill: New York, 1962, pp.188-201.
- 17) Borgen, G.; Dale, J. *Acta Chem. Scand.* **1972**, 26, 952.
- 18) Galli, C.; Giovannelli, G.; Illuminati, G.; Mandolini, L. *J. Org. Chem.* **1979**, 44, 1258.
- 19) Illuminati, G.; Mandolini, L.; Masci, B. *J. Am. Chem. Soc.* **1977**, 99, 6308.
- 20) Galli, C.; Illuminati, G.; Mandolini, L. *J. Am. Chem. Soc.* **1973**, 95, 8374.
- 21) Galli, C.; Mandolini, L. *Chem. Comm.* **1982**, 251.
- 22) Ruzieka, L.; Stoll, M.; Sehin, H. *Helv. Chem. Act.* **1926**, 9, 249.
- 23) Knops, P.; Sendhoff, N.; Mekelbirger, H.-B.; Vögtle, F. ‘High Dilution Reactions- New Synthetic Applications” Topics in Current Chemistry: Macrocycles ed. Dewar, M.J.S.; Dunitz, J.D.; Hafner, K.; Ito, S.; Lehn, J.-M.; Niedenzu, K.; Raymond, K.N.; Rees, C.W.; Vögtle, F. Springer-Verlag:Berlin, 1992 , pp.1-106.
- 24) Kramer, U.; Guggisberg, A.; Hesse, M.; Schmid, H. *Angew. Chem., Int. Ed. Engl.* **1978**, 17, 200.
- 25) Hesse, M. Ring Enlargement in Organic Chemistry VCH: New York, 1991.
- 26) Corey, E.J.; Nicolaou, K.C. *J. Am. Chem. Soc.* **1974**, 96, 5614.
- 27) Nicolaou, K.C.; Ninkovic, S.; Sarabia, F.; Vourloumis, D.; He, .Y.; Vallberg, H.; Finlay, M.R.V.; Yang, Z. *J. Am. Chem. Soc.* **1997**, 119, 7974.

- 28) Dwoden, J.; Edwards, P.D.; Flack, S.S.; Kilburn, J.D. *Chem. Eur. J.* **1999**, *5*, 79.
- 29) Nicolaou, K.C.; Ritzén, A.; Namoto, K.; Buey, R.M.; Díaz, J.F.; Andreu, J.M.; Wartmann, M.; Altmann, K.-H.; O'Brate, A.; Giannakakou, G. *Tetrahedron* **2002**, *58*, 6413.
- 30) Nicolaou, K.C.; Zak, M.; Safina, B.S.; Lee, S.H.; Estrada, A.A. *Angew. Chem. Int. Ed.* **2004**, *43*, 5092.
- 31) Takeda, K.; Yano, S. Yoshii, E. *Tetrahedron Lett.* **1988**, *29*, 6951.
- 32) Danishefsky, S.J.; Mantlo, N.B.; Yamashita, D.S. *J. Am. Chem. Soc.* **1988**, *110*, 6890.
- 33) Takahashi, T.; Nagashima, T.; Tsuji, J. *Tetrahedron Lett.* **1981**, *22*, 1359.
- 34) Marshall, J.A.; Cleary, D.G. *J. Org. Chem.* **1986**, *51*, 858.
- 35) Porter, N.A.; Chang, V.H-T. *J. Am. Chem. Soc.* **1987**, *109*, 4976.
- 36) Cox, N.J.G.; Pattenden, G.; Mills, S.D. *Tetrahedron Lett.* **1989**, *30*, 621.
- 37) Boger, D.L.; Mathvink, R.J. *J. Am. Chem. Soc.* **1990**, *112*, 4008.
- 38) Graetz, B.R.; Rychnovsky, S.D. *Org. Lett.* **2003**, *5*, 3357.
- 39) McCauley, J.A.; Nagasawa, K.; Lander, P.A.; Mischke, S.G.; Semones, M.A.; Kishi, Y. *J. Am. Chem. Soc.* **1998**, *120*, 7647.
- 40) Evans, D.A.; Ripin, D.H.B.; Halstead, D.P.; Campos, K.R. *J. Am. Chem. Soc.* **1999**, *121*, 6816.
- 41) Yang, W.; Digits, C.A.; Hatada, M.; Narula, S.; Rozamus, L.W.; Huestis, C.M.; Wong, J.; Dalgarno, D.; Holt, D.A. *Org. Lett.* **1999**, *1*, 2003.
- 42) Zajac, M.A.; Vedejs, E. *Org. Lett.* **2004**, *6*, 237.
- 43) Belanger, G.; Deslongchamps, P. *J. Org. Chem.* **2000**, *65*, 7070.
- 44) Dineen, T.A.; Rousch, W.R. *Org. Lett.* **2004**, *6*, 2043.
- 45) Smith, A.B.; Adams, C.M.; Kozmin, S.A.; Paone, D.V. *J. Am. Chem. Soc.* **2001**, *123*, 5925.
- 46) McMurray, J.E. *Acc. Chem. Res.* **1983**, *16*, 405.
- 47) Corey, E.J.; Hamanaka, E. *J. Am. Chem. Soc.* **1964**, *86*, 1641.
- 48) Dauben, W.G.; Beasley, G.H.; Broadhurst, M.D.; Muller, B.; Peppard, D.J.; Pesnelle, P.; Sutter, C. *J. Am. Chem. Soc.* **1974**, *96*, 4724.
- 49) Paterson, I.; Lombart, H.-G.; Allerton, C. *Org. Lett.* **1999**, *1*, 19.
- 50) Quéron, E.; Lett, R. *Tetrahedron Lett.* **2004**, *45*, 4539.
- 51) Boger, D.L.; Mathvink, R.J. *J. Am. Chem. Soc.* **1990**, *112*, 4008.
- 52) Trost, B.M.; Ohmori, M.; Boyd, S.A.; Okawara, H.; Brickner, S.J. *J. Am. Chem. Soc.* **1989**, *111*, 8281.
- 53) Märkl, G.; Amrhein, J.; Stoiber, T.; Stiebl, U.; Kreitmeier, P. *Tetrahedron* **2002**, *58*, 2551.
- 54) Zheng, G.; Shibata, M.; Dougherty, T.J.; Pandey, R.K. *J. Org. Chem.* **2000**, *65*, 543.
- 55) Marshall, J.A.; Jenson, T.M.; DeHoff, B.S. *J. Org. Chem.* **1986**, *51*, 4316.
- 56) Nicolaou, K.C.; Duggan, M.E.; Hwang, C.-K. *J. Am. Chem. Soc.* **1986**, *108*, 2468.
- 57) Reid, R.C.; Kelso, M.J.; Scanion, M.J.; Fairlie, D.P. *J. Am. Chem. Soc.* **2002**, *124*, 5673.

- 58) Goekjian, P.G.; Wu, G.-Z.; Chen, S.; Zhou, L.; Jirousek, M.R.; Gillig, J.R.; Balla, L.M.; Dixon, J.T. *J. Org. Chem.* **1999**, *64*, 4238.
- 59) Rodriguez, G.; Lutz, M.; Spek, A.L.; van Koten, G. *Chem. Eur. J.* **2002**, *8*, 46.
- 60) Trnka, T.M.; Grubbs, R.H. *Acc. Chem. Res.* **2001**, *34*, 18.
- 61) Tsuji, J.; Hashiguchi, S. *Tetrahedron Lett.* **1980**, *21*, 2955.
- 62) Gaul, C.; Njardarson, J.T.; Shan, D.; Wu, K.-D.; Tong, W.P.; Huang, X.-Y.; Moore, M.A.S.; Danishefsky, S.J. *J. Am. Chem. Soc.* **2004**, *126*, 11326.
- 63) Ojima, I.; Lin, S.; Inoue, T.; Miller, M.L.; Borella, C.P.; Geng, X.; Walsh, J.J. *J. Am. Chem. Soc.* **2000**, *122*, 5343.
- 64) Mohr, B.; Lynn, D.M.; Grubbs, R.H. *J. Am. Chem. Soc.* **1998**, *120*, 1627.
- 65) Kulkowit, S.; McKervey, M.A. *J. Chem. Soc., Chem. Commun.* **1981**, 616.
- 66) Toma, K.; Miyazaki, E.; Murae, T.; Takahashi, T. *Chem. Lett.* **1982**, 863.
- 67) Doyle, M.P.; Protopopova, M.N.; Poulter, C.D.; Rogers, D.H. *J. Am. Chem. Soc.* **1995**, *117*, 7281.
- 68) Padwa, A.; Austin, D.J. *Angew. Chem., Int. Ed. Engl.* **1994**, *33*, 1797.
- 69) Doyle, M.P.; Bagheri, V.; Wandless, T.J.; Harn, N.K.; Brinker, D.A.; Eagle, C.T.; Loh, K.-L. *J. Am. Chem. Soc.* **1990**, *112*, 1906.
- 70) Doyle, M.P.; McKervey, M.A.; Ye, T. Modern Catalytic Methods for Organic Synthesis with Diazo Compounds: from Cyclopropanes to Ylides, Wiley-Interscience: New York, 1998.
- 71) Pauissenen, R.; Reimlinger, H.; Hayez, E.; Hubert, A.J.; Teyssie, P. *Tetrahedron Lett.* **1973**, 2233.
- 72) Davies, H.M.L. *Tetrahedron*, **1993**, *49*, 5203.
- 73) Padwa, A.; Krumpe, K.E. *Tetrahedron*, **1992**, *48*, 5385.
- 74) Mass, G. *Top. Curr. Chem.* **1987**, *137*, 76.
- 75) Doyle, M.P. *Chem. Rev.* **1986**, *86*, 919.
- 76) Rempel, G.A.; Legzdins, P.; Smith, H.; Wilkinson, G. *Inorg. Syn.* **1972**, *13*, 90.
- 77) Ahsan, M.Q.; Bernal, I.; Bear, J.L. *Inorg. Chem.* **1986**, *25*, 260.
- 78) Lifsey, R.S.; Lin, X.Q.; Chavan, M.Y.; Ahsan, M.Q.; Kadish, K.M.; Bear, J.L. *Inorg. Chem.* **1987**, *26*, 830.
- 79) Doyle, M.P.; Raab, C.E.; Roos, G.H.P.; Lynch, V.; Simonsen, S.H. *Inorg. Chim. Acta* **1997**, *266*, 13.
- 80) Doyle, M.P.; Winchester, W.R.; Hoorn, J.A.A.; Lynch, V.; Simonsen, S.H.; Ghosh, R. *J. Am. Chem. Soc.* **1993**, *115*, 9968.
- 81) Woodward, R.B. *Angew. Chem.*, **1957**, *69*, 50.
- 82) Doyle, M.P.; Hu, W. *Synlett* **2001**, 1364.
- 83) Ruggli, P. *Ann.* **1912**, *392*, 92.
- 84) Doyle, M.P.; Hu, W.; Chapman, B.; Marnett, A.B.; Peterson, C.S.; Vitale, J.P.; Stanley, S.A. *J. Am. Chem. Soc.* **2000**, *122*, 5718.
- 85) Doyle, M.P.; Peterson, C.S.; Parker, D.L. *Angew. Chem. Int. Ed. Eng.* **1996**, *35*, 1334.
- 86) Doyle, M.P.; Ene, D.G.; Peterson, C.S.; Lynch, V. *Angew. Chem. Int. Ed.* **1999**, *38*, 700.

- 87) Doyle, M.P.; Protopopova, M.N.; Peterson, C.S.; Vitale, J.P. *J. Am. Chem. Soc.* **1996**, *118*, 7865.
- 88) Doyle, M.P.; Chapman, B.J.; Hu, W.; Peterson, C.S.; McKervery, M.A.; Garcia, C.F. *Org. Lett.* **1999**, *1*, 1327.
- 89) Pfaltz, A. *Acc. Chem. Res.* **1993**, *26*, 339.
- 90) Müller, P.; Baud, C.; Ene, D.; Motallebi, S.; Doyle, M.P.; Brandes, B.D.; Dyatkin, A.B.; See, M.M. *Helv. Chim. Acta* **1995**, *78*, 459.
- 91) Nishiyama, H. Itoh, Y.; Sugawara, Y.; Matsumoto, Aoki, K.; Itoh, K. *Bull. Chem. Soc. Jpn.* **1995**, *68*, 1247.
- 92) Doyle, M.P.; Dyatkin, A.B.; Autry, C.L.J. *J. Chem. Soc., Perkin Trans. 1* **1995**, 619.
- 93) Doyle, M.P.; Austin, R.E.; Bailey, A.S.; Dwyer, M.P.; Dyatkin, A.B.; Kalinin, A.V.; Kwan, M.M.Y.; Liras, S.; Oalman, C.J.; Pieters, R.J.; Protopopova, M.N.; Raab, C.E.; Roos, G.H.P.; Zhou, Q.-L.; Martin, S.F. *J. Am. Chem. Soc.* **1995**, *117*, 5763.
- 94) Doyle, M.P.; Peterson, C.S.; Protopopova, M.N.; Marnett, A.B.; Parker, D.L., Jr.; Ene, D.G.; Lynch, V. *J. Am. Chem. Soc.* **1997**, *119*, 8826.
- 95) Martin, S.F.; Spaller, M.R.; Liras, S.; Hartmann, B. *J. Am. Chem. Soc.* **1994**, *116*, 4493.
- 96) Doyle, M.P.; Hu, W. *J. Org. Chem.* **2000**, *65*, 8839.
- 97) Doyle, M.P.; Hu, W. *Tetrahedron Lett.* **2000**, *41*, 6265.
- 98) Doyle, M.P.; Hu, W.; Phillips, I.M.; Moody, C.J.; Pepper, A.G.; Slawin, A.M.Z. *Adv. Synth. Catal.* **2001**, *343*, 112.
- 99) Doyle, M.P.; Zhou, Q.-L.; Simonsen, S.H.; Lynch, V. *Synlett*, **1996**, 697.
- 100) Doyle, M.P.; Phillips, I.M. *Tetrahedron Lett.* **2001**, *42*, 3155.
- 101) Kulkowit, S.; McKervery, M.A. *J. Chem. Soc., Chem. Commun.* **1983**, 1069.
- 102) Doyle, M.P.; Hu, W.; Phillips, I.M.; Wee, A.G.H. *Org. Lett.* **2000**, *2*, 1777.
- 103) Helsin, J.C.; Moody, C.J. *J. Chem. Soc., Perkin Trans. 1* **1988**, 1417.
- 104) *Catalytic Asymmetric Synthesis*, 2nd Ed.; Ojima, Iwao editor; Wiley-VCH: New York, 2000.
- 105) Masamune, S.; Choy, W.; Petersen, J.S.; Sita, L.R. *Angew. Chem. Int. Ed. Engl.* **1985**, *24*, 1.
- 106) Kolodiazny, O.I. *Tetrahedron* **2003**, *59*, 5953.
- 107) Doyle, M.P.; Davies, S.B.; May, E.J. *J. Org. Chem.* **2001**, *66*, 8112.
- 108) Doyle, M.P.; Kalinin, A.V.; Ene, D.G. *J. Am. Chem. Soc.* **1996**, *118*, 8837.
- 109) Martin, S.F.; Spaller, M.R.; Liras, S.; Hartmann, B. *J. Am. Chem. Soc.* **1994**, *116*, 4493.
- 110) Doyle, M.P.; Dyatkin, A.B.; Kalinin, A.V.; Ruppar, D.A.; Martin, S.F.; Spaller, M.R.; Liras, S. *J. Am. Chem. Soc.* **1995**, *117*, 11021.
- 111) Kim, P.; Nantz, M.H.; Kurth, M.J.; Olmstead, M.M. *Org. Lett.* **2000**, *2*, 1831.
- 112) Roush, W.R.; Hoong, L.K.; Palmer, M.A.J.; Straub, J.A.; Palkowitz, A.D. *J. Org. Chem.* **1990**, *55*, 4117.
- 113) Still, W.C.; Darst, K.P. *J. Am. Chem. Soc.* **1980**, *102*, 7385.
- 114) Horeau, A.; Kagan, H.B.; Vigneron, J.-P. *Bull. Soc. Chim. Fr.*, **1968**, 3795.

- 115) Izumi, Y.; Tai, A. *Stereodifferentiating Reactions*, Academic Press: New York, **1977**.
- 116) Heathcock, C.H.; White, C.T. *J. Am. Chem. Soc.* **1979**, *101*, 7076.
- 117) Eliel, E.L.; Wilen, S.H.; Mander, L.N. *Stereochemistry of Organic Compounds*, Wiley: New York, 1994; p. 969.
- 118) Masamune, S.; Ali, S.A.; Snitman, D.L.; Garvey, D.S. *Angew. Chem. Int. Ed. Engl.* **1980**, *19*, 557.
- 119) Müller, P.; Baud, C.; Ene, D.; Motallebi, S.; Doyle, M.P.; Brandes, B.D.; Dyatkin, A.B.; See, M.M. *Helv. Chim. Acta* **1995**, *78*, 459.
- 120) Tei, T.; Sato, Y.; Hagiya, K.; Tai, A.; Okuyama, T.; Sugimura, T. *J. Org. Chem.* **2002**, *67*, 6593.
- 121) Douglas, N. L.; Ley, S.V.; Osborn, H.M.I.; Owen, D.R.; Priepke, H.W.M.; Warriner, S.L. *Synlett* **1996**, 793-5.
- 122) Montchamp, J.-L.; Tian, F.; Hart, M.E.; Frost, J.W. *J. Org. Chem.* **1996**, *61*, 3897-9.
- 123) *Handbook of Thin-Layer Chromatography* J. Sherman and B. Fried, Eds., Marcel Dekker, New York, NY, 1991.
- 124) Danheiser, R.L.; Miller, R.F.; Brisbois, R.G.; Park, S.Z. *J. Org. Chem.* **1990**, *55*, 1959-64.
- 125) Kubas, G.J. *Inorg. Synth.* **1979**, *19*, 90.
- 126) Evans, D.A.; Peterson, G.S.; Johnson, J.S.; Barnes, D.M.; Campos, K.R.; Woerpel, K.A. *J. Org. Chem.* **1998**, *63*, 4541-44.
- 127) Doyle, M.P.; Dyatkin, A.B.; Protopopova, M.N.; Yang, C.I.; Miertschin, C.S.; Winchester, W.R.; Simonsen, S.I.; Lynch, V.; Ghosh, R. *Recueil Trav. Chim. Pays-Bas*, **1995**, *114*, 163.
- 128) Doyle, M.P.; Davies, S.B.; Hu, W.H. *J. Org. Chem.*, **2000**, *65*, 8839.
- 129) Davies, H.M.L.; Bruzinski, P.R.; Lake, D.H.; Kong, N.; Fall, M.J. *J. Am. Chem. Soc.* **1996**, *118*, 6897.
- 130) Goldberg, I.; Stein, Z.; Weber, E.; Doeringhaus, N.; Franklin, S. *J. Chem. Soc., Perkin II* **1990**, 953.
- 131) Prelog, V. *J. Chem. Soc.* **1950**, 420.
- 132) Yeung, K.-S.; Paterson, I. *Angew. Chem. Int. Ed.* **2002**, *41*, 4632.
- 133) Taber, D.F.; Petty, E.H. *J. Org. Chem.* **1982**, *47*, 4808.
- 134) Taber, D.F.; Ruckle, R.E., Jr. *J. Am. Chem. Soc.* **1986**, *108*, 7686.
- 135) Wilson, L.J. Recent Advances in Solid-Phase Synthesis of Natural Products. In *Solid-Phase Organic Synthesis*, Burgess, K. Ed.; Wiley:New York, 2000; pp. 247-367.
- 136) Dörwald, F..Z. *Organic Synthesis on Solid Phase*, Wiley:New York, 2002; pp.18-38.
- 137) Gaul, C.; Njardarson, J.T.; Shan, D.; Dom, D.C.; Wu, K.-D.; Tong, W.P.; Huang, X.-Y.; Moore, M.A.S.; Danishefsky, S.J. *J. Am. Chem. Soc.*, **2004**, *126*, 11326.
- 138) Corey, E.J.; Myers, A.G. *Tetrahedron Lett.* **1984**, *25*, 3359.
- 139) Clark, J.S.; Krowiak, S.A. *Tetrahedron Lett.* **1993**, *34*, 4385.
- 140) Doyle, M.P.; Bagheri, V.; Wandless, T.J.; Harn, N.K.; Brinker, D.A.; Eagle, C.T.; Loh, K.-L. *J. Am. Chem. Soc.*, **1990**, *112*, 1906.

- 141) Nishiyama, H.; Itoh, Y.; Matsumoto, H.; Park, S.-B.; Itoh, K. *J. Am. Chem. Soc.* **1994**, *116*, 2223.
- 142) Panghonr, A.B.; Giardello, M.A.; Grubbs, R.H.; Rosen, R.K.; Timmers, F.J. *Organometallics*, **1996**, *15*, 1518.
- 143) House, H.O.; Blankley, C.J. *J. Org. Chem.* **1968**, *33*, 53.
- 144) Blankely, C.J.; Sauter, F.J.; House, H.O. *Org. Synth.* **1969**, *49*, 22.
- 145) Doyle, M.P.; Peterson, C.S.; Protopopova, M.N.; Marnett, A.B.; Parker, D.L., Jr.; Ene, D.G.; Lynch, V. *J. Am. Chem. Soc.* **1997**, *119*, 8826.
- 146) Entel, J.; Ruof, C.F.; Howar, H.C. *J. Am. Chem. Soc.* **1952**, *74*, 441.
- 147) Ruzieka, L.; Brugger, W.; Pfeiffer, M.; Sehinz, H.; Stoll, M. *Helv. Chem. Act.* **1926**, *9*, 499.
- 148) Busch, D.H. *J. Inclusion Phenom.* **1992**, *12*, 389.
- 149) Gerbeleu, N.V.; Arion, V.B.; Burgess, J. *Template Synthesis of Macrocyclic Compounds*, Wiley-VCH:New York, 1999.
- 150) Anderson, S.; Anderson, H.L.; Sanders, J.K.M. *J. Chem. Soc., Perkin Trans. I* **1995**, 2247.
- 151) Baker, W.; McOmie, J.F.W.; Ollis, W.D. *J. Chem. Soc.* **1951**, 200.
- 152) Mandolini, L.; Masci, B.; Roelens, S. *J. Org. Chem.* **1997**, *42*, 3733.
- 153) Pedersen, C.J. *J. Am. Chem. Soc.* **1967**, *89*, 7071.
- 154) Shaw, B.L. *J. Am. Chem. Soc.* **1975**, *97*, 3856.
- 155) Ochiai, E.I. *Coord. Chem. Rev.* **1968**, *3*, 49.
- 156) Mandolini, L.; Masci, B. *J. Am. Chem. Soc.* **1977**, *99*, 7709.
- 157) Ercolani, G.; Mandolini, L.; Masci, B. *J. Am. Chem. Soc.* **1981**, *103*, 2780.
- 158) Dunitz, J.D.; Dobler, M.; Seiler, P.; Phizackerley, R.P. *Acta Crst. B* **1974**, *30*, 2733.
- 159) Cotton, F.A.; Wilkenson, G.; Murillo, C.A.; Bochmann, M. *Advanced Inorganic Chemistry*, 6th ed.; Wiley & Sons: New York, 1999; pp. 854-876.
- 160) Comarmond, J.; Plumeré, P.; Lehn, J.-L.; Agnus, Y.; Louis, R.; Weiss, R.; Kahn, O.; Morgenstern-Badarau, O. *J. Am. Chem. Soc.* **1982**, *104*, 6330.
- 161) Beall, L.S.; Mani, N.S.; White, A.J.P.; Williams, D.J.; Barrett, A.J.M.; Hoffman, B.M. *J. Org. Chem.* **1998**, *63*, 5806.
- 162) Martens, C.F.; Gebbink, R.J.M.K.; Feiters, M.C.; Kooijman, G.H.; Smeets, W.J.J.; Spek, A.L.; Nolte, R.J.M. *Inorg. Chem.* **1994**, *33*, 5541.
- 163) Yamamoto, K.; Garbaccio, R.M.; Stachel, S.J.; Solit, D.B.; Chiosis, G.; Rosen, N.; Danishefsky, S.J. *Angew. Chem. Int. Ed.* **2003**, *42*, 1280.